Phosphorus Legacies and Water Quality Trajectories Across Canada

by

Lamisa Malik

A thesis
presented to the University of Waterloo
in fulfillment of the
thesis requirement for the degree of
Doctor of Philosophy
in
Civil and Environmental Engineering (Water)

Waterloo, Ontario, Canada, 2024

© Lamisa Malik 2024

Examining Committee Membership

The following served on the Examining Committee for this thesis. The decision of the Examining Committee is by majority vote.

External Examiner
Roxane Maranger
Professor
Department of Biological Sciences, University of Montreal

Supervisor
Nandita Basu
Professor
Civil and Environmental Engineering, University of Waterloo

Internal Members
Bruce MacVicar
Associate Professor
Civil and Environmental Engineering, University of Waterloo

Internal-external Members
Helen Jarvie
Professor
Geography and Environmental Management, University of Waterloo

Kimberly J Van Meter
Adjunct Professor
Department of Earth and Environmental Sciences, University of Waterloo

Author's Declaration

This thesis consists of material all of which I authored or co-authored: see Statement of Contributions included in the thesis. This is a true copy of the thesis, including any required final revisions, as accepted by my examiners.

I understand that my thesis may be made electronically available to the public.

Statement of Contributions

All three research chapters were written in the journal manuscript format. I am the first author of all these chapters, and the contributions of co-authors are summarized below

Chapter 2: Estimation of Legacy Phosphorus and its Drivers across the Lake Erie Basin using Data Synthesis and Machine Learning Integration

Nandita Basu, Nitin Singh, and I designed, led and wrote the study which has two parts: data synthesis and machine learning. I led the data synthesis part. The USA side of Lake Erie phosphorus mass balance uses data prepared by Danyka Byrnes, Shuyu Chang, and Kimberly J. Van Meter. Nitin Singh led the machine learning part of the study.

Chapter 3: Modeling Legacy Phosphorus Storage across the Lake Erie Basin Using ELEMeNT-P Model

Nandita Basu, Kimberly J. Van Meter, and I led the study. The ELEMeNT-P model framework was developed by Kimberly J. Van Meter. I aggregated data, rebuilt the model for the Lake Erie scale, calibrated the model and performed the analysis. I wrote the chapter with inputs from Nandita Basu. I thank Meghan McLeod for her help during the model development stage.

Chapter 4: Pan Canada Phosphorus Budget: Insight from a 60 years Dataset

I and Nandita Basu designed the study. I synthesized the data set with valuable inputs from Nandita Basu, Kimberly J. Van Meter and Danyka Byrnes. Shuyu Chang assisted me by providing valuable feedback on the map downscaling task. I wrote the chapter with inputs from Nandita Basu. I thank my co-ops Anisha and Nikita for their contributions to data collection, map digitization and quality control.

Abstract

Phosphorus (P) pollution in freshwater is a critical environmental issue, primarily driven by agricultural runoff, wastewater discharge, and industrial effluents. Across Canada, lakes such as Lake Erie and Lake Winnipeg experience severe and persistent algal blooms driven mainly due to excess phosphorus loading. Excessive phosphorus loading leads to eutrophication, which causes harmful algal blooms and hypoxia which disrupt aquatic life, reduce biodiversity, and impair water quality, making human consumption and recreational activities unsafe. Despite policies aimed at reducing phosphorus loading, such as improved farming practices and wastewater treatment upgrades, we have not seen a marked decrease in riverine loads. Phosphorus management goals often fall short due to the persistence of legacies – phosphorus that has accumulated in soils and sediments over decades of agricultural applications – which continue to release phosphorus into water bodies for decades after its initial application. Despite recognizing the existence and significant regional and global impact of legacy P on water quality and aquatic ecosystems, our understanding of the magnitude and spatial distribution of these P stores remains limited. Understanding the legacy P stores and their contributors is crucial for efficiently managing water quality, highlighting the importance of studying these factors to develop more effective and sustainable management strategies.

The central theme of this thesis is the exploration of the phosphorus legacy across various landscapes. My work has three objectives. First, I explore phosphorus legacies and water quality trajectories across the Lake Erie basin. Second, I quantify various legacy P stores and evaluate their current and future impacts on water quality. Third, I quantified phosphorus accumulation for Pan Canada.

In the first objective, I develop a comprehensive phosphorus budget for the Lake Erie Basin, a 60,000 km² transboundary region between the U.S. and Canada, by collecting, harmonizing, and synthesizing agricultural, climate, and population data. The phosphorus inputs included fertilizer, livestock manure, human waste, detergents, and atmospheric deposition, while outputs focused on crop and pasture uptake, covering a historical period from 1930 to 2016. The budget allowed us to calculate excess phosphorus as phosphorus surplus– surplus defined as the difference between P inputs and non-hydrological exports. A random forest model was then employed to describe in-stream phosphorus export as a function of cumulative P surplus and streamflow. The results indicated a significant accumulation of legacy P in the watersheds of the Lake Erie Basin. Notably, higher legacy P accumulation corresponded strongly with greater manure inputs (R^2=0.46, $p < 0.05$), whereas fertilizer inputs showed a weaker relationship.

For the second objective, I model the long-term nutrient dynamics of phosphorus across 45 watersheds in the Lake Erie basin using the ELEMeNT-P model. This aimed to quantify legacy phosphorus accumulation and depletion across different landscape compartments, including soils, landfills, reservoirs, and riparian zones, and to assess the potential for phosphorus load reductions

under future management scenarios. The model sought to identify key legacy phosphorus pools and explore the feasibility of achieving significant reductions in phosphorus loading, with results indicating that 40% reductions are attainable only through aggressive management efforts.

For the last objective, I develop a high-resolution phosphorus budget dataset for Canada, spanning the years 1961 to 2021, at both county and 250-meter spatial scales. This dataset aimed to capture phosphorus inputs from fertilizers, manure, and domestic waste, along with phosphorus uptake by crops and pastureland, across all ten provinces. With this dataset, I aim to better understand the state and progress of phosphorus management across space and time. The results reveal significant variation in P surplus attributable to differences in land use and management practices. The highest surpluses were observed in southern Ontario and Quebec, with approximately 50 kilotons in 2021, contributing to an accumulation of over 2 tera tons of phosphorus over the past 60 years.

Acknowledgements

I would like to thank Nandita Basu, my supervisor, for her invaluable support and guidance, without which this thesis would not have been completed. I am also grateful to her for introducing me to the field of phosphorus research, allowing me to gain a deep understanding of nutrient dynamics and management.

I would like to thank my committee members Helen Jarvie, Bruce MacVicar and Kimberley J Van Meter for their time, support, and feedback.

I would like to thank Lake Futures-Global Water Futures for providing me with funding throughout my degree.

I am immensely thankful to my lab mates in BasuLab for helping me grow as a researcher. To my nutrient buddies, Danyka Byrnes, Garima Lakhanpal, and Meghan McLeod, for being there during stressful times and always offering a listening ear. I am truly blessed to have friends and colleagues like you. To Nitin Singh, Tyler Hampton, and Joy Liu, thank you for your help and your words of encouragement.

Fahad, I can't thank you enough for your support throughout this journey. To my parents, thank you for everything. To my undergraduate and master's supervisor, Dr. Abdul Matin, thank you for always encouraging me. Your guidance and inspiration have helped shape me into who I am today.

Thanks to my friends, especially Arpita, Humaira, Shamonti and Jovana I am so lucky to have such incredible friends like you.

Dedication

To my butterfly, Yaara

Table of Contents

LIST OF FIGURES ..... **XII**

LIST OF TABLES ..... **XIV**

CHAPTER 1 ..... **1**

INTRODUCTION **1**

1.1 INTRODUCTION 1
1.1.1 Phosphorus Pollution Scenario in the Lake Erie Basin and Beyond *2*
1.1.1.1 Lake Erie Basin: General Description and Land Use 2
1.1.1.2 Mitigating Phosphorus Pollution in Lake Erie: A Historical Perspective 3
1.1.1.3 Harmful Algal Blooms in North America and its Response 5
1.2 FATE AND TRANSPORT OF PHOSPHORUS 7
1.2.1 Legacy Phosphorus and Time Lags *7*
1.3 QUANTIFYING PHOSPHORUS INPUTS AND MODELING LEGACIES- GAPS AND CAPABILITIES 8
1.4 RESEARCH OBJECTIVES 10

CHAPTER 2 ..... **12**

ESTIMATION OF LEGACY PHOSPHORUS AND ITS DRIVERS ACROSS THE LAKE ERIE BASIN **12**

2.1 INTRODUCTION 12
2.2 MATERIALS AND METHODS 14
2.2.1 Phosphorus Mass Balance across Lake Erie Basin *14*
2.2.1.1 P Surplus 16
2.2.2 Stream Phosphorus Export *17*
2.2.3 Estimation of Legacy Phosphorus *18*
2.3. RESULTS AND DISCUSSION 18
2.3.1 Phosphorus Inputs and Surplus across the Transboundary Lake Erie Basin (1930-2016) *18*
2.3.2 Phosphorus Surplus and Riverine P Loads *21*
2.3.3 Legacy Phosphorus Accumulation across the Lake Erie Basin *23*
2.4. CONCLUSIONS 26

CHAPTER 3 ..... **28**

MODELING LEGACY PHOSPHORUS STORAGE ACROSS THE LAKE ERIE BASIN USING ELEMENT-P MODEL **28**

3.1 BACKGROUND 28
3.2 THE ELEMENT-P MODEL FRAMEWORK 31
3.2.1 Source Zone Dynamics *33*
3.2.1.1 P Surplus as Input to the Source Zone 33
3.2.2 Surface P Transport: Erosion and Retention *34*
3.2.3 Domestic P Inputs *35*
3.3 METHODS AND DATA SOURCES 36
3.3.1 Model Inputs and Outputs *36*
3.3.1.1 Watershed Selection, Discharge and Total Phosphorus Concentration Data 36
3.3.1.2 Input from P Mass Balance 39

3.3.1.3 Watershed Land Use Trajectories....43
3.3.1.4 Watershed Erosion Parameter....44
3.3.1.5 Model Calibration....46
3.3.1.6 Generating Future Scenarios....48
3.4 RESULTS AND DISCUSSION....48
3.4.1 Model Performance....49
3.4.2 Phosphorus Fluxes and Stores....50
3.4.2.1 Estimation of Stream P Loading for Over 100 Years....50
3.4.2.2 P Accumulation across the Lake Erie Basin....52
3.4.3 Future Scenarios....56
3.5 CONCLUSION....61
CHAPTER 4....63
PAN CANADA PHOSPHORUS BUDGET: INSIGHT FROM A 60 YEAR DATASET....63
4.1 BACKGROUND....63
4.2 MATERIALS AND METHODS....67
4.2.1 Dataset Preparation: County-scale Phosphorus Mass Balance....67
4.2.1.1 Inorganic Fertilizer....68
4.2.1.2 P from Livestock Manure....70
4.2.1.3 Domestic Waste....72
4.2.1.4 Phosphorus Uptake....73
4.2.1.5 P Surplus....78
4.2.2 Mapping the P inputs to the county scale....78
4.2.2.1 Downscaling County Scale P Surplus Components....80
4.2.3 Phosphorus Use Efficiency (PUE)....82
4.3 RESULTS AND DISCUSSIONS....83
4.3.1 Trajectories of P surplus and its components across Canada (1961-2021)....83
4.3.1.1 P Surplus Across the Provinces in Canada....85
4.3.1.2 Addressing Legacy P with Cumulative P Surplus....88
4.3.2 Phosphorus Use Efficiency (PUE) in Legacy P Management....90
4.3.2.1 PUE at the National and Provincial Scale....90
4.3.2.2 PUE Metric from a Management Perspective....93
4.3.3 Technical Evaluation of Results and Limitations....95
4.3.3.1 Comparison of County-scale Mass Balance Data....95
4.3.3.2 Validation of Gridded Phosphorus Data with County-scale Data....97
4.4 CONCLUSIONS....99
CHAPTER 5....101
CONCLUSION....101
5.1 SUMMARY....101
5.2 MAJOR CONTRIBUTION....103
5.3 LIMITATIONS AND RECOMMENDATIONS FOR FUTURE WORK....103
REFERENCES....105
APPENDIX A- SUPPLEMENTAL INFORMATION FOR CHAPTER 2....129
S1. METHODS....129
S1.1 Phosphorus in Fertilizer....129

S1.2 Phosphorus from Livestock Manure *130*
S1.3 Domestic Phosphorus Waste *132*
S1.4 Phosphorus Uptake *133*
S1.5 Downscaling Phosphorus Mass Balance Component *137*

APPENDIX B- SUPPLEMENTARY MATERIALS FOR CHAPTER 3 143

TEXT S1 SOURCE ZONE DYNAMICS 143
S1.1 Organic P (Msop) in the Source Zone *143*
S1.2 Mineral P (Mmin) in the Source Zone *143*
S1.3 Dissolved P Fluxes: Travel Time-based Approach *145*
TEXT S2 SURFACE P TRANSPORT 145

APPENDIX C- SUPPLEMENTAL INFORMATION FOR CHAPTER 4 159

List of Figures

Figure 1.1: Lake Erie watershed 2
Figure 1.2: Western Lake Erie bloom severity index from 2002-2022. 4
Figure 2.1: P surplus and its components. 16
Figure 2.2: Maps of the major components for the agricultural phosphorus mass balance 20
Figure 2.3: Basin-scale phosphorus (P) inputs (fertilizer, atmospheric deposition, manure and domestic P) and outputs (crop P export) across the Lake Erie Basin in (a) USA and (b) Canada..... 21
Figure 2.4: Relationship between percent change in P export vs percent change in P surplus..... 23
Figure 2.5: Legacy P accumulation in kg P per hectare of watershed area for the 57 watersheds of the Lake Erie Basin during the 87-year period (1930-2016). 24
Figure 2.6: Relationship between legacy P and agricultural phosphorus inputs..... 25
Figure 3.1: Conceptual diagram for ELEMeNT-P model for estimating catchment-scale P loads based on both legacy P and inputs from the current year (Van Meter et al., 2021). 32
Figure 3.2: Spatial distribution of 45 stations across the Lake Erie basin 37
Figure 3.3:Land use of Lake Erie Basin. a) Spatial distribution of agricultural areas and urban area in 2016. b) trajectories of crops, pasture and population density..... 44
Figure 3.4: Model performance for 45 studied Lake Erie watersheds. a 49
Figure 3.5: Modeled and measured loading at the watershed outlet from 1920 to 2016.. 51
Figure 3.6: Phosphorus accumulation trajectory (kilogram per hectare) in the landscape compartments for two major watersheds in the Lake Erie basin.. 53
Figure 3.7: Fate of applied P since 1900. [panel a-d] Trajectories of P Flux and P stores in different land compartments for four major watersheds in the Lake Erie basin..... 55
Figure 3.8: Change in P load (2018 -2045) for Maumee River Watershed at Waterville, Ohio, under six simulated future scenarios..... 59
Figure 3.9: Change in P load (2018 -2045) for Grand River Watershed at York, Ontario, under six simulated future scenarios..... 60
Figure 4.1: The data source and workflow for creating the gridded Pan-Canada dataset..... 80
Figure 4.2: County scale maps for P surplus and its components: (a-b) fertilizer P, (c-d) manure P, (e-f) domestic P waste, (g-h) crop P uptake and (i-j) total P surplus all in kg-P ha^{-1} yr^{-1} 84
Figure 4.3: Phosphorus mass balance and its components for Canadian provinces. 87
Figure 4.4: P accumulation in Canada from 1961-2021. 88
Figure 4.5: Relationship between Cumulative agricultural P surplus from 1961 to 2021 and PUE.... 90
Figure 4.6: (a-j) Trajectories of PUE and percentage of cropland; (k-t) trajectories of PUE compared with the agricultural P surplus components (fertilizer, manure and crop uptake) for ten provinces of Canada. 92
Figure 4.7: Cumulative agricultural phosphorus surplus and PUE are shown for the years 1981 (a, b) and 2021 (c, d).. 94
Figure 4.8: Comparison of agricultural phosphorus surplus components across major Canadian provinces using datasets from Pan Canada, IPNI (2014), and Wang (2022).. 96
Figure 4.9: Relationship between county-scale phosphorus estimates of Pan Canada P mass balance components and gridded phosphorus estimates, re-aggregated to the county scale. 98
Figure S1.1: Studied 57 watersheds across the Lake Erie basin 142
Figure S2.1 ELEMeNT-P modelling framework (Van Meter et al., 2021) 147

Figure S2.2: Modeled and measured loading at the outlet of 45 studied Lake Erie watersheds from 1920 to 2016. 148
Figure S2.3: Trend of total P surplus and its component from 1901 to 2016 for 45 sub-watersheds in the Lake Erie basin. 149
Figure S2.4: P accumulation trajectories in different land compartments for 45 watersheds in the Lake Erie basin. 150
Figure S2.5: Relationship between percentage of tiled area and modeled travel time for studied sub-watersheds of Lake Erie basin. 151
Figure S2.6: Ranges of 16 calibrated parameters across 45 watersheds of the Lake Erie basin. described in 152
Figure S2.7: Model performance-KGE..... 153
Figure S2.8: Model performance-p-Bias 154
Figure S3.1: Maps of the major components for the agricultural phosphorus mass balance..... 165

List of Tables

Table 3.1:List of all studied sub-watersheds 37
Table 4.1: Table for Canadian mass balance studies at different spatial and temporal scales 65
Table 4.2: Data summary for components of Pan-Canada P mass balance 67
Table S1.1:P excretion rate from manure of different animal 131
Table S1.2: Harmonized field crop categories and their P content 134
Table S1.3: P content in Pasture 137
Table S1.4: Description of the Stations used in this study 139
Table S2.1: List of model performance parameters 154
Table S2.2: Change in P load from 2018 to 2045 under six different future scenarios. 156
Table S2.3: Description of the calibration parameters with their mean value 157
Table S3.1: Livestock phosphorus excretion parameters ($p_(_{lvstk,excr})$) for 2008. 159
Table S3.2: Normalized livestock weights (1961-2021)…….…… …159
Table S3.3: Data for calculating P from laundry and dish detergent use for census years …….…….....162
Table S3.4: P content and fraction dry crop matter for all crop types…….……163
Table S3.5: Livestock Phosphorus consumption parameters by livestock category for 2018……..164
Table S3.6: Confinement factor for each province. …….…….....164
Table S3.7: Investigation report for mismatched county IDs…….…..…....166

Chapter 1

Introduction

1.1 Introduction

Harmful algal blooms (HABs) pose a persistent and significant challenge to numerous freshwater ecosystems worldwide (Stephen R. Carpenter, 2005; Paerl et al., 2018; A. Sharpley et al., 2000). The underlying cause of this issue can be attributed to the enrichment of nutrients in water bodies, primarily resulting from intensified human activities (S. R. Carpenter et al., 1998.; Nwankwegu et al., 2019; Peters et al., 2000). Among these nutrients, nitrogen (N) and phosphorus (P) are the two limiting nutrients in freshwater ecosystems, entering water bodies through various sources such as agricultural runoff, wastewater treatment plant discharge, and groundwater leaching (Basu et al., 2022; Boyer et al., 2002; Han et al., 2012; P. Kleinman et al., 2011). This nutrient enrichment, termed eutrophication, stimulates the growth of algae and aquatic plants, leading to the development of hypoxic zones in both inland and coastal waters (Diaz et al., 2009). Consequently, the impact of eutrophication extends to the well-being of humans and aquatic organisms, recreational opportunities, and local economies (S. R. Carpenter et al., 1998; Manning et al., 2019; Michalak et al., 2013). Countless resources have been allocated globally to mitigate the costs associated with eutrophication-induced damages (Dodds et al., 2009; Pretty et al., 2003).

Numerous lakes, rivers, and coastal areas worldwide, such as Lake Erie and Chesapeake Bay in the USA, the Baltic Sea in Europe, the Yangtze River in China, and Lake Victoria in Africa, bear the brunt of eutrophication adverse effects (International Lake Environment Committee, 1993). While both N and P contribute to eutrophication, nitrogen tends to be more prevalent in coastal regions, while phosphorus predominates in freshwater systems (Fouzia, 2019; McDowell et al., 2001; Paerl, 2009; A. N. Sharpley, 1995). In this thesis, our focus centers on P pollution and its environmental impact.

1.1.1 Phosphorus Pollution Scenario in the Lake Erie Basin and Beyond

1.1.1.1 Lake Erie Basin: General Description and Land Use

Lake Erie, the fourth-largest of the Great Lakes, spans 78100 square kilometres, has a volume of approximately 119 cubic miles and is positioned between Lake Huron and Lake Ontario (Great Lake Information Network. 2012; Division of Geological Survey, 2013; Lake Erie Lakewide Action and Management Plan 2002); Andrews, 2019). It stands out as the warmest and shallowest among the Great Lakes, with an average depth of about 62 feet (Lake Erie Lakewide Action and Management Plan, 2002; Andrews, 2019). However, the basin is also the most stressed and altered among the Great Lake basins, despite being a vital resource that supports a population of approximately twelve million people, including seventeen metropolitan areas with over 50,000 residents (U.S. Action Plan for Lake Erie, 2018).



Figure 1.1: Lake Erie watershed

The drainage basin of Lake Erie spans parts of Indiana, Michigan, Ohio, Pennsylvania, New York, and Ontario. This extensive basin is fed by significant tributaries, including the Maumee, Sandusky, Cuyahoga, Raisin, and Huron Rivers in the United States, as well as the Thames (via

Lake St. Clair) and Grand Rivers in Canada. Approximately 19.3 billion litres (~5 billion gallons) of water flow into Lake Erie each hour from Lake Huron through the St. Clair and Detroit Rivers, which accounts for about 80% of its average total inflows (Scavia et al., 2019). Precipitation contributes 11% of the total inflow, while the remaining 9% comes from runoff in the watershed, including tributary flows (Lake Erie LAMP (2019-2023), 2019).

Since the 1960s, Lake Erie has faced a persistent issue with phosphorus pollution due to abundant runoff from human-impacted watersheds (Han et al., 2012; Michalak et al., 2013; Rosa et al., 1987). This runoff, stemming from agricultural, industrial, and urban development, has significantly increased phosphorus levels, leading to a deterioration in the lake's water quality. The issue of phosphorus pollution, however, has deeper historical roots tied to historical changes in agricultural practices.

After World War II, the increased use of phosphorus (P) fertilizer became a concern for shallow lakes in North America (Cordell et al., 2009). This situation was further exacerbated by the growing use of phosphorus in laundry and dishwashing detergents, which led to an excess of phosphorus in water bodies during the 1960s and 1970s (GLWQ report, 2018). While efforts to manage point source phosphorus pollution initially controlled harmful algal blooms (HABs) in Lake Erie, by 2010, these blooms resurged, and hypoxic events became frequent occurrences during summers. These environmental stressors were severe enough to cause massive fish die-offs in 2012 and even led to the shutdown of the drinking water system in Ohio in 2014 (Bukhari et al., 2015; Rao et al., 2014), illustrating the ongoing and evolving challenge of managing phosphorus pollution in Lake Erie.

1.1.1.2 Mitigating Phosphorus Pollution in Lake Erie: A Historical Perspective

During the late 1970s and early 1980s, Lake Erie faced a significant surge in phosphorus load, primarily driven by point sources (70%) (Lake Erie Ecosystem Priority, 2019). In response, Canada and the USA signed the inaugural Great Lakes Water Quality Agreement (GLWQA) in 1972. This landmark agreement aimed to enhance wastewater treatment and eliminate phosphorus from detergents through federal regulations (Sweeney, 1974). As a result, point source pollution decreased, and harmful algal blooms remained absent from Lake Erie between 1980 and the mid-

1990s. However, recent years have seen a resurgence in blooms, with the five worst occurrences recorded since 2011 (Kane et al., 2014; Wilson et al., 2019).

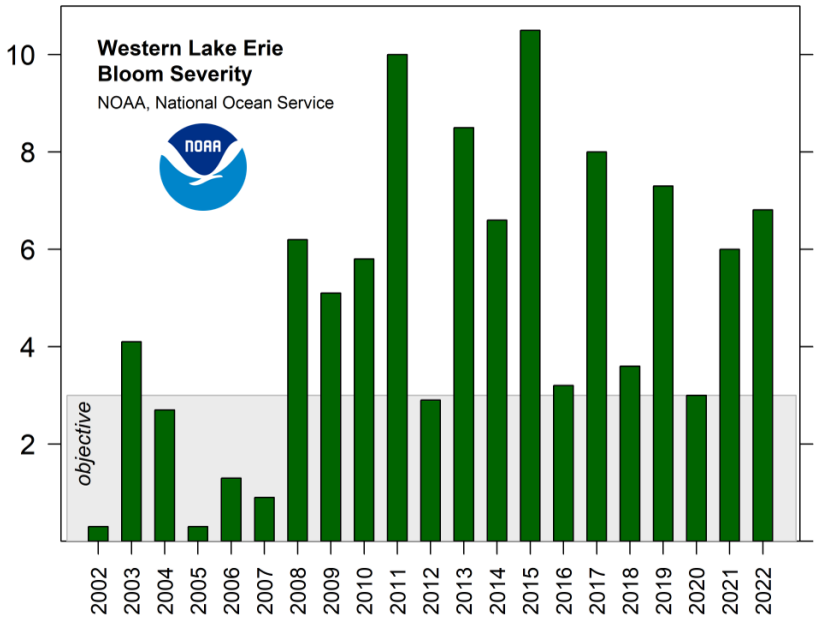


Figure 1.2: Western Lake Erie bloom severity index from 2002-2022. A severity index below 4 is considered mild and above 4 indicates a potentially harmful bloom. (NOAA, 2022).

To address the recurring eutrophication issue, the United States and Canada established binational priorities for science and action under the GLWQA to protect the waters of the Great Lakes. Recommendations were made to reduce P loading from the Maumee River and Western Basin tributaries by 40% (Kalcic et al., 2019; Reg, 2015). The target was to achieve 860 metric tons or less of total phosphorus (TP) and 186 metric tons or less of dissolved reactive phosphorus (DRP), corresponding to flow-weighted mean concentrations (FWMC) of 0.23 mg/L and 0.05 mg/L, respectively for Maumee River (Lake Erie Ecosystem Priority 2019.; Wilson et al., 2019) et al., 2019). The International Joint Commission also endorsed maintaining dissolved oxygen concentrations in the central basin above 2.0 mg/L and TP load below 6000 metric tons (MTA) (Lake Erie Ecosystem Priority 2019.; Wilson et al., 2019). The US and Canadian Governments approved these recommendations in 2016, with a collaborative agreement between Ohio, Michigan, and Ontario to achieve a 40% reduction by 2025 and an aspirational goal of a 20% reduction by 2020 (Wilson et al., 2019). In response to recommendations for reducing phosphorus

(P) levels, various strategies have been adopted to address contributions from both agricultural and municipal sources while restoring watersheds (U.S. Action Plan for Lake Erie, 2018). These strategies include reducing fertilizer use, managing land use practices such as tillage and tile drainage, implementing the 4R Nutrient Stewardship strategy, optimizing wastewater infrastructure, promoting Low Impact Development (LID) and green infrastructure, and restoring natural hydrology and ecological buffers to intercept nutrient runoff **(**U.S. Action Plan for Lake Erie, 2018).

In response to recommendations for reducing P levels, various strategies have been adopted to address contributions from both agricultural and municipal sources while restoring watersheds (U.S. Action Plan for Lake Erie: Commitments and Strategy for Phosphorus Reduction 2018). These strategies include reducing fertilizer use, managing land use practices such as tillage and tile drainage, implementing the 4R Nutrient Stewardship strategy, optimizing wastewater infrastructure, promoting Low Impact Development (LID) and green infrastructure, and restoring natural hydrology and ecological buffers to intercept nutrient runoff **(**U.S. Action Plan for Lake Erie, 2018).

To assess progress towards reducing P load and combatting harmful algal blooms in Lake Erie, monitoring programs and modeling have been developed and put into action (LAMP 2022, 2023). The 2022 Lake Erie Lakewide Action and Management Plan Annual Report indicates that the total phosphorus (TP) load to the western and central basins was 6,464 metric tons annually, exceeding the desired target of 6,000 metric tons. Additionally, the spring (March-July) load from the Maumee River in 2022 was 273 metric tons of dissolved reactive phosphorus (DRP), higher than the target of 186 metric tons annually. The report highlighted that the desired loading targets have yet to be achieved, indicating the need for further research and concerted efforts to address this ongoing challenge.

1.1.1.3 Harmful Algal Blooms in North America and its Response

While much attention is directed towards the issue of harmful algal blooms (HABs) in Lake Erie, it's worth noting that these occurrences extend beyond this region, manifesting in various shorelines across North America. Instances of such blooms are well-documented, spanning locations such as Muskegon Bay and Green Bay in Lake Michigan, Saginaw Bay and Georgian

Bay in Lake Huron, Hamilton Harbor, Chesapeake Bay, Oswego Harbor, Pinto Lake, Lake Okeechobee, the West Coast of the USA from California to Alaska, and the Bay of Quinte in Lake Ontario (Environment and Climate Change Canada and Ontario Ministry of the Environment and Climate Change, 2018; Environment and Climate Change Canada, 2021, U.S. Environmental Protection Agency, 2017).

Reports of HABs have surfaced across all U.S. coastal states and the surrounding Great Lakes area, with their frequency and intensity steadily increasing (US Department of Commerce et al., 2018). These issues aren't confined solely to the United States, as Canada shares similar concerns. In fact, between 2005 and 2007, over one-third of water quality monitoring sites in Canada exceeded established guidelines, highlighting the significant challenge of nutrient enrichment in surface waters (EC, 2010).

While current studies focus on addressing recent harmful algal bloom (HAB) events, Canada has a longstanding history of HABs dating back to the 1970s (Pick, 2016). Notable lakes such as Champlain, Ontario, Erie, St. Lawrence River, the Lake of the Woods (LOW), and Lake Winnipeg have all witnessed extensive blooms since 1970s. A comprehensive study detected the cyanobacterial toxin microcystin in 246 water bodies across Canada, underscoring the widespread nature of the issue (Orihel et al., 2012). Additional alarming events have emerged, such as Lake Winnipeg being deemed the world's most threatened lake due to recurring eutrophication in 2013 (Ali et al., 2019), a significant surge in eutrophication and hypoxia in the St. Lawrence sub-basin (Altieri et al., 2015; Glibert et al., 2014; Goyette et al., 2016), concerns over Quinton Bay in Lake Ontario, and the Georgian Bay (Favot et al., 2023; Nicholls et al., 2011; Watson et al., 2008), as well as the Strait of Georgia in British Columbia (Esenkulova et al., 2021), all of which have cast a shadow over Canadian water quality. Noteworthy regions in the USA, including Chesapeake Bay, declared 'impaired' by the U.S. Environmental Protection Agency (Chesapeake Progress, retrieved on 2023), and Lake Okeechobee, where a striking 95 percent of the lake's surface was covered by an algal bloom in 2018 (Schaefer et al. 2020), also underscore the severity of the issue.

Efforts to address the challenge of HABs have been ongoing since the early 1970s, with various policies and strategies implemented in North America. These initiatives encompass the Clean Water Act and the Great Lakes Water Quality Agreement of 1972, the Canada-Wide Strategy for

the Management of Municipal Wastewater Effluent, the Agricultural Policy Framework (APF), and the 4R nutrient Stewardship Program, among others. Despite these efforts, the persistence of frequent and severe blooms throughout North America remains a challenging reality.

1.2 Fate and Transport of Phosphorus

Phosphorus is an essential element for biological functions and cycles through the environment via natural processes (Filippelli, 2008). It is primarily derived from the weathering and erosion of rocks, existing in both soluble and insoluble forms (M. Chen et al., 2008; Y. Liu et al., 2008). In soil, P can be found in organic and inorganic forms, with organic P being mineralized by soil microbes into inorganic forms. P can be taken up by plants or transported out of the system by water (A. N. Sharpley, 1995). Runoff, especially after heavy rainfall, is a critical pathway for the movement of P, particularly in areas with high supply and transport potential (Daniel et al., 1994; P. Kleinman et al., 2011).

Over-application of P fertilizers and manure in agricultural soils impacted the global P cycle, leading to water pollution (A. N. Sharpley, 1995). These P inputs can accumulate in the soil and transport to surface water even after the input has stopped (Bennett et al., 2001; Philip M. Haygarth et al., 1999; P. M. Haygarth et al., 2005; P. Kleinman et al., 2011). Tile drains in agricultural fields also contribute to P transport to surface water (Daniel et al., 1994; Holman et al., 2008; King et al., 2015; P. Kleinman et al., 2011; Macrae et al., 2007; Smith et al., 2015; P. J. Withers et al., 2001). The loss of P through tile drains in the subsurface is particularly concerning due to its contribution to water pollution in agricultural landscapes (Andersson et al., 2013; Philip M. Haygarth et al., 1999).

1.2.1 Legacy Phosphorus and Time Lags

Decades of intensive application of P in the landscape resulted in a buildup of P in our landscape, such as, in soils, groundwater, sediment, and wetlands (Jarvie et al., 2014; Muenich et al., 2016; K. J. Van Meter et al., 2021; P. J. A. Withers, Sylvester-Bradley, et al., 2014). These pools are often referred to as legacy P and they can be released slowly from the field, and continue to cause water pollution decades after cessation of P input (Bennett et al., 2001; Philip M. Haygarth et al., 1999; P. M. Haygarth et al., 2005; P. Kleinman et al., 2011). The legacy pool can result in significant delays between the implementation of management measures and the desired

improvement in water quality, which is commonly referred to as time lags or legacy effects (Chang et al., 2021; Fenton et al., 2011; Hamilton, 2012; Philip M. Haygarth et al., 2014; J. Liu et al., 2021; Meals et al., 2010; Kimberly J. Van Meter et al., 2015; K. J. Van Meter et al., 2017; Vero et al., 2018)

Time lags at the watershed level can be categorized into two distinct types: hydrologic and biogeochemical time lags (Basu et al., 2010, 2011; Thompson et al., 2011; K. J. Van Meter et al., 2016, 2017; Worrall et al., 2012). Hydrologic time lag refers to the duration it takes for nutrients and contaminants to travel from their sources to receptor areas through hydrological pathways (K. J. Van Meter et al., 2016). The hydrologic time lags are influenced by soil type, climatic conditions, and bedrock geology. Conversely, biogeochemical time lag arises from sorption reactions that solute undergo in the landscape, resulting in their accumulation in a sorbed form (Hamilton, 2012; Kimberly J. Van Meter et al., 2015; K. J. Van Meter et al., 2016, 2017; Worrall et al., 2015). Various mechanisms contribute to the occurrence of both time lags, ranging from temporary nutrient storage in soil or vegetation (Loecke et al., 2017; K. J. Van Meter et al., 2017) to protracted hydrologic transport times through the subsurface and nutrient retention in stream sediments and surface water reservoirs (K. J. Van Meter et al., 2016, 2017, 2021).

1.3 Quantifying Phosphorus Inputs and Modeling Legacies- Gaps and Capabilities

Researchers have frequently used phosphorus mass balance to quantify phosphorus inputs into landscapes. These studies estimate phosphorus surplus for different regions and timeframes as the difference between phosphorus inputs (fertilizer, manure, domestic waste) and outputs (crop harvest) (Baker et al., 2002; Goyette et al., 2016; Han et al., 2012; MacDonald et al., 2009; Powers et al., 2016; Russell et al., 2008; Sabo et al., 2021; Sattari et al., 2012; K. J. Van Meter et al., 2021; Van Staden et al., 2022; Wang et al., 2022). Some of these studies address legacy phosphorus accumulation (Powers et al., 2016; Reid et al., 2019; Sabo et al., 2021; K. J. Van Meter et al., 2021; Van Staden et al., 2022). For instance, Powers et al., (2016) examined legacy phosphorus in Ohio's Maumee River, a Lake Erie tributary. MacDonald et al., (2009) reported legacy phosphorus accumulation in the St. Lawrence River basin due to increased fertilizer use. Van Staden et al., (2022) analyzed soil phosphorus accumulation from 1961 to 2016 in Ontario, Canada. Despite these contributions, most studies do not account for riverine phosphorus export and legacy

accumulation, limiting insights into the transformation and transportation of phosphorus surplus to rivers and its downstream effects. Some short-term studies report a wide range of 5-30% of phosphorus surplus being exported to rivers (Boardman et al., 2019; Han et al., 2012; Russell et al., 2008; Sabo et al., 2021), which makes it an important component for estimating phosphorus input to the landscape. Research linking phosphorus mass balance to riverine phosphorus export is particularly limited in the Lake Erie Basin (Han et al., 2011, 2012; Powers et al., 2016; Scavia et al., 2019; K. J. Van Meter et al., 2021). These studies, while insightful, are often limited in temporal scope and geographical coverage. Our study addresses the need for comprehensive long-term phosphorus mass balance research that quantifies legacy phosphorus contributions to waters across the transboundary Great Lakes and beyond.

Quantifying the magnitude and dynamics of legacy phosphorus, which accumulates in the landscape over decades, remains a considerable challenge (Lintern et al., 2020; Meals et al., 2010; A. Sharpley et al., 2013; P. J. A. Withers, Neal, et al., 2014). Legacy phosphorus continues to contribute to phosphorus loads in water bodies, complicating efforts to meet reduction targets (P. J. A. Kleinman et al., 2019; McCrackin et al., 2018; Mississippi River/Gulf of Mexico Watershed Nutrient Task Force. Monitoring et al., 2004; Muenich et al., 2016; Powers et al., 2016; Stackpoole et al., 2019). Various modelling techniques, such as GWLF, SPARROW, GlobalNEWS, PolFlow, SWAT, INCA, DPPS, AGNPS, and ANSWERS, have been used to quantify legacy phosphorus. While these models can estimate total phosphorus accumulation within a watershed, they are often limited in quantifying legacy phosphorus across different landscapes like soils, reservoirs, and landfills, and they frequently lack the long-term perspective or mechanistic approach necessary to fully understand and manage these legacy effects (A. B. Bottcher et al., 2012; D. Chen et al., 2018; H. Chen et al., 2023; Condron et al., 2013; Harrison et al., 2019; Hwang et al., 2006; Jarvie et al., 2012; Khare et al., 2021; Martin JL, 2013; Motew et al., 2017; Muenich et al., 2016; Schippers et al., 2006; Zhang et al., 2020). For example, (Muenich et al., 2016) employed the SWAT model to simulate the impact of legacy phosphorus in the western Lake Erie watershed. (Schippers et al., 2006) developed a two-compartment model to estimate phosphorus time lags in soil, but these models did not consider the gradual buildup of legacy phosphorus over extended periods. To address these gaps, we developed the Exploration of Long-tErM Nutrient Trajectories-Phosphorus (ELEMeNT-P) model. This novel mechanistic model utilizes long-term data to explore

phosphorus accumulation and depletion within watersheds and assess the contribution of legacies to riverine phosphorus loads (K. J. Van Meter et al., 2021). By applying ELEMeNT-P to the Lake Erie Basin, we can simulate long-term phosphorus dynamics and develop scenarios to evaluate potential reductions in phosphorus loads, aligned with current policy recommendations.

Our analysis begins by examining historical and current phosphorus pollution in the Lake Erie Basin. Moving beyond basin-scale analysis, we have developed a comprehensive phosphorus mass balance dataset at a pan-Canadian scale. This dataset aggregates county-level data from various sources, despite numerous studies conducted at multiple spatial and temporal scales, ranging from provincial to basin-wide assessments (Bittman et al., 2023; Bruulsema et al., 2011; IPNI, 2014; Reid et al., 2019; Wang et al., 2022; Minpeng Chen et al., 2016; MacDonald et al., 2011; Mekonnen et al., 2018), there is still a significant lack of high-resolution and consistent data for the entire country. These gaps hinder our ability to study small watersheds and implement precise and effective management practices. In response to these challenges, we have created a long-term estimate (1961-2021) of the phosphorus budget. It includes inputs from fertilizers, livestock manure, domestic waste, and phosphorus uptake by crops and pasturelands. Our high-resolution estimates cover both county-scale and 250-meter grid scales, significantly enhancing our understanding of spatial distribution and legacy phosphorus accumulation.

1.4 Research Objectives

The primary goal of this research is to understand phosphorus dynamics by quantifying phosphorus input and legacy accumulation in the landscapes. A key aspect of this study is investigating the impact of legacy phosphorus stores on the time lag between changes in the landscape and the subsequent response in streams. To achieve this, I have outlined three sub-objectives:

> **Objective 1:** Quantify long-term phosphorus inputs, stream phosphorus loads and legacy phosphorus patterns across the transboundary Lake Erie basin.
>
> **Objective 2**: Use the ELEMeNT-P model to quantify legacy stores in various landscape reservoirs and analyze the effect of legacy P on current and future water quality.

Objective 3: Develop a comprehensive phosphorus mass balance dataset at a pan-Canadian scale to provide a long-term (1961-2021) estimate of the phosphorus budget at both county and 250-meter grid scales.

Chapter 2

Estimation of Legacy Phosphorus and its Drivers across the Lake Erie Basin

2.1 Introduction

Over the last century, human activities have significantly disrupted the global phosphorus (P) cycle (Bennett et al., 2001; Cordell et al., 2009; Goyette et al., 2016). The intensification of agriculture and urbanization has led to an increase in P-rich runoff from farm fields to downstream waters (Powers et al., 2016; Sharpley et al., 2013; Smith et al., 2009), fueling eutrophication (Carpenter, 2005; Dodds et al., 2009; Withers et al., 2014). This has led to a cascade of detrimental effects including algal blooms, hypoxic zones, fish kills, and loss of biodiversity (Bonsdorff, 2021; Conley et al., 2009; Diaz et al., 2009; Goyette et al., 2016; Vitousek et al., 1997). To address this issue, regulatory agencies worldwide have implemented phosphorus management strategies, including reducing fertilizer and manure applications, minimizing erosion during high flows, and reducing phosphorus in wastewater (Bindraban et al., 2020; Bruulsema, 2022; Kleinman, Sharpley, et al., 2015; Liu et al., 2018; Schindler et al., 2016). Despite decades of intensive management efforts, eutrophication persists and has recently worsened in many lakes and water bodies (Meals et al., 2010; Zhang et al., 2020). This ongoing issue has been partly attributed to the legacy phosphorus accumulated in the landscape over the years (Carleton et al., 2023; Condron et al., 2013; Jarvie et al., 2013; Kleinman, Smith, et al., 2015; Muenich et al., 2016; Sharpley et al., 2013; Van Meter et al., 2021a; T. L. Van Staden et al., 2022; Wironen et al., 2018).

Studies have quantified legacy phosphorus across spatiotemporal scales by analyzing the difference between phosphorus inputs (fertilizer, manure, and domestic waste) and P outputs (crop uptake) (Baker et al., 2002; Goyette et al., 2016; Han et al., 2011, 2012; Powers et al., 2016; Russell et al., 2008; Sabo et al., 2021; Sattari et al., 2012; Van Meter et al., 2021a). For example, Powers et al., (2016) estimated a legacy P rate of about 13 kg-ha^{-1}yr^{-1} (Maumee, US), 9.4 kg-ha^{-1}yr^{-1} (Thames, UK) and 8.2 kg-ha^{-1}yr^{-1} (Yangtze, China) in the last four decades. MacDonald et al., (2009) reported legacy P of 8.1 kg-ha^{-1}yr^{-1} over a century (1901-2001) in the St. Lawrence River basin (US and Canada). Hong et al., (2012) modelled legacy and found 44 Mton phosphorus accumulation in the Baltic Sea drainage basin in Europe. Recently, Van Staden et al., (2022) computed phosphorus accumulation ranging from 0 to over 850 kg-ha^{-1} between 1961 and 2016 at

the county scale for Ontario, Canada. Similarly, Sabo et al., (2021) demonstrated that more than 100 kg-ha^{-1} of phosphorus accumulated in central and western USA from 1945 to 2001. These studies highlight the heterogeneity in phosphorus accumulation based on its inputs and outputs across agricultural watersheds worldwide. However, it is important to note that only a subset of such legacy studies account for the hydrologic P output in addition to P inputs and output (Baker et al., 2002; Bennett et al., 1999; Goyette et al., 2016; Han et al., 2012; Hong et al., 2012; Hu et al., 2020; Maccoux et al., 2016; Meng et al., 2022; Metson et al., 2017; Russell et al., 2008).

Although short-term, some legacy studies document the export of 5-10% of P accumulation to rivers downstream (Han et al., 2011; Hu et al., 2020; Russell et al., 2008). Boardman et al., (2019) found that 17% of P accumulation can be exported to rivers, while a few watersheds exported more than 30% of P stores to rivers at a regional scale in MN (USA). As a result, our understanding of the fraction of legacy phosphorus exported as riverine phosphorus and its influence on downstream waters remains limited. Moreover, some legacy phosphorus studies that link phosphorus mass balance to riverine phosphorus export, only a limited amount of work focuses on the Great Lakes region. (Han et al., 2011, 2012; T. L. Van Staden et al., 2022). Understanding the magnitude of accumulated phosphorus leaving via streams at a regional scale is especially critical in the Lake Erie basin, where efforts are being made to reduce total phosphorus by 40% under the Great Lakes Water Quality Agreement (Environment et al., 2020; Farley, 2023; Team, 2015; Wilson et al., 2019). Despite these efforts, progress is slow, and past work on the topic has been limited to a few watersheds. For the Maumee River, USA, a tributary to Lake Erie, Powers et al., (2016) showed that phosphorus accumulation in soils exceeded river export from 1975 to 1995, whereas the opposite trend was observed from 1995 to 2010. Recently, a study estimates that 12% of the accumulated P can contribute to Lake Erie based on the approximate discharge and riverine P values for a few Canadian watersheds that drain into Lake Erie (Maccoux et al., 2016; T. L. Van Staden et al., 2022). These studies provide insightful but short-term (<40 years) perspectives, focusing on a single watershed that contributes to Lake Erie, without explicitly estimating riverine P exports for their study watersheds. To date, no study has quantified the contribution of legacy P to receiving waters over the long term across the transboundary Lake Erie basin (US and Canada).

This study provides the first comprehensive inventory of phosphorus (P) inputs and outputs throughout the 20th century (1930-2016) across the transboundary Lake Erie basin. By coupling

accumulated phosphorus with riverine phosphorus exports for a diverse set of watersheds (n=57) that drain into Lake Erie, this research addresses several key questions: How have phosphorus inputs and outputs evolved in agricultural landscapes over the past century across the transboundary Lake Erie basin? How do legacy phosphorus estimates vary spatially across the Lake Erie basin? What fraction of legacy phosphorus leaves as riverine export from these watersheds? These questions aim to enhance our understanding of phosphorus dynamics and inform effective management strategies for the region.

2.2 Materials and Methods

2.2.1 Phosphorus Mass Balance across Lake Erie Basin

The components of the P mass balance were calculated for the period 1930–2016 at the county and watershed scales across the Lake Erie Basin. The P surplus was quantified as the difference between P inputs (P fertilizers, livestock manure, household and wastewater P, and atmospheric P deposition) and non-hydrological outputs (crop P uptake). The watershed-scale P budget is simply a downscaled version of county-scale P inputs and outputs. The gridded P components were averaged over the delineated boundaries for each watershed.

Phosphorus in Fertilizer

Fertilizer P use datasets at a county scale for the USA and Canada were compiled annually from 1930 to 2016. For the USA, county-scale annual fertilizer P inputs were derived from four sources: i) 1945 to 1985 (Alexander et al., 1990), 1987 to 2012 (USGS, 2020), 2013 to 2017 from the Food and Agriculture Organization of the United Nations (FAO) (Food and Agriculture Organization of the United Nations (FAO), 2022). To the best of our knowledge, no dataset regarding P fertilizer usage during the period 1930-1944 was available. Thus, we employed the USGS Phosphate Rock Statistics to estimate P fertilizer use for this timeframe (USGS, Retrieved on 2019). For Canada, annual P fertilizer inputs were obtained from the provincial fertilizer sales datasets (Government of Canada 2023b). For additional details regarding the development of the P fertilizer use dataset from 1930-2016, see **Appendix A section S1.1**.

Livestock Inputs

Manure P inputs, defined as waste excretion from livestock, were obtained for census years from USDA NASS (United States) and Statistics Canada (Canada). We selected 13 different livestock categories- dairy cattle, beef cattle, heifers, steers, bull, calves, chickens, broilers, turkeys, hogs, sheep, goats and horses, to estimate manure P. Manure P (kg ha^{-1}) was calculated as the product of reported heads of livestock and P content in manure generated per animal for each census year and then normalized by the county area. Further, these manure P values were linearly interpolated between the census years to generate the annual estimates. More details regarding the approach used to estimate manure P can be obtained from **Appendix A section S1.2**.

Domestic P Inputs

Domestic P inputs included P from laundry and dish detergent usage, P associated with human excreta, and P generated from food waste. All four components of domestic P inputs were derived from county-scale population census data from the US (US Census Bureau, 2023) and Canada (Government of Canada et al., 2001)) and a suite of parameters such as annual per capita P from laundry and dishwashing detergent, human P consumption rates. More details on the approach and the selection of parameters have been provided in the supplement (**Appendix A section S1.3**).

P Uptake

Crop and pasture P uptake was calculated using county-scale crop-specific production data from the Agricultural Census obtained from USDA NASS (USA) and Statistic Canada (Canada). We utilized a set of 20 crops and 2 pasture types that were relevant for the counties on each side (Canada and USA) of the LE basin. The harvested area for all crops was largely available for the census years from 1930-2017, and the cropped areas were linearly interpolated between the census years. The approach and the parameters (e.g., P content fraction) used to compute P uptake (kg $ha^{-1}year^{-1}$) are available in the supplementals (**Appendix A section S1.4**).

Atmospheric P Deposition

Atmospheric phosphorus deposition (ATM) originates from sources such as sea salt, dust, biogenic aerosol particles, and emissions from fuel combustion. Atmospheric P deposition is a minor P input component and it was obtained from a global P deposition data set (Wang et al. 2017). The deposition dataset contains P exposition data for 52 different years spanning from 1850-2100 and

it is at 1x1 degree spatial resolution. The global deposition data were clipped with the county boundaries and linearly interpolated in between the modelled years to obtain county-scaled yearly P deposition data in kg $ha^{-1}year^{-1}$.

2.2.1.1 P Surplus

The phosphorus surplus and its components were calculated using a downscaled version of county-scale data for both the USA and Canada, presented on a 250m x 250m grid (see **Appendix A, section S1.5** for details). The downscaled P surplus components included: P fertilizer, manure P, crop and pasture P uptake, and domestic P waste (including detergents, human and food waste).

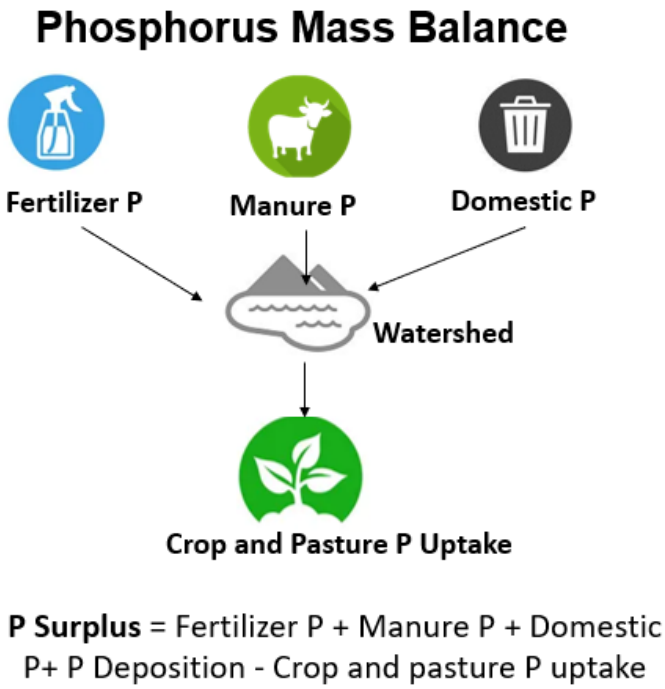


Figure 2.1: P surplus and its components. Atmospheric deposition is not shown in the figure since it contributes to less than 1% of total P input

At the basin scale, the phosphorus surplus is calculated by subtracting phosphorus uptake (crop and pasture) from the total phosphorus input, which includes fertilizers, manure, waste, and deposition. For the watershed scale analysis, phosphorus surplus and its components were determined by clipping the corresponding downscaled phosphorus grid with watershed

boundaries. Given that atmospheric deposition contributes to less than 1% of the total phosphorus input to the Lake Erie basin, we excluded this component from further watershed scale analysis.

2.2.2 Stream Phosphorus Export

We selected 57 sub-watersheds (18 in the US and 39 in Canada), with a minimum of 12 years of data for total phosphorus (TP) concentration and 25 years of discharge data between 1970-2016 (For details on watersheds refer to **Appendix A-Table S4 and Figure S1**). In-stream total phosphorus concentrations were obtained from the Provincial Water Quality Monitoring Network (PWQMN) for Canada and the United States Geological Survey (USGS), National Centre for Water Quality Research (NCWQR) by Heidelberg University, Water Quality eXchange (WQX), and Storage and retrieval Data Warehouse (STORET) databases for the USA. The discharge data corresponding to the TP monitoring stations were retrieved from the Water Survey of Canada and the United States Geological Survey. Further, we used the weighted regression on time, discharge, and season (WRTDS) modeling approach (Hirsch et al., 2010, 2015) to estimate the daily time series of P exports from the sparse concentration and daily flow data. However, for the five select watersheds (Ohio, USA) that have high frequency (daily to sub-daily) TP concentrations and discharge data, we used observed daily exports and not WRTDS simulated P export. We summed the daily loads to compute annual P export for each watershed and each year between 1970-2016.

We found that there were gaps (n=812; 30% of total observations) in annual P export due to missing discharge observations across the study watersheds between 1970-2016. So to fill the gaps in P export, we used a Random Forest model.

Random Forest (RF) is a non-parametric, multivariate regression approach based on supervised learning (Attanasi et al., 2020). The RF uses an ensemble of a large number of decision trees and integrates bootstrap aggregation with randomization to simulate the dependent variable. Overall, the RF approach is robust to overfitting and collinearity and equipped to simulate non-linearity in the relationships between dependent and independent variables. In total, we used seven input variables (Manure P, Fertilizer P, P Surplus, cumulative P Surplus, watershed area, percent of wetland in watershed, and discharge) to develop RF models to simulate P export. There were gaps (n=767, 28%) in observed discharge datasets for the watersheds during 1970-2016. So to fill the gaps, we used a simulated discharge time series available through Terra Climate (Abatzoglou et

al., 2018). After selecting a set of variables, we identified an optimal set of hyperparameters that can maximize the model performance for the given variables. We employed a grid search approach over a range of commonly used values for each parameter and then selected the parameters that returned the maximum R^2. The search grid was developed using the key RF parameters that included- number of trees (500, 1000, 2000, 3000, 4000, 5000), variables to consider at split (1, 2, 3, 4, 5, 6, 7), fraction of sample to replace (0.5, 0.6, 0.7, 0.8), and the number of nodes (1, 2, 3, 5, 7, 9, 10). Overall, the Random Forest model performed well (R^2=0.74, MSE=0.11) from out-of-bag samples with the independent variables used.

2.2.3 Estimation of Legacy Phosphorus

We estimated legacy P as a difference between cumulative phosphorus surplus and stream phosphorus export for each watershed over an 87-year period (1930-2016). Annual phosphorus surplus values were summed for each watershed to obtain cumulative phosphorus surplus during the study period. The annual phosphorus export values simulated from the RF model were summed for each watershed to estimate the total phosphorus export between 1970-2016. However, P export observations were unavailable before 1970. To estimate stream phosphorus export between 1930-1970, we calculated median phosphorus export during the first 10 years (1970-1980) for each watershed times the number of years (40 years). Here, we assume that P export is constant from 1930-1970.

2.3. Results and Discussion

2.3.1 Phosphorus Inputs and Surplus across the Transboundary Lake Erie Basin (1930-2016)

Phosphorus inputs across the transboundary Lake Erie Basin are dominated by fertilizer and manure in agricultural areas, and domestic waste in urban regions near Detroit and Cleveland in the US (**Figure 2.2**). Manure inputs are concentrated in the northern parts of the Lake Erie basin in Canada, while fertilizer inputs are greater in the western Lake Erie Basin in the US. Fertilizer and manure inputs have increased since the 1930s, but so has crop uptake, such that phosphorus surplus magnitudes are currently lower compared to the 1990s **(Figure 2.2s,t**). Indeed, current P surplus magnitudes across the basin range between (-)2.7 - 19.5 kg ha^{-1} yr^{-1} (5 to 95th percentile), with 32% of the area with negative surplus magnitudes and a median surplus of 2.7 kg ha^{-1} yr^{-1}

across the entire basin (**Figure 2.2q-t**). Phosphorus budgets have changed dramatically over the last decade (1930 - 2016), due to agricultural intensification and urbanization (**Figures 2.2 and 2.3**). Fertilizer inputs have increased over 4-fold since the 1930s, from 1.84 kg ha^{-1} yr^{-1} in 1930 to 7.2 kg ha^{-1} yr^{-1} in 2016. Inputs have since then stabilized in the US side of the basin, while there has been a recent increase (~24%) in fertilizer sales in the eastern Lake Erie basin in Canada. Manure P inputs have increased similarly ranging from 0 to 9.71 kg ha^{-1} yr^{-1} in 1930, and 0 to 22.8 kg ha^{-1} yr^{-1} (5 to 95th percentile) in 2016 (**Figure 2.2e,h**). Phosphorus inputs in domestic waste have decreased since the 1970s from 0 - 14.2 kg ha^{-1} yr^{-1} to 0-7.7 kg ha^{-1} yr^{-1} (5 to 95th percentile) in 2016, and this can be attributed to P ban in detergents (Maki et al., 1984; Vallentyne, 1978; Wilson et al., 2019). Crop production is the primary P output pathway from the landscape, with crop P export almost doubling over the last 50 years due to improved crop varieties (**Figure 2.2 and Figure 2.3**). The increase in crop uptake, despite a decrease in inputs, has contributed to a peak in P surplus in both the US and the Canadian sides of the basin in the 1970s, with a steady decline of 6-fold on the US side from 12 to 2.3 kg ha^{-1} yr^{-1}. In contrast, we see a recent (2006 to 2016) increase in P surplus from 2 to 6 kg ha^{-1} yr^{-1} on the Canadian side of the basin due to a rise in fertilizer input (**Figure 2.3**). However, despite the recent increase, the P surplus has decreased by 77% on the US side and 24% on the Canadian side of the Lake Erie Basin. Overall, the P surplus has decreased 65% since the 1970s for the Lake Erie basin with the current 3.4 kg ha^{-1} yr^{-1} (IQR 0.1-4.4). At the basin scale, livestock manure comprises a greater proportion of the inputs on the Canadian budget side compared to the US side (72% of inputs in Canada and 28% in the US) (**Figure 2.3**).

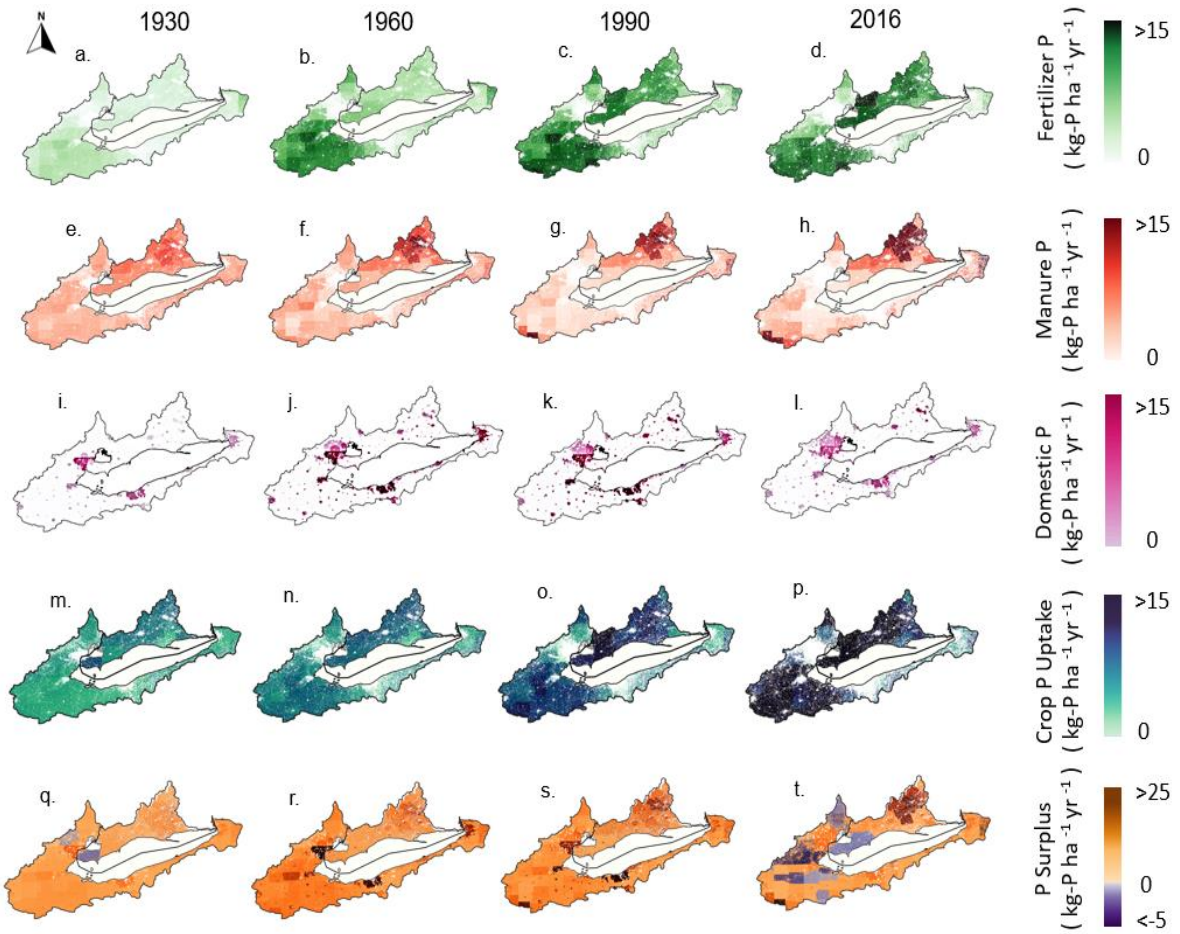


Figure 2.2: Maps of the major components for the agricultural phosphorus mass balance: (a-d) fertilizer P, (e-h) manure P, and (i-l) domestic P, (m-p) crop P uptake, and (q-t) P surplus, all kg ha^{-1} yr^{-1}. Each map is divided showing four time periods to capture the start and the end of the time series, along with two intermediate years.

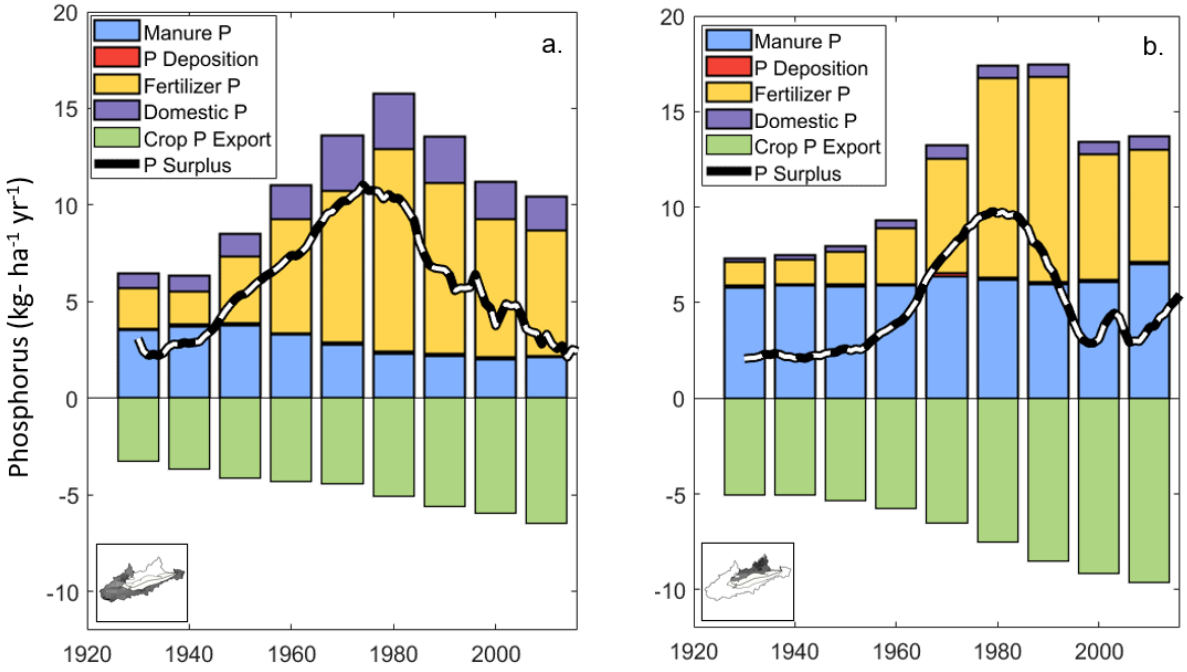


Figure 2.3: Basin-scale phosphorus (P) inputs (fertilizer, atmospheric deposition, manure and domestic P) and outputs (crop P export) across the Lake Erie Basin in (a) USA and (b) Canada. Inputs and outputs are shown as positive and negative values, while the dashed line represents the long-term, basin-scale P surplus. P budget components are presented in kg ha^{-1} yr^{-1} units, with the area representing the basin area on the US (56103 km^2) and the Canadian side (22615 km^2); shown as insets in the figures.

2.3.2 Phosphorus Surplus and Riverine P Loads

The relationships between phosphorus surplus and riverine loads vary across the basin, with some watersheds like the Maumee in the US where phosphorus surplus has significantly decreased over time, to magnitudes that are similar to magnitudes of riverine P loads. In contrast, watersheds like the Grand and Thames in Canada document a more recent increase in P surplus from increasing fertilizer sales in the basin (**Figure 2.4**). In these watersheds, however, P surplus magnitudes are much greater compared to riverine P load, highlighting the potential of more efficient nutrient management practices to improve water quality.

Across all the 57 watersheds we analyzed, the P surplus decreased over the 47-year timeframe (1970 - 2016), with 60% of the watersheds documenting a significant decrease ($p < 0.05$). The median P surplus across these watersheds decreased from 10.8 kg/ha in the 1970s to 5.8 kg/ha in

the current decade. The percentage decrease varied from 0.32% per year to 3.73% per year, with a median decrease of 1.1%. As discussed in the previous section, a large proportion of this decrease can be attributed to improved crop varieties that contributed to a greater yield for the same fertilizer inputs.

In contrast to the P surplus trends, P exports were found to decrease in only 41 of the 57 watersheds, with only 26 of them showing a significant decrease. P exports are increasing in 16 watersheds, with four of them documenting a significant increase. Significant increases in P export occur in Cattaraugus Creek at Gowanda, Huron River at Milan, Mary's River near Fort Wayne, and Auglaize River near Fort Jennings watersheds on the US side of the basin, while decreases are concentrated on the Canadian side. This is interesting given the percent decreases in P surplus are greater on the US side compared to the Canadian side of the basin and might allude to the buildup of past legacies.

Further, we found that even in watersheds where P exports are decreasing, the magnitude of the decrease is much smaller than the decrease in P surplus, ranging from 0.024% to 2% across the 41 watersheds documenting a decrease. The substantially lower decrease in exports compared to decrease in inputs arises likely due to the accumulation of legacy P sources over the decades of application. Indeed, we find that even in watersheds where the P surplus is negative (Rasin River near Monroe in the USA, Ruscom River near Ruscom and Canard River near Lukerville watersheds in Canada), P export magnitudes are still high (0.03- 2 kg ha^{-1} yr^{-1}), highlighting the role of legacy phosphorus in sustaining the riverine P loads in these basins. Thus, reducing riverine P loads requires an understanding of the magnitude of legacy phosphorus that has built up in this landscape.

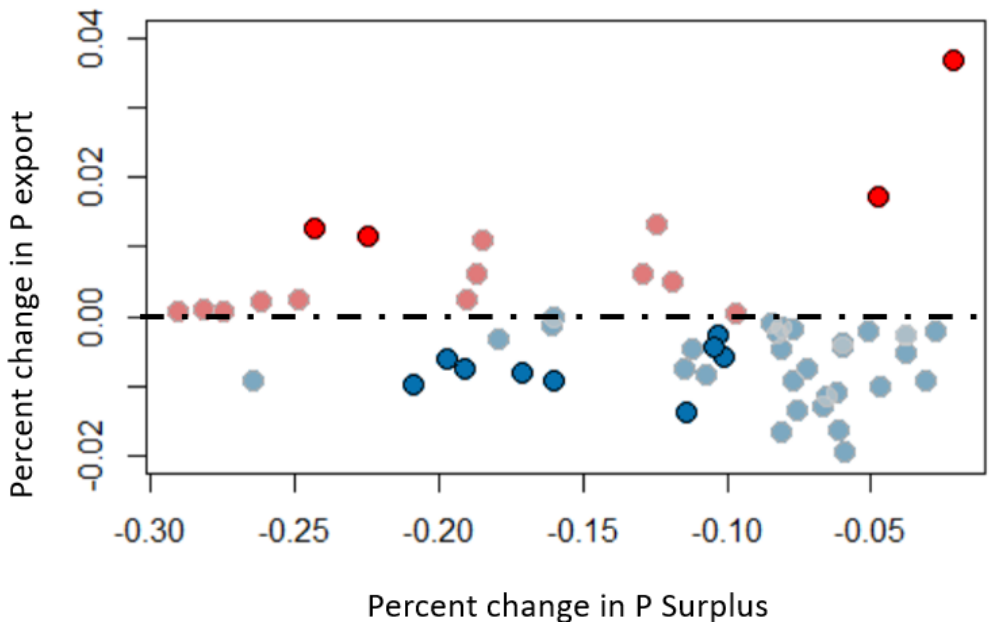


Figure 2.4: Relationship between percent change in P export vs percent change in P surplus. The percent change is calculated by dividing the Sen's slope (1970-2016) by the mean value (1970-1979). Red points indicate an increase in P export, while blue points indicate a decrease in P export. Darker colors represent watersheds with significant changes, and lighter colours represent watersheds with insignificant changes.

2.3.3 Legacy Phosphorus Accumulation across the Lake Erie Basin

The lack of response in phosphorus export despite significant decreases in surplus across the basin arises most likely due to the accumulation of legacy phosphorus that buffers the effects of current management practices. We estimated legacy phosphorus accumulation from 1930s to current by subtracting the cumulative watershed export from the cumulative surplus. We found legacy P accumulation rates to range between 0.7 to 10 kg ha^{-1} yr^{-1} across all 57 watersheds analyzed in our study, with no discernible spatial patterns across the basin (**Figure 2.5**). This is a substantial amount given phosphorus application rates range between 1 to 21.5 kg ha^{-1} yr^{-1}. Over the 86 years of the analysis, this leads to an accumulation of 190 kg ha^{-1} to 935 kg ha^{-1}, with very similar accumulation rates across the major agricultural basins across the US and Canada: 573 kg ha^{-1} for the Grand, 505 kg ha^{-1} Thames in Canada, and 413 kg ha^{-1} for the Maumee watershed in the US.

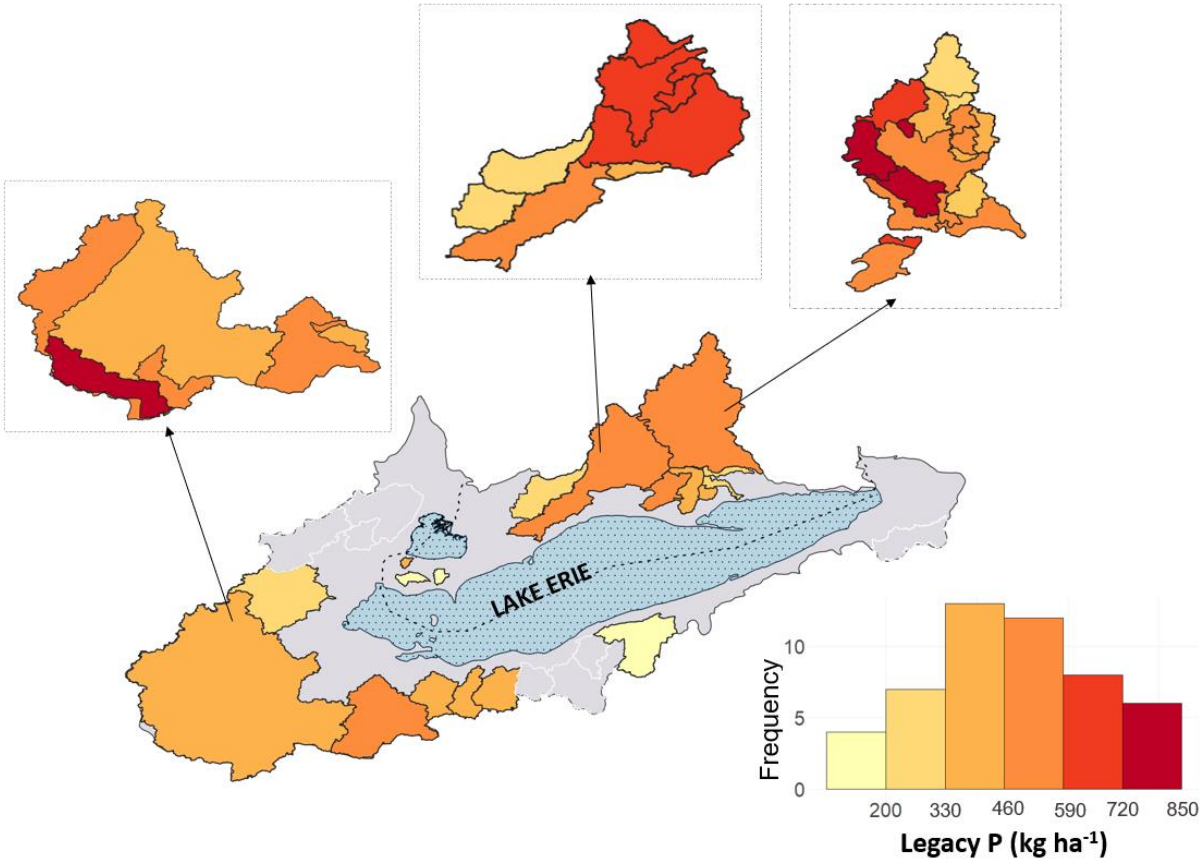


Figure 2.5: Legacy P accumulation in kg P per hectare of watershed area for the 57 watersheds of the Lake Erie Basin during the 87-year period (1930-2016).

Across the 57 watersheds (**Appendix A Table 1.4**) in the basin, we found P export to range between 1.2% to 25% of the cumulative P inputs, while crop uptake ranges between 7% and 66%, such that 5 to 91% of the phosphorus is potentially retained in the landscape as legacy phosphorus.

When normalized to cropland area, our magnitudes are similar to (Reid et al., 2019) reported P accumulation from 3.2 kg ha^{-1} yr^{-1} to more than 19 kg ha^{-1} yr^{-1} during 1981-2011 (31 years) across the province of Ontario (Canada). When compared to the findings of Sabo et al., (2021), our values align closely with their reported legacy phosphorus surplus near the Lake Erie Basin, which ranges from 0.9 to 7 kg ha^{-1} yr^{-1} for the period 1945-2001. For the Maumee River (OH, USA), a tributary to Lake Erie, Powers et al. (2016) documented a legacy phosphorus accumulation rate of 4 kg ha^{-1} yr^{-1} between 1976 and 2010, which is lower than our estimate of 4.9 kg ha^{-1} yr^{-1} for the same watershed. This discrepancy can be attributed to the inclusion of a wider variety of crop categories in our studies, whereas Powers' study focused solely on four major field crops. Additionally, the

study did not account for domestic waste generated from the 11% urban area within the watershed. Our legacy accumulation magnitudes are also consistent with the findings of various studies beyond the Lake Erie basin. For instance, Wironen et al., (2018) reported an accumulation rate of 10 kg ha^{-1} yr^{-1} in Vermont's watersheds from 1925 to 2012. Similarly, Kusmer et al., (2019) observed an accumulation rate of 2.6 kg ha^{-1} yr^{-1} in the St. Lawrence River watersheds between 1901 and 2011. Furthermore, the magnitude of our legacy P accumulation aligns with the results from (McDowell et al., 2020), who found approximately 58-207 kg ha^{-1} of P in the soil in New Zealand. Similarly, Hou et al., (2013) and Li et al., (2011) observed a mean soil phosphorus accumulation of more than 242 kg ha^{-1} in China between 1980-2007. There are two different studies in Western Europe and France both showed an accumulation rate of 18 kg ha^{-1} yr^{-1} which is higher than our highest estimated legacy phosphorus accumulation rate of 10 kg ha^{-1} yr^{-1} (Sattari et al., 2012).

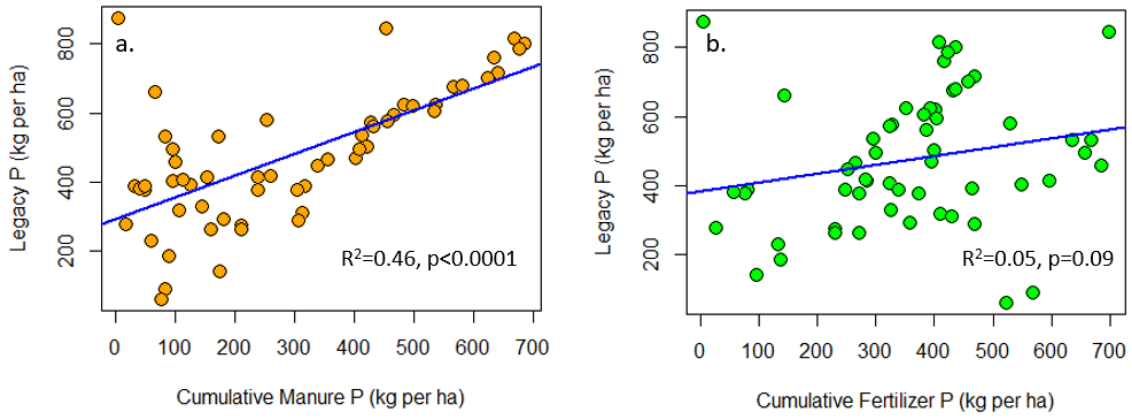


Figure 2.6: Relationship between legacy P and agricultural phosphorus inputs. a) Legacy P vs. cumulative phosphorus from livestock manure, b) Legacy P vs. cumulative phosphorus from fertilizer use. Cumulative phosphorus from manure and fertilizer is calculated using data from 1970-2016. Each point in the figure represents an individual watershed in the basin. The blue line is the linear regression line.

We next explored the drivers of legacy accumulation. We find that the spatial pattern of legacy P is largely explained by the manure P (R^2=0.46; p<0.0001) but not by the fertilizer P (R^2=0.05; p=0.09) inputs to the watershed in the LEB (**Figure 2.6**). These findings indicate that livestock operations are the primary driver of legacy P accumulation.

For example, in two major Canadian watersheds, the Grand and Thames River watersheds, more than 50% of P input is attributed to livestock manure, resulting in a substantial P accumulation of 573 kg ha^{-1} and 505 kg ha^{-1} yr^{-1}, respectively over the past century. Canagagigue Creek near Elmira watershed showed one of the highest legacy accumulations at 815 kg ha^{-1}, with more than 60% of phosphorus input from livestock manure. Conversely, in the USA, the Huron River at Ann Arbor, MI shows only 230 kg ha^{-1} of legacy P, with only 30% of agricultural phosphorus input coming from livestock manure. These findings are corroborated by Reid et al., (2019), who found that hotspots of P accumulation corresponded to areas of high livestock density (e.g., poultry, swine, cows). Similarly, the importance of manure application in driving legacy P accumulation has also been noted in other geographical regions (Bouwman et al., 2013; Glibert, 2020; Wironen et al., 2018). Thus, our study offers crucial insights for developing more targeted and efficient nutrient management practices, indicating that effective phosphorus management strategies must focus on reducing manure P inputs to mitigate the impacts of legacy phosphorus.

2.4. Conclusions

This study presents the first comprehensive inventory of phosphorus inputs and outputs throughout the 20th century (1930-2016) across the transboundary Lake Erie basin. By coupling accumulated phosphorus with riverine phosphorus exports for 57 watersheds, we have addressed key questions regarding the evolution of phosphorus dynamics in agricultural landscapes over the past century. Our analysis reveals significant spatial variability in legacy phosphorus estimates across the basin and highlights the proportion of legacy phosphorus that contributes to riverine export.

The findings indicate that phosphorus inputs, primarily from fertilizers and manure, have increased significantly since the 1930s, while domestic waste contributions have decreased since the 1970s due to regulatory measures. Crop and pasture phosphorus uptake has also increased, reflecting improvements in agricultural practices. Despite these changes, phosphorus surplus remains a critical issue, with current magnitudes suggesting significant legacy phosphorus accumulation in the landscape.

This study underscores the importance of considering legacy phosphorus in watershed management. Despite reduced phosphorus inputs, riverine phosphorus exports remain substantial

due to the historical buildup of phosphorus in the soil, which acts as a buffer and sustains high phosphorus levels in water bodies despite current management efforts. Our findings reveal that manure phosphorus, rather than fertilizer phosphorus, is the primary driver of legacy phosphorus accumulation, particularly in regions with intensive livestock operations.

This comprehensive analysis of phosphorus dynamics in the Lake Erie basin enhances our understanding and provides valuable insights into developing effective nutrient management strategies. Addressing legacy phosphorus accumulation is crucial for improving water quality and achieving long-term sustainability in agricultural watersheds. Future research should focus on quantifying the specific contributions of legacy phosphorus to riverine exports and exploring targeted mitigation strategies to reduce its impact on water quality.

Chapter 3

Modeling Legacy Phosphorus Storage across the Lake Erie Basin Using ELEMeNT-P Model

3.1 Background

The extensive application of phosphorus (P) fertilizers, intensified livestock production, high population densities, and the use of P-rich detergents have led to widespread eutrophication in coastal and inland waters (Boesch, 2002; Huang et al., 2017; Le Moal et al., 2019; David W. Schindler et al., 2016; D. W. Schindler, 1974; Sharpley et al., 2013). Since 1950, global P fertilizer use has quadrupled, exacerbating eutrophication in places like North America's Lake Erie, Gulf of Mexico and China's Lake Taihu (Kröger et al., 2011; Sharpley et al., 2014; Van Vuuren et al., 2010). Initially, mitigation efforts focused on reducing point-source pollution through enhanced wastewater treatment and reduced P content in detergents (Chapra et al., 1977). Recently, the focus has shifted towards addressing nonpoint sources of phosphorus pollution, with strategies like erosion control and reduced fertilizer use being implemented (Haygarth et al., 2014; Jarvie et al., 2013). Despite these measures, P pollution persists, causing eutrophication and algal blooms in freshwater and coastal systems, with notable re-eutrophication and cyanobacterial blooms in the Great Lakes region (Carmichael et al., 2016; Jarvie et al., 2017; Litke, 1999; Steffen et al., 2014). It is increasingly recognized that a persistent lack of improvement in water quality can partly be attributed to the presence of legacy phosphorus (Sabo et al., 2021; Van Meter et al., 2021; Van Staden et al., 2022). This form of phosphorus has accumulated in soils and sediments over decades due to intensive agriculture (Van Meter et al., 2021).

The accumulation of legacy phosphorus has hindered efforts to meet phosphorus load reduction targets in river basins globally (Kleinman et al., 2019; McCrackin et al., 2018; Mississippi River/Gulf of Mexico Watershed Nutrient Task Force. Monitoring et al., 2004 ; Muenich et al., 2016; Powers et al., 2016; Stackpoole et al., 2019). Quantifying the magnitude and dynamics of legacy P and its impact on water quality is challenging (Lintern et al., 2020; Meals et al., 2010; Sharpley et al., 2013; Withers et al., 2014). Various modelling techniques have been employed to assess how changes in watershed management practices might affect riverine P. However, only some of these have effectively considered the ongoing contributions of legacy P to surface waters

(R. B. Alexander et al., 2004; Arheimer et al., 2012; Han et al., 2011; Hong et al., 2012; Motew et al., 2017; Scavia et al., 2016; Schoumans et al., 2000; Van Meter et al., 2021). Most research that addresses legacy P adopts a data-driven, mass balance methodology, compiling the annual P surplus over time (Han et al., 2011; MacDonald et al., 2009; Mittelstet et al., 2016; Wironen et al., 2018). Statistical or process-based models such as GWLF, SPARROW, GlobalNEWS, PolFlow, SWAT, INCA, DPPS, AGNPS, and ANSWERS, have also been applied to improve our quantitative understanding of watershed phosphorus dynamics (D. Chen et al., 2018; H. Chen et al., 2023; Condron et al., 2013; Harrison et al., 2019; Hwang et al., 2006; Muenich et al., 2016; T. Zhang et al., 2020). However, these models generally lack an explicit mechanism to describe the dynamics of legacy phosphorus and the associated delivery lag.

Several recent studies have employed mathematical models to assess the impact of legacy phosphorus, but many of these studies lack a long-term perspective or a mechanistic approach. For instance, (D. Chen et al., 2016) established statistical relationships between river TP flux and current and past P inputs in China's Yongan watershed, estimating that legacy P sources contributed 13-32% of annual riverine TP flux from 1980 to 2011. Van Meter et al., (2021) estimated lag times in a Southern Ontario watershed between 1900 and 2016 by examining relationships between P inputs and outputs. In a more intricate empirical model, McCrackin et al., (2018) employed a 3-parameter, 2-box spatially lumped model to capture 100-year legacy P dynamics, revealing that legacy P in the mobile pool contributed over half of the water-borne P load to the Baltic Sea. Jarvie et al., (2012) used empirical approaches to investigate the retention of legacy P from wastewater effluent in stream channels and its impact on river P loads.

Process-based models such as AGNPS, ANSWERS, INCA, ICECREAMDB, and SWAT often fail to adequately capture legacy effects, including the quantification of historical inputs and the accumulation and depletion of legacy phosphorus (D. Chen et al., 2018; Kleinman et al., 2015; Martin JL, 2013; Radcliffe et al., 2015). For example, Muenich et al., (2016) used the SWAT model to simulate legacy P effects in the western Lake Erie watershed but ran the model for only 12 years, whereas legacy P can accumulate over longer timescales. Schippers et al., (2006) developed a two-compartment model for estimating P time lags in soil but did not account for the long-term buildup of legacy stores. Ilampooranan et al., (2022) coupled SWAT with a travel time distribution model to describe legacy nitrogen dynamics, but the computational demands were

excessive. Motew et al., (2017) developed a more complex modelling framework that combined the Agro-IBIS and THMB models to assess the influence of legacy P on water quality, highlighting the significant impact of legacy P on stream loads. Accurately quantifying legacy P buildup in the landscape is crucial, but current watershed legacy P models often overlook this aspect. Additionally, complex models like the Watershed Assessment Model (WAM) and GRAFS-DPPS have been developed to understand watershed responses and analyze soil dynamics to assess legacy P contributions in specific regions (A. B. Bottcher et al., 2012; Khare et al., 2021; Le Noë et al., 2020). Studies using WAM model found that legacy P contributes to 63% of baseline TP load in watersheds in Lake Okeechobee (A. B. Bottcher et al., 2012; Khare et al., 2021). Coupled model GRAFS-DPPS and DPPS- LePA assesses the annual P budget on the landscape to analyze soil dynamics and estimate and asses legacy P stocks in the soil (Le Noë et al., 2020; Yu et al., 2021).

These models often lack a long-term perspective or mechanistic understanding. To address these gaps, we combine long-term phosphorus mass balance data with a mechanistic model designed to explore P accumulation and depletion within watersheds. The model, Exploration of Long-term Nutrient Trajectories-Phosphorus (ELEMeNT-P), previously applied to Grand River watersheds (Van Meter et al., 2021), goes beyond simple mass-balance approaches. By utilizing long-term data, it identifies where P accumulates in the landscape and assesses the contribution of legacies to riverine P loads. This approach allows for more reliable hypothesis testing regarding the impact of management interventions on water-quality trajectories.

In this chapter, ELEMeNT-P was used to simulate long-term P dynamics for 45 sub-watersheds of the Lake Erie Basin. The model was calibrated using total phosphorus load data. Future scenarios were developed to evaluate the potential for reducing P loads in line with current policy recommendations for Lake Erie watersheds. In this work, we have attempted to address the following questions: (a) What are the magnitudes of legacy P that have accumulated across the Lake Erie basin? (b) What are the most important landscape stores for legacy P accumulation, for example, soils, reservoirs, and groundwater? (d) How long will it take, and what measures are necessary, to achieve reductions in P loading in human-impacted watersheds?

3.2 The ELEMeNT-P Model Framework

In this analysis, the ELEMeNT-P model was used to simulate P storage and fluxes across the sub-watersheds of Lake Erie's basin by considering source-zone dynamics with a travel time-based approach and transport and retention mechanisms. ELEMeNT-P model was initially developed to simulate the accumulation and depletion of phosphorus to predict total P loading in Grand River watersheds in southern Ontario (Van Meter et al., 2021). This model is an extension of the ELEMeNT model, which was originally designed for nitrogen and used to simulate the loading of several watersheds in the past such as the Grand river watershed in Ontario, Weser watershed in Germany, Mondego basin in Portugal, Chesapeake Bay in the USA, and very recently for Lake Erie Basin (S. Y. Chang et al., 2021; Liu et al., 2021; Marques et al., 2022; McLeod, 2023; Sarrazin et al., 2022).

The ELEMeNT-P model considers both current-year inputs and legacy nutrient stores to explore how nutrient fluxes may change over time in response to changes in land use and management. Rather than breaking up the watershed into spatial units, it divides the landscape into non-spatial units, each with a distinct land use pattern over time. For example, cropland that has been converted into non-agricultural areas or suburban lawns behaves differently than cropland that has never been used for agriculture. The ELEMeNT-P model differentiates between these two types of non-agricultural land based on their past land-use trajectories. By taking into account past land use and changes in nutrient inputs, the model maintains a "memory" of past land use within its structure. By treating different land-use trajectories separately, the model provides a more accurate simulation of long-term nutrient dynamics than other watershed models.

ELEMeNT-P model has some additional components to the nitrogen model. It adds an overland flow component to the process-based approach of the nitrogen version to account for erosion effects and P transport on the land surface. It also considers P sorption processes to capture equilibrium dynamics within the source zone and irreversible precipitation in soil and groundwater (Van Meter et al., 2021). The model enables us to estimate legacy P accumulation and depletion in soils, groundwater, landfills, reservoirs, and riparian zones. This model simulates stream P loading as total phosphorus to assess the accumulation and depletion dynamics of legacy P in watersheds in the Lake Erie Basin.

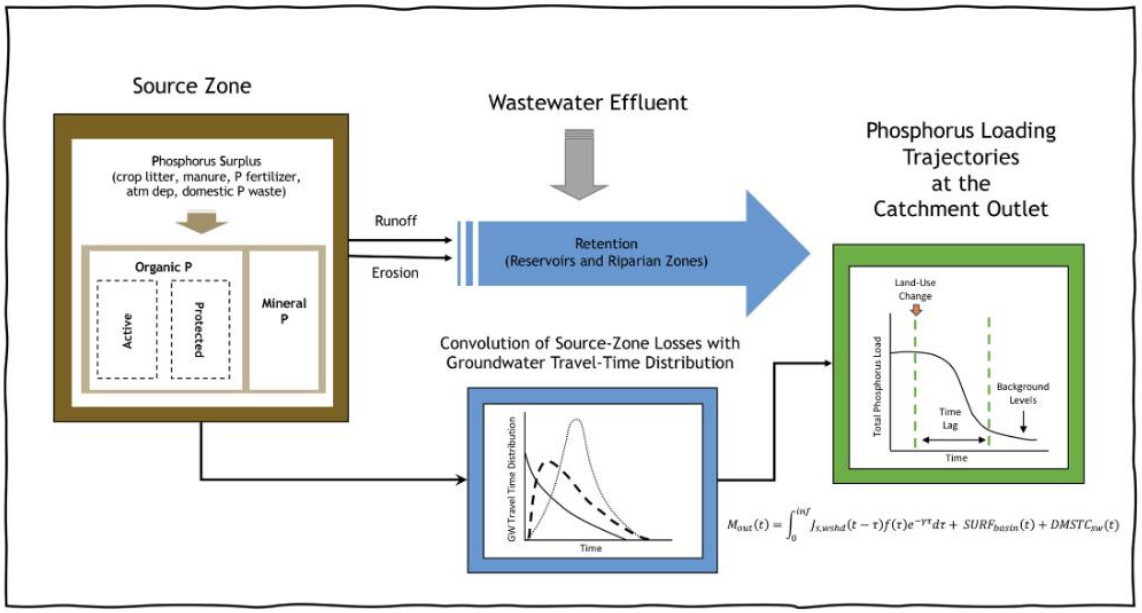


Figure 3.1: Conceptual diagram for ELEMeNT-P model for estimating catchment-scale P loads based on both legacy P and inputs from the current year (Van Meter et al., 2021).

To model P loading at the outlet of the watershed, the model treats the landscape as a collection of stream tubes, each with its unique path to the outlet. ELEMeNT-P accounts for three different pathways in order to simulate total phosphorus loading at the outlet: a) subsurface P transport, b) overland P transport, and c) wastewater inputs (**Fig S1 in Appendix b**). TP load trajectory at the outlet ($M_{out(t)}$)

$$M_{out}(t) = \int_0^{inf} J_{s,wshd}(t-\tau)f(\tau)e^{-\gamma\tau}d\tau + SURF_{basin}(\tau) + DMSTC_{SW}(\tau) \qquad \text{(Eq. 3.1)}$$

Here, the source function $J_{s,wshd}(t-\tau)[ML^{-2}T^{-1}]$, $f(\tau)[T^{-1}]$ is the distribution of travel time and $\gamma\left[T^{-1}\right]$ is the rate constant representing first-order sorption of P along surface pathways, the basin scale surface P yield $SURF_{basin}(t)[ML^{-2}T^{-1}]$, and the, $DMSTC_{SW}(t)[ML^{-2}T^{-1}]$ is domestic wastewater P discharged from waste water treatment plants (WWTPs).

The unique feature of ELEMeNT-P, distinguishing it from other watershed models, is its explicit consideration of both current-year phosphorus inputs and the influence of historical land use, land management, and in stream phosphorus fluxes (Van Meter et al., 2017, 2021). To accommodate this, the watershed is segmented into distinct units, each characterized by a unique land-use history. The evolution of these land-use trajectories over time is captured within a two-dimensional land-

use array, *LU (s, t)*. Each unit, s represents an index in the land-use array, which spans over time t. Specifically, LU is represented by the following equation

$$LU(s,t) = \begin{cases} 2 & s \leq A_{crop}(t) & cropland \\ 1 & A_{crop}(t) < s \leq \left[A_{crop}(t) + A_{past}(t)\right] & pastureland \\ 0 & s > \left[A_{crop}(t) + A_{past}(t)\right] & other \end{cases}$$

(Eq. 3.2-3.4)

Here, A_{crop} and A_{past} correspond to watershed percent cropland and percent pastureland, respectively.

3.2.1 Source Zone Dynamics

The source zone refers to the uppermost one-meter layer of biogeochemically active soil that contains both organic and mineral P stores. It is estimated as a function of the P surplus to the soil surface, and soil hydrological and biogeochemical factors responsible for transport and transform P (**Section 3.2.1.1 and 3.2.2**).

$$M_{source}(s,t) = M_{sop}(s,t) + M_{min}(s,t) \quad \text{(Eq. 3.5)}$$

Where $M_{source}(s,t)[ML^{-2}]$ the mass of P in the source zone for land use s at time $t, M_{sop}(s,t)[ML^{-2}]$ is the P in soil organic matter, and $M_{min}(s,t)[ML^{-2}]$ is mineral P, in both dissolved and sorbed forms. These P stores within the source zone change over time (**Appendix B Text S1.1 S1.2**) as a function of changes in land use net P inputs.

3.2.1.1 P Surplus as Input to the Source Zone

The source zone receives an annual P surplus, derived from the P mass balance approach. P surplus is calculated separately for cropland, pasture land, and non-agricultural land to feed into the model

$$N_p(crop,t) = FERT_{p,crop}(t) + MAN_{p,crop}(t) + DEP_p(t) + DMSTC_{p,crop}(t) - CROP_p(t) \quad \text{(Eq. 3.6)}$$

$$N_p(past,t) = FERT_{p,past}(t) + MAN_{p,past}(t) + DEP_p(t) - GRASS_p(t) \quad \text{(Eq. 3.7)}$$

$$N_{p,other}(t) = DEP_p(t) \quad \text{(Eq. 3.8)}$$

Where $N_p(s,t)$ is P surplus applied at the soil surface to cropland, pastureland, and non-agricultural land, respectively; $FERT_{p,crop}(t)$ and $FERT_{p,past}(t)$ are inorganic P fertilizer applied to cropland and pastureland, respectively; $MAN_{p,crop}(t)$ is manure P applied to cropland; $MAN_{p,past}(t)$ is manure P applied to pastureland plus animal P excreted during grazing, $DEP_p(t)$ is atmospheric P deposition; $DMSTC_{p,crop}(t)$ is land-applied domestic P from WWTPs and septic systems; $CROP_p(t)$ is crop-specific P uptake; and $GRASS_p(t)$ to grass P consumption by grazing livestock. All units are in $ML^{-2}T^{-1}$

3.2.2 Surface P Transport: Erosion and Retention

The basin-scale P yield from surface transport pathways, $SURF_{basin}(t)$ $[ML^{-2}T^{-1}]$, can be described as the sum of two terms, $SURF_{eros}(t)$ and $MAN_{p,losses}(t)$. $SURF_{eros}(t)$ is P erosion from the landscape which includes runoff from manure applied as fertilizer and runoff of surplus P from manure, and $MAN_{p,losses}(t)$ manure handling losses.

$$SURF_{basin}(t) = \left(1 - K_{ret}(t)\right) * \left(SURF_{eros}(t) + MAN_{p.losses}(t)\right) \quad \text{(Eq.3.9)}$$

The P erosion from the landscape, $SURF_{eros}$ is quantified as a function of the gross erosion rate constant, $k_{eros}(s, t)(y-1)$, and the mass of mineral and organic P in the source zone. These erosion (k_{eros}) and retention (k_{ret}) terms are calculated using a modified version of the semi-quantitative Gavrilovic method (Gavrilovic, 1976; (de Vente et al., 2005). The Gavrilovic method is modified to account for temporal variations in these rates, as a function of flow variability. Details on using this method to estimate $k_{eros}(s, t)$ and $K_{ret}(t)$ are described in the **text S2 in Appendix B**

$$SURF_{eros}(t) = \sum_{s-1}^{n} \left[k_{eros}(s,t)\left(M_p(s,t) + M_a(s,t) + M_{sorb,i}(s,t) + M_{sorb,r}(s,t)\right)\right] \quad \text{(Eq.3.10)}$$

The manure loss component on the farm scale, $MAN_{p,losses}(t)$, is determined by estimating based on studies of farm-scale manure handling systems, that suggested 3% to 7% of manure phosphorus is lost through runoff during the storage of manure (Lin et al., 2017; Magdoff et al., 2009).

$$MAN_{p,losses}(t) = K_{manure} * f_{conf}(t) * MAN_{p,tot}(t) \quad \text{(Eq.3.11)}$$

where $MAN_{p,losses}(t)$ [$ML^{-2}T^{-1}$] is farm-scale manure loss component, $MAN_{p,tot}(t)$ is the total annual manure P, $f_{conf}(t)$ is the time-varying fraction of manure P produced in confinement, and k_{manure} [T^{-1}] is a calibrated partitioning coefficient.

Finally, an eroded portion is retained in the reservoir and riparian zone and sediment and follows the following equation

$$RES_p(t) = K_{ret}(t) * \left(SURF_{eros}(t) + MAN_{p,losses}(t)\right) \quad \text{(Eq.3.12)}$$

Where of eroded phosphorus retained in reservoirs, riparian zones, and stream sediments, $SURF_{eros}(t)$ is P erosion from the landscape.

3.2.3 Domestic P Inputs

Domestic P sources are waste from human consumption and the P-containing dish and laundry detergents. Most of domestic P transports through septic systems and municipal wastewater pathways. These system, septic and WWTPs retain P, which can either be disposed of in landfills or applied to cropland. The remaining of it is released into surface water. However, food waste is directly directed to landfills. The mass of domestic wastewater P discharged to surface water, $DMSTC_{sw}(t)$, [$ML^{-2}T^{-1}$], is quantified using the following equation

$$DMSTC_{sw}(t) = \left(1 - k_{h,wwtp}\right) * DMSTC_{wwtp}(t) + \left(1 - k_{h,sep}(t)\right) * DMSTC_{sep}(t) \quad \text{(Eq. 3.13)}$$

where, $DMSTC_{wwtp}(t)[MT^{-1}]$ and $DMSTC_{sep}(t)[MT^{-1}]$ represent the waste P routed through septic systems and WWTPs, and $k_{h,wwtp}$ (t) and $k_{h,sep}$ (t)(y^{-1}) are time-varying P retention coefficients in these two systems.

Total P input to landfills, $LF_p(t)$ [MT^{-1}], include P from food waste, septic systems, and WWTPs. Which is described as following

$$LF_p(t) = FOOD_{p,waste}(t) + \left(k_{h,sep} * DMSTC_{sep}(t)\right) + \left(k_{h,wwtp} * DMSTC_{wwtp}(t)\right) \quad \text{(Eq.3.14)}$$

In the ELEMeNT-P model, landfills are treated as a permanent pool for P. As a result, phosphorus that is deposited in landfills does not contribute to phosphorus levels in surface water or groundwater.

3.3 Methods and Data Sources

3.3.1 Model Inputs and Outputs

This section provides an overview of the inputs and outputs of the ELEMeNT-P model. The inputs for the ELEMeNT-P model include discharge, total phosphorus load, phosphorus in fertilizer, P from livestock excretion, crop P production, domestic P waste, long-term land use data, and catchment property data. Additionally, this section describes the methods used for model calibration, including the criteria for selecting parameters.

3.3.1.1 Watershed Selection, Discharge and Total Phosphorus Concentration Data

Daily stream discharge and total phosphorus (TP) concentrations were collected from various databases for both the American and Canadian sides of the Lake Erie basin. Similar to the 1st objective, water quality modelling stations were chosen based on several criteria: (a) availability of at least 13 years of overlapping flow and concentration data, (b) fewer than 10 years of data gaps in the concentration-time series, (c) a minimum of 25 years of flow data (applicable only in Canada), and (d) proximity to a flow monitoring station (also only in Canada). In the US, discharge data were already supplemented by concentration data, whereas in Canada, discharge and concentration data were extracted from two separate databases. Consequently, two additional criteria (criteria c and d) were applied specifically for Canadian stations. For co-locating discharge and concentration gauges in Canada, we ensured that the drainage areas for both gauges had a maximum discrepancy of less than 10%, meaning that flow and water quality stations were only paired if their drainage areas differed by less than 10%. Consequently, we obtained data from 57 stations. However, for this study, we selected the top-performing 45 stations across the Lake Erie basin for modeling with ELEMeNT-P. Among these stations, 28 are located in Canada and 17 in the USA (**Figure 3.2**). Detailed information regarding the watershed IDs and additional characteristics of the watersheds can be found in **Table 3.1**.

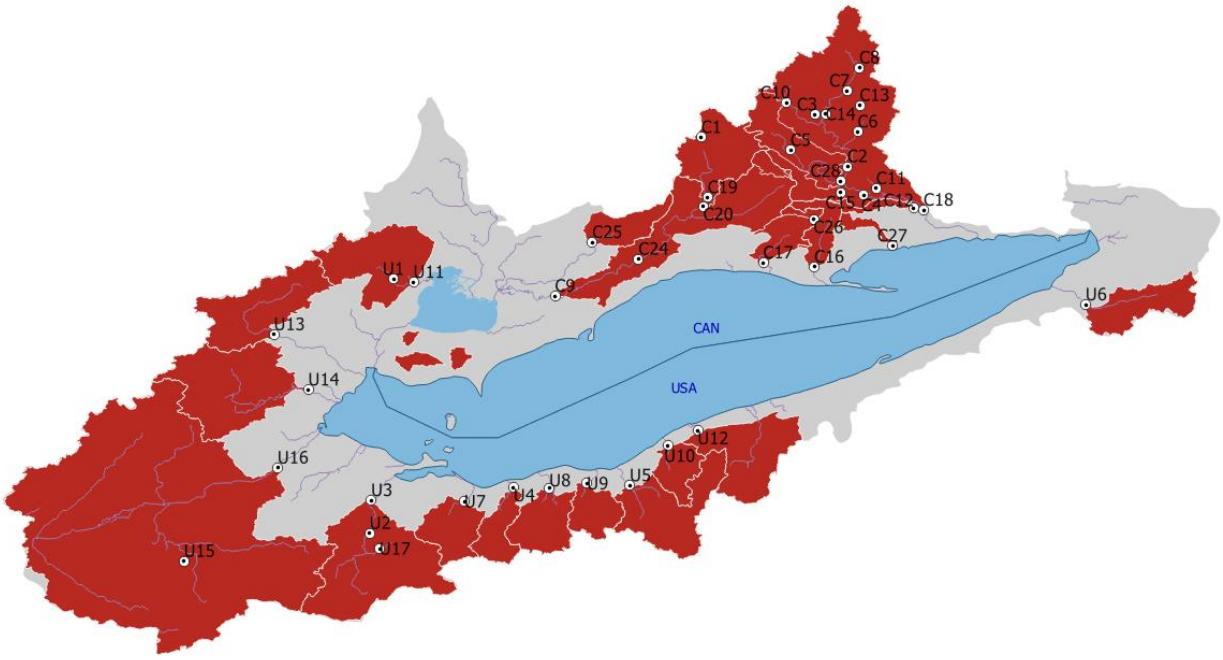


Figure 3.2: Spatial distribution of 45 stations across the Lake Erie basin

Table 3.1:List of all studied sub-watersheds

ID	Name	Latitude	Longitude	Area sq km
U1	Clinton River at Sterling Heights	42.61	-83.03	799.99
U2	Rock Creek at Tiffin	41.11	-83.17	95.38
U3	Sandusky River near Fremont	41.31	-83.16	3250.01
U4	Vermilion River near Vermillion	41.38	-82.32	687.62
U5	Cuyahoga River at Independence	41.40	-81.63	1840.73
U6	Cattaraugus Creek at Gowanda	42.46	-78.93	1136.16
U7	Huron River at Milan	41.30	-82.61	949.09
U8	Black River at Elyria	41.38	-82.11	1028.77
U9	Rocky River near Berea	41.41	-81.88	691.91
U10	Chagrin River at Willoughby	41.63	-81.40	638.44
U11	Clinton River at Mt. Clemens	42.60	-82.91	1894.59
U12	Grand River near Painesville	41.72	-81.23	1787.75
U13	Huron River at Ann Arbor	42.29	-83.73	1888.11
U14	River Rasin near Monroe	41.96	-83.53	2689.77
U15	Auglaize River near Fort Jennings	40.95	-84.27	860.98
U16	Maumee River at Waterville	41.50	-83.71	16943.43
U17	Honey Creek at Melmore	41.02	-83.11	388.94
C1	North Thames River Near Mitchell	43.45	-81.21	317.35
C2	Grand River At Galt	43.28	-80.34	3487.45
C3	Canagagigue Creek Near Elmira	43.59	-80.54	111.26

C4	Grand River At Brantford	43.11	-80.25	5100.29
C5	Nith River At New Hamburg	43.38	-80.68	549.35
C6	Speed River Below Guelph	43.53	-80.25	526.13
C7	Grand River Below Shand Dam	43.73	-80.34	788.52
C8	Grand River Near Marsville	43.86	-80.27	665.07
C9	Thames at Thamesville	42.51	-82.07	4540.90
C10	Conestogo River At Glen Allan	43.65	-80.70	573.00
C11	Fairchild Creek Near Brantford	43.15	-80.17	360.08
C12	Mckenzie Creek Near Caledonia	43.03	-79.95	174.20
C13	Speed River Near Armstrong Mills	43.64	-80.27	176.71
C14	Grand River At West Montrose	43.59	-80.47	1157.30
C15	Whitemans Creek Near Mount Vernon	43.13	-80.38	397.65
C16	Big Creek At Walsingham	42.69	-80.54	565.76
C17	Big Otter Creek At Calton	42.71	-80.84	655.78
C18	Grand River at York	43.02	-79.89	6015.09
C19	North Thames River Near Thorndale	43.10	-81.17	1337.13
C20	North Thames River Below Fanshawe Dam	43.04	-81.19	1416.70
C21	Canard River Near Lukerville	42.16	-83.02	159.00
C22	Ruscom River Near Ruscom Station	42.21	-82.63	125.00
C23	Little River At Windsor	42.31	-82.93	55.30
C24	Thames River At Innerkip	42.73	-81.58	150.42
C25	Sydenham River Near Alvinston	42.83	-81.85	704.16
C26	Big Otter Creek Above Otterville	42.97	-80.54	99.15
C27	Nanticoke Creek At Nanticoke	42.81	80.08	179.24
C28	Nith River Near Canning	43.19	-80.38	1128.10

We used four multiple sources to obtain longer TP data for watersheds in the USA. They are National Water-Quality Assessment (NAWQA) by USGS, National Center for Water Quality Research (NCWQR) at Heidelberg University, Michigan Department of Environmental Quality (MIDEQ) and the Ohio Environmental Protection Agency (OHEPA)(USGS, 2020; EGLE, 2019; NCWQR, 2020; OHEPA, 2019). To obtain data from National Water Information System (NWIS) and National Water-Quality Assessment (NAWQA) we used R dataRetrieval package (Hirsch, Archfield, et al., 2015).

Flow and water quality data for Canadian watersheds are collected from hydrometric monitoring stations of Environment and Climate Change Canada (Environment and Climate Change Canada Historical Hydrometric Data, 2018) and Provincial (Stream) Water Quality Monitoring Network (PWQMN) (Provincial (Stream) Water Quality Monitoring Network, 2018) respectively.

TP data were sparse in both USA and Canadian stations, thus we applied the weighted regression on time, discharge, and season (WRTDS) modelling approach (Hirsch et al., 2010; Hirsch & De Cicco, 2015) to estimate daily concentration data from sparse data. Following this, we calculated flow-weighted concentrations (FWCs) and determined the daily continuous data for annual loads. WRTDS, which is an advanced approach to assessing water quality. Unlike conventional models that only consider the relationship between concentration and discharge, WRTDS also takes into account seasonal and temporal variations. It analyzes the interactions between discharge, time of year, and season to calculate daily concentrations (Maestre et al., 2014). To facilitate its application in monitoring water quality, WRTDS was implemented through the EGRET package in R, a software tool provided by the USGS. The model's underlying equation is as follows

$$\ln(c) = \beta_0 + \beta_1 t + \beta_2 \ln(Q) + \beta_3 \sin(2\pi t) + \beta_4 \cos(2\pi t) + \epsilon \quad \text{(Eq.3.15)}$$

where c is concentration, β,0-4 are regression coefficients, t is the time as a fraction of the year, Q is the average daily streamflow and ε is the residual error.

3.3.1.2 Input from P Mass Balance

Phosphorus inputs at the watershed scale from 1901 to 2016 were calculated using 250-meter grid maps of the components of the phosphorus mass balance. Since the mass balance dataset for the USA began in 1930, we estimated the unavailable data from 1901 to 1929 by assuming a constant value equivalent to the recorded value in 1930. The phosphorus components were measured in kilograms of phosphorus per hectare of watershed area. The data were then used in the ELEMeNT-P model to estimate phosphorus inputs on a larger watershed scale.

P Fertilizer

Estimates of P fertilizer use (FERT) on a county scale for the USA and Canada have been compiled for every year from 1930 to 2016. The data was gathered from various sources with different spatiotemporal resolutions and then normalized with the county area. To maintain consistency across both countries, the compilation exclusively utilizes farm P fertilizer usage data.

In the USA, the county-scale annual phosphorus fertilizer inputs were compiled from several sources. Phosphate fertilizer sales data from 1945 to 1985 were obtained from (Richard B.

Alexander et al., 1990). For the period 1987 to 2012, information was sourced from the USGS report (*County-Level Estimates of Nitrogen and Phosphorus from Commercial Fertilizer for the Conterminous United States, 1987-2012*, 2020). Data from 2013 to 2017 were obtained by the Food and Agriculture Organization of the United Nations (FAO) (Food and Agriculture Organization of the United Nations (FAO), 2022). For the years 1930-1944, where no specific dataset on P fertilizer usage was available, we used county-specific scaling factors to estimate usage. Details on the estimation of phosphorus from fertilizer are described in **Appendix A Section 1.1**.

For Canada, annual P fertilizer inputs were obtained from the provincial fertilizer sales datasets. The average provincial fertilizer application rate was calculated from provincial fertilizer sales data, assuming that all fertilizer sold was applied to farmland within the same year. The Ontario provincial sales data from 1966 to 2016 was obtained from the Fertilizer Shipment Survey provided by Statistics Canada (Government of Canada et al., 2023) and 1930 to 1965 from Fertilizer Trade Data provided by Statistics Canada. P fertilizer application rate of Ontario before 1930 was calculated using the Phosphate Rock Statistics data, similar to that used in the USA to calculate fertilizer from 1930-1944 (**Eq. S1.1**).

Livestock Inputs

To estimate the P input from livestock manure at the county scale for the census year across both countries (USDA National Agricultural Statistics Service Agriculture Census; Agricultural Census of Canada). Included livestock categories in this study are- dairy cattle, beef cattle, heifers, steers, bulls, calves, chickens, broilers, turkeys, hogs, sheep, goats and horses. However, in the USA, survey data between census years were used for seven livestock categories (Byrnes et al., 2020)0), while in Canada, phosphorus estimates from livestock were linearly interpolated between census years.

P from livestock manure (MAN) is calculated by multiplying livestock inventory, animal excretion rate and weight factor (**Eq. S1.4**). P content in manure was estimated based on the *Agricultural Waste Management Field Handbook* (USDA NRCS, 2008). Detail on calculation of phosphorus input from livestock manure is described in **Appendix A Section 1.2**.

Crop P Uptake

Crop P uptake (CROP) was calculated using crop area and crop production data from the Agricultural Census. First, we identified common field crops across both countries. Next, we obtained crop area areas for census years and multiplied them with crop yield (kg per area) to convert the area into mass units. The mass of the crop harvested was converted into kg of phosphorus by multiplying it with the P content of each crop. The final equation (**Eq. S1.8**) for calculating crop P uptake is described in **section S1.4 in Appendix A**. The crop uptake is then normalized with county area.

Crop mass data for the USA from (Byrnes et al., 2020), which used harvested crop area data from the ICPSR data archive (1930–2012) and NASS Quick Stats (2017) (Haines et al., 2014); (*USDA - national agricultural statistics service - data and statistics*, n.d.). Harvested crop area data for Canada is from the Census of Agriculture by Statistics Canada. Details are in **Section S1.4 in Appendix A**.

An update was made to the crop phosphorus parameters to account for a decrease in P uptake levels in certain field crops, attributed to reduced protein content in these crops (Ciampitti et al., 2012; Scott et al., 2006; Villamil et al., 2019). As a result, lower P parameter values for corn, soybean, and wheat were used in Chapter 2. However, in this chapter, the P content values for corn, soybean, and wheat were sourced from the values of the International Plant Nutrition Institute (IPNI) and Hong et al. (2012). The values for corn, soybean, and wheat used as input are tabulated in **Table S4 in Appendix C**.

Domestic P Input

Total flux for domestic P (WASTE) comprises P from laundry and dish detergent usage, human food consumption and food waste. These four elements of domestic P inputs were calculated using population data from the US (US Census Bureau, 2023) and Canada ((Government of Canada et al., 2001)), alongside a set of variables including the annual per capita phosphorus contribution from laundry and dishwashing detergents, and human phosphorus consumption rates. Further details about the methodology and the selection of these parameters are available in **Section S1.3 in Appendix A**.

Atmospheric P Deposition

Atmospheric phosphorus deposition (ATM) originates from sources such as sea salt, dust, biogenic aerosol particles, and emissions from fuel combustion. Atmospheric P deposition is a minor P input component, and it was obtained from a global P deposition data set (Wang et al., 2017). The deposition dataset contains P exposition data for 52 different years spanning from 1850-2100 and it is at 1x1 degree spatial resolution. The global deposition data were clipped with the county boundaries and linearly interpolated in between the modelled years to obtain county-scaled yearly P deposition data in kg-P per hectare.

3.3.1.2.1 Downscaling Model Inputs

The watershed-scale P surplus and its components were calculated from a downscaled version of county-scale data for both the USA and Canada, presented on a 250m x 250m grid. The downscaled P surplus components included: fertilizer P input, crop P uptake, and manure P input specific to each type of livestock (such as beef cows, milk cows, other cows, hogs, chickens, broilers, turkeys, horses, sheep, and goats), and domestic P inputs (including detergents, human and food waste).

For the USA, the gridded map of P surplus and its components was obtained using two different land use data. The data from 1931-2005 was downscaled using historical land use data from (Sohl et al., 2016) and from 2006-2017 was downscaled using National Land Cover Database (NLCD). (*National Land Cover Database (NLCD) 2019 products (ver. 2.0, June 2021)*). The gridded map of P surplus and its components for Canada was obtained using annual crop inventory maps (ACI) from 2011 to 2016 (Agriculture and Agri-Food Canada 2020).

On the Canadian side, we used a gridded map downscaled from the ACI (Annual Crop Inventory, 2016). Although the NLCD and ACI data are available at a 30m x30m resolution, we resampled it to 250m x 250m grids to reduce processing time and ensure methodological consistency. For the study, agricultural land is considered as cultivated cropland. On the other hand, urban land is a developed land. In cases where land use data was not available for a specific year, the previously available land use raster was utilized as a substitute. A detailed downscaled methodology is described in **Section S1.5 in Appendix A**.

To estimate the watershed-scale inputs of P from these downscaled maps, we clipped the watersheds with the P grid maps. This allowed us to determine the fertilizer P input, crop P uptake,

domestic P inputs (including detergents, human and food waste), as well as the manure P input specific to each type of livestock (such as beef cows, milk cows, other cows, hogs, chickens, broilers, turkeys, horses, sheep, and goats). These P input components were quantified in kg P per hectare of watershed area and were subsequently utilized in the ELEMeNT-P model.

3.3.1.2.2 Total and Agricultural P Surplus

I computed the phosphorus surplus, which indicates the amount of excess phosphorus present in the landscape. Total P surplus is defined as the difference between P inputs (fertilizer P, manure P, domestic waste P and atmospheric P deposition) and P outputs (crop P uptake) (Byrnes et al., 2020) and agricultural P surplus as the difference between agricultural P input and P outputs.

$$_{tot}PS_{grid}\,(i,t) = FERT_{grid}\,(i,t) + MAN_{grid}\,(i,t) + WASTE_{grid}\,(i,t) + ATM\,(i,t) - UPTAKE_{grid}\,(i,t) \quad \text{(Eq.3.16)}$$

$$_{ag}PS_{grid}\,(i,t) = FERT_{grid}\,(i,t) + MAN_{grid}\,(i,t) + - UPTAKE_{grid}\,(i,t) \quad \text{(Eq.3.17)}$$

where FERT is inorganic P fertilizer (kg-P ha^{-1} yr^{-1}), MAN is P from livestock manure, WASTE is the P from domestic waste (kg-P ha^{-1} yr^{-1}), and UPTAKE is the P removed through crop harvesting or pastureland (kg-P ha^{-1} yr^{-1}). Here, *i* and *t* denote the iteration of each county and year respectively.

3.3.1.3 Watershed Land Use Trajectories

ELEMeNT-P, the model uses a historical record of land use (LU) for each sub-watershed to accurately allocate P surplus inputs into their crop, pasture, and non-agricultural components. LU trajectory summarizes the proportion of crops, pastures, and non-agricultural land occupied over time. We created a 316-year (1700-2016) LU trajectory for each sub-watershed, which is an input component of the model. To construct this trajectory, we used census data on crops and pastureland from 1930 to 2016. We summed up all categories of crop and pasture area used for our mass balance and supplemented that data from the historical global croplands dataset (Ramankutty et al., 1999) from 1700 to 2007.

The model also uses county-scale population data to calculate domestic waste input. We compiled population data at the county level from the United States and Canada's population census starting from 1900. Additionally, We supplemented the data with historical national population records to

estimate population figures before 1900. The spatial and temporal distribution of landuse in the Lake Erie basin is presented below:

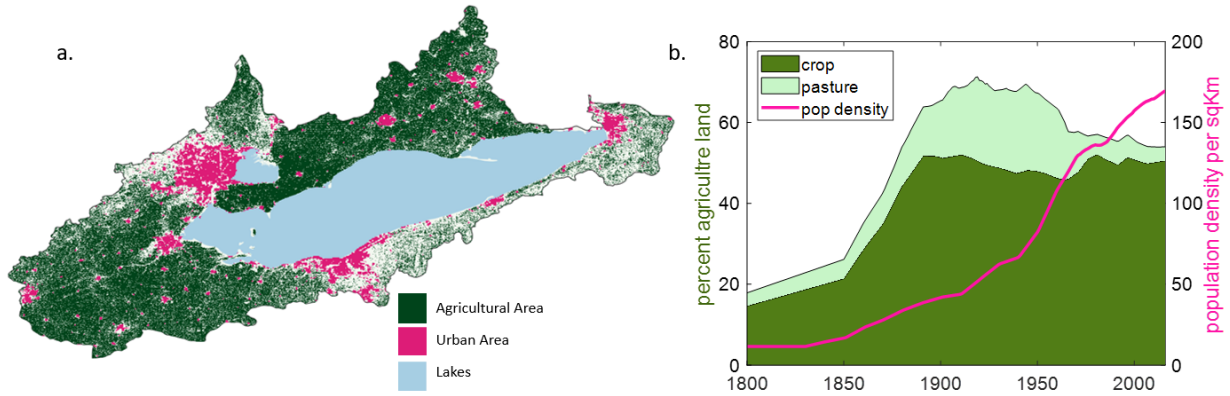


Figure 3.3:Land use of Lake Erie Basin. a) Spatial distribution of agricultural areas and urban area in 2016. b) trajectories of crops, pasture and population density.

3.3.1.4 Watershed Erosion Parameter

To calculate the erosion and retention of P in the landscape the model uses the modified Gavrilovic method (**Section 3.2.2 and Text S2 in Appendix B**) (Van Meter et al., 2021). The Erosion rate constant is calculated based on watershed-dependent parameters such as temperature, slope, and precipitation and the sediment retention ratio is calculated using watershed perimeter, elevation difference and length of principal waterways (**Eq. S12-S16**) (Van Meter et al., 2021).

The methodology and data sources for estimating the erosion parameters vary between the two countries. For the United States, precipitation and temperature data were obtained from the WorldClim database at a resolution of 1 km (Fick et al., 2017). The climate variables used in the calculations include the average annual precipitation in millimetres per year and the average annual temperature in degrees Celsius of the watershed. Slope data for the United States was obtained from the hydrologic landscape regions of the United States dataset (Wolock et al., 2004). The maximum and minimum elevation for the USA watersheds were obtained from the 30m resolution Elevation Derivatives for National Applications (EDNA) Digital elevation raster by USGS (U.S. Geological Survey, 2005). The length of principal waterways within each USA watershed was estimated using the USGS streamer (U.S. Geological Survey, 2014). We traced upstream and downstream streams in each watershed to calculate stream length. On the other hand, all the

necessary data for Ontario, Canada, including precipitation, temperature, slope, and elevation, were acquired from the Ontario Flow Assessment Tool (OFAT) (C. Chang et al., 2002). This tool provides a 30m digital elevation model specifically designed for Ontario's watersheds (Dony, 2020).

3.3.5 Model Parameter Selection and Sensitivity Analysis

The ELEMeNT-P model uses seventeen parameters (**Table 3.2**), representing the watershed's physical properties (Van Meter et al., 2021). Among these seventeen parameters we calibrated fifteen of them and two of them were calculated based on soil data. The parameter was chosen based on sensitivity analysis done by (Van Meter et al., 2021). Global parameter sensitivity analysis was performed to identify the largest impactful parameter (Mishra, 2009; Muleta et al., 2005) and then a maximum and minimum range were set for parameter calibration (Van Meter et al., 2021).

Table 3.2: Description of ELEMeNT-P model parameters (Van Meter et al., 2021)

Parameter	Description [units]	Type	Range	
			Max	**Min**
$\mathbf{M_{pris}}$	Total soil P mass in pristine soil [kg/ha]	Calibrated	100	3900
$\mathbf{h_c}$	Protection coefficient, cultivated land	Calibrated	0.21	0.4
$\mathbf{h_{nc}}$	Protection coefficient, non-cultivated land	Calibrated	0.35	0.65
$\mathbf{k_a}$	Mineralization rate constant, active pool [y-1]	Calibrated	0.001	0.2
$\mathbf{k_p}$	Mineralization rate constant, protected pool [y-1]	Calibrated	1.9E-06	7.6E-05
n	Soil porosity	Measured	.	.
s	Soil water content	Measured	.	.

k_f	Proportionality constant for Freundlich model	Calibrated	0.005	0.2
n_{fr}	Empirical constant for Freundlich model	Calibrated	0.5	0.9
P_{sorb_o}	Fraction of sorbed soil P in pristine soil	Calibrated	0.003	0.6
K_{sorb}	Fraction of reversibly sorbed source zone P	Calibrated	1E-05	0.02
K_{sc}	Coefficient of soil cover	Calibrated	0.35	0.65
K_{sr}	Coefficient of soil resistance	Calibrated	1.2	2.2
K_e	coefficient of type and extent of erosion	Calibrated	0.35	0.65
μ	Mean groundwater travel time [y]	Calibrated	0.5	19.5
Υ_p	Groundwater P sorption coefficient [y-1]	Calibrated	0.03	0.98
K_{manure}	Manure partitioning coefficient	Calibrated	0.001	0.04

Soil saturation (s) and porosity (n) are determined for each sub-watershed using observed data. We calculate them by averaging soil characteristics from the Soil Landscapes of Canada database (for Canadian sub-watersheds) (Agriculture and Agri-Food Canada, 2016) and the USGS Soil Properties Dataset (for U.S. sub-watersheds) (Boiko et al., 2021).

3.3.1.5 Model Calibration

We developed separate ELEMeNT-P models for all 45 watersheds in the Lake Erie Basin. Model inputs included P surplus and its components, while the model was calibrated with TP load at the watershed outlet. Each sub-watershed was calibrated separately using the OSTRICH modeling platform, and best-performing parameters were accepted and used to create a set of ensemble runs

for each sub-watershed. The models were calibrated to the entire period that P concentration data were available, to optimize the performance of the calibration.

Calibration was performed using OSTRICH (Tolson et al., 2007), which is independent of the model used and incorporates various parameter optimization algorithms to identify the most effective model parameters (Matott, 2017). We employed the Pareto Archived Dynamically Dimensioned Search (PADDS) algorithm in this study. This algorithm generates parameter sets (solutions) encompassing the allowable ranges of parameters for a global search (Asadzadeh et al., 2013). This algorithm continues until OSTRICH assembles a set of dominant and non-dominated solutions (parameter sets). As the iterations progress toward the specified maximum number, the algorithm dynamically and probabilistically focuses on perturbing fewer parameters. During each iteration, PADDS retains the set of non-dominated solutions, while generating a new candidate solution by perturbing randomly selected parameters using magnitudes randomly sampled from a normal distribution with a mean of 0. If the candidate solution is either dominating or non-dominated when compared to the archived set of solutions, it is added to the archive and subject to random perturbation in the next iteration. Conversely, if the candidate solution is dominated, another non-dominated set is chosen for perturbation in the same iteration (Asadzadeh et al., 2013). By utilizing the PADDS algorithm for model calibration, a considerable number of distinct parameter sets optimized for our objective functions can be generated.

We conducted five runs of the OSTRICH model, each consisting of 200 iterations for all 45 sub-watersheds. In total, 1000 iterations were used to calibrate the model, encompassing both dominant and non-dominant parameter sets. The objectives were twofold: they were to maximize the Kling-Gupta Efficiency (KGE) (Gupta et al., 2009) and to minimize the percent bias (PBIAS) between the modelled and measured P loading at the outlet. The equations for these objectives are provided below.

$$KGE(obs, sim) = 1 - \sqrt{(CC - 1)^2 + (\frac{\mu sim}{\mu obs} - 1)^2 + (\frac{\sigma sim}{\sigma obs} - 1)^2} \qquad \text{(Eq.3.18)}$$

$$PBIAS(obs, sim) = \frac{\sum(obs - sim)}{\Sigma obs} \qquad \text{(Eq.3.19)}$$

Where ‘obs’ is the observed and ‘sim’ is the modelled P load at the outlet. CC is the Pearson correlation coefficient between obs and sim; μ_{sim} and μ_{obs} are the means of simulated and observed

value respectively; σ_{sim} and σ_{obs} are the standard deviations of simulated and observed value respectively. A KGE of 1 indicates a perfect match between the observed and simulated load at the outlet.

After calibrating the model, we obtained 1000 parameter sets for each sub-watershed. To select parameters for the model ensembles, we set specific acceptance criteria. The main requirements were that the Kling-Gupta Efficiency (KGE) for P loading should be at least 50%, and the percent bias (PBIAS) for P loading should be at most 20%. For sub-watersheds that didn't meet all these conditions (about 13% of them), we accepted parameter sets with up to 30% KGE and a maximum PBIAS of 40% for P loading. Finally, we generated diverse outputs using the chosen parameter range to account for inherent uncertainty related to the parameters.

3.3.1.6 Generating Future Scenarios

In this study, we developed and simulated six future scenarios to estimate load reductions and determine their potential to achieve the International Joint Commission (IJC) proposed 40% reduction target. The first scenario (S1) represents the business-as-usual approach, with no changes to current management practices. The second scenario (S2) explores the cessation of all farm fertilizer applications, relying instead on plants absorbing nutrients from the legacy soil pool. The third scenario (S3) simulates conditions with no manure handling losses, maintaining existing management practices otherwise. The fourth scenario (S4) eliminates phosphorus fertilizer application and all manure handling losses. The fifth scenario (S5) proposes the elimination of fertilizer input along with an 80% reduction in current wastewater P effluent. Finally, the sixth scenario (S6) involves no fertilizer application combined with a 20% reduction in soil phosphorus erosion.

3.4 Results and Discussion

I used the ELEMeNT-P framework to study 45 catchments and understand the effect of legacy phosphorus across a diverse landscape. First, we analyzed the historical P surplus trajectory in Lake Erie Basin watersheds. Then, we explored its connection with P accumulation trajectories.

3.4.1 Model Performance

The models were able to capture TP loads across all 45 watersheds over 110 years (**Figure 3.4**), with a median Kling-Gupta Efficiency (KGE) value of 0.71 (IQR 0.55 to 0.75) and a median Percent Bias (PBIAS) of 4% (IQR of 1.8% to 8%) (**Table S1 in Appendix B)**. This suggests a good predictive capacity for a parsimonious model (Ilampooranan, 2019).

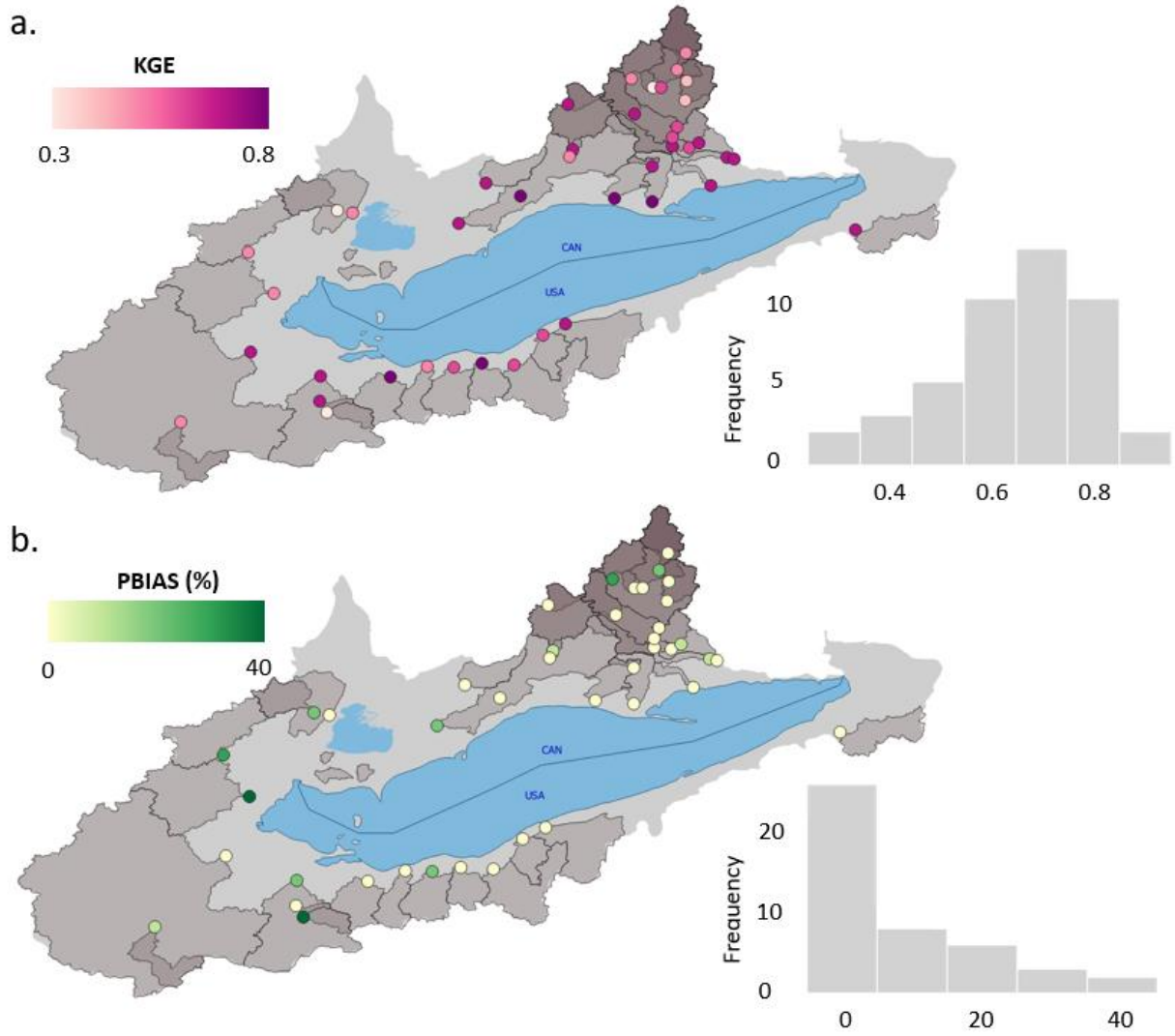


Figure 3.4: Model performance for 45 studied Lake Erie watersheds. a) Distribution of median KGE for each sub-watershed's ensemble runs. b) Distribution of median percent PBIAS for each sub-watershed's ensemble runs

Four sub-watersheds—Clinton (U1), Canagagigue (C3), and two in Speed River (C6, C13)—displayed KGE values below 0.5. The Clinton River Watershed in the USA had a KGE value of 0.32 and a PBIAS of 0.25 (**Figure 3.4 and Table S1 in Appendix B**). This watershed is primarily urban and located near Detroit, which likely contributed to the challenges in accurately representing P loading dynamics and resulted in lower KGE scores.

3.4.2 Phosphorus Fluxes and Stores

3.4.2.1 Estimation of Stream P Loading for Over 100 Years

The modeled phosphorus load provides valuable insights into historical phosphorus use within the basin. To simulate the loading in the 45 watersheds of the Lake Erie Basin (LEB) from 1900 to 2016, we used the ELEMeNT-P model (**Figure S2 in Appendix B**). This simulation is based on observed P load and historical phosphorus input to the landscape. From 1900 to 1945, the simulated average riverine phosphorus loads were approximately 0.35 kg-P $ha^{-1}year^{-1}$, with a range from 0.04 kg-P $ha^{-1}year^{-1}$ to 1.7 kg-P $ha^{-1}year^{-1}$. This period experienced relatively low P inputs to the watershed, likely due to the impacts of the World Wars and the Great Depression (Smiley, 2002).

Following World War II, the North American economy and population experienced significant growth (Field, 2011), coinciding with the advent of the Green Revolution. During this period, the availability and use of synthetic P fertilizers increased dramatically (Tilman, 1998), leading to a notable rise in phosphorus inputs into the watersheds. Our analysis reveals that the median P load began to increase from 1945, aligning with the post-war revolution era, and has continued to rise within the Lake Erie Basin. Between 1945 and 2011, the median P load to Lake Erie watersheds surged nearly fourfold, ranging from 0.38 kg-P $ha^{-1}year^{-1}$ to 1.48 kg-P $ha^{-1}year^{-1}$. This significant rise is particularly evident in the agricultural watersheds of Lake Erie, as shown in **Figure 3.5a, b and c**.

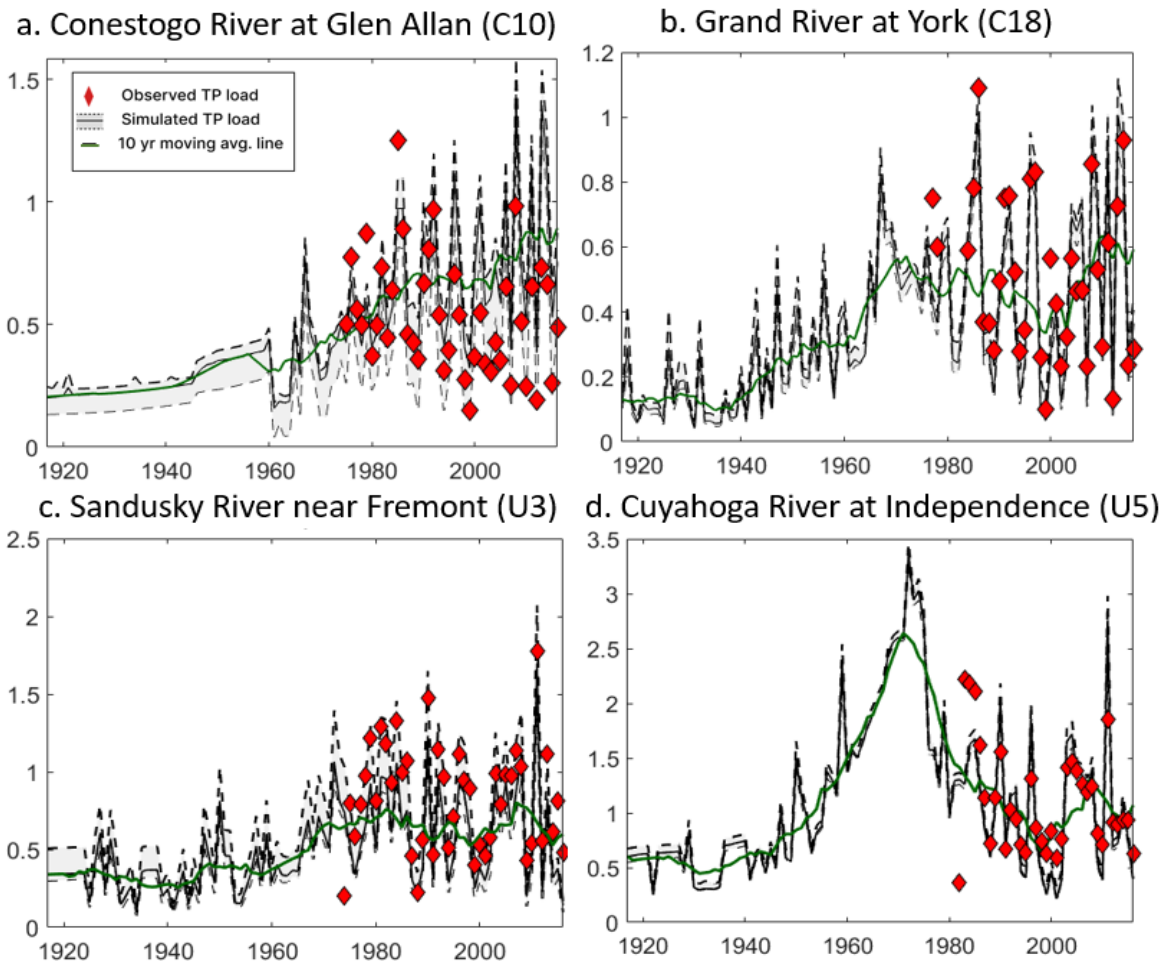


Figure 3.5: Modeled and measured loading at the watershed outlet from 1920 to 2016. The grey bounds represent the upper and lower limit of loading, the green line represents the 10-year moving mean of simulated TP load and the red points represent the observed TP load. Load trajectory for a) Conestogo River Watershed at Glen Allan, ON (C10) with 81% agricultural area; b) Grand River Watershed at York, ON (C18) with 68% agricultural area; c) Sandusky River Watershed at Fremont, OH (U3) with 81% agricultural area; and d) Cuyahoga River at Independence, OH (U5) with 17% agricultural area.

In contrast, a peak in phosphorus load was observed in 1972 in the urban watersheds of the Lake Erie Basin. For instance, the Cuyahoga River at Independence experienced P loading of approximately 3.5 kg-P $ha^{-1}year^{-1}$ (**Figure 3.5d**). This peak was followed by a subsequent decline, largely due to the enactment of the Clean Water Act and the associated ban on phosphorus in detergents in the early 1970s (Litke, 1999); (Us Epa, 2012).

3.4.2.2 P Accumulation across the Lake Erie Basin

The trajectories of phosphorus accumulation and its distribution across different landscape pools in the LEB have evolved due to varied land management practices in the watersheds. The modeled results estimate the magnitude of phosphorus accumulation in various stores throughout the Lake Erie Basin. We estimated storage in four different landscape compartments: soil, groundwater, landfills, and the river network (including reservoirs, riparian zones, and stream beds). We analyzed individual watershed phosphorus accumulation trajectories for these four landscape compartments from 1900 to 2016 (**Figure S4 in Appendix B**). For this discussion, we will first focus on the cumulative accumulation of phosphorus from 1900 to 2016 in the two largest watersheds of LEB: the Maumee River Watershed in Waterville (MRW), Ohio, and the Grand River Watershed at York (GRW), Ontario (**Figure 3.6**).

Our results suggest that, from 1900 to 2016, both MRW and GRW watersheds have served as a net sink for P, with an estimated accumulation of 276 Kg-Pha^{-1} and 600 Kg-Pha^{-1} respectively (**Figure 3.6a,f)**. Our findings, indicating that 80% of legacy P is accumulated in the soil, align with Sharpley et al. (2013) and Van Meter et al. (2021), which demonstrate that P accumulation in agricultural soils is the most pervasive source of legacy P to the environment and the largest sink within watersheds. Specifically, the GRW has 89% in the soil pool, 6.5% in landfills, and 4.5% in the riparian zone. These percentages align with a previous study by Van Meter et al. (2021), which reported similar soil P pool accumulation and distribution. The MRW has 82% in the soil pool, 10.5% in landfills, 5.5% in the riparian zone, and 2% in the groundwater pool.

The MRW has accumulated 226 Kg-P ha^{-1} of phosphorus in the soil. Of this total, model results suggest that 57% is in the form of organic phosphorus, while the remaining phosphorus exists in irreversible sorbed (7%) and reversible sorbed (36%) forms (**Figure 3.6b**). Our simulation results for the Maumee watershed reveal approximately 75 Kg-Pha^{-1} (127 Kton) of phosphorus in the inorganic soil pool. These findings align with soil tests conducted in nearby watersheds, as reported by Muenich et al. Muenich et al., (2016), which observed phosphorus accumulations ranging from 21 to 71 ppm (approximately 90-301 Kton). In the case of GRW, 532 kg-P/ha has accumulated in the soil legacy pool. Model results indicate that approximately 38% of this is soil organic phosphorus, with the rest being irreversible sorbed (38%) and reversible sorbed (24%) forms aligned with number form (Van Meter et al., 2021) (**Figure 3.6g**).

Further investigation into soil accumulation trends reveals two distinct rates: pre-1950 (slope ~1.1) and post-1950 (slope ~5). This indicates that the rate of soil accumulation in LEB increased nearly fourfold after 1950, likely due to the excessive application of fertilizers beyond crop demand. However, after 1990, the rate of soil accumulation decreased for MRW (**Figure 3.6b**), potentially due to increased awareness and the implementation of various best management practices.

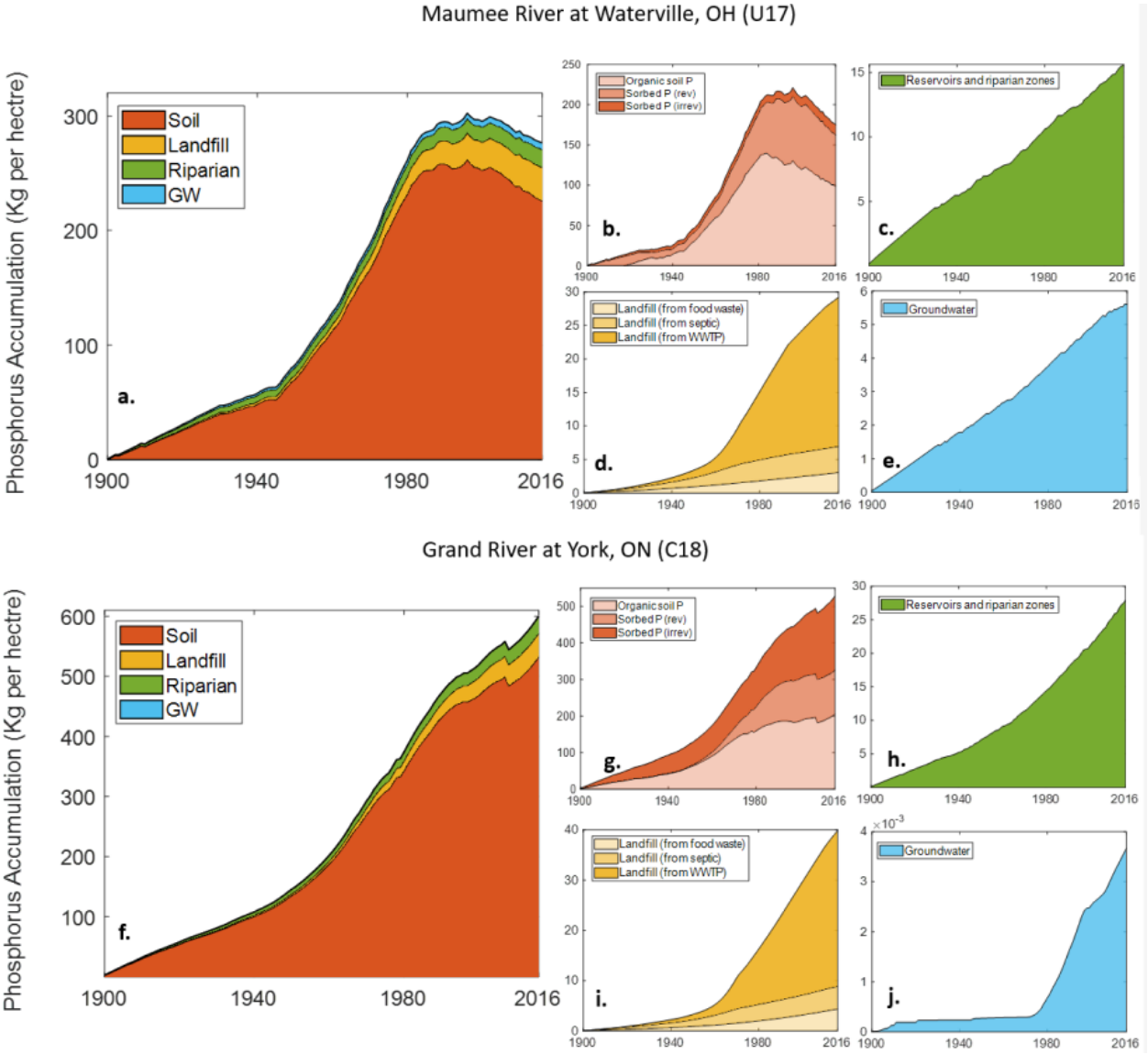


Figure 3.6: Phosphorus accumulation trajectory (kilogram per hectare) in the landscape compartments for two major watersheds in the Lake Erie basin, 1900–2016. [panel a-e] Maumee

River watershed at Waterville, OH, USA; [panel f-j] Grand River watershed at York, ON, Canada.

Landfills serve as the second large sink for excess P after the soil pool. Food waste, septic tank sludge, and outflow from WWTPs contribute to the P pool in landfills, with WWTPs being the primary source (>75%). The accumulation magnitudes of landfill pool have increased over time due to both population growth and enhanced phosphorus removal rates at WWTPs (Nicholls et al., 2001). Model results indicate that approximately 10% of landfill phosphorus can be attributed to food waste, and 8% to septic tank sludge. Some researchers suggest that landfill pool may eventually become an important source of reusable phosphorus as conventional global sources of mineral phosphorus begin to fall short of human demand (Dawson et al., 2011; Haarstad et al., 2016).

Riparian zones and reservoir areas serve as significant legacy phosphorus pools in the Lake Erie Basin, following landfills and soil pools, especially in watersheds with instream reservoirs and dams (Maavara et al., 2020). These reservoirs, riparian zones, and stream beds accumulate phosphorus transported by erosional processes. The analysis indicates an increase in phosphorus accumulation in these areas post-1900. Specifically, the GRW exhibited a phosphorus accumulation of 28 Kg ha^{-1} (**Figure 3.6**c) in riparian zones, comparable to sediment core findings of 35 Kg ha^{-1}. While groundwater is not a major source of phosphorus pollution, it has accumulated only 2 Kg ha^{-1} of P in the groundwater pool since 1900 in MRW (**Figure 3.6e**). Nonetheless, groundwater can contribute to elevated instream phosphorus concentrations, especially during periods of low (Welch et al., 2010).

In **Figure 3.7**, we illustrate the outlet total phosphorus load along with the distribution across four landscape compartments for all watersheds of the LEB since 1900. Our model estimates that a median of 13.5% (IQR 8% to 22%) of accumulated phosphorus has been exported to downstream waters via the watersheds of LEB since 1900. Major watersheds such as the Cuyahoga River at Independence (CRW), the Maumee River Watershed (MRW), the Thames River at Thamesville (TRW), and the Grand River Watershed (GRW) have exported 22%, 26%, 15%, and 6% of accumulated phosphorus, respectively (**Figure 3.7a-d**). These values are consistent with previous findings on phosphorus export and retention. For instance, riverine phosphorus fluxes in the Baltic Sea region range from 3% to 23% of catchment net phosphorus inputs (Hong et al. 2012).

Similarly, in the Lake Erie and Lake Michigan watersheds, these fluxes ranged from 3% to 25% of net inputs between 1974 and 1992 (Han et al. 2011).

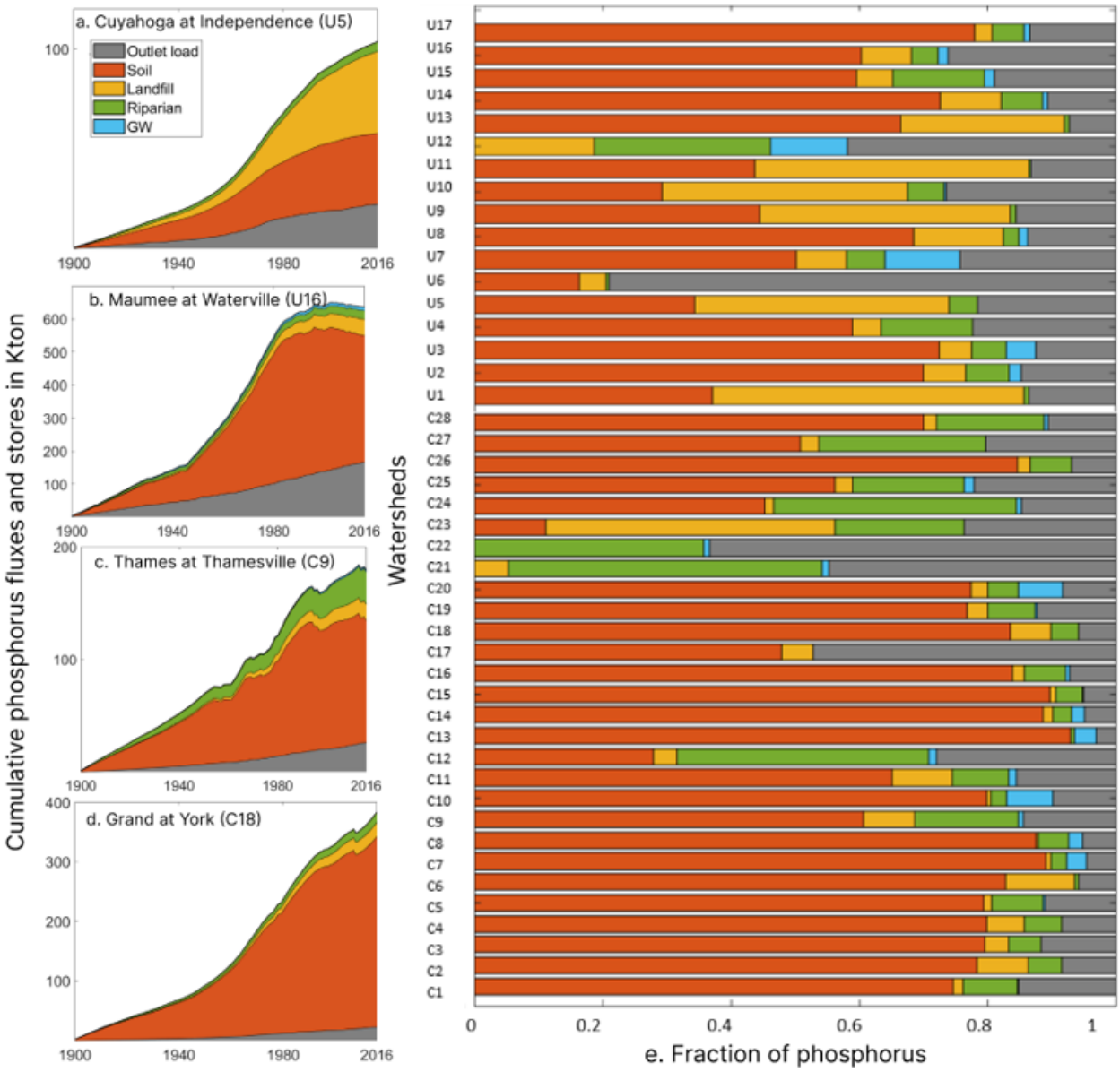


Figure 3.7: Fate of applied P since 1900. [panel a-d] Trajectories of P Flux and P stores in different land compartments for four major watersheds in the Lake Erie basin- a) Cuyahoga River watershed at Independence (U5), b) Maumee River watershed at Waterville (U16), c)

Thames River watershed at Thamesville (C9), and d) Grand River watershed at York (C18). [e] The proportion of P attributed to fluxes and stores in all modelled sub-watersheds.

Despite having a similar percentage of agricultural land (~70%), the GRW, MRW, and TRW exhibited different riverine export rates. This discrepancy is partly due to the higher proportion of tiled areas in the MRW (65%) and TRW (60%), compared to 37% in the GRW. The increased tiled area, along with conservation tillage practices, enhances the flushing of phosphorus, resulting in shorter travel times and greater phosphorus export (**Figure S5 in Appendix B**). This finding aligns with studies such as Jarvie et al. (Jarvie et al., 2017), which emphasize the impact of agricultural practices on phosphorus mobility.

Similarly, the high export of phosphorus in the CRW is attributed to point sources, as this densely populated watershed contains industries and dense urban zones, with only 17% agricultural area (**Figure 3.7a**). Consequently, the watershed has 60% phosphorus accumulation in the landfill compartment. Additionally, Cattaraugus Creek exhibits the highest phosphorus export rate at 79% (**Figure 3.7e**). This is due to its extensive forest cover (58%) and predominantly rural landscape, which limit agricultural activity and thus reduce phosphorus retention in the soil (NYSOGS, 2022). This comparative analysis indicates that explaining legacy accumulation based solely on present land-use practices is challenging. Other factors, such as historical land practices, land conversions, soil type, and canopy cover, may also significantly impact phosphorus accumulation.

3.4.3 Future Scenarios

To address the recurring harmful algal blooms in the western basin and hypoxia in the central basin of Lake Erie, the International Joint Commission (IJC) proposed a target of a 40% reduction in total phosphorus (TP) and dissolved reactive phosphorus (DRP) loads by 2025, based on 2008 levels (Team, 2015; Wilson et al., 2019). However, from 2008 to 2018, no improvement was observed in the basin-scale TP load. In fact, in 2018, the basin load increased to 11,800 tonnes per year from the 2008 level of 10,500 tonnes per year (Environment et al., 2020). Understanding future scenarios can provide valuable insights into the current phosphorus levels, the timeframe required to achieve the desired reductions and the feasibility of these reduction targets.

We generated six future scenarios for all our study watersheds and estimated the percentage of load reduction by the year 2045 from the level of the 2018 load (**Table S2, Appendix B**). Here, we illustrate and discuss in detail two major watersheds in the Lake Erie basin: the Maumee River Watershed (MRW) in the USA and the Grand River Watershed (GRW) in Canada, with interventions starting in 2018. Land use and population trends for the other watersheds are similar to those on both the USA and Canadian sides of the Lake Erie basin.

The results of these simulations first show that with business-as-usual practices (S1), meaning no changes in current management practices, we observed two opposite trends for the MRW and GRW watersheds. The MRW showed a 19% decrease (**Figure 3.8a**) in phosphorus load, while the GRW experienced a 15% increase (**Figure 3.9a**) by 2045. The decrease in MRW is due to improved phosphorus use efficiency (PUE) with better nutrient management. In contrast, the increase in GRW is due to the continued accumulation of P in agricultural soils, reservoirs, and riparian zones, leading to higher annual export of legacy particulate P through erosion. Thus, maintaining the current P surplus will result in increases in legacy P stores and modest annual rises in riverine P loads over the next two decades in GRW.

In the second scenario (S2), we simulate a situation where no additional fertilizer is applied to the landscape. This scenario resulted in a dramatic drop in P loading for all agricultural watersheds. Particularly in the GRW, we observed phosphorus use efficiency (PUE) increased from 59% to 100%, with a 4% decrease in P loading (**Figure 3.9b**). Notably, 100% PUE is desired for the sustainable management of the crop-soil system. For the MRW, we observed a 33% decrease in P load with a threefold increase in PUE (**Figure 3.8b**). These significant reductions in P load indicate that limiting fertilizer application and allowing plants to reuse existing soil P may be an effective management strategy.

The third scenario involves eliminating all manure handling losses. This approach provides decreases in phosphorus loads in GRW from a 15% increase to a 20% decrease (**Figure 3.9c**), even without changes in overall phosphorus use efficiency (PUE). In MRW, it showed a 25% decrease in P load (**Figure 3.8c**). These results suggest that managing manure housing and storage losses can significantly reduce P loading. Typically, about 3% to 7% of manure P is lost to runoff during storage (Lin et al., 2017; Magdoff et al., 2009; Oenema et al., 2007). This loss can be higher

if practices like winter manure spreading or cattle grazing are allowed (Bhandari et al., 2021; McDowell et al., 2007). However, even after a large decrease in P loading due to improved manure handling, riverine P loads showed to increase again (**Figure 3.9c**). This is due to the continued accumulation of P in agricultural soils, reservoirs, and riparian zones, and the ongoing contributions of this legacy P to riverine loading. Our fourth scenario aims to enhance PUE together with eliminating manure handling losses to prevent the rise in riverine loads observed in the third scenario.

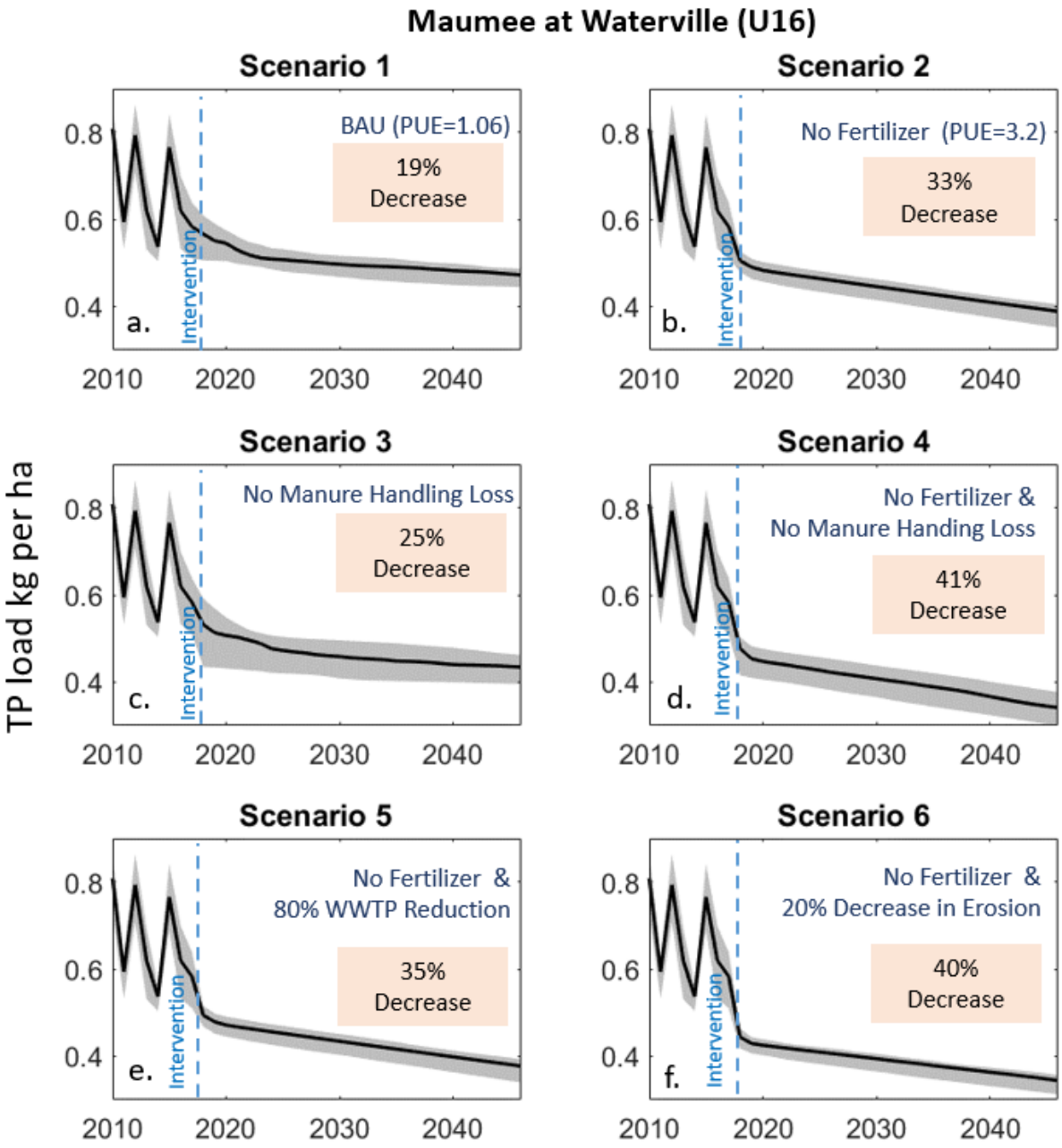


Figure 3.8: Change in P load (2018 -2045) for Maumee River Watershed at Waterville, Ohio, under six simulated future scenarios.

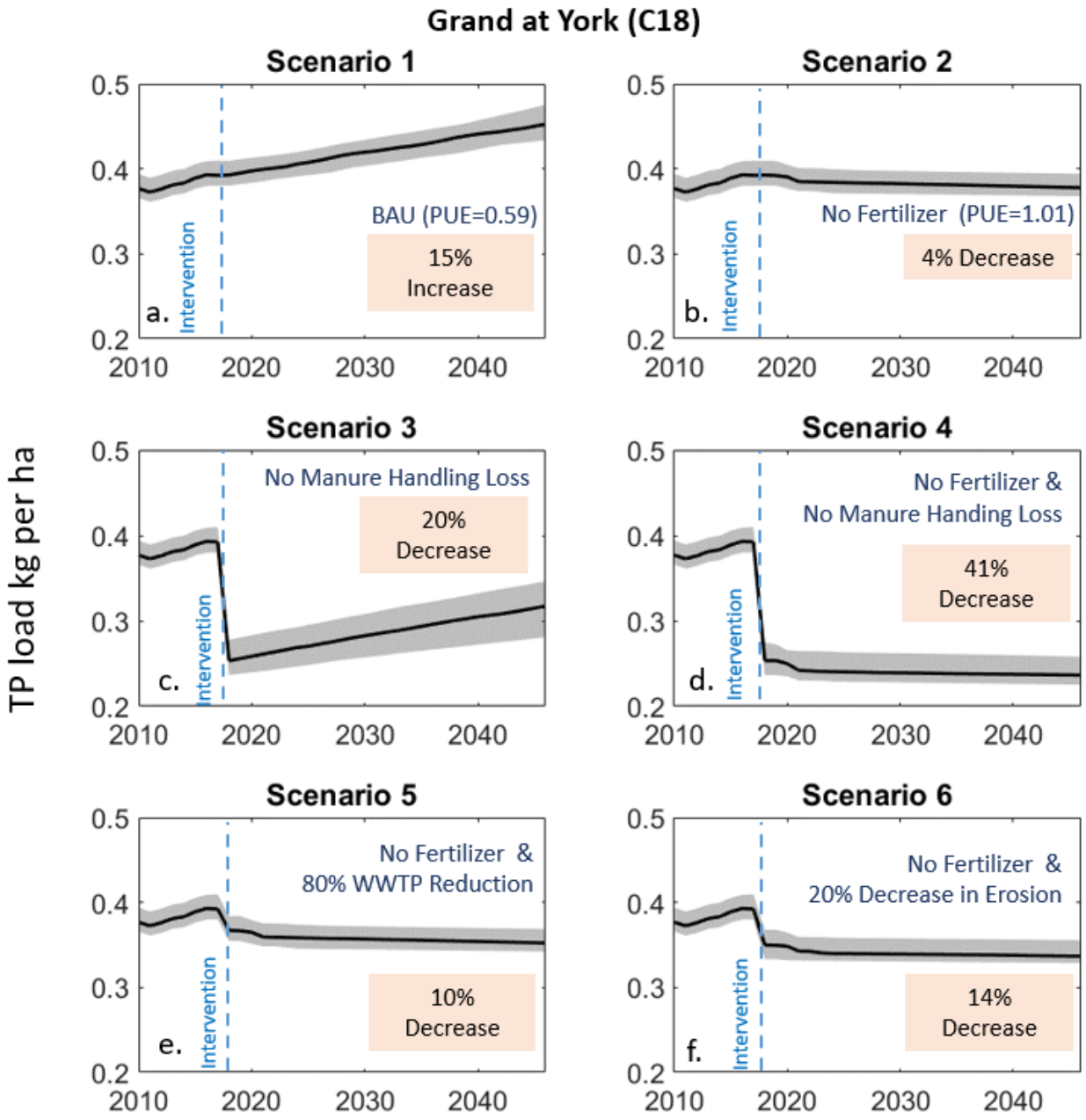


Figure 3.9: Change in P load (2018 -2045) for Grand River Watershed at York, Ontario, under six simulated future scenarios.

In the fourth scenario fertilizer application is ceased and manure handling loss is eliminated, as a result, we observe the highest reduction of P load for MRW and GRW. Under the 4th scenario, both GRW and MRW showed approximately a 40% decrease by 2045 (**Figure 3.8d, Figure 3.9d**). These results suggest that management of manure housing and storage losses addition to limiting

fertilizer application may be one of the most powerful tools available to achieve substantial reductions in P loading to downstream waters in the Lake Erie basin.

The fifth scenario involves upgrading to a more efficient wastewater treatment plant (WWTP), which may not significantly impact a highly agricultural basin like the Lake Erie Basin. However, when combined with the no fertilizer scenario, we observed a reduction in phosphorus loads, particularly significant for urban watersheds like Cuyahoga in Cleveland and Clinton in Detroit, where notable P reductions were observed. Alternatively, in the sixth scenario, WWTP loads are kept constant while agricultural management practices are implemented to achieve a 20% reduction in soil P erosion. The results showed a reduction of 14% in P load for the Grand River Watershed (GRW) (**Figure 3.9f**) and 40% for the Maumee River Watershed (MRW) (**Figure 3.8f**). This reduction can be achieved by adopting well-recognized practices such as reduced tillage, reinforcing stream banks, utilizing non-perforated tile systems, implementing cover crops, and other applicable methods (Aronsson et al., 2016; Basche et al., 2016; Duncan et al., 2019; Seitz et al., 2018; Zaimes et al., 2019; T. Q. Zhang et al., 2017).

3.5 Conclusion

In this chapter, we utilized the ELEMeNT-P model to simulate long-term phosphorus dynamics in 45 sub-watersheds of the Lake Erie Basin, by taking the legacy P accumulation into account. By incorporating long-term data and a mechanistic approach, the model effectively addressed gaps in traditional mass-balance models, providing deeper insights into P accumulation and depletion within the landscape. This approach allowed us to identify the magnitudes and locations of legacy P accumulation, evaluate the contributions of various landscape stores, and assess the timeframes and measures needed to reduce P loading in human-impacted watersheds.

Our findings revealed significant variability in P dynamics across the sub-watersheds, influenced by historical land use, agricultural practices, and human activities. The ELEMeNT-P model successfully captured P loading trajectories, showing that 80% of legacy P stores are found in soils, which form the largest component of this legacy. This legacy P can potentially serve as a resource for crop growth, allowing for reduced fertilizer application rates. In contrast, legacies in the riparian zone and groundwater, although smaller, require downstream control measures such as wetlands and riparian buffers to mitigate their impact on surface water quality.

These insights are further supported by future simulations, which reveal differing load trajectories for watersheds in the US and Canada. Despite aggressive management practices, reducing P loads remains challenging due to legacy phosphorus stores in the landscape. While Canadian watersheds face significant difficulty in achieving reduction targets, some US watersheds show promising trends of decreasing P loads, suggesting potential for effective nutrient reduction strategies. This study underscores critical policy implications for enhancing water quality, emphasizing that legacy phosphorus in the soil presents a major obstacle to meeting water quality goals in the Lake Erie watersheds.

Continuation of current management practices is likely to result in increased P loads in many watersheds over the next 25 years, particularly on the Canadian side. Simply reducing P fertilizer use will not suffice to achieve the targeted P load reductions, especially for Canadian watersheds. While reducing P fertilizer use is essential to prevent further P accumulation, additional measures are necessary in many watersheds. These include erosion control and reducing manure handling losses, which are imperative to meet current policy goals. One of the most significant findings of this study is the immediate and substantial impact of reducing fertilizer application and improving manure handling practices on stream total phosphorus loads.

In conclusion, our research findings hold significant implications for watershed management aimed at minimizing lag times and achieving water quality targets, particularly regarding phosphorus in agricultural watersheds. First, our study shows that improving water quality after implementing conservation measures takes many decades. Policy decisions should consider these long timelines to effectively address water quality issues. Our findings suggest that management efforts may benefit from focusing on legacy hotspots—areas with the highest accumulation of phosphorus—rather than adopting a one-size-fits-all approach. By targeting specific sites, we can speed up water quality improvements and achieve measurable success. This targeted approach is more efficient and can produce faster and more significant results. Finally, achieving lasting water quality improvements requires ongoing long-term nutrient management plans. Evidence from targeted strategies can help guide future efforts to reduce phosphorus loading in streams. Our study highlights the need for tailored management approaches and persistence in addressing water quality issues over extended periods.

Chapter 4

Pan Canada Phosphorus Budget: Insight from a 60 Year Dataset

4.1 Background

The increase in phosphorus levels in the environment, driven by agricultural intensification and population growth, poses significant risks to human health and aquatic ecosystems. One major consequence of increased phosphorus levels is the formation of algal blooms, including harmful algal blooms (HABs). These blooms negatively impact water quality, biodiversity, and the provision of ecosystem services (Lin et al. 2024; Amorim and Moura 2021). Given that phosphorus is often the critical limiting nutrient in freshwater environments, addressing phosphorus contribution from different sources is crucial for preventing freshwater eutrophication (Smith and Schindler 2009; Elser et al. 1990; Paerl et al. 2018).

Globally, the widespread use of fertilizers and manure in agriculture is a major contributor to this eutrophication (Kirchmann and Thorvaldsson 2000; Sattari et al. 2012; Stackpoole et al. 2019; MacDonald et al. 2011; Haygarth et al. 2014). Agricultural runoff reflects not only current farming practices but also the release of legacy phosphorus, accumulated in soil and other landscape compartments over decades due to past applications of fertilizers and manure (Reid and Schneider 2019; Sharpley et al. 2013; van Bochove et al. 2012; Stackpoole et al. 2019; Van Staden et al. 2022; Van Meter and Basu 2015; Jarvie et al. 2013). This continual discharge of legacy phosphorus can cause blooms and diminish the effect of nutrient reduction actions (Van Meter et al. 2021; Stackpoole et al. 2019). In this chapter, we focus on Canada, which has a long history of algal blooms across human-impacted areas throughout the country.

In Canada, home to over a million freshwater lakes and numerous ponds, severe water pollution issues are exacerbated by population growth, increasing farming activity and northern warming, (Pick, 2016; David W. Schindler et al., 2006; D. W. Schindler, 2001). Farmlands in Canada, which make up about 0.6 million km² (6.2% of the land area of Canada), are predominantly located in the southern parts of Ontario, Quebec, and Prairie region (AAFC, 2023). These agricultural areas are often near significant water bodies, such as the Great Lakes in Ontario, the St. Lawrence River basin in Quebec, Lake Winnipeg, which are susceptible to harmful algal blooms due to phosphorus

runoff from adjacent farmlands. According to Environment Canada (2011), from 2005 to 2007, 32% of surface water quality monitoring sites in Canada exceeded the phosphorus guideline more than half the time. This has had devastating consequences for biodiversity, water quality, and economies. For instance, Smith et al. (2019) showed that HABs in Lake Erie cost the Canadian government around $272 million annually.

Algal blooms are not a recent phenomenon in Canada; the country has experienced a significant history of cyanobacterial blooms since the 1970s. Several notable lakes with a history of multiple algal blooms include Lake Champlain, Lake Ontario, Lake Erie, the St. Lawrence River, and the Lake of the Woods (Becker et al., 2009; Budd et al., 2001; Favot et al., 2023; Pick, 2016; Vincent et al., 2004; Winter et al., 2011), Among these, Lake Winnipeg stands out, having been labelled "Canada's sickest lake" by a national newspaper in 2013, and it is frequently cited as one of the world's most threatened lakes (Ali et al., 2019). Research showed increasing agricultural activities in the prairie region, loss of wetlands, and shifts in the hydrological regime are causing accelerated eutrophication in Lake Winnipeg (David W. Schindler et al., 2012). Similarly, algal blooms are common in the fall near lakes in Western Quebec (LeBlanc et al., 2008), and from 2004 to 2010, blooms were reported in various water bodies (24 to 150) in Quebec Province (Pick, 2016; MDDEFP, 2014). The St. Lawrence sub-basin is experiencing increasing events of eutrophication and hypoxia due to invasive farming, urbanization, and global warming. (Altieri et al., 2015; Glibert et al., 2014; Goyette et al., 2016). In Ontario, cyanobacteria blooms are more common near Lake Erie, Quitine Bay in Lake Ontario, and the Georgian Bay ecoregion (Favot et al., 2023; Nicholls et al., 2011; Watson et al., 2008), with the Bay of Quinte also suffering from persistent blooms and frequent shoreline advisories in the summer (Favot et al., 2023; Nicholls et al., 2011; Watson et al., 2008). Additionally, the transboundary Lake of the Woods, shared by Manitoba, Ontario, and Minnesota, has experienced annual blooms over the past decades, despite a threefold decrease in total phosphorus delivery from point sources since the 1970s (Macgillivray et al., 2023). Prolonged warming of the lake is thought to be contributing to an increased number of blooming events. (Macgillivray et al., 2023; Pick, 2016). While toxic blooming events less common in British Columbia compared to other provinces, they still occur and have led to the issue of health advisories and cases of fish and animal fatalities (Jacoby et al., 2007; Kotak et al., 2007; Pick, 2016). The persistence of these issues across Canada underscores the need for a deeper

understanding of phosphorus budgets and management strategies, which are critical for mitigating eutrophication and its impacts on aquatic ecosystems.

The contemporary P budgets cover a range of spatial scales, periods, and coarse resolutions. Many P budget studies have been conducted for the USA (Sabo et al., 2021; Sprague et al., 2012; Stackpoole et al., 2019; Swaney et al., 2019c) at various regional and temporal scales, while few P studies have been conducted for Canada. In Canada, phosphorus budget studies are primarily compiled at the provincial, watershed, or basin scale (Bruulsema et al., 2011; IPNI 2011; Wang et al., 2022; Goyette et al, 2016). Notable provincial scale studies on the Canadian P budget were either developed for one or two provinces or the entire country with various temporal scales (Bruulsema et al., 2011; IPNI, 2014; Wang et al., 2022). These studies are useful for understanding P trends over a broad spatial time scale; however, the data's coarse resolution is insufficient for watershed-scale or more detailed studies. In contrast, there are several basin-scale (S. Bittman et al., 2017; Goyette et al., 2016) and provincial-scale (T. L Van Staden et al., 2022) studies use county data to examine P accumulation and loss within specific regions over time. Additionally, there are few county scale studies (Reid, Schneider, et al., 2019; van Bochove et al., 2012) that take county scale data and re-allocate it into Soil Landscape of Canada (SLC) (Agriculture et al., 2013) polygon as a proxy of soil test P. These studies, however, did not publish data and do not explicitly account for historical county boundary changes. P budget studies were also conducted on global scale for different time periods (Chen et al., 2016; MacDonald et al., 2011; Mekonnen et al., 2018) which often helps to quantify the history of P losses in Canada and compare the efficiencies across the globe. Some notable P budget studies of Canada are tabulated in the following table

Table 4.1: Table for Canadian mass balance studies at different spatial and temporal scales

Spatial Extent	Temporal Extent	Limitation	Citation
Provincial Scale	1961-2018	Coarse scale	Wang et al., 2022
Provincial Scale	1973-2013	Coarse scale	IPNI, 2011
Watershed Scale Lower Fraser Valley, British Columbia	2011/2012	-Watershed scale -One year	S. Bittman et al., 2017

Watershed Scale St. Lawrence sub-basin	1901-2012	-Watershed scale	Goyette et al., 2016
County Scale Data re-allocated to SLC polygon scale	1981 to 2006	-limited resolution -agricultural inputs only	Van Bochove et al., 2012
County Scale Ontario	1961 to 2016	-limited to ON	Van Staden et al., 2022
County scale Canada	1981 to 2011	-limited temporal scale	Reid, Schneider, et al., 2019
Provincial Scale Ontario, Michigan, Ohio	1955-2008	-Only agricultural sources are considered	Bruulsema et al., 2011
Watershed Scale Lake of the Woods and the Rainy River catchment	1960-2009	-limited to point sources	Hargan et al., 2011
Zonal scale 2 productions; Manitoba and Ontario crop areas	-	-limited year -62 production zone in US and CA	Williams et al., 2022

In this chapter, we have developed a comprehensive phosphorus mass balance dataset at a pan-Canadian scale by aggregating county-scale data from various sources. This dataset covers over 6.4 million km2 of land area and excludes northern regions -Yukon, Nunavut, and the Northwest Territories due to minimal agricultural activities and challenging soil conditions characterized by extreme cold climates and prevalent permafrost. This dataset offers a long-term (1961-2021) estimate of the P budget at both county and 250-meter grid scales. It encompasses phosphorus inputs from fertilizers, livestock manure, domestic waste, and phosphorus uptake from crops and pasturelands. This dataset is the first of its kind to provide high-resolution estimates of phosphorus surplus and its components at both county-scale and 250-meter grid scales. Additionally, we have quantified legacy phosphorus accumulation across the Canadian landscape to identify and analyze hotspots requiring targeted intervention. This analysis aims to enhance the understanding and management of phosphorus dynamics in agricultural settings across Canada.

4.2 Materials and Methods

The Pan-Canadian scale dataset provides estimation on both the current and historical usage of phosphorus and its impacts across the nation. Our methodology integrates and builds upon existing datasets like the TREND dataset by Byrnes et al. (2020), which provides a long-term trajectory of nitrogen use in the conterminous USA, and the phosphorus mass balance study by Van Staden et al. (2022) focused on southern Ontario.

4.2.1 Dataset Preparation: County-scale Phosphorus Mass Balance

The components of the phosphorus mass balance were calculated for the census years (every 5 years) between 1961 to 2021 at a county scale, and across Canada. "We excluded territories northern Canada-Yukon, northwest territories and Nunavut from our analysis as the census does not report for these regions throughout the study period. Here, we describe our methods for estimating the different components of the mass balance, focusing on harmonizing methodologies between the US and Canada, and across diverse datasets that vary over time.

For our crop and livestock P fluxes analysis, we use data from the Statistics Canada Census of Agriculture, administered every five years. From the census data, we include 22 major crops and 10 livestock types in our analysis.

Table 4.2: Data summary for components of Pan-Canada P mass balance

P Surplus Component	Data Type	Data Source	Temporal Resolution	Spatial Resolution
Fertilizer (+)	Fertilizer Sales	Statistics Canada	1961-2021	Provincial
	Fertilized Area	Canadian Agricultural Census	1961-2021	Census Division
Livestock Manure (+)	Livestock Count	Canadian Agricultural Census	1961-2021	County

	Excretion and Consumption Value	USDA NRCS, 2008) Department of Agriculture	Constant	National
	Weight Factor	US Department of Agriculture	1961-2021	National
Domestic Waste (+)	Population Count	Canadian Census of Population	1961-2021	Census Division
	Dish Coeff.	Han et al., 2012	1961-2011	National
	Laundry Coeff.	Han et al., 2012	1961-2011	National
	Human Waste Coeff.	(Han et al. 2012)	Constant	National
	Food Waste Coeff.	Parfitt et al., 2010	Constant	National
Crop and Pasture Removal (-)	Crop Area	Canadian Agricultural Census	1961-2021	Census Division
	Crop Yield	Field Crop Survey-Statistic Canada	1961-2021	Provincial

4.2.1.1 Inorganic Fertilizer

To estimate county-scale phosphorus fertilizer rate in any given year, we used the provincial phosphate fertilizer application rate and the crop area of the county. The provincial fertilizer rates

($R_{fert,p}$) were calculated using the mass of phosphate obtained from provincial sales data and the total crop area of the province. The provincial phosphate fertilizer sales data, reported in metric tons, were sourced from Statistics Canada (Government of Canada et al., 2013). The provincial crop area was calculated by summing the areas of all major field crops listed in **Table S4 in Appendix C**, as reported in the Census of Agriculture by Statistics Canada, with measurements provided in hectares.

$$R_{fert,p}(t) = (M_{fert,p}(t) / A_{crop,p}(t)) * 1000 * 0.43 \quad \text{(Eq. 4.1)}$$

Where, $R_{fert,p}(t)$ is the provincial fertilizer application rate in kg per hectare in t year, $M_{fert,p}(t)$ is the mass of P fertilizer sold in *t* year in the province, $A_{crop,p}(t)$ is the total crop area of the province in *t* year and 0.43 is the conversion of P from phosphate (IPNI, 2014).

Finally, county-scale total phosphorus fertilizer (*FERT)* in kg-P/yr is estimated using the following equation assuming that all fertilizer sold within each province was applied onto the farmland within that year.

$$FERT(i,t) = R_{fert,p}(t) * A_{crop,c}(i,t) \quad \text{(Eq. 4.2)}$$

Where, $R_{fert,p}(t)$ is the provincial fertilizer application rate in *t* year, and $A_{crop,c}(i,t)$ is the crop area for *i* county in *t* year.

To ensure data consistency across census years, we addressed inconsistencies in the phosphate fertilizer sales data with two key estimations. The first estimation dealt with missing phosphate sales data for 2016 in British Columbia (BC). We calculated the average phosphate-to-nitrogen fertilizer sales ratio for BC using data from 2021, 2011, and 2006. We then used this average ratio to estimate the missing phosphate fertilizer sales for 2016 by multiplying it with the nitrogen fertilizer sales data for that year.

$$M_{fert,BC}(2016) = mean\left(\frac{Pfert,BC(2006)}{Nfert,BC(2006)} + \frac{Pfert,BC(2011)}{Nfert,BC(2011)} + \frac{Pfert,BC(2021)}{Nfert,BC(2021)}\right) * Nfert,BC(2016) \quad \text{(Eq. 4.3)}$$

Where, $M_{fert,BC}(2016)$ is the estimated fertilizer mass for 2016 in metric tons for BC, $Pfert,BC$ is phosphate fertilizer mass and $Nfert,BC$ is nitrogen fertilizer mass in metric tonnes in year indicated by parenthesis.

The second estimation addressed the separation of fertilizer sales data for the Atlantic provinces (New Brunswick, Newfoundland and Labrador, Nova Scotia, and Prince Edward Island) as they are reported collectively. Using data from 1966, we established a scaling factor based on the ratio of each province's phosphate fertilizer sales to the combined total of all four provinces. This factor allowed us to estimate consistent phosphate fertilizer sales data for each Atlantic province throughout the census years.

4.2.1.2 P from Livestock Manure

Manure P inputs, MAN, refer to the phosphorus in urine and manure excreted by livestock. We grouped livestock data into ten different categories for our analysis: dairy cattle, beef cattle, other cattle (heifers, steers, bulls, and calves), broilers (broilers, roasters, and Cornish), other chickens (hens, pullets, chicks), turkeys, pigs, sheep and lambs, goats, and horses and ponies. All livestock inventory data originates from the Census of Agriculture provided by Statistic Canada and are reported at 5-year intervals. The grouping of the categories was done to ensure consistency with a parallel dataset being developed across the continental US by Byrnes et al.. To further maintain this consistency, we disaggregated the broiler and other chicken categories for some census years. To estimate the “other chicken” category from 1971-2021 we subtracted the number of broilers from the total number of chickens. Since the 1961 and 1966 censuses did not report broilers, the "total chickens" category in those censuses corresponds directly to our current definition of "other chickens." We also disaggregated total chicken for 1981, 1986 and 1991 to estimate broiler inventory for the years. According to the census of 1981, 1986 and 1991 total chicken category includes subcategories such as "Hens and Pullets 20 weeks and over," "Pullets and Pullet Chicks under 20 weeks," and "Other chickens." We assumed that broilers were included in the "Other chickens" subcategory on those three years. To estimate broiler numbers for those three missing years, we used the total chicken-to-broiler ratio from 1976 and scaled the total chicken numbers accordingly.

There are two types of data gaps in the census data: (1) livestock inventory for specific categories in certain counties is undisclosed due to privacy concerns, and (2) certain livestock categories are missing for a particular census year. The undisclosed livestock numbers were estimated by

calculating the difference between reported provincial-level livestock numbers and the sum of all reported county-level livestock numbers. This difference was then distributed among counties with missing data based on the ratio between county-scale and provincial-scale numbers for the nearest census year where data was available. The latter type of data gaps are filled by using the data from the most recent year for which there is existing data for that county and livestock type (Falcone, 2021). However, there are exceptional cases, such as the broiler numbers for the years 1961 and 1966, where no data was available prior to the missing year 1961. For these years, broiler numbers were estimated using the rate of change in broiler consumption from 1971. We used the rate of broiler consumption (kg consumed) and live broiler weight (kg meat/chicken) from 1961 to 1971 to calculate per capita broiler consumption. We then estimated the percent change in per capita broiler consumption in 1961 and 1966 from the value of per capita broiler consumption in 1971. All the data were obtained from US broiler performance by the National Chicken Council (Surhone et al., 2011).

The phosphorus excretion rates per animal is influenced by animal weight, which has increased over time due to genetic evolution and improved feeding practices (Falcone, 2021). Recognizing the importance of these changes, we have adopted a methodology for adjusting livestock weights over time in our dataset, based on USGS methods (Falcone, 2021). In the current methodology, we use time-varying livestock weights based on the use of annual slaughtered livestock weight data (USDA NRCS, 2008). Reported weights were available for the period from 1961 to 2017, with any data gaps filled using linear interpolation. For years after 2017, we assumed no change in livestock weights. Since no time-varying weights were available for horses, their weight was assumed to remain constant throughout the study period. In this approach, 2008 was chosen as a base year due to the availability of phosphorus excretion parameters for 2008 livestock weights (USDA NRCS, 2008). Temporally varying, livestock type-specific scaling factors, $S_{wt}(j,t)$, were developed based on the ratio of the 2008 weight to the reported weight for any given year (**Table S2 in Appendix C**).

Phosphorus from livestock excretion (kg-P per animal per yr) are obtained by multiplying county scale livestock number with P content in manure and weight coefficient using the following equation

$$MAN\ (i,j,t)=INV(i,j,t) * p(j)_{lvstk,excr} * S_{wt}(j,t) \quad \text{(Eq. 4.4)}$$

Here, *MAN (i,j,t)* is the phosphorus excreted(*kg-P* y^{-1}*)* from livestock type j in county *i* for the year *t*. The variable $INV(i,j,t)$ is the number of livestock type *j* in county *i* for the year *t*, as obtained from Statistics Canada. The parameter $p(j)_{lvstk,excr}$ is the estimated P content in manure (kg-P $head^{-1}y^{-1}$) for livestock type *j* (**Table S1 in Appendix C)**, and $S_{wt}(j,t)$ is the time-varying scaling factor for livestock weights for livestock type *j* in year *t* (**Table S2 in Appendix C**). Both the phosphorus excretion ($p(j)_{lvstk,excr}$) and weight parameter, ($S_{wt}(j,t)$) were based on the USDA Agricultural Waste Management Field Handbook (USDA NRCS, 2008). Finally, the phosphorus excretion magnitudes for all of the livestock types were then aggregated to provide one annual, county-scale value:

$$MAN(i,t) = \sum_{j=1}^{n} MAN(i,j,t) \quad \text{(Eq. 4.5)}$$

where *n* is the number of different livestock types.

4.2.1.3 Domestic Waste

Domestic waste components include phosphorus waste from laundry and dish detergent usage, as well as phosphorus generated from human food consumption and food waste, with detailed methodology provided below.

Laundry and Dish Detergent

Detergent P was estimated based on per capita detergent use and P content in detergents. Total detergent P waste (*DET*) is estimated using the following equation

$$DET\ (i,t)= (\ DISH(t)\ *\ USE_{dish}(t)\ *\ P_{dish}(t) + USE_{laun}(t)\ *\ P_{laun}(t)) * POP(i,t)) \quad \text{(Eq. 4.6)}$$

Where, $DISH(t)$ is the fraction of households with dishwashers in year t, $USE_{dish}(t)$ represents the national detergent use per capita in year *t* (spoons per capita per year), $P_{dish}(t)$ denotes the phosphorus content in detergents in year *t* (kg of P per spoon),, $USE_{laun}(t)$ represents the laundry detergent use in year *t* (kg of laundry detergent use per capita per year), $P_{laun}(i,t)$ denotes the P content in the detergent in year *t* and (P per kg detergent), *POP (i,t)* is the population of *i* county in *t* year. Time-varying per capita laundry and dishwashing detergent use data were obtained from

Goyette et al., (2016), Han et al., (2012) and Van Meter et al., (2021) (**Table S3 in Appendix C**) and countyscale yearly population data were obtained from Statistic Canada.

Human Consumption and Food Waste

Human P consumption and food waste were estimated based on a constant human consumption rate. We assumed a constant human P consumption rate (P_{hum}) of 0.6 kg person^{-1} y^{-1} (Russell et al. 2008; Han et al. 2012) and food P waste is a constant fraction (P_{food}= 0.11) of food consumption (Parfitt et al., 2010). Here, it should be noted that a significant portion of human waste undergoes processing in wastewater treatment facilities or septic systems before being released into downstream waters. Quantifying these treatment trajectories is beyond the scope of the current work. The total P waste generated by humans,

$$HUM\ (i,t) = POP(i,t) * (P_{hum} + P_{hum} * P_{food}) \quad \text{(Eq. 4.7)}$$

Where, *HUM (i,t)* represents the total waste from humans in county *i* for the year *t*, *POP (i,t)* is the population for county *i* for the year *t*, P_{hum} is human P consumption rates and P_{food} is the fraction of food that goes into the landfill as food waste.

The total domestic P waste is calculated using the following equation

$$WASTE\ (i,t) = DET\ (i,t) + HUM\ (i,t) \quad \text{(Eq. 4.8)}$$

Where, *WASTE (i,t)* is the total domestic P waste generated from *i* county for *t* year, *DET (i,t)* is the total waste generated by detergent (**Eq. 4.6**), and *HUM (i,t)* is the P waste generated from human consumption and food waste (**Eq. 4.7**). All units are in kg-P y^{-1}.

4.2.1.4 Phosphorus Uptake

We define P uptake as the sum of crop and pasture P uptake, with methodology details below.

Crop P Uptake

The crop-specific, county-scale P uptake values in kg-P yr^{-1}, CROP (i,j,t), were calculated using the harvested area, $HARV(i,j,t)$, of each crop at the county level in hectares, by crop yield, $YIELD$ (p,j,t), at the provincial level in kilogram per hectare, by the crop-specific percent dry matter,

d(j), where applicable, and then by the crop-specific P uptake values, Pcrop(j) obtained from literature.

$$CROP\ (i,j,t) = HARV\ (i,j,t) \times\ YIELD\ \ (p,j,t) \times d\ (j)\ x\ P_{crop}\ (j) \qquad \text{(Eq. 4.9)}$$

Where, subscript *i* represents county, *j* represents crop type, *p* represents province and t represent year. Finally, the total phosphorus uptake for crops at the county scale, was calculated by adding together the uptake values for all crop categories.

$$CROP(i,t) = \sum_{j=1}^{n}\ CROP(i,j,t) \qquad \text{(Eq. 4.10)}$$

Here, n represents the number of crop types included in the study (n=22). We only included field crops in this dataset, which, according to the 2021 census, accounted for at least 94% of all crop and fruit tree areas across Canada. The dry matter values, and P uptake parameters for field crops are provided in supplemental **Table S4 in Appendix C**. County-scale annual crop area data, HARV(i,j,t), was obtained from the Census of Agriculture from Statistic Canada, which reports data for every 5 years.

To create a consistent crop category across these years, we have disaggregated hay categories for certain census years. In the 1986 census, hay was reported under one category, "All Tame Hay." However, in our dataset, we report "alfalfa" and "all other tame hay excluding alfalfa" separately. Therefore, we disaggregated the alfalfa and all other tame hay areas for 1986. To estimate the alfalfa area, we used the average ratio of alfalfa to "All Tame Hay" from the 1981, 1986, and 1991 data, with the remaining tame hay considered as all other tame hay excluding alfalfa. Additionally, from 2001 onwards, we further disaggregated "All other tame hay except alfalfa" because this category was modified to include fodder crops, becoming "All other tame hay except alfalfa and fodder crop." To separate fodder crops from this category, we scaled them using data from the years 1961, 1966, 1971, 1976, and 1981. In our calculations for fodder crops, we focused on three types: oats for fodder, barley for fodder, and other fodder crops. The scaling factor was derived from the mean ratio of these fodder crops over the specified years and applied to the "All other tame hay excluding alfalfa and fodder crop" category to disaggregate fodder crops and create a consistent category.

Like the livestock inventory census, the crop area census has two types of data gaps: (1) crop areas for specific categories in certain counties are undisclosed due to privacy concerns, and (2) certain crop categories are unreported for a particular census year. To estimate the undisclosed crop areas, we employed the methodology used by Byrnes et al. (2020), which involves calculating the difference between reported provincial-level crop area values and the sum of all reported county-level values. This difference was then apportioned among the counties with classified data, based on the ratio between county-scale and provincial-scale values from the nearest census years with reported data. When previous census year data were available for a county, we used the ratio between county-scale and province-scale values to apportion the missing data. For instance, to fill in the 1996 data gaps, we would first look at the ratios from 1991. If data from 1991 was missing, we would then use the data from 1986, and if that was unavailable, from 1981. This technique assumes that the proportion of crop areas in counties with classified data remains consistent over time.

In addition to the censored county-level data, certain crop categories were unreported in specific census years. These data gaps were addressed by using the data from the most recent year for which there is existing crop area data for that county. For example, crop areas for tobacco from 2011-2021, total beans from 2006-2021, other field crops from 1996-2001, lentils and triticale from 1961-1976 were estimated using the aforementioned gap-filling method.

Provincial-scale annual crop yield data, *YIELD* (p,j,t), was obtained from the Census of Agriculture from Statistic Canada, which reports data for every year. Similar to crop area data, some crop yield data were also unavailable. If crop yield data for a province is missing, we initially replace it with the national average yield for that year. If the national average is also missing, we use the provincial yield from the most recent available year. For instance, if the corn yield for Ontario is missing for 2001, we use the national average. If that is unavailable, we check Ontario's yield for 2000, and if that's missing, we use the 1999 value, and so on. The alfalfa yield is not reported separately in the provincial yield database; therefore, we estimate it using the yield values for tame hay. Additionally, tobacco yield data is also not included in the provincial yield database and is only reported for Ontario according to the Census of Agriculture. To address this, we obtained tobacco yield data from the Ontario Ministry of Agriculture, Food and Rural Affairs (OMAFRA), which has been reporting these values since 2004. Given the negligible reported tobacco areas

before 2004, we assume there was no significant tobacco cultivation prior to that year. For the "other field crops" category, where specific yield data is absent, we use the yield values of common field crop, such as barley, as a substitute.

Pasture P Uptake

Pasture phosphorus uptake is defined as phosphorus taken up by grazing livestock (cattle, horses, goats, and sheep), based on both the total area of available pasture and the population of grazing livestock within a given county. We used two types of pasture areas: improved pasture and unimproved or natural pastureland. Improved pasture is land that has been improved from its natural state by seeding, draining, irrigating, and fertilizing, whereas unimproved land for pasture is grazable land that has not been recently improved, including native pasture, native hay, rangeland, and grazable bush (Statistic Canada, 1981). After 1991, improved pasture is termed as tamed or seeded pasture in the Agricultural Census of Canada.

We used constant-area-based P uptake parameters for these two types of pastures (Swaney et al., 2019) to determine the amount of P uptake per hectare of pastureland. In certain cases, the P uptake values derived exceeded the estimated P consumption by grazing cattle, suggesting a potential overestimation of P uptake. Therefore, when the total P consumption by cattle in a county was less than the P uptake from pastures calculated using area-based methods, we adjusted the P uptake to match the cattle's P consumption. The following equation was used to calculate pasture uptake with the area-based method (**Eq. 4.10**). If consumption values exceeded the calculated maximum P uptake for the pasture area, values were capped at the area-based P uptake value.

$$\mathrm{PAST}_{\max}(i,j,t) = \mathrm{AREA}_{\mathrm{past}}(i,j,t) \times \mathrm{Y}_{\mathrm{past}}(j) \times \mathrm{PC}_{\mathrm{past}}(j) \qquad \text{(Eq. 4.10)}$$

Where $\mathrm{PAST}_{\max}(i,j,t)$ is the mass of P uptake by pasture land (Kg-P yr^{-1}) for pasture type j in county i in year t, $\mathrm{AREA}_{\mathrm{past}}(i,j,t)$ is the pasture area (hectare) for pasture type j in county i in year t, $\mathrm{Y}_{\mathrm{past}}(j)$ is the constant pasture yield (Kg ha^{-1}) for pasture type j, $\mathrm{PC}_{\mathrm{past}}(j)$ is the P content of pasture type j, in kg-P per kg of pasture per year. Then pasture types for both types were summed to calculate total P uptake from pastureland.

To estimate the maximum P consumption by grazing cattle, we employed consumption rates across different types of grazing livestock (**Table S5 in Appendix C**). We incorporated both spatial and temporal variations by considering the percentage of cattle reared in enclosures versus those grazing freely. This was achieved by applying a provincial confinement factor ($f_{conf}(i,j)$) (**Table S6 in Appendix C**), calculated using the levels observed in nearby states within the US (USDA NRCS, 2008). The equation for calculating the highest P consumption by livestock on pastures is

$$CONS_{max}(i,j,t) = (1-f_{conf}(i,j)) \times POP_{lvstl}(i,j,t) \times P_{cons}(j) \times W_{coeff}(j,t) \quad \text{(Eq. 4.11)}$$

Here, $CONS_{max}$ represents pasture consumption by livestock, $f_{conf}(i,j)$ is confinement factor for livestock type *j* in county *i*, $POP_{lvstl}(i,j,t)$ is number of *j* livestock type in *i* county for *t* year, $P_{cons}(j)$ is P consumption by *j* livestock type and $W_{coeff}(j,t)$ is weight coefficient (**Table S2 in Appendix C**). We assumed that horses, goats, and sheep were allowed to graze all year round ($f_{conf} = 0$).

All grazing consumption was then summed as total livestock pasture consumption, $CONS_{max}(i,t)$. To estimate the pasture P uptake the minimum between $PAST_{max}(i,t)$ and $CONS_{max}(i,t)$ is used.

$$PAST(i,t) = \begin{cases} PAST_{max}(i,t), & CONS_{max}(i,t) \geq PAST_{max}(i,t) \\ CONS_{max}(i,t), & CONS_{max}(i,t) < PAST_{max}(i,t) \end{cases} \quad \text{(Eq. 4.12)}$$

where $PAST(i,t)$ is the pasture uptake in kg-P per hectare per year for county *i* in year *t*.

Finally, phosphorus uptake ($UPTAKE(i,t)$) by crops and pasture was calculated from the following equation

$$UPTAKE(i,t) = CROP(i,t) + PAST(i,t) \quad \text{(Eq. 4.13)}$$

Where UPTAKE (i,t) is the sum of crop and pasture P uptake (Kg-P yr^{-1}) for all the categories for i county in year t. CROP (i,t) and PAST (i,t) are the crop and pasture P uptake for i county in t year respectively, in Kg-P yr^{-1}.

4.2.1.5 P Surplus

We calculated P surplus, which measures excess P in the landscape (Byrnes et al., 2020; Sabo et al., 2021). We define the county-scale P surplus, *PScnty*, as the difference between P inputs (fertilizer P, manure P, domestic waste P) and P outputs (crop and pastureland P uptake) (Byrnes et al., 2020).

$$PS_{cnty}\,(i,t) = FERT\,(i,t) + MAN\,(i,t) + WASTE(i,t) - UPTAKE(i,t) \quad \text{(Eq. 4.14)}$$

where FERT is inorganic P fertilizer, MAN is P from livestock manure, WASTE is the P from domestic waste, and UPTAKE is the P removed through crop harvesting or pastureland. Here, i and t denote the iteration of each county and year respectively. We normalized the P surplus (PS_{cnty}) with county area to obtain P surplus in kg-P ha^{-1} yr^{-1}.

4.2.2 Mapping the P inputs to the county scale

All county-scale components of phosphorus mass balance were presented as maps, covering the census years between 1961 and 2021. These maps were created using Canadian census division maps obtained from Statistics Canada for the study period. Note that the census division is the general term used by Statistics Canada for provincially legislated areas such as counties (Government of Canada 2023). These divisions are further subdivided into census subdivisions, which are equivalent to townships.

To provide context for the development of these maps, it is important to note that since 1961, Statistics Canada has conducted a census every five years. Since then, they have made changes to the census format, categories, and geographic boundaries. These changes aim to standardize census boundaries and integrate large amounts of census data into an automated format (Statistic Canada 2010). This need led to an agreement in 1966, where the Quebec Bureau of Statistics and Statistics Canada adopted a standard geographic code (SGC) to standardize the boundaries. As a result, many changes occurred in the census boundaries after 1966. For instance, in 1970, the Province of British Columbia replaced its 10 census divisions with 29 Regional Districts. Similarly, Manitoba's census divisions underwent significant changes in 1976 as part of a larger restructuring of census geography to reflect population and economic growth more accurately and improve data usability. This restructuring aimed to reflect population and economic growth more accurately and improve

data usability by standardizing boundaries across the country. Changes in census subdivisions (CSD) also took place on a large scale, with between 50 and 100 CSDs involved in boundary changes reported in 1974 (Government of Canada, 1981). By 2016, 1,024 CSDs had experienced boundary changes since 2011, reflecting ongoing adjustments to accommodate demographic and administrative shifts.

To account for changes in census divisions, we mapped each census year using the respective census division maps. For example, P surplus components for 1961 were mapped using the census division map of 1961, and P surplus components for 2016 were mapped using the census division map of 2016. Digital format of census division scale maps for the years 1961, 1981, and 1986 were obtained from Scholars Portal Geoportal, while maps for 1991, 1996, 2001, 2006, 2011, 2016, and 2021 were sourced from Statistics Canada (Stat Canada 2020; Leahey 2016). We digitized the county scale map for 1966, 1971, and 1976 as their digital version were unavailable. Upon investigating agricultural census data and county IDs we assumed that county boundaries did not change between the census year 1961 and 1966 thus, we used 1961 county boundaries for 1966. For 1971 and 1976, we had undigitized county scale maps. We used georeferencing techniques and georeferenced the maps of 1971 and 1976 using the map of 1981. Later, we manually adjusted the boundaries to account for the county boundary changes. There were some county polygons on the maps that did not have IDs associated with it. When the polygons are in the agricultural region, we manually matched the IDs with census IDs and assigned IDs to them. For non-agricultural regions, we left them with null values. The table of investigations is provided in **Extra Table S7 and Text S7 in Appendix C**. Although most of the maps are available for download in digital formats, the formats varied over the years. To ensure consistency across all maps for the census years, we standardized them by removing large lakes, harmonizing the boundaries at land-water intersections, maintaining uniformity in the representation of large islands, and applying a consistent numbering convention for county IDs. The four-digit county IDs are structured so that the first two digits represent the province, and the last two digits indicate the subdivisions. Additionally, we dissolved any unnecessary polygons.

4.2.2.1 Downscaling County Scale P Surplus Components

We downscaled the county scale data to a 250-m grid scale using the annual crop inventory maps (ACI) of 2016 and 2021 provided by Agriculture and Agri-Food Canada (AAFC) (*Annual crop inventory 2016, Annual crop inventory 2021*). We selected the most recent land use rasters from 2016 and 2021 because ACI did not offer comprehensive maps for all ten provinces for census years prior to 2016. Specifically, we used the 2021 ACI data to downscale the 2021 census data, while the 2016 ACI data was used for all other census years prior to 2021.

The ACI data, originally at a 30-meter resolution, includes various land use categories such as farmland, pastures, fallow lands, developed areas, wetlands, peatlands, barren lands, and forests (Agri-food Canada, Agriculture, 2018). For our analysis, we resampled the 30-meter map to 250-meter grids using nearest neighborhood sampling method.

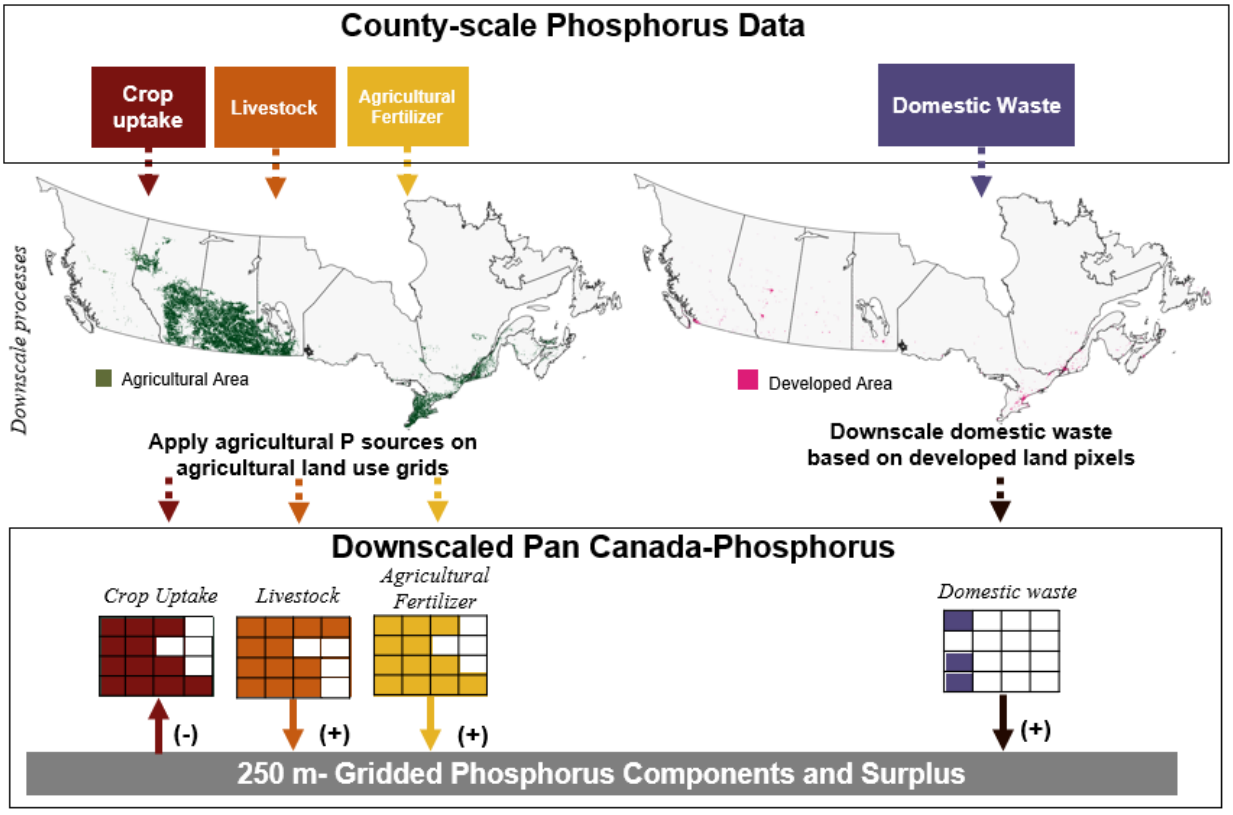


Figure 4.1: The data source and workflow for creating the gridded Pan-Canada dataset: Agricultural components of the P mass balance such as crop uptake, manure, and agricultural

fertilizer were downscaled to areas with agricultural land use; and Human waste was downscaled based on developed land area map provided by ACI.

During the generation of the gridded Pan-Canada dataset (**Figure 4.1**), agricultural components of the P mass balance, such as crop uptake, manure, and agricultural fertilizer, were downscaled to match areas identified as agricultural land use by ACI. We utilized pixels labelled as field crop and pasture areas in the ACI land use map for this purpose, categorizing pixel codes 120 to 199 as cropland and pastureland. (Agri-food Canada, Agriculture, 2018). Similarly, for downscaling domestic waste and its associated components, we selected pixels identified as urban or developed land, pixel code 34 (Agri-food Canada, Agriculture, 2018, p. 20).

Agricultural Components

For downscaling the agricultural components of the mass balance, the ACI dataset was resampled to a 250-meter grid for croplands and pastureland across the country. County-scale agricultural components, including fertilizer (FERT), livestock manure (MAN), and crop and pasture uptake (UPTAKE), were allocated equally to the cropland and pastureland grids within each county. The detailed downscaling processes for agricultural components are described below

1) We created a binary raster from the ACI land use map. A binary agricultural raster is represented as a raster where each agricultural pixel has a value of one and all non-cropland pixels have a value of zero [$gLU_{ag}(k,t) = 0/1$]. We consider attribute codes 120 to 199 as cropland and pastureland (Agri-food Canada, Agriculture, 2018, pp. 20–22) to create a binary raster for cropland.
2) The total agricultural area in each county in each year, $AREA_{ag}(i,t)$ (ha), was then calculated as the sum of the gridded agricultural land. For each agricultural component of the P mass balance, j, county-scale P flux ($P_{county}(i,j,t)$) values normalized by agricultural area. $P_{ag,county}(i,j,t)$ (kg ha-agland^{-1} y^{-1}) were calculated by dividing the total county P flux by the agricultural area of each county, i:

$$P_{ag,county}(i,j,t) = \frac{P_{county}(i,j,t)}{AREA_{ag}(i,t)} \quad \text{(Eq. 4.15)}$$

3) The final downscaled agriculture components were created by multiplying the binary annual agricultural rasters (step 1) by the rasterized annual agricultural inputs and outputs data (step 2).

$$gP_{ag}(k,j,t) = P_{ag,county}(k,j,t) * gLU_{ag}(k,t) \quad (\text{Eq. } 4.16)$$

Domestic Waste Components

Domestic waste (WASTE) was downscaled using the urban/developed land pixels (Agri-food Canada, 2018). We followed a similar methodology for downscaling agricultural input and urban input; however, instead of using crop and pasture pixels, we used developed land pixels to create a binary raster. After creating a binary raster (step 1 **Section 4.2.3.6.1**) we calculated the urban P flux normalized by developed area, $P_{ur,county}(i,j,t)$ (kg ha-urban^{-1} y^{-1})

$$P_{ur,county}(i,j,t) = \frac{P_{county}(i,j,t)}{AREA_{devloped}(i,t)} \quad \text{(Eq. 4.17)}$$

The final downscaled waste component was created by multiplying the binary annual urban rasters (step 1) by the rasterized annual waste inputs (step 2) using **Eq. 4.17**. It should be noted that the amount of human waste we estimated here was the amount without taking into account contemporary wastewater treatment plants or septic systems, which is comparable to other Pinputs and outputs in the database that focused on land surface values, without treatment and hydrological process.

4.2.3 Phosphorus Use Efficiency (PUE)

We calculated Phosphorus Use Efficiency (PUE) for Canada using the gridded map. The agricultural PUE is the ratio between P output and P inputs on agricultural land (Lassaletta et al., 2014; Swaney et al., 2019c; Van Meter et al., 2021; Wang et al., 2022). P inputs on agricultural land ($gI_{crop}(t)$) are fertilizer and manure in kg/ha. P output (*Y(t))* is crop and pasture uptake in kg/ha.

$$gI_{crop}(t) = gFERT_{crop}(t) + gMAN_{crop}(t) \quad \text{(Eq. 4.18)}$$

$$gY_{\square}(t) = gUPTAKE_{N,crop,past}(t) \quad \text{(Eq. 4.19)}$$

The PUE is then calculated as the ratio of yield to inputs:

$$PUE(t) = \frac{gY(t)}{gI(t)} \quad \text{(Eq. 4.20)}$$

It should be noted that the PUE metric is used to evaluate the ideal case of the use of P on cropland. We did not consider how much manure is typically allocated to cropland.

4.3 Results and Discussions

4.3.1 Trajectories of P surplus and its components across Canada (1961-2021)

We have presented 60 years of P surplus estimate for census years across 10 provinces of Canada at two spatial resolutions- county scale and 250m X 250 m grid. The spatio-temporal variability in the P surplus and the component is presented in **Figure 4.2 (**Additional 250m X 250 m grid-scale maps in **Figure S1 in Appendix C)**.

We observed a higher P surplus in the agricultural active areas like the southern region of Canada and prairie provinces. Over six decades from 1961 to 2021, there has been a marked increase in the use of P fertilizer in Canada, the major contributor of P surplus. The median value of P fertilizer use has escalated threefold, from 0.4 $kgha^{-1}yr^{-1}$ (interquartile range [IQR]: 0.1-1.56) in 1961 to 1.35 $kgha^{-1}yr^{-1}$ (IQR: 0.12-5.6) in 2021. The trend of median fertilizer P use initially rose until 1986, reaching 1.31 $kgha^{-1}yr^{-1}$, before decreasing to 0.6 $kgha^{-1}yr^{-1}$ by 2006, and then ascending sharply thereafter. Notably, regions such as southern Ontario and Manitoba have emerged as hotspots with exceedingly high fertilizer inputs, peaking at 18.2 $kgha^{-1}yr^{-1}$ in 2021. Similarly, the Atlantic province, particularly counties in Prince Edward Island (PEI), demonstrated a significant rise in median fertilizer P usage from 4.5 to 19 $kgha^{-1}yr^{-1}$ over the same period.

Conversely, phosphorus from manure sources did not exhibit the same upward trajectory. Instead, there was a 1.5-fold decrease in median manure P values from 1.15 $kgha^{-1}yr^{-1}$ (IQR: 0.24-3.85) in 1961 to 0.73 $kgha^{-1}yr^{-1}$ (IQR: 0.08-2.6) in 2021. The median value of manure phosphorus initially declined until 1986, reaching 0.78 $kgha^{-1}yr^{-1}$, then rose back to 1961 levels by 2006 before continuing its downward trend. The primary contributions of manure P were concentrated in southern Ontario and Quebec, areas hosting nearly two-thirds of the nation's beef and dairy cattle, with 2021 manure P inputs reaching as high as 26 $kgha^{-1}yr^{-1}$.

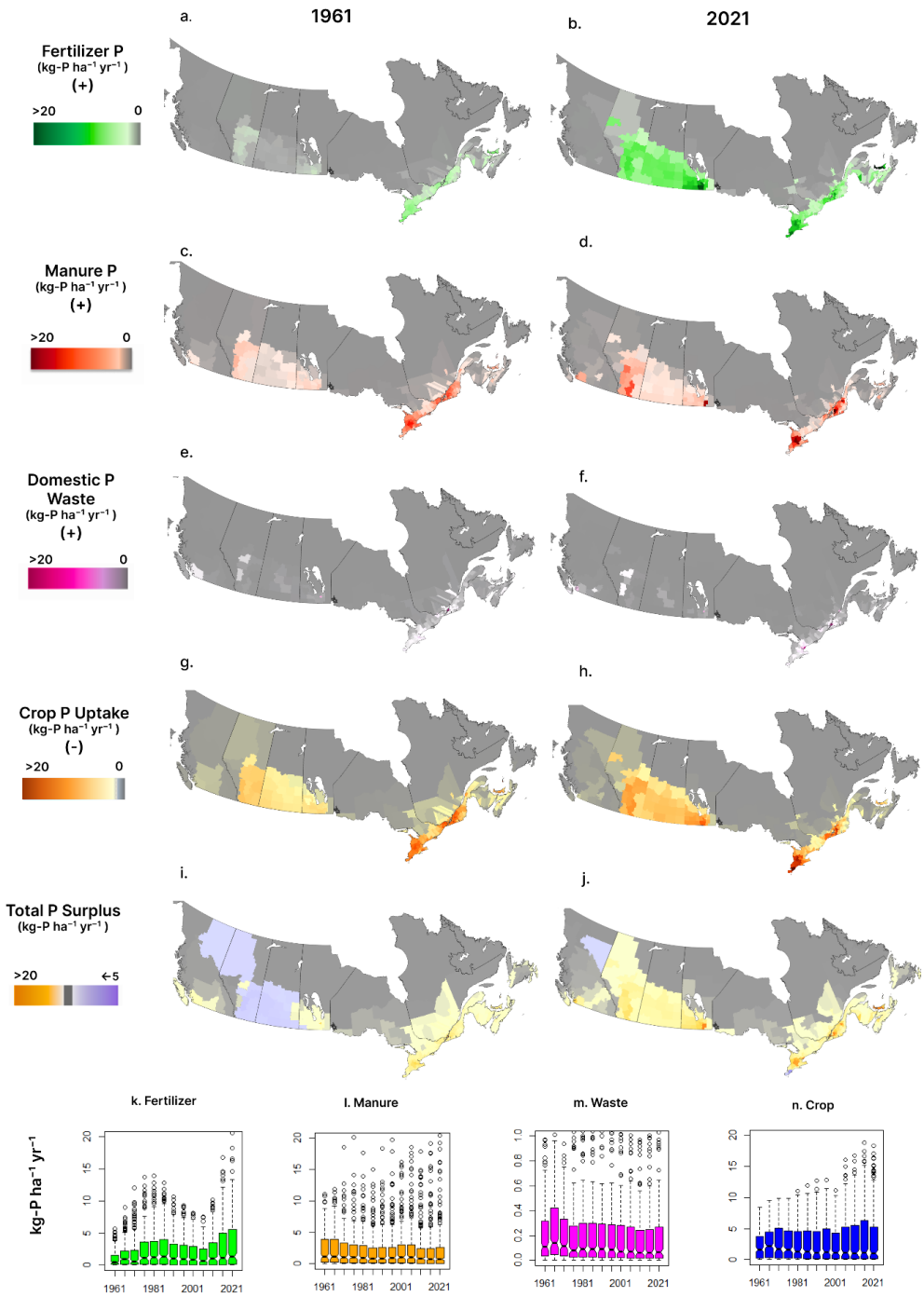


Figure 4.2: County scale maps for P surplus and its components: (a-b) fertilizer P, (c-d) manure P, (e-f) domestic P waste, (g-h) crop P uptake and (i-j) total P surplus all in kg-P ha^{-1} yr^{-1}. Each map is divided showing the beginning, and end of the time series. The box plot shows the mean and interquartile range (25%-75%) of the magnitude of P mass balance components (k-n) for census years.

In contrast, domestic waste P inputs have remained minimal, constituting only 3% of the total national P inputs. There has been a twofold reduction in median domestic P waste from 0.11 $kgha^{-1}yr^{-1}$ (IQR: 0.03-0.31) in 1961 to 0.064 $kgha^{-1}yr^{-1}$ (IQR: 0.01-2.75) in 2021. A significant drop was noted post-1971, following the nationwide ban on phosphorus in household detergents. However, ongoing urbanization and population growth have sustained high levels of domestic P inputs in metropolitan areas like Toronto and Montreal, where levels reached 31 $kgha^{-1}yr^{-1}$ in 2021.

Phosphorus uptake by crops and pastures is the sole significant removal pathway in the P surplus mass balance. There was no substantial change in the median crop and pasture P uptake over the study period, which slightly decreased from 1.66 $kgha^{-1}yr^{-1}$ (IQR: 0.22-3.3) in 1961 to 1.1 $kgha^{-1}yr^{-1}$(IQR: 0.1-5.0) in 2021. However, a notable increase in uptake was observed in the Prairie provinces, from 1.4 $kgha^{-1}yr^{-1}$ in 1961 to 4.5 $kgha^{-1}yr^{-1}$ in 2021, paralleling increased wheat yields as documented by McCallum et al., (2008).

The overall P surplus has also intensified, with the median value increasing from 0.5 $kgha^{-1}yr^{-1}$ (IQR: 0.1-2.7) in 1961 to 1.3 $kgha^{-1}yr^{-1}$ (IQR: 0.15-4.2) in 2021. In 1961, the highest P surplus was recorded in Montreal (41 $kgha^{-1}yr^{-1}$), whereas the lowest was in Division No. 5 of Alberta (-0.5 $kgha^{-1}yr^{-1}$). By 2021, the highest surplus shifted to the Toronto metropolitan area (31 $kgha^{-1}yr^{-1}$) , with the lowest observed in Chatham-Kent, ON (-2.5 $kgha^{-1}yr^{-1}$).

4.3.1.1 P Surplus Across the Provinces in Canada

Our provincial scale analysis (**Figure 4.3)** reveals that high P surpluses are observed in Ontario and Quebec with a mean magnitude of 38 Kton per year and 34 Kton per year respectively, during the study period. Fertilizer and livestock manure are both important P inputs to these provinces. The average amount of P applied as fertilizer in Ontario and Quebec each year is 45 Kton and 21.6 Kton, and the average amount of P generated from livestock manure is 43.6 Kton and 33.5 Kon, respectively. Fertilizer P input increased in Ontario from 1961 to 1981 (62 Kton per year), decreased to 24 Kton per year in 2006, and then started to rise again in 2021 with a magnitude of 61.5 Kton per year. With high fertilizer P inputs of 31 Kton per year in 1986, 14 Kton per year in 2006, and an increase of 29 Kton per year in 2021, we observed a comparable pattern for Quebec. The dry weather that Ontario and Quebec experienced in 2001 and 2005 can be attributed to the

decrease in fertilizer input (Tam et al., 2019), furthermore, high fertilizer P inputs in 2021 are consistent with the Statistic Canada data indicating record fertilizer shipments in 2020 (F. Canada, 2020). However, only 10% (~ 8 Kton per year) of the P inputs are contributed from domestic P waste. Based on our estimates of crop and pasture uptake, Ontario's agricultural output is double that of Quebec. Ontario's annual mean crop and pasture uptake is 59 Kton, while Quebec's is 27 Kton. Over the study period, we found no significant increase in crop uptake between the two provinces.

The prairie provinces demonstrated consistently low surplus values during the study period. The P surplus in Manitoba remained at a mean of 10.5 Kton between 1961 and 2011, while Saskatchewan and Alberta both had negative P surpluses at -25 Kton and -2.5 Kton, respectively. However, in more recent years, there has been a noticeable spike in yearly P surplus values, with Manitoba, Saskatchewan, and Alberta experiencing surpluses of 56 Kton, 75 Kton, and 81 Kton, respectively. This increase in surplus values is due to the rising levels of fertilizer input levels across Canada. Notably, these provinces also exhibited similar fertilizer usage throughout the study period, with Manitoba and Saskatchewan experiencing an approximately 28-fold increase in fertilizer P input, while for Alberta, it increased 10-fold. It is worth noting that Alberta had a higher P contribution from manure sources, with P input from manure rising from 37 Kton per year to 75 Kton per year over the years, which is more than double the amount of manure input from Manitoba and Saskatchewan. P surpluses in the prairie regions are driven by increasing crop and pasture P uptake over the years. Our study showed a threefold increase in P uptake in these provinces over the study period, which may be due to the higher production of wheat (Newlands et al., 2014) and large pasture areas available for grazing (Bork et al., 2021).

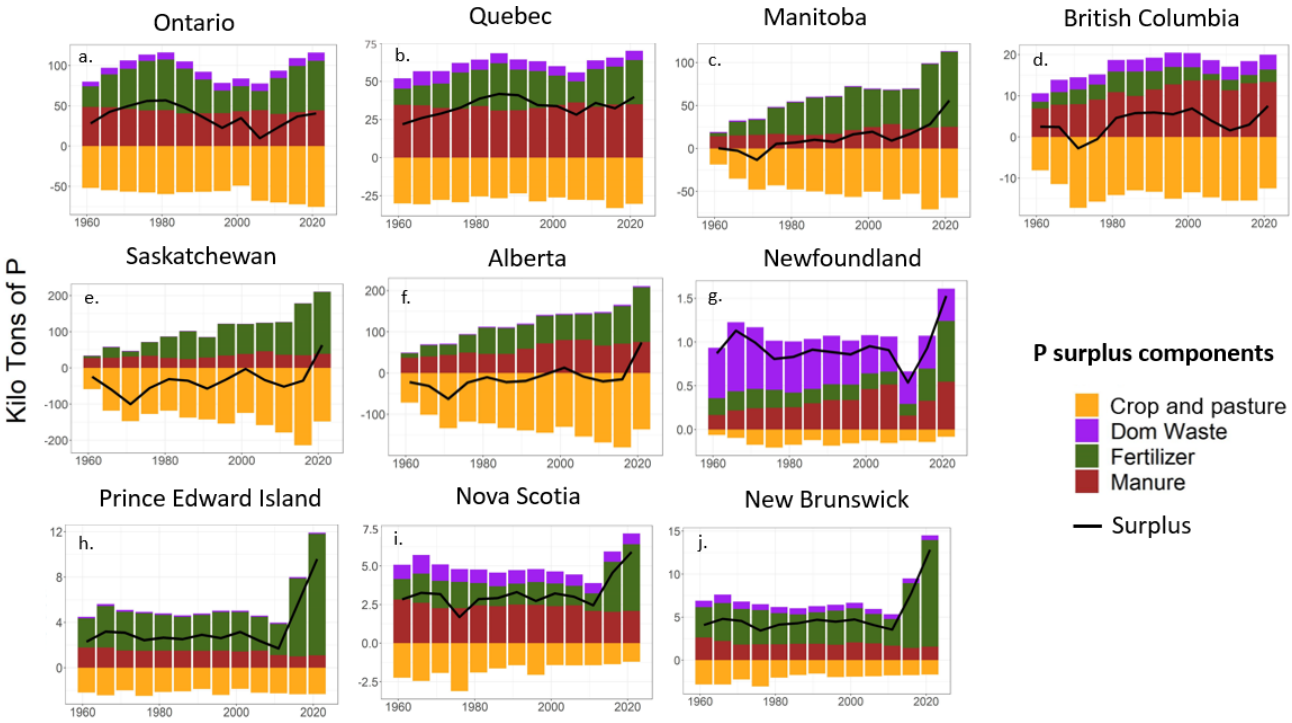


Figure 4.3: Phosphorus mass balance and its components for Canadian provinces.

The agricultural surplus in the eastern provinces of Canada is relatively low, which can be attributed to the fact that these provinces have only 19% of cropland (Statistics Canada, 2021). Our study has revealed that the major source of P inputs for Prince Edward Island and New Brunswick is fertilizer P, whereas Nova Scotia relies on manure P and Newfoundland on domestic P waste. Over the study period, we have observed a significant increase in P surpluses ranging from 2 to 4-fold in these provinces. The spike in the P surplus after 2006 can be attributed to the increase in fertilizer sales during this time.

In contrast, British Columbia has less than 5% of suitable land for farming (Deng, 2022), leading to a relatively low magnitude of overall provincial scale P inputs. However, we have noticed a 2-fold rise in P surplus from 4.8 Kton per year in 1961 to 10.6 Kton per year in 2021 for this province. This rise in P surplus can be attributed to the high manure P input (13 Kton per year in 2021), as this 5% of farmland accounts for 5% of the beef cattle industry of the country (Statistic Canada, 2022).

4.3.1.2 Addressing Legacy P with Cumulative P Surplus

The P surplus trajectories from 1961 to 2021 were used to estimate the cumulative P surplus, which can indicate legacy accumulation in the landscape over the time frame. To fill gaps between census years, we used linear interpolation to estimate P surplus values for non-census years. Estimating the P accumulation in the landscape can be crucial in reducing P loss because the accumulated P will flow down to the stream at some point (Van Meter et al., 2021; Wang et al., 2022). **Figure 4.4** below displays the P accumulation for all P components, but in our subsequent analysis, we primarily focused on agricultural P surplus. This is because domestic waste is mostly treated in WWTPs and does not accumulate in the environment.

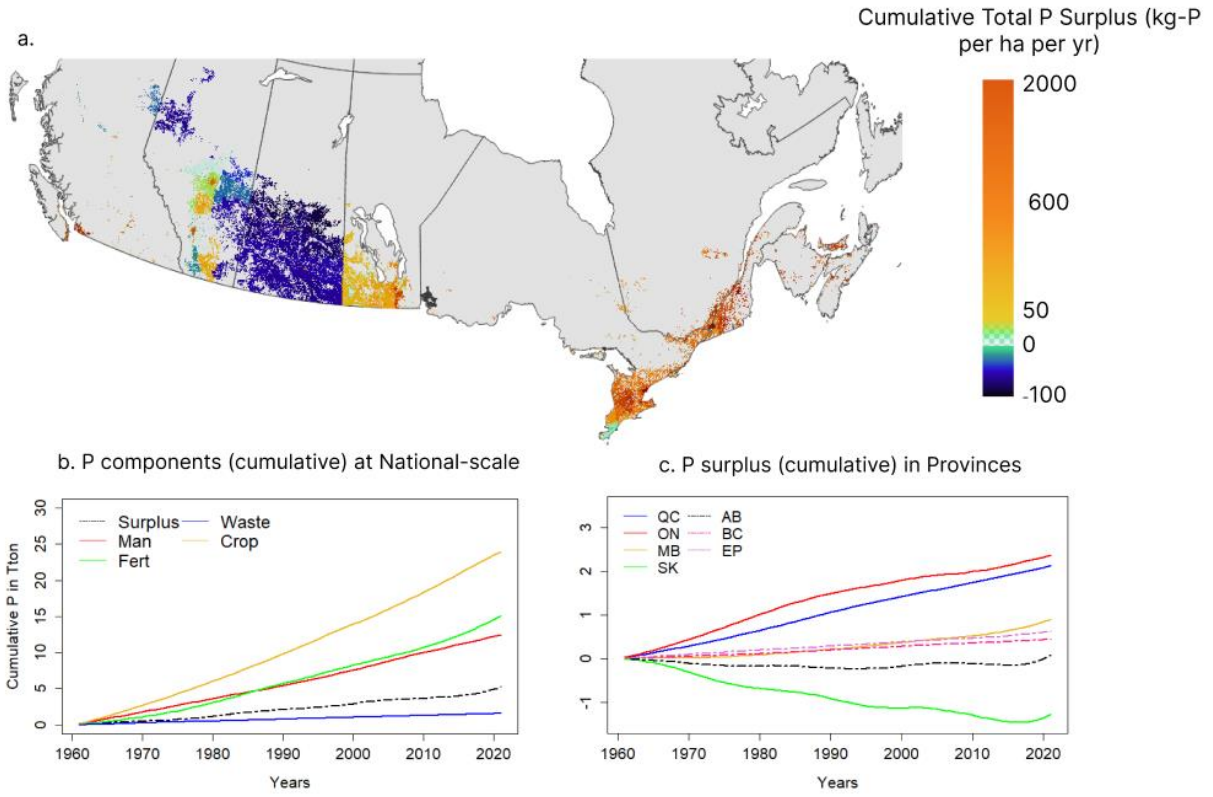


Figure 4.4:P accumulation in Canada from 1961-2021. a) Cumulative P surplus across agricultural areas of Canada. b) Cumulative P surplus in Tton on a National Scale. c) Cumulative Total P surplus in Tton for provinces across Canada.

We observe more than 5 Tera tons (Tton) of P accumulation across Canada. The provincial cumulative P surplus varies between -1.2 Tton to 2.3 Tton, with the lowest magnitude being

observed in Saskatchewan and the highest magnitude in Ontario. Ontario and Quebec have the highest P accumulation, accounting for 85% of P accumulation in Canada. These provinces also have the highest population density; thus, they contribute one ton of P from domestic waste. The cumulative agriculture surplus in Ontario and Quebec is approximately 1.8 Tton each. Manitoba, British Columbia, and the Eastern Province contribute to the remaining P accumulation with a cumulative agricultural P surplus of 1.6 Tton altogether. The 2021 statistics from the Census of Agriculture showed that Saskatchewan and Alberta make up 70% of Canada's croplands, and they have yet to accumulate P, which resulted in low national P accumulation similar to the findings from Wang et al. (2024). In fact, Saskatchewan has shown P mining from the soil with a decreasing P surplus, while Alberta has demonstrated a recent P recovery, resulting in a cumulative P surplus of 83 Kton.

The cumulative P surplus and its components over the study period are shown in (**Figure4.4b**), with cropland P having the largest cumulative P levels followed by fertilizer P, animal P, and household P waste. We see a similar pattern for livestock P accumulation and fertilizer P accumulation, which shows that both factors equally contributed to P buildup. However, only 17% of P inputs were accumulated across Canada, with the remaining amount taken up by crop and pasture lands. Although Canada has low national scale P accumulation, there are certain provinces with hotspots that have high legacy accumulation, which requires targeted incentives. For instance, agricultural regions in Rouville, Maskoutains, and La Nouvelle-Beauce counties in Quebec, as well as Waterloo and Perth counties in Ontario, have accumulated more than 1000 kg P Ag-ha^{-1}. The Fraser Valley in British Columbia has a legacy P accumulation of 3000 kg P-Ag-ha^{-1} in its landscape. Even after adopting various management practices, Ontario and Quebec continue to accumulate legacy P, putting agricultural watersheds in those provinces at risk of potential water pollution. (Reid, Schneider, et al., 2019; Van Meter et al., 2021; T. L. Van Staden et al., 2022).

4.3.2 Phosphorus Use Efficiency (PUE) in Legacy P Management

4.3.2.1 PUE at the National and Provincial Scale

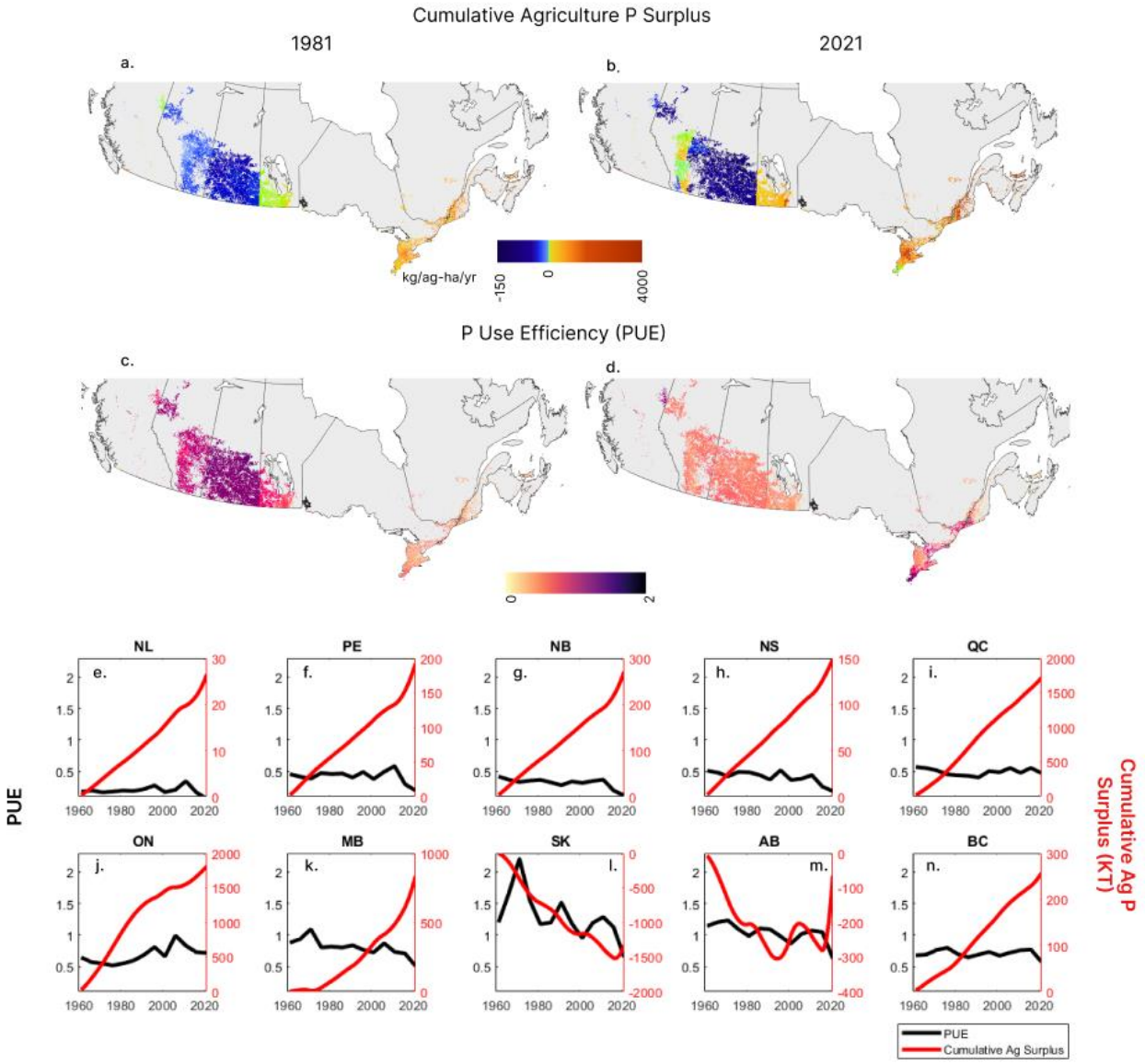


Figure 4.5:Relationship between Cumulative agricultural P surplus from 1961 to 2021 and PUE: a,b) Spatial distribution of cumulative agricultural surplus, (c.d) PUE, and (e-n) trajectories of cumulative agricultural P surplus and PUE separated for ten study provinces.

We estimated PUE, which measures the amount of input removed through crop yield. It is important to note that PUE is an metric, where a value of 1 denotes the most efficient use of phosphorus in the system. Any deviation from this value signifies the impact of landscape

characteristics and the disparity between agricultural input and output. Our study showed that national scale PUE exhibited considerable variation over the study period, declining from 1.02 in 1981 to 0.63 in 2021 (**Figure 4.5c,d)**. The decrease in PUE suggests a shift towards inefficient P use, despite the implementation of management strategies such as the 4R stewardship for P fertilization and conservative tillage practices (Grant et al., 2019; Vollmer-Sanders et al., 2016; Wang et al., 2022). This reduction in P efficiency is a cause for concern and warrants further attention.

We also estimated the PUE for each province and discovered that Saskatchewan and Alberta had a PUE greater than 1, while all other provinces had a PUE less than 1 (**Figure 4.5l,m**). Next, we compared the PUE with the provincial cumulative agricultural surplus and the percent of cropland, finding three relationship categories (**Figure 4.5e-n, Figure 4.6a-j**). These categories are: 1) decreasing PUE with increasing cumulative agricultural surplus and cropland; 2) decreasing PUE and cumulative agricultural surplus with increasing cropland; and 3) plateauing PUE with increasing cumulative agricultural surplus and little or no change in cropland. Manitoba was categorized in the first group because it showed a 40% decrease in PUE and a 30% increase in cropland over the last 60 years (**Figure 4.6g**). Despite an increase in cropland, this province is not using P efficiently, as the PUE is driven by increased P fertilizer use (**Figure 4.6q**). Saskatchewan and Alberta were grouped in the second category because they showed a 45% decrease in PUE and a >50% increase in cropland with a sharp decrease (9-fold for AB and 40-fold for SK) in cumulative agricultural surplus (**Figure 4.5l,m, Figure 4.6h,i**). However, PUE in these provinces was higher than in any other province, as it was highly driven by crop P uptake (**Figure 4.6r,s**). Increased organic farming methods emphasizing limiting the use of inorganic P fertilizer (Schneider et al., 2019; Wang et al., 2022), Canadian Organic Trade Association, 2018 together with increased farmland and yield, can be attributed to the unidirectional relationship between PUE and cumulative agricultural surplus in the Prairies.

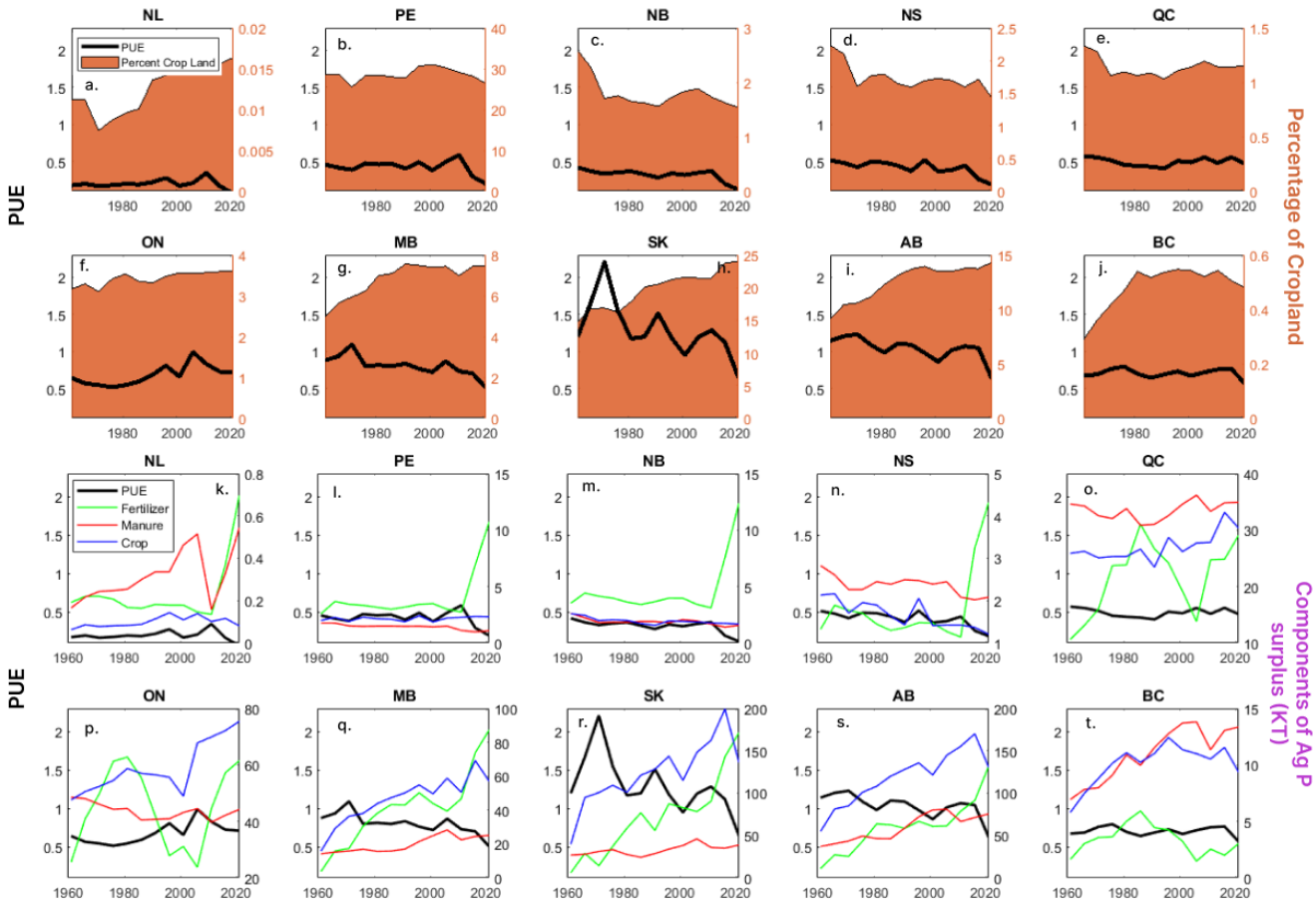


Figure 4.6: (a-j) Trajectories of PUE and percentage of cropland; (k-t) trajectories of PUE compared with the agricultural P surplus components (fertilizer, manure and crop uptake) for ten provinces of Canada.

The third category included all other provinces that exhibited negligible or minimal changes in PUE and crop area value. Typically, these provinces demonstrate PUE values below 1, with a growing agricultural surplus. However, the eastern provinces and BC showed a low P accumulation of less than 300 Kton (**Figure 4.5n**). The low PUE and increasing magnitude of cumulative agricultural surplus in these provinces are primarily due to manure from expanding livestock operations in NL, NS, and BC (**Figure 4.6k,n,t**). This finding is consistent with a previous study by (Shabtai Bittman et al., 2023; Reid & Schneider, 2019; Withana Herath, 2013). ON and QC had the highest P accumulation of around 2000 Kton, despite PUE and total cropland remaining relatively stable over the last 60 years (**Figure 4.5j,k**). These intensifications of

agriculture resulted in high P accumulation in the landscape and more frequent water quality issues in these provinces. There has been a significant increase in ON crop production due to increasing crop yield (Cabas et al., 2010; Van Meter et al., 2021; T. L. Van Staden et al., 2022) while there has been a 48% decrease in cattle over the past 55 years (T. L. Van Staden et al., 2022) which resulted in PUE being driven by crop production in ON (**Figure 4.6p**). In contrast, in QC, PUE was driven by livestock operations (**Figure 4.6o**), as evidenced by high-density dairy cattle and swine farms in the southern part of the province (Shabtai Bittman et al., 2023; Reid & Schneider, 2019).

4.3.2.2 PUE Metric from a Management Perspective

In this section, our investigation focused on PUE and cumulative agricultural P surplus in Canadian agriculture in 1981 and 2021 to assess the state of P management across the country. Our hypothesis was that a perfect system would have a cumulative agricultural P surplus of 0 and a PUE of 1. Based on this, we categorized the land system into four quadrants. The first quadrant, Q1, includes areas with a positive cumulative surplus and a PUE above 1. We labelled this the "recovery zone" from overapplication, as the surplus is currently in a reduction phase due to PUE being greater than 1. The second quadrant, Q2, covers areas with a negative cumulative surplus and PUE > 1. This indicates that the system is mining phosphorus. The third quadrant, Q3, encompasses areas with no P stores and a PUE of less than 1, indicating that the land is recovering from soil phosphorus mining. We termed this the "recovery zone" from soil depletion. Finally, the fourth quadrant, Q4, covers areas with P accumulation and a PUE less than 1, where excess P is enriching the soil. We labelled this the "Overapplication zone."

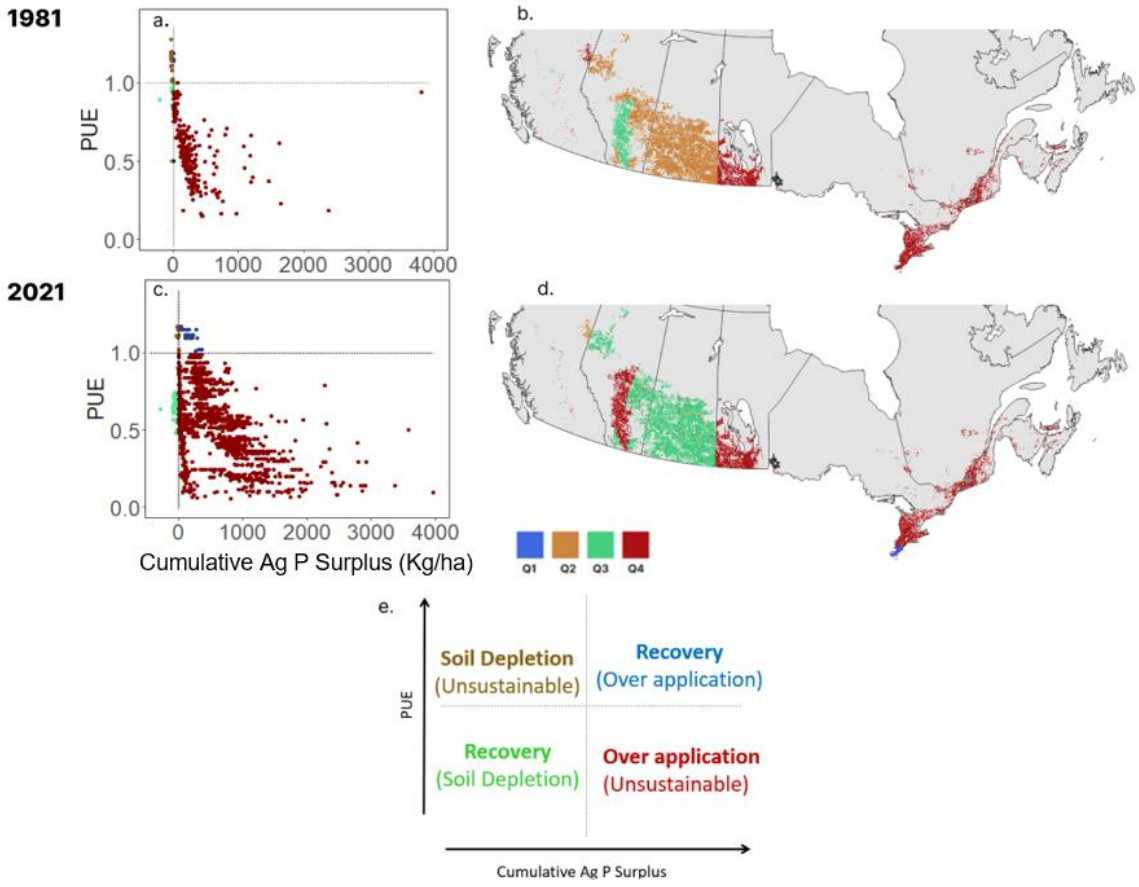


Figure 4.7: Cumulative agricultural phosphorus surplus and PUE are shown for the years 1981 (a, b) and 2021 (c, d). Panel (e) categorizes grid cells into four modes: Q1 Recovery from overapplication, Q2 P depletion from soil, Q3 Recovery from soil depletion, and Q4 Over application of P.

In 1981, 61.7% of Canada's agricultural land was categorized as Q2 (Soil Depletion), 9.7% as Q3 (Recovery from soil depletion), and 28.4% as Q4 (Overapplication), with a negligible amount (less than 0.1%) in Q1 (Recovery due to overapplication) as shown in **Figure 4.7a**. In Ontario, Quebec, and Manitoba, the agricultural lands fell predominantly within the Q4 zone, indicating over application and unsustainable use of P with an average cumulative P surplus of 130 kg-P ag-ha^{-1} (**Figure 4.7a,b)**. Given that the PUE in these areas is less than 1, it suggests that P continues to accumulate in the landscape due to inefficient usage. Conversely, Saskatchewan and Alberta primarily fell into zones Q2 and Q3, indicating no P accumulation in the landscape. Specifically, the western part of Alberta showed signs of land recovering from previous soil P depletion (as PUE<1). Meanwhile, both Saskatchewan and eastern Alberta were in a phase of P mining (**Figure 4.7b)**.

By 2021, we have observed significant changes in land practices that have resulted in shifts in the PUE across Canada. We have observed that 0.9% of agricultural land is in each of the Q1 and Q2 zones, while the highest percentage is observed in the Q3 zone with land accounting for 55% of the agricultural area and 42.5% of the land falling into the Q4 zone (**Figure 4.7c)**. Over the past 40 years, a large percentage of land has shifted from the Q2 zone to the Q3 and Q4 zones. Interestingly, over the past 40 years, the land in Saskatchewan has transitioned from a PUE of higher than 1 to a less PUE, signaling a recovery from soil P depletion. This improvement is likely due to change in fertilizer application, supported by the region's rich agricultural soil and high crop yields (Pierre and Mhlanga, 2022). In contrast, the western parts of Alberta have moved into a P Q4 zone, driven by overapplication of phosphorus due to the continuous increase in phosphorus inputs over the years, from both fertilizer and manure sources. Meanwhile, Ontario, Quebec, and Manitoba continue to stay in overapplication zone, with the average cumulative P surplus now at 260 kg-P ag-ha^{-1}, which is double the amount recorded in 1981 (**Figure 4.7c)**. This persistent high phosphorus highlights the ongoing challenges in managing phosphorus effectively in these regions.

4.3.3 Technical Evaluation of Results and Limitations

4.3.3.1 Comparison of County-scale Mass Balance Data

In our study, we compared our results with several phosphorus mass balance studies and found them to be consistent. We aggregated P surplus and its components from county to provincial scales for comparison with values from IPNI (2014) and Wang et al. (2022) as shown in **Figure 4.8**. IPNI has provincial-scale values for agricultural components from 1973 to 2013, and Wang et al. 2022 have provincial values from 1961 to 2018. These provincial-scale values were aggregated every year and only included crop uptake as the output component for P mass balance, excluding pasture land. Thus for comparison purposes, we used only crop uptake data in **Figure 4.8**. For the Pan-Canada P fertilizer trend and IPNI P fertilizer, the R-squared value was >0.95, while for BC, the R-squared value between Wang et al. 2022 and our dataset was 0.8. This is because we filled in the classified fertilizer sales value using previous N:P fertilizer sales ratios. Manure P input showed a relationship with IPNI with a median R-squared of 0.95. We observed

variation from (Wang et al., 2022) as we employed the new USDA method, which accounts for livestock weight changes throughout the study year. Our crop P uptake trend also displayed strong R-squared values (>0.9) compared to these two studies.

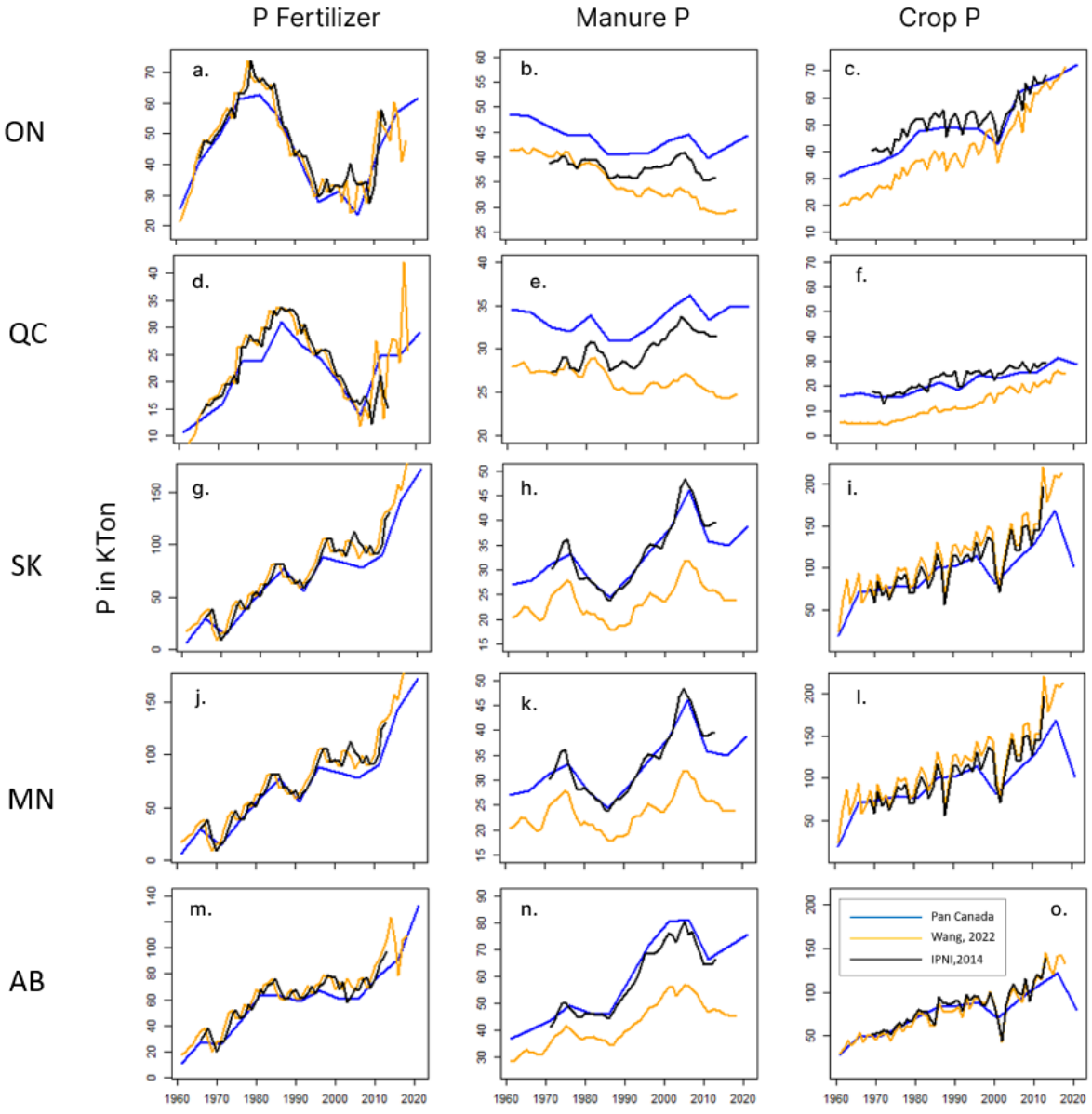


Figure 4.8: Comparison of agricultural phosphorus surplus components across major Canadian provinces using datasets from Pan Canada, IPNI (2014), and Wang (2022). Note: British Columbia is excluded from this figure as it is not included in the IPNI, 2014 mass balance dataset.

We also compared our study with (T. L. Van Staden et al., 2022) and found that the values were comparable. The study found the highest P surplus to be in the Toronto Metropolitan Area in 1976, with a magnitude of 37 $kgha^{-1}yr^{-1}$, and our investigation revealed 34 $kgha^{-1}yr^{-1}$ for that area. Our study demonstrated that the highest cumulative agricultural surplus is near the Waterloo Region (700-1100 $kgha^{-1}$ of crop area per year), which is consistent with the findings in Van Staden's work. Our result is also comparable with the Lower Fraser Valley study by (S. Bittman et al., 2017), which reported a P surplus of 2.3 $kgha^{-1}yr^{-1}$ in 2011, while our study revealed 2.5 $kgha^{-1}yr^{-1}$ of TP in the Lower Fraser Valley county in BC. Our findings are also similar to (Reid & Schneider, 2019) which identified the highest P surplus in QC and ON, with Saskatchewan displaying a negative P surplus. The study is also comparable to (Goyette et al., 2016) which reported an NAPI of ~1400 $kg.km^2$ in the nearby watersheds of Montreal in 2011, while our research revealed 1494 $kg.km^2$ in Montreal.

4.3.3.2 Validation of Gridded Phosphorus Data with County-scale Data

We compared county scale data with the gridded data to ensure the accuracy of the downscaling method. To avoid potential errors from GIS software and to ensure the integrity of the dataset, every product was carefully examined. We assessed phosphorus surplus by comparing data aggregated from the gridded Pan-Canada dataset at the county level with the Pan-Canada county-scale version. Since the annual P surplus in the gridded dataset is derived by summing all P components, any discrepancies indicate potential errors in the individual component data.

Figure 4.9 shows a comparison of county scale mass balance against the mean county values from the gridded Pan-Canada, in kg-P per ha per year, for each census year from 1961 to 2021, covering all P surplus components. Linear regression analyses of these datasets reveal that the R-squared values for all surplus components are consistently equal to or greater than 0.99. Several factors could cause the downscaled data not to align perfectly with the county-scale results. For instance, the land use map from 2016 might not accurately depict the agricultural and urban areas as they were in 1961 due to significant changes in land development driven by increased human activity. Additionally, the location of areas heavily impacted by human activity—often on islands or near water bodies—poses challenges for the rasterization process. For instance, in our gridded mass balance dataset, the Magdalen Islands (Îles de la Madeleine) in the Gulf of Saint Lawrence,

Quebec, displayed notable discrepancies with the county-scale values. This issue arises because the Magdalen Islands consist of a group of 12 small islands, some of which are smaller than our 250m x 250m raster grid size. The limited grid size hindered the accurate capture of county-scale data for these smaller areas. Although using a finer grid size could potentially resolve this issue by better representing the Pan-Canada dataset, we opted to maintain the current grid size. This decision was made to ensure consistency with the resolution of the TREND-N dataset and to avoid the computational costs associated with downsizing to a finer grid. Despite these challenges, a strong correlation is still evident between the two datasets. This consistent high correlation across components validates the accuracy of our downscaling methodology.

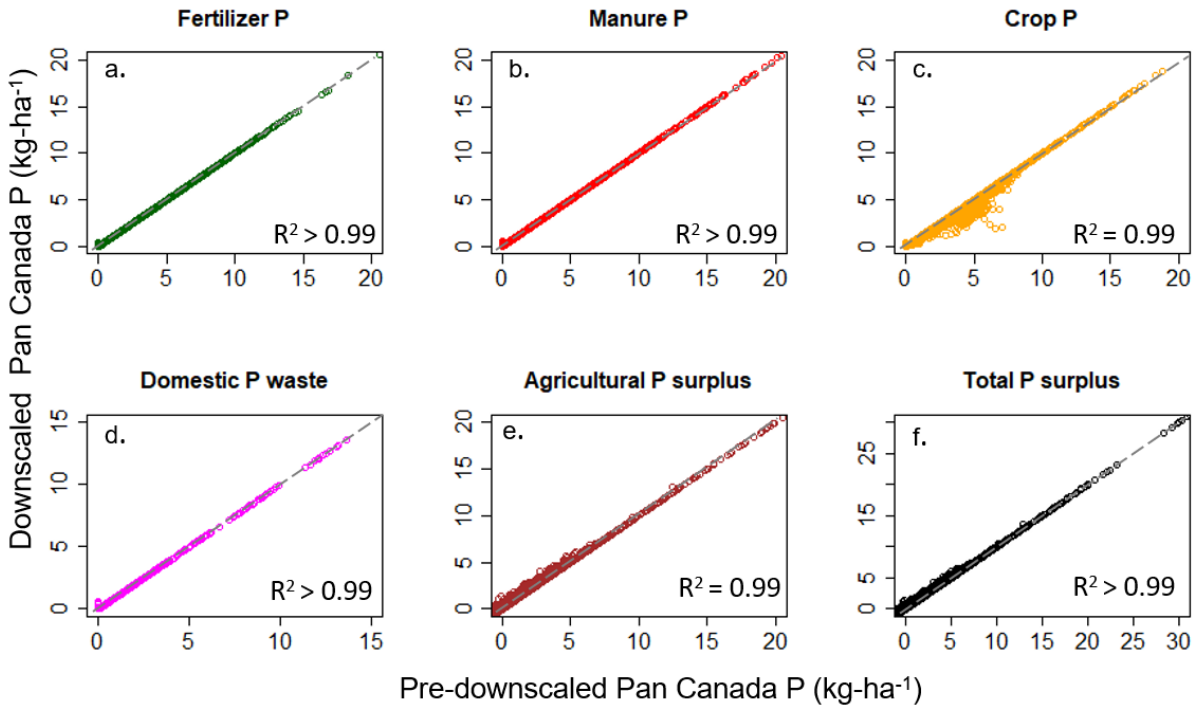


Figure 4.9: Relationship between county-scale phosphorus estimates of Pan Canada P mass balance components and gridded phosphorus estimates, re-aggregated to the county scale. Data points represent estimates for each county for each census year from 1961 to 2021. The dashed lines represent a 1:1 relationship.

The study has some limitations that should be noted. Firstly, we only considered major field crops, grains, and livestock in Canada for our simple mass balance, and disregarded the fruits and vegetables as they contribute very little (2% of total agricultural land) to P input in Canada. Additionally, we did not consider atmospheric P deposition due to its negligible impact. We

assumed that manure stays where it is generated and did not account for the possibility of manure transport, which may not always be the case. From 1966 to 1976, we had to make some assumptions regarding county boundary changes as we could not find any county-scale digitized maps for those years, which may have led to some estimation errors. We estimated undisclosed data using provincial differences or previous census data, which may have also introduced some errors in our county-scale estimation. Additionally, we did not consider the export of P to waterbodies during our estimation of legacy, which could limit the accuracy of our legacy estimates. Moving forward, we aim to address this limitation in future studies.

4.4 Conclusions

This chapter presents estimates of phosphorus surplus and its components across Canada from 1961 to 2021, calculated at both county and 250-meter grid scales, excluding northern Canada. While there have been several published phosphorus mass balance datasets for Canada (Dillon et al., 1993; Goyette et al., 2016; *IPNI, 2014.*; Liu et al., 2020; Reid, Schneider, et al., 2019; T. L. Van Staden et al., 2022; Wang et al., 2022), they have not been published at the county scale or finer grid sizes like 250 meters. Our study introduces the first dataset of its kind that provides estimates of county-scale phosphorus surplus and its components at such a high resolution. Our dataset estimates phosphorus from fertilizer, livestock manure, domestic waste, and crops and pasture land. The total surplus, agricultural surplus, and phosphorus use efficiency were estimated using the P component dataset. The dataset reveals how agricultural practices and land use changes over six decades have significantly impacted P dynamics within Canada. The dataset presents an unprecedented opportunity for understanding spatiotemporal characteristics of P use in human-impacted landscapes and will be critical to advancing our understanding of how surplus P impacts water quality, and ecosystem health.

Our dataset analysis highlighted the increase in P fertilizer use, especially in southern Ontario and Manitoba, regions that have become notable hotspots for high fertilizer inputs. This increase is paralleled by a decline in manure P inputs, reflecting shifts in livestock management practices and intensification of agricultural production in specific areas. Despite these changes, domestic waste P inputs have remained minimal but persistent, influenced largely by urbanization and regulatory changes such as the ban on phosphorus in detergents. The study also demonstrated the enduring

challenge of managing P surplus efficiently to prevent environmental degradation. Notably, Ontario and Quebec exhibited the highest P accumulations, suggesting a critical need for targeted management practices in these high-surplus areas. Conversely, despite historically low P surplus values, the Prairie provinces have shown a recent increase in P surplus, linked to rising fertilizer applications and enhanced agricultural productivity.

Additionally, we compared our dataset against existing P mass balance datasets across Canada, which was on a provincial scale. Our assessments confirm that our results align consistently with those from key existing studies, corroborating findings that demonstrate similar P surplus values across major Canadian regions (*IPNI, 2014*.; Wang et al., 2022). However, challenges persist in accurately estimating P surplus due to issues related to grid size. Despite these challenges, our methodology for downscaling and validating gridded data against county-scale data has proven highly effective, achieving correlation coefficients (R^2) greater than 0.99. This strong validation not only confirms the reliability of our approach but also identifies areas that could benefit from further refinement in future research.

Chapter 5

Conclusion

5.1 Summary

In this thesis, the persistent issue of phosphorus (P) pollution was addressed which was known to be, exacerbated by human activities such as intensive agriculture and urbanization, These activities have significantly altered the global phosphorus cycle, leading to increased phosphorus runoff from agricultural lands into downstream water bodies. Such runoff contributes to eutrophication, manifested as algal blooms, hypoxia, fish kills, and biodiversity loss. Despite longstanding efforts to manage phosphorus through various strategies, such as reducing fertilizer use and controlling erosion, eutrophication remains a worsening problem in many water bodies, including the Laurentian Lake Erie Basin. Once a success story of eutrophication management in the 1980s, this basin has seen a resurgence of the problem in recent decades, driven in part by the accumulation of legacy phosphorus in soils.

In the first objective (chapter 2), a phosphorus mass balance approach was used from 1930 to 2016 across both the USA and Canadian sides of the Lake Erie basin (60,000 km^2) to address the issue of legacy phosphorus. This method calculated the difference between phosphorus inputs—fertilizers, manure, domestic waste, and atmospheric deposition—and outputs, primarily from crop and pasture uptake. This approach determined the phosphorus surplus, which was then linked to riverine phosphorus exports to estimate legacy phosphorus. These exports were estimated using a Random Forest model that predicted phosphorus export based on cumulative phosphorus surplus and stream flow dynamics. The results indicated that, despite reductions in phosphorus inputs, the effects of accumulated legacy phosphorus persistently influence riverine exports. It was found that only a median of 8% of phosphorus accumulated in the basin is exported via streams, with the vast majority—458 kg ha^{-1} (ranging from 62 to 875 kg ha^{-1})—accumulating as legacy phosphorus across the 57 study watersheds over the past nine decades. Further analysis revealed that this accumulation of legacy phosphorus is predominantly driven by livestock manure inputs, as evidenced by a strong correlation (R^2=0.46; P<0.0001), while fertilizer inputs had a minimal impact (R^2=0.05; P=0.09).

In the second objective (chapter 3), the legacy phosphorus across various land compartments, and phosphorus loads at watershed outlets of the Lake Erie basin were simulated using the ELEMeNT-P model. This process-based model considers current-year inputs with historical nutrient stores and land use trends to simulate phosphorus fluxes and storage. Calibration of the model was conducted using observed phosphorus loads at the watershed outlets, demonstrating good performance with median Kling-Gupta Efficiency (KGE) and Percent Bias (PBIAS) values of 0.71 and 4%, respectively. The analysis estimated that approximately 80% of the legacy phosphorus is stored in the soil pool, with 10% in landfills, 8% in reservoirs and riparian zones, and the remaining phosphorus in the groundwater flux. Future scenario simulations indicated that meeting the International Joint Commission's target of a 40% reduction in total phosphorus loading by 2025 poses significant challenges, necessitating more focused and intensified nutrient management strategies. The future scenarios showed potential outcomes with varying degrees of P surplus reduction and highlighted the importance of addressing manure handling losses to reduce phosphorus load. The study showed that Canadian watersheds have large amounts of phosphorus input coming from livestock manure and reducing phosphorus loss from manure handling can lead to a 22% reduction in phosphorus loading by the next 20 years.

In the 3rd objective (chapter 4), a phosphorus mass balance dataset for Canada was developed, covering the period from 1961 to 2021. This dataset, the first of its kind, offers high-resolution estimates of phosphorus inputs and outputs across Canada, covering 6.4 million km², at both county and 250-meter grid scales, excluding the northern regions. Key components included in the dataset are fertilizers, livestock manure, domestic waste, and crop and pasture uptake. Phosphorus mass balance calculations were done for each census year, with gaps in classified census data filled. The results were subsequently mapped using historical census division maps that reflected changes in administrative boundaries over time. The analysis indicated a significant increase in phosphorus fertilizer use over the six decades, particularly notable in southern Ontario and Manitoba. Here, the median application of fertilizer phosphorus escalated threefold, reaching up to 18.2 kg/ha in 2021. In contrast, phosphorus from manure sources and crop uptake did not exhibit significant changes over the period, except for a notable increase in recent years in the Prairie provinces, which corresponded with increased wheat yields. Domestic waste phosphorus inputs remained minimal, accounting for only 3% of the total national phosphorus inputs. Additionally,

the dataset aligns well with multiple phosphorus mass balance studies such as IPNI (2014) and Wang et al. (2022), demonstrating a strong correlation in agricultural phosphorus surplus across Canadian provinces.

5.2 Major Contribution

The thesis has three significant contributions. Firstly, it establishes the first comprehensive phosphorus mass balance for the transboundary Lake Erie basin spanning 86 years, which is then utilized to estimate legacy phosphorus through coupling with stream phosphorus exports. Secondly, a Lake Erie scale ELEMeNT-P model framework was developed to simulate phosphorus load at the outlet and legacies at different landscape components. Thirdly, it introduces a novel dataset providing high-resolution estimates of phosphorus inputs and outputs across Canada, covering 6.4 million km² at both county and 250-meter grid scales. This dataset not only incorporates changes in historical county boundaries but also addresses gaps in census data.

5.3 Limitations and Recommendations for Future Work

This thesis has successfully achieved its objective by developing a phosphorus mass balance and estimating legacy phosphorus through data synthesis, process-based modelling, and statistical analysis. Nonetheless, this field presents ample scope for further research and development.

Phosphorus Mass Balance

The phosphorus mass balance data presented in this thesis was aggregated at the county level. However, agricultural censuses in Canada provide data at the subdivision or municipal scales, suggesting a potential area for increasing resolution in future studies. This dataset relied on assumptions to fill gaps in classified census data, introducing uncertainties into our mass balance calculations. The study focused solely on field crops, which constitute over 94% of Canada's cropland, yet future expansions could include analyses on fruits and vegetable crops to broaden its scope. We utilized provincial crop yield data for major field crops and assumed constant pasture yields throughout the study period, which may raise concerns about variability in yields across provinces and years. Additionally, we assumed that manure phosphorus remains within the county of its origin, despite the possibility of inter-county manure trading, for which data were unavailable.

For this thesis, a pan-Canada mass balance was conducted for census years due to the absence of consistent, yearly county-scale agricultural census data. However, yearly provincial-scale data on fertilizer use and crop yields are available and could be downscaled to the county level in future work to provide more frequent mass balance updates. Assumptions made during the digitization of historical census maps for 1966, 1971, and 1976 also introduce potential inaccuracies in defining exact county boundaries, underscoring the need for careful consideration in future methodological improvements.

Some inconsistencies can be addressed during downscaling county scale phosphorus mass balance data using land use maps. For instance, some counties report agricultural phosphorus fluxes based on agricultural census data, yet have no agricultural land according to land-use raster. Because our downscaling method relies on land use data, agricultural phosphorus fluxes in these counties are set to zero in all grid cells, slightly reducing the total phosphorus mass in our analysis. A similar issue arises with the downscaling of domestic waste data. This happens because these maps may not accurately represent the population in small rural communities, affecting the accuracy of phosphorus estimates.

Estimation of Phosphorus Legacy

In the first objective of this thesis, legacy phosphorus was estimated using modeled phosphorus load data, due to gaps in available data. Since actual load data before 1970 was unavailable for any of the watersheds, legacy phosphorus dating back to 1930 was estimated using a constant yearly load for years before 1970. This method may introduce some uncertainty in the estimation of legacy phosphorus.

In Chapter 3 of this thesis, the ELEMeNT-P model was utilized to model legacy phosphorus across various watersheds in the Lake Erie basin. Although many sub-watersheds were covered, some were not modeled due to a lack of stream phosphorus export data. There are opportunities to refine these results in future work by exploring a broader range of model parameters and assumptions to enhance model performance. Additionally, future studies could include more detailed descriptions of wastewater treatment plants to better estimate phosphorus in landfill pools and incorporate soil test phosphorus data in the calibration and validation processes.

References

Abatzoglou, J. T., Dobrowski, S. Z., Parks, S. A., & Hegewisch, K. C. (2018). TerraClimate, a high-resolution global dataset of monthly climate and climatic water balance from 1958-2015. Scientific Data, 5(1), 170191. doi: 10.1038/sdata.2017.191

A. B. Bottcher, B. J. Whiteley, A. I. James, & J. G. Hiscock. (2012). Watershed assessment model (WAM): Model use, calibration, and validation. Transactions of the ASABE, 55(4), 1367–1383. doi: 10.13031/2013.42248

Agriculture, & Canada, A.-F. (2013, December 13). Soil landscapes of Canada (SLC). Retrieved from https://sis.agr.gc.ca/cansis/nsdb/slc/index.html

Agri-food Canada, Agriculture. (2018). ISO 19131 Annual Crop Inventory–Data Product Specifications. Agriculture and Agri-Food Canada.

Alexander, R. B., & Smith, R. A. (1990). County-level estimates of nitrogen and phosphorus fertilizer use in the United States, 1945 to 1985 (No. 90-130). U.S. Geological Survey ;Books and Open-File Reports [distributor],. doi: 10.3133/ofr90130

Ali, G., & English, C. (2019). Phytoplankton blooms in Lake Winnipeg linked to selective water-gatekeeper connectivity. Scientific Reports, 9(1), 8395. doi: 10.1038/s41598-019-44717-y

Allinger, L. E., & Reavie, E. D. (2013). The ecological history of Lake Erie as recorded by the phytoplankton community. Journal of Great Lakes Research, 39(3), 365–382. doi: 10.1016/j.jglr.2013.06.014

Altieri, A. H., & Gedan, K. B. (2015). Climate change and dead zones. Global Change Biology, 21(4), 1395–1406. doi: 10.1111/gcb.12754

Amorim, C. A., & Moura, A. do N. (2021). Ecological impacts of freshwater algal blooms on water quality, plankton biodiversity, structure, and ecosystem functioning. The Science of the Total Environment, 758, 143605. doi: 10.1016/j.scitotenv.2020.143605

Andersson, H., Bergström, L., Djodjic, F., Ulén, B., & Kirchmann, H. (2013). Topsoil and subsoil properties influence phosphorus leaching from four agricultural soils. Journal of Environmental Quality, 42(2), 455–463. doi: 10.2134/jeq2012.0224

Andrews, L. (2019, May 10). 2018 Great Lakes Commission Annual Report. Great Lakes Commission. Retrieved from https://www.glc.org/library/2018-glc-annual-report

Annual crop inventory 2016. Retrieved from https://open.canada.ca/data/en/dataset/b8e4da73-fb5f-4e6e-93a4-8b1f40d95b51

Annual crop inventory 2021. Retrieved from https://open.canada.ca/data/en/dataset/199e4ab6-832b-4434-ac39-e4887d7cc4e5

Annual report … .: En161-14E-PDF - Government of Canada Publications - Canada.ca. (2002, July 1). Retrieved from https://publications.gc.ca/site/eng/9.512580/publication.html

Aronsson, H., Hansen, E. M., Thomsen, I. K., Liu, J., Øgaard, A. F., Känkänen, H., & Ulén, B. (2016). The ability of cover crops to reduce nitrogen and phosphorus losses from arable land in

southern Scandinavia and Finland. Journal of Soil and Water Conservation, 71(1), 41–55. doi: 10.2489/jswc.71.1.41

Asadzadeh, M., & Tolson, B. (2013). Pareto archived dynamically dimensioned search with hypervolume-based selection for multi-objective optimization. Engineering Optimization, 45(12), 1489–1509. doi: 10.1080/0305215X.2012.748046

Attanasi, E. D., & Coburn, T. C. (2020). Random Forest. In B. S. Daya Sagar, Q. Cheng, J. McKinley, & F. Agterberg (Eds.), Encyclopedia of Mathematical Geosciences (pp. 1–4). Cham: Springer International Publishing. doi: 10.1007/978-3-030-26050-7_265-1

Baker, D. B., & Richards, R. P. (2002). Phosphorus budgets and riverine phosphorus export in northwestern Ohio watersheds. Journal of Environmental Quality, 31(1), 96–108. doi: 10.2134/jeq2002.9600

Basche, A. D., Archontoulis, S. V., Kaspar, T. C., Jaynes, D. B., Parkin, T. B., & Miguez, F. E. (2016). Simulating long-term impacts of cover crops and climate change on crop production and environmental outcomes in the Midwestern United States. Agriculture, Ecosystems & Environment, 218, 95–106. doi: 10.1016/j.agee.2015.11.011

Basu, N. B., Destouni, G., Jawitz, J. W., Thompson, S. E., Loukinova, N. V., Darracq, A., Zanardo, S., Yaeger, M., Sivapalan, M., Rinaldo, A., & Rao, P. S. C. (2010). Nutrient loads exported from managed catchments reveal emergent biogeochemical stationarity. Geophysical Research Letters, 37(23). doi: 10.1029/2010GL045168

Basu, N. B., Thompson, S. E., & Rao, P. S. C. (2011). Hydrologic and biogeochemical functioning of intensively managed catchments: A synthesis of top-down analyses. Water Resources Research, 47(10), 1–12. doi: 10.1029/2011WR010800

Basu, N. B., Van Meter, K. J., Byrnes, D. K., Van Cappellen, P., Brouwer, R., Jacobsen, B. H., Jarsjö, J., Rudolph, D. L., Cunha, M. C., Nelson, N., Bhattacharya, R., Destouni, G., & Olsen, S. B. (2022). Managing nitrogen legacies to accelerate water quality improvement. Nature Geoscience, 15(2), 97–105. doi: 10.1038/s41561-021-00889-9

Batool, M., Sarrazin, F. J., Attinger, S., Basu, N. B., Van Meter, K., & Kumar, R. (2022). Long-term annual soil nitrogen surplus across Europe (1850-2019). Scientific Data, 9(1), 612. doi: 10.1038/s41597-022-01693-9

Becker, R. H., Sultan, M. I., Boyer, G. L., Twiss, M. R., & Konopko, E. (2009). Mapping cyanobacterial blooms in the Great Lakes using MODIS. Journal of Great Lakes Research, 35(3), 447–453. doi: 10.1016/j.jglr.2009.05.007

Bennett, E. M., Carpenter, S. R., & Caraco, N. F. (2001). Human impact on erodable phosphorus and eutrophication: a global perspective: increasing accumulation of phosphorus in soil threatens rivers, lakes, and coastal oceans with eutrophication. Bioscience, 51(3), 227–234. Retrieved from https://academic.oup.com/bioscience/article-abstract/51/3/227/256199

Bennett, E. M., Reed-Andersen, T., Houser, J. N., Gabriel, J. R., & Carpenter, S. R. (1999). A phosphorus budget for the Lake Mendota watershed. Ecosystems, 2(1), 69–75. doi: 10.1007/s100219900059

Bhandari, A. B., Gelderman, R., German, D., & Todey, D. (2021). Manure Application Timing and Tillage Influence on Nutrient Loss from Snowmelt Runoff. Soil Systems, 5(4), 67. doi: 10.3390/soilsystems5040067

Bindraban, P. S., Dimkpa, C. O., & Pandey, R. (2020). Exploring phosphorus fertilizers and fertilization strategies for improved human and environmental health. Biology and Fertility of Soils, 56(3), 299–317. doi: 10.1007/s00374-019-01430-2

Bittman, S., Sheppard, S. C., Poon, D., & Hunt, D. E. (2017). Phosphorus flows in a peri-urban region with intensive food production: A case study. Journal of Environmental Management, 187, 286–297. doi: 10.1016/j.jenvman.2016.11.040

Bittman, S., Worth, D., Hunt, D., Spiegal, S., Kleinman, P., Nanayakkara, S., Vendramini, J., Silveira, M., Flynn, C., Reid, K., Martin, T., VanderZaag, A., & Javorek, S. (2023). Distribution of livestock sectors in Canada: Implications for manureshed management. Journal of Environmental Quality. doi: 10.1002/jeq2.20457

Boardman, E., Danesh-Yazdi, M., Foufoula-Georgiou, E., Dolph, C. L., & Finlay, J. C. (2019). Fertilizer, landscape features and climate regulate phosphorus retention and river export in diverse Midwestern watersheds. Biogeochemistry, 146(3), 293–309. doi: 10.1007/s10533-019-00623-z

Bolster, C. H., Wessel, B. M., Vadas, P. A., & Fiorellino, N. M. (2022). Sensitivity and uncertainty analysis for predicted soil test phosphorus using the Annual Phosphorus Loss Estimator model. Journal of Environmental Quality, 51(2), 216–227. doi: 10.1002/jeq2.20328

Bonsdorff, E. (2021). Eutrophication: Early warning signals, ecosystem-level and societal responses, and ways forward: This article belongs to Ambio's 50th Anniversary Collection. Theme: Eutrophication. Ambio, 50(4), 753–758. doi: 10.1007/s13280-020-01432-7

Bork, E. W., Döbert, T. F., Grenke, J. S. J., Carlyle, C. N., Cahill, J. F., & Boyce, M. S. (2021). Comparative Pasture Management on Canadian Cattle Ranches With and Without Adaptive Multipaddock Grazing. Rangeland Ecology & Management, 78, 5–14. doi: 10.1016/j.rama.2021.04.010

Bouwman, L., Goldewijk, K. K., Hoek, K. W. V. D., Beusen, A. H. W., Van Vuuren, D. P., Willems, J., Rufino, M. C., & Stehfest, E. (2013). Exploring global changes in nitrogen and phosphorus cycles in agriculture induced by livestock production over the 1900–2050 period. Proceedings of the National Academy of Sciences, 110(52), 20882–20887. doi: 10.1073/pnas.1012878108

Boyer, E. W., Goodale, C. L., Jaworski, N. A., & Howarth, R. W. (2002). Anthropogenic nitrogen sources and relationships to riverine nitrogen export in the northeastern U.S.A. Biogeochemistry, 57(1), 137–169. doi: 10.1023/A:1015709302073

Bruulsema, T. (2022). Nutrient stewardship: Taking 4R further. Crops & Soils, 55(1), 34–40. doi: 10.1002/crso.20165

Bruulsema, T. W., Mullen, R. W., O'Halloran, I. P., & Warncke, D. D. (2011). Agricultural phosphorus balance trends in Ontario, Michigan and Ohio. Canadian Journal of Soil Science, 91(3), 437–442. doi: 10.4141/cjss10002

Budd, J. W., Beeton, A. M., Stumpf, R. P., Culver, D. A., & Charles Kerfoot, W. (2001). Satellite observations of Microcystis blooms in western Lake Erie. In SIL Proceedings, 1922-2010 (Vol. 27, Issue 7, pp. 3787–3793). doi: 10.1080/03680770.1998.11901692

Bukhari, H., Elkin, J., Hemken, M., Lichten, N., Pettit, R., & Shattuck, S. (2015). Evaluation of Different Approaches for Controlling Phosphorus Pollution in the Maumee River Watershed. Retrieved from https://deepblue.lib.umich.edu/handle/2027.42/111006

Byrnes, D. K., Van Meter, K. J., & Basu, N. B. (2020). Long-term shifts in U.S. nitrogen sources and sinks revealed by the new TREND-nitrogen data set (1930–2017). Global Biogeochemical Cycles, 34(9), e2020GB006626. doi: 10.1029/2020gb006626

Cabas, J., Weersink, A., & Olale, E. (2010). Crop yield response to economic, site and climatic variables. Climatic Change, 101(3), 599–616. doi: 10.1007/s10584-009-9754-4

Canada, F. (2020, August 31). Fertilizer industry achieves record fertilizer shipments in 2020. Fertilizer Canada. Retrieved from https://fertilizercanada.ca/news-events/news/fertilizer-industry-achieves-record-fertilizer-shipments-in-2020/

Canada, S. (2010, October 4). History of the census of Canada. Retrieved from https://www12.statcan.gc.ca/census-recensement/2011/ref/about-apropos/history-histoire-eng.cfm

Carleton, J. N., & Lee, S. S. (2023). Modeling Lake Recovery Lag Times Following Influent Phosphorus Loading Reduction. Environmental Modelling and Software[R], 162, 1–15. doi: 10.1016/j.envsoft.2023.105642

Carpenter, S. R. (2005). Eutrophication of aquatic ecosystems: bistability and soil phosphorus. Proceedings of the National Academy of Sciences of the United States of America, 102(29), 10002–10005. doi: 10.1073/pnas.0503959102

Carpenter, S. R., Caraco, N. F., & Correll, D. L. (1997). Nonpoint pollution of surface waters with phosphorus and nitrogen. Ecological. doi: 10.1890/1051-0761(1998)008[0559:NPOSWW]2.0.CO;2

Chang, C., Ashenhurst, F., Damaia, S., & Mann, W. (2002). Ontario Flow Assessment Techniques (OFAT). WIT Transactions on Ecology and the Environment, 52. Retrieved from https://www.witpress.com/elibrary/wit-transactions-on-ecology-and-the-environment/52/475

Chang, S. Y., Zhang, Q., Byrnes, D. K., Basu, N. B., & Van Meter, K. J. (2021). Chesapeake legacies: the importance of legacy nitrogen to improving Chesapeake Bay water quality. Environmental Research Letters: ERL [Web Site], 16(8), 085002. doi: 10.1088/1748-9326/ac0d7b

Chen, D., Hu, M., Wang, J., Guo, Y., & Dahlgren, R. A. (2016). Factors controlling phosphorus export from agricultural/forest and residential systems to rivers in eastern China, 1980–2011. Journal of Hydrology, 533, 53–61. doi: 10.1016/j.jhydrol.2015.11.043

Chen, D., Shen, H., Hu, M., Wang, J., Zhang, Y., & Dahlgren, R. A. (2018). Chapter Five - Legacy Nutrient Dynamics at the Watershed Scale: Principles, Modeling, and Implications. In D. L. Sparks (Ed.), Advances in Agronomy (Vol. 149, pp. 237–313). Academic Press. doi: 10.1016/bs.agron.2018.01.005

Chen, H., Yin, J., Song, M., Ding, H., Mo, F., Ren, Q., Li, G., Song, S., & Wang, Y. (2023). The evaluation of N/P fate using the SPARROW model: a case study in an arid and semi-arid region, northern China. Environmental Science and Pollution Research International, 30(19), 55662–55677. doi: 10.1007/s11356-023-26240-w

Chen, M., Chen, J., & Sun, F. (2008). Agricultural phosphorus flow and its environmental impacts in China. The Science of the Total Environment, 405(1-3), 140–152. doi: 10.1016/j.scitotenv.2008.06.031

Chen, M., & Graedel, T. E. (2016). A half-century of global phosphorus flows, stocks, production, consumption, recycling, and environmental impacts. Global Environmental Change: Human and Policy Dimensions, 36, 139–152. doi: 10.1016/j.gloenvcha.2015.12.005

Ciampitti, I. A., & Vyn, T. J. (2012). Physiological perspectives of changes over time in maize yield dependency on nitrogen uptake and associated nitrogen efficiencies: A review. Field Crops Research, 133, 48–67. doi: 10.1016/j.fcr.2012.03.008

Condron, L. M., Spears, B. M., Haygarth, P. M., Turner, B. L., & Richardson, A. E. (2013). Role of legacy phosphorus in improving global phosphorus-use efficiency. Environmental Development, 8, 147–148. doi: 10.1016/j.envdev.2013.09.003

Conley, D. J., Paerl, H. W., Howarth, R. W., Boesch, D. F., Seitzinger, S. P., Havens, K. E., Lancelot, C., & Likens, G. E. (2009). Ecology. Controlling eutrophication: nitrogen and phosphorus. Science, 323(5917), 1014–1015. doi: 10.1126/science.1167755

Cordell, D., Drangert, J.-O., & White, S. (2009). The story of phosphorus: Global food security and food for thought. Global Environmental Change: Human and Policy Dimensions, 19(2), 292–305. doi: 10.1016/j.gloenvcha.2008.10.009

County-Level Estimates of Nitrogen and Phosphorus from Commercial Fertilizer for the Conterminous United States, 1987-2012. (2020, August 26). Retrieved from https://www.sciencebase.gov/catalog/item/5851b2d1e4b0f99207c4f238

Crop Nutrient Balance - Canada - Phosphorus. Retrieved from http://phosphorus.ipni.net/article/NANE-3104. Retrieved on 2021

Daniel, T. C., Sharpley, A. N., Edwards, D. R., Wedepohl, R., & Lemunyon, J. L. (1994). Minimizing surface water eutrophication from agriculture by phosphorus management. Journal of Soil and Water Conservation. Retrieved from https://pubag.nal.usda.gov/catalog/20712

Davis, C. C. (1964). Evidence for the eutrophication of lake Erie from phytoplankton records. Limnology and Oceanography, 9(3), 275–283. doi: 10.4319/lo.1964.9.3.0275

de Vente, J., & Poesen, J. (2005). Predicting soil erosion and sediment yield at the basin scale: Scale issues and semi-quantitative models. Earth-Science Reviews, 71(1), 95–125. doi: 10.1016/j.earscirev.2005.02.002

Diaz, R. J., & Rosenberg, R. (2009). Spreading Dead Zones and Consequences for Marine Ecosystems. 2009. Retrieved from http://science.sciencemag.org/

Dillon, P. J., Reid, R. A., & Evans, H. E. (1993). The relative magnitude of phosphorus sources for small, oligotrophic lakes in Ontario, Canada. SIL Proceedings, 1922-2010, 25(1), 355–358. doi: 10.1080/03680770.1992.11900133

Dodds, W. K., Bouska, W. W., Eitzmann, J. L., Pilger, T. J., Pitts, K. L., Riley, A. J., Schloesser, J. T., & Thornbrugh, D. J. (2009). Eutrophication of U.S. freshwaters: analysis of potential economic damages. Environmental Science & Technology, 43(1), 12–19. doi: 10.1021/es801217q

Dony, J. (2020). A random forest in the Great Lakes: Exploring nutrient water quality in the Laurentian Great Lakes watersheds [University of Waterloo]. Retrieved from https://uwspace.uwaterloo.ca/handle/10012/16347

Duncan, E. W., Osmond, D. L., Shober, A. L., Starr, L., Tomlinson, P., Kovar, J. L., Moorman, T. B., Peterson, H. M., Fiorellino, N. M., & Reid, K. (2019). Phosphorus and soil health management practices. Agricultural & Environmental Letters, 4(1), 190014. doi: 10.2134/ael2019.04.0014

Elser, J. J., Marzolf, E. R., & Goldman, C. R. (1990). Phosphorus and Nitrogen Limitation of Phytoplankton Growth in the Freshwaters of North America: A Review and Critique of Experimental Enrichments. Canadian Journal of Fisheries and Aquatic Sciences. Journal Canadien Des Sciences Halieutiques et Aquatiques, 47(7), 1468–1477. doi: 10.1139/f90-165

Environment, & Canada, C. C. (2020, October 14). Phosphorus loading to Lake Erie. Retrieved from https://www.canada.ca/en/environment-climate-change/services/environmental-indicators/phosphorus-loading-lake-erie.html

Erie, L., Phosphorus, B., Agriculture, •., & Canada, A.-F. (2019). Lake Erie Binational Phosphorus Reduction Strategy Prepared by the Great Lakes Water Quality Agreement Nutrients Annex Subcommittee.

Esenkulova, S., Suchy, K. D., Pawlowicz, R., Costa, M., & Pearsall, I. A. (2021). Harmful algae and oceanographic conditions in the Strait of Georgia, Canada based on citizen science monitoring. Frontiers in Marine Science, 8. doi: 10.3389/fmars.2021.725092

Falcone, J. A. (2021). Estimates of county-level nitrogen and phosphorus from fertilizer and manure from 1950 through 2017 in the conterminous United States (No. 2020-1153). U.S. Geological Survey. doi: 10.3133/ofr20201153

Fang, Y., & Jawitz, J. W. (2018). High-resolution reconstruction of the United States human population distribution, 1790 to 2010. Scientific Data, 5, 180067. doi: 10.1038/sdata.2018.67

Farley, M. (2023). Bold action needed to meaningfully reduce algal blooms in western Lake Erie. Alliance for the Great Lakes. Retrieved from https://greatlakes.org/2023/02/bold-action-needed-to-meaningfully-reduce-algal-blooms-in-western-lake-erie/

Favot, E. J., Holeton, C., DeSellas, A. M., & Paterson, A. M. (2023). Cyanobacterial blooms in Ontario, Canada: Continued increase in reports through the 21st century. Lake and Reservoir Management, 1–20. doi: 10.1080/10402381.2022.2157781

Fenton, O., Schulte, R. P. O., Jordan, P., Lalor, S. T. J., & Richards, K. G. (2011). Time lag: A methodology for the estimation of vertical and horizontal travel and flushing timescales to nitrate

threshold concentrations in Irish aquifers. Environmental Science & Policy, 14(4), 419–431. doi: 10.1016/j.envsci.2011.03.006

Fick, S. E., & Hijmans, R. J. (2017). WorldClim 2: new 1-km spatial resolution climate surfaces for global land areas. International Journal of Climatology, 37(12), 4302–4315. doi: 10.1002/joc.5086

Field, A. J. (2011). A Great Leap Forward: 1930s Depression and U.S. Economic Growth. Yale University Press. Retrieved from https://play.google.com/store/books/details?id=n2tXIWa8PoYC

Filippelli, G. M. (2008). The Global Phosphorus Cycle: Past, Present, and Future. Elements , 4(2), 89–95. doi: 10.2113/GSELEMENTS.4.2.89

Focus volume 13, issue 1 (march/April 1988). (2018, July 26). International Joint Commission. Retrieved from https://www.ijc.org/en/focus-volume-13-issue-1-marchapril-1988

Food and Agriculture Organization of the United Nations (FAO). (2022). Fertilizers by Nutrient [Data set]. Retrieved from https://www.fao.org/faostat/en/#data/RFN

Fouzia, H. B. (2019). Monitoring of Marine Pollution. BoD – Books on Demand. Retrieved from https://play.google.com/store/books/details?id=mTj8DwAAQBAJ

Glibert, P. M. (2020). From hogs to HABs: impacts of industrial farming in the US on nitrogen and phosphorus and greenhouse gas pollution. Biogeochemistry, 150(2), 139–180. doi: 10.1007/s10533-020-00691-6

Glibert, P. M., Maranger, R., Sobota, D. J., & Bouwman, L. (2014). The Haber Bosch–harmful algal bloom (HB–HAB) link. Environmental Research Letters, 9(10), 105001. doi: 10.1088/1748-9326/9/10/105001

Government of Canada, & Canada, S. (2001, January 15). Census of Population. Retrieved from https://www12.statcan.gc.ca/census-recensement/index-eng.cfm

Government of Canada, & Canada, S. (2013). Fertilizer shipments to Canadian agriculture markets, by nutrient content and fertilizer year [Data set]. Government of Canada, Statistics Canada. Retrieved from https://www150.statcan.gc.ca/t1/tbl1/en/tv.action?pid=3210027401

Government of Canada, & Canada, S. (2023a). Estimated areas, yield, production, average farm price and total farm value of principal field crops, in metric and imperial units [Data set]. Government of Canada, Statistics Canada. Retrieved from https://www150.statcan.gc.ca/t1/tbl1/en/tv.action?pid=3210035901

Government of Canada, & Canada, S. (2023b). Fertilizer shipments to Canadian agriculture markets, by nutrient content and fertilizer year, cumulative data (x 1,000) [Data set]. Government of Canada, Statistics Canada. Retrieved from https://www150.statcan.gc.ca/t1/tbl1/en/tv.action?pid=3210003901

Government of Canada, & Canada, S. (2023c). Appendix A – glossary. Retrieved from https://www12.statcan.gc.ca/census-recensement/2021/ref/98-306/2021001/app-annA-eng.cfm

Goyette, J.-O., Bennett, E. M., Howarth, R. W., & Maranger, R. (2016). Changes in anthropogenic nitrogen and phosphorus inputs to the St. Lawrence sub-basin over 110 years and impacts on riverine export. Global Biogeochemical Cycles, 30(7), 1000–1014. doi: 10.1002/2016gb005384

Grant, C. A., & Flaten, D. N. (2019). 4R Management of Phosphorus Fertilizer in the Northern Great Plains. Journal of Environmental Quality, 48(5), 1356–1369. doi: 10.2134/jeq2019.02.0061

Gupta, H. V., Kling, H., Yilmaz, K. K., & Martinez, G. F. (2009). Decomposition of the mean squared error and NSE performance criteria: Implications for improving hydrological modelling. Journal of Hydrology, 377(1), 80–91. doi: 10.1016/j.jhydrol.2009.08.003

Haines, M., Fishback, P., & Rhode, P. (2014). United States Agriculture Data, 1840 - 2012 [Data set]. ICPSR - Interuniversity Consortium for Political and Social Research. doi: 10.3886/ICPSR35206.V4

Hamilton, S. K. (2012). Biogeochemical time lags may delay responses of streams to ecological restoration. Freshwater Biology, 57(SUPPL. 1), 43–57. doi: 10.1111/j.1365-2427.2011.02685.x

Han, H., Allan, D. J., & Bosch, N. S. (2012). Historical pattern of phosphorus loading to Lake Erie watersheds. Journal of Great Lakes Research, 38(2), 289–298. doi: 10.1016/j.jglr.2012.03.004

Han, H., Bosch, N., & Allan, J. D. (2011). Spatial and temporal variation in phosphorus budgets for 24 watersheds in the Lake Erie and Lake Michigan basins. Biogeochemistry, 102(1), 45–58. doi: 10.1007/s10533-010-9420-y

Hargan, K. E., Paterson, A. M., & Dillon, P. J. (2011). A total phosphorus budget for the Lake of the Woods and the Rainy River catchment. In Journal of Great Lakes Research (Vol. 37, Issue 4, pp. 753–763). doi: 10.1016/j.jglr.2011.09.001

Harrison, J. A., Beusen, A. H. W., Fink, G., Tang, T., Strokal, M., Bouwman, A. F., Metson, G. S., & Vilmin, L. (2019). Modeling phosphorus in rivers at the global scale: recent successes, remaining challenges, and near-term opportunities. Current Opinion in Environmental Sustainability, 36, 68–77. doi: 10.1016/j.cosust.2018.10.010

Haygarth, P. M., Jarvie, H. P., Powers, S. M., Sharpley, A. N., Elser, J. J., Shen, J., Peterson, H. M., Chan, N.-I., Howden, N. J. K., Burt, T., Worrall, F., Zhang, F., & Liu, X. (2014). Sustainable phosphorus management and the need for a long-term perspective: the legacy hypothesis. Environmental Science & Technology, 48(15), 8417–8419. doi: 10.1021/es502852s

Haygarth, P. M., & Jarvis, S. C. (1999). Transfer of Phosphorus from Agricultural Soil. In D. L. Sparks (Ed.), Advances in Agronomy (Vol. 66, pp. 195–249). Academic Press. doi: 10.1016/S0065-2113(08)60428-9

Haygarth, P. M., Wood, F. L., Heathwaite, A. L., & Butler, P. J. (2005). Phosphorus dynamics observed through increasing scales in a nested headwater-to-river channel study. The Science of the Total Environment, 344(1-3), 83–106. doi: 10.1016/j.scitotenv.2005.02.007

Heagy, E. (n.d.). Nutrient project catalogue. Upper Thames River Conservation Authority. Retrieved from https://thamesriver.on.ca/about-us/publications/nutrient-project-catalogue/?doing_wp_cron=1688485173.5558240413665771484375

Hirsch, R. M., Archfield, S. A., & De Cicco, L. A. (2015). A bootstrap method for estimating uncertainty of water quality trends. Environmental Modelling and Software, 73, 148–166. doi: 10.1016/j.envsoft.2015.07.017

Hirsch, R. M., & De Cicco, L. A. (2015). User guide to Exploration and Graphics for RivEr Trends (EGRET) and dataRetrieval: R packages for hydrologic data. In Techniques and Methods (No. 4-A10). US Geological Survey. doi: 10.3133/tm4a10

Hirsch, R. M., Moyer, D. L., & Archfield, S. A. (2010a). Weighted Regressions on Time, Discharge, and Season (WRTDS), With an Application to Chesapeake Bay River Inputs. Journal of the American Water Resources Association, 46(5), 857–880. doi: 10.1111

Hirsch, R. M., Moyer, D. L., & Archfield, S. A. (2010b). Weighted Regressions on Time, Discharge, and Season (WRTDS), with an Application to Chesapeake Bay River Inputs. Journal of the American Water Resources Association, 46(5), 857–880. doi: 10.1111/j.1752-1688.2010.00482.x

Holman, I. P., Whelan, M. J., Howden, N. J. K., Bellamy, P. H., Willby, N. J., Rivas-Casado, M., & McConvey, P. (2008). Phosphorus in groundwater-an overlooked contributor to eutrophication? Hydrological Processes, 22(26), 5121–5127. doi: 10.1002/hyp.7198

Hong, B., Swaney, D. P., Mörth, C. M., Smedberg, E., Eriksson Hägg, H., Humborg, C., Howarth, R. W., & Bouraoui, F. (2012). Evaluating regional variation of net anthropogenic nitrogen and phosphorus inputs (NANI/NAPI), major drivers, nutrient retention pattern and management implications in the multinational areas of Baltic Sea basin. Ecological Modelling, 227, 117–135. doi: 10.1016/j.ecolmodel.2011.12.002

Hou, Y., Ma, L., Gao, Z. L., Wang, F. H., Sims, J. T., Ma, W. Q., & Zhang, F. S. (2013). The driving forces for nitrogen and phosphorus flows in the food chain of china, 1980 to 2010. Journal of Environmental Quality, 42(4), 962–971. doi: 10.2134/jeq2012.0489

Hu, M., Liu, Y., Zhang, Y., Shen, H., Yao, M., Dahlgren, R. A., & Chen, D. (2020). Long-term (1980-2015) changes in net anthropogenic phosphorus inputs and riverine phosphorus export in the Yangtze River basin. Water Research, 177, 115779. doi: 10.1016/j.watres.2020.115779

Hwang, S.-W., Jang, T.-I., Park, S.-W., & Kang, M.-S. (2006). The Application of the GWLF model for Rural Small Watershed. Journal of The Korean Society of Agricultural Engineers, 48(3), 23–34. doi: 10.5389/KSAE.2006.48.3.023

Ilampooranan, I., Van Meter, K. J., & Basu, N. B. (2022). Intensive agriculture, nitrogen legacies, and water quality: Intersections and implications. Environmental Research Letters: ERL [Web Site], 17(3). doi: 10.1088/1748-9326/ac55b5

Inorganic fertilizers 2000–2021. Food and Agriculture Organization of the United Nations. Retrieved from https://www.fao.org/food-agriculture-statistics/data-release/data-release-detail/en/c/1644432/

IPNI estimates of nutrient uptake and removal. (2011). Retrieved from http://www.ipni.net/article/IPNI-3296

IPNI Estimates of Nutrient Uptake and Removal. (2011). Retrieved from http://www.ipni.net/article/IPNI-3296

Jacoby, J. M., & Kann, J. (2007). The occurrence and response to toxic cyanobacteria in the Pacific Northwest, North America. Lake and Reservoir Management, 23(2), 123–143. doi: 10.1080/07438140709353916

Janssen, B. H. (1984). A simple method for calculating decomposition and accumulation of "young" soil organic matter. In J. Tinsley & J. F. Darbyshire (Eds.), Biological Processes and Soil Fertility (pp. 297–304). Dordrecht: Springer Netherlands. doi: 10.1007/978-94-009-6101-2_26

Jarvie, H. P., Johnson, L. T., Sharpley, A. N., Smith, D. R., Baker, D. B., Bruulsema, T. W., & Confesor, R. (2017). Increased Soluble Phosphorus Loads to Lake Erie: Unintended Consequences of Conservation Practices? Journal of Environmental Quality, 46(1), 123–132. doi: 10.2134/jeq2016.07.0248

Jarvie, H. P., Sharpley, A. N., Brahana, V., Simmons, T., Price, A., Neal, C., Lawlor, A. J., Sleep, D., Thacker, S., & Haggard, B. E. (2014). Phosphorus retention and remobilization along hydrological pathways in karst terrain. Environmental Science & Technology, 48(9), 4860–4868. doi: 10.1021/es405585b

Jarvie, H. P., Sharpley, A. N., Scott, J. T., Haggard, B. E., Bowes, M. J., & Massey, L. B. (2012). Within-river phosphorus retention: Accounting for a missing piece in the watershed phosphorus puzzle. Environmental Science and Technology, 46(24), 13284–13292. doi: 10.1021/es303562y

Jarvie, H. P., Sharpley, A. N., Spears, B., Buda, A. R., May, L., & Kleinman, P. J. A. (2013). Water quality remediation faces unprecedented challenges from "legacy phosphorus." Environmental Science & Technology, 47(16), 8997–8998. doi: 10.1021/es403160a

Kalcic, M. M., Muenich, R. L., Basile, S., Steiner, A. L., Kirchhoff, C., & Scavia, D. (2019). Climate Change and Nutrient Loading in the Western Lake Erie Basin: Warming Can Counteract a Wetter Future. Environmental Science & Technology, 53(13), 7543–7550. doi: 10.1021/acs.est.9b01274

Kane, D. D., Conroy, J. D., Peter Richards, R., Baker, D. B., & Culver, D. A. (2014). Re-eutrophication of Lake Erie: Correlations between tributary nutrient loads and phytoplankton biomass. Journal of Great Lakes Research, 40(3), 496–501. doi: 10.1016/j.jglr.2014.04.004

Khare, Y. P., Paudel, R., Wiederholt, R., Abiy, A. Z., Van Lent, T., Davis, S. E., & Her, Y. (2021). Watershed Response to Legacy Phosphorus and Best Management Practices in an Impacted Agricultural Watershed in Florida, U.S.A. Land, 10(9), 977. doi: 10.3390/land10090977

King, K. W., Williams, M. R., Macrae, M. L., Fausey, N. R., Frankenberger, J., Smith, D. R., Kleinman, P. J. A., & Brown, L. C. (2015). Phosphorus transport in agricultural subsurface drainage: a review. Journal of Environmental Quality, 44(2), 467–485. doi: 10.2134/jeq2014.04.0163

Kirchman, D. L. (2021). Dead Zones: The Loss of Oxygen from Rivers, Lakes, Seas, and the Ocean. Oxford University Press. Retrieved from https://play.google.com/store/books/details?id=jHEWEAAAQBAJ

Kirchmann, H., & Thorvaldsson, G. (2000). Challenging targets for future agriculture. European Journal of Agronomy: The Journal of the European Society for Agronomy, 12(3), 145–161. doi: 10.1016/S1161-0301(99)00053-2

Kleinman, P. J. A., Fanelli, R. M., Hirsch, R. M., Buda, A. R., Easton, Z. M., Wainger, L. A., Brosch, C., Lowenfish, M., Collick, A. S., Shirmohammadi, A., Boomer, K., Hubbart, J. A., Bryant, R. B., & Shenk, G. W. (2019). Phosphorus and the Chesapeake Bay: Lingering Issues and Emerging Concerns for Agriculture. Journal of Environmental Quality, 48(5), 1191–1203. doi: 10.2134/jeq2019.03.0112

Kleinman, P. J. A., Sharpley, A. N., Withers, P. J. A., Bergström, L., Johnson, L. T., & Doody, D. G. (2015). Implementing agricultural phosphorus science and management to combat eutrophication. Ambio, 44 Suppl 2(Suppl 2), S297–S310. doi: 10.1007/s13280-015-0631-2

Kleinman, P. J. A., Smith, D. R., Bolster, C. H., & Easton, Z. M. (2015). Phosphorus Fate, Management, and Modeling in Artificially Drained Systems. Journal of Environmental Quality, 44(2), 460–466. doi: 10.2134/jeq2015.02.0090

Kleinman, P., Sharpley, A., Buda, A., McDowell, R., & Allen, A. (2011). Soil controls of phosphorus in runoff: Management barriers and opportunities. Canadian Journal of Soil Science, 91(3), 329–338. doi: 10.4141/cjss09106

Kotak, B. G., & Zurawell, R. W. (2007). Cyanobacterial toxins in Canadian freshwaters: A review. Lake and Reservoir Management, 23(2), 109–122. doi: 10.1080/07438140709353915

Kusmer, A. S., Goyette, J. O., MacDonald, G. K., Bennett, E. M., Maranger, R., & Withers, P. J. A. (2019). Watershed Buffering of Legacy Phosphorus Pressure at a Regional Scale: A Comparison Across Space and Time. Ecosystems , 22(1), 91–109. doi: 10.1007/s10021-018-0255-z

Lake Erie Ecosystem Priority, & International Joint Commission. (2014.). A balanced diet for Lake Erie : reducing phosphorus loadings and harmful algal blooms (p. 96).

Lake Erie lakewide action and management plan annual report 2022. (2023). Retrieved from https://binational.net/2023/05/15/lake-erie-lakewide-action-and-management-plan-annual-report-2022/

Lander, C. H., Moffitt, D., & Alt, K. (1998). Nutrients Available from Livestock Manure Relative to Crop Growth Requirements. U.S. Department of Agriculture, Natural Resources Conservation Service. Retrieved from https://www.nrcs.usda.gov/wps/portal/nrcs/detail/national/technical/nra/?cid=nrcs143_014175

Lassaletta, L., Billen, G., Grizzetti, B., Anglade, J., & Garnier, J. (2014). 50 year trends in nitrogen use efficiency of world cropping systems: the relationship between yield and nitrogen input to cropland. Environmental Research Letters, 9(10), 105011. doi: 10.1088/1748-9326/9/10/105011

Leahey, A. Accessing digital historical census boundaries just got a whole lot easier! . Retrieve on 2022. Retrieved from http://geohist.ca/2016/05/accessing-digital-historical-census-boundaries-just-got-a-whole-lot-easier/

LeBlanc, S., Pick, F. R., & Hamilton, P. B. (2008). Fall cyanobacterial blooms in oligotrophic-to-mesotrophic temperate lakes and the role of climate change. SIL Proceedings, 1922-2010, 30(1), 90–94. doi: 10.1080/03680770.2008.11902091

Le Noë, J., Roux, N., Billen, G., Gingrich, S., Erb, K.-H., Krausmann, F., Thieu, V., Silvestre, M., & Garnier, J. (2020). The phosphorus legacy offers opportunities for agro-ecological transition (France 1850–2075). Environmental Research Letters, 15(6), 064022. doi: 10.1088/1748-9326/ab82cc

Li, H., Huang, G., Meng, Q., Ma, L., Yuan, L., Wang, F., Zhang, W., Cui, Z., Shen, J., Chen, X., Jiang, R., & Zhang, F. (2011). Integrated soil and plant phosphorus management for crop and environment in China. A review. Plant and Soil, 349(1-2), 157–167. doi: 10.1007/s11104-011-0909-5

Lindström, G., Pers, C., Rosberg, J., Strömqvist, J., & Arheimer, B. (2010). Development and testing of the HYPE (Hydrological Predictions for the Environment) water quality model for different spatial scales. Hydrology Research, 41(3-4), 295–319. Retrieved from https://iwaponline.com/hr/article-abstract/41/3-4/295/822

Lintern, A., McPhillips, L., Winfrey, B., Duncan, J., & Grady, C. (2020). Best Management Practices for Diffuse Nutrient Pollution: Wicked Problems Across Urban and Agricultural Watersheds. Environmental Science & Technology, 54(15), 9159–9174. doi: 10.1021/acs.est.9b07511

Lin, X., Zhang, R., Jiang, S., & El-Mashad, H. (2017). Losses of Solids, Moisture, Nitrogen, Phosphorus, Potassium, Carbon, and Sulfur from Laying-Hen Manure in Storage Facilities. Water, Air, & Soil Pollution: Focus, 228(3), 102. doi: 10.1007/s11270-017-3275-y

Lin, X., Zhu, L., Sun, D., Li, S., Fang, H., Zhou, W., & Xu, J. (2024). Submerged Plants in River Water Quality Improvement and Algal Bloom Control: A Mini Review. Environmental Governance, Ecological Remediation and Sustainable Development, 381–387. doi: 10.1007/978-3-031-52901-6_37

Litke, D. W. (1999). Review of Phosphorus Control Measures in the United States and Their Effects on Water Quality. U.S. Department of the Interior, U.S. Geological Survey. Retrieved from https://play.google.com/store/books/details?id=CKEJXDN7TOIC

Liu, D., Zheng, C., Qiu, Q., Tang, J., & Xu, Y. (2020). Global pattern of studies on phosphorus at watershed scale. Environmental Science and Pollution Research International, 27(13), 14872–14882. doi: 10.1007/s11356-020-07771-y

Liu, J., Kleinman, P. J. A., Aronsson, H., Flaten, D., McDowell, R. W., Bechmann, M., Beegle, D. B., Robinson, T. P., Bryant, R. B., Liu, H., Sharpley, A. N., & Veith, T. L. (2018). A review of regulations and guidelines related to winter manure application. Ambio, 47(6), 657–670. doi: 10.1007/s13280-018-1012-4

Liu, J., Van Meter, K. J., McLeod, M. M., & Basu, N. B. (2021). Checkered landscapes: hydrologic and biogeochemical nitrogen legacies along the river continuum. Environmental Research Letters: ERL [Web Site], 16(11), 115006. doi: 10.1088/1748-9326/ac243c

Liu, Y., Villalba, G., Ayres, R. U., & Schroder, H. (2008). Global phosphorus flows and environmental impacts from a consumption perspective. Journal of Industrial Ecology, 12(2), 229–247. doi: 10.1111/j.1530-9290.2008.00025.x

Loecke, T. D., Burgin, A. J., Riveros-Iregui, D. A., Ward, A. S., Thomas, S. A., Davis, C. A., & Clair, M. A. S. (2017). Weather whiplash in agricultural regions drives deterioration of water quality. Biogeochemistry, 133(1), 7–15. doi: 10.1007/s10533-017-0315-z

Maavara, T., Chen, Q., Van Meter, K., Brown, L. E., Zhang, J., Ni, J., & Zarfl, C. (2020). River dam impacts on biogeochemical cycling. Nature Reviews Earth & Environment, 1(2), 103–116. doi: 10.1038/s43017-019-0019-0

Maccoux, M. J., Dove, A., Backus, S. M., & Dolan, D. M. (2016). Total and soluble reactive phosphorus loadings to Lake Erie: A detailed accounting by year, basin, country, and tributary. Journal of Great Lakes Research, 42(6), 1151–1165. doi: 10.1016/j.jglr.2016.08.005

MacDonald, G. K., & Bennett, E. M. (2009). Phosphorus accumulation in saint lawrence river watershed soils: A century-long perspective. Ecosystems , 12(4), 621–635. doi: 10.1007/s10021-009-9246-4

MacDonald, G. K., Bennett, E. M., Potter, P. A., & Ramankutty, N. (2011). Agronomic phosphorus imbalances across the world's croplands. Proceedings of the National Academy of Sciences of the United States of America, 108(7), 3086–3091. doi: 10.1073/pnas.1010808108

Macgillivray, K. A., Greenwood, W. J., Paterson, A. M., Watmough, S. A., Williams, A. J., & Eimers, M. C. (2023). Complex patterns of phosphorus delivery in the Lake of the Woods watershed. Journal of Great Lakes Research, 49(1), 21–31. doi: 10.1016/j.jglr.2022.06.002

Macrae, M. L., English, M. C., Schiff, S. L., & Stone, M. (2007). Intra-annual variability in the contribution of tile drains to basin discharge and phosphorus export in a first-order agricultural catchment. Agricultural Water Management, 92(3), 171–182. doi: 10.1016/j.agwat.2007.05.015

Maestre, A., El-Sheikh, E., Williamson, D., & Ward, A. (2014). A Machine Learning Tool for Weighted Regressions in Time, Discharge, and Season. International Journal of Advanced Computer Science and Applications (IJACSA), 5(3). doi: 10.14569/IJACSA.2014.050314

Magdoff, F., & Es, H. V. (2009). Animal manures for increasing organic matter and supplying nutrients. Sustainable Soil Management.

Maki, A. W., Porcella, D. B., & Wendt, R. H. (1984). The impact of detergent phosphorus bans on receiving water quality. Water Research, 18(7), 893–903. doi: 10.1016/0043-1354(84)90275-6

Manning, N. F., Wang, Y.-C., Long, C. M., Bertani, I., Sayers, M. J., Bosse, K. R., Shuchman, R. A., & Scavia, D. (2019). Extending the forecast model: Predicting Western Lake Erie harmful algal blooms at multiple spatial scales. Journal of Great Lakes Research, 45(3), 587–595. doi: 10.1016/j.jglr.2019.03.004

Map: Provincial (stream) Water Quality Monitoring Network. Ontario.ca. Retrieved from https://www.ontario.ca/page/map-provincial-stream-water-quality-monitoring-network

Marques, J., Liu, J., Cunha, M. C., Van Meter, K. J., & Basu, N. B. (2022). Nitrogen legacies in anthropogenic landscapes: a case study in the Mondego Basin in Portugal. Environmental Science and Pollution Research International, 29(16), 23919–23935. doi: 10.1007/s11356-021-16725-x

Martin JL, D.-R. J. (2013). Modelling Phosphorus Export from Humid Subtropical Agricultural Fields: A Case Study Using the HSPF Model in the Mississippi Alluvial Plain. Journal of Earth Science & Climatic Change, 04(06). doi: 10.4172/2157-7617.1000162

Matott, L. S. (2017). OSTRICH--an optimization software toolkit for research involving computational heuristics documentation and user's guide version 17.12. 19. University at Buffalo Center for Computational Research, 1, 79. Retrieved from http://www.civil.uwaterloo.ca/jrcraig/CIVE781/Ostrich_Manual_17_12_19.pdf

McCallum, B. D., & DePauw, R. M. (2008). A review of wheat cultivars grown in the Canadian prairies. Canadian Journal of Plant. Retrieved from https://cdnsciencepub.com/doi/abs/10.4141/CJPS07159

McCrackin, M. L., Muller-Karulis, B., Gustafsson, B. G., Howarth, R. W., Humborg, C., Svanbäck, A., & Swaney, D. P. (2018). A Century of Legacy Phosphorus Dynamics in a Large Drainage Basin. Global Biogeochemical Cycles, 32(7), 1107–1122. doi: 10.1029/2018GB005914

McDowell, R., Dodd, R., Pletnyakov, P., & Noble, A. (2020). The ability to reduce soil legacy phosphorus at a country scale. Frontiers of Environmental Science & Engineering in China, 8. doi: 10.3389/fenvs.2020.00006

McDowell, R. W., Nash, D. M., & Robertson, F. (2007). Sources of phosphorus lost from a grazed pasture receiving simulated rainfall. Journal of Environmental Quality, 36(5), 1281–1288. doi: 10.2134/jeq2006.0347

McDowell, R. W., Sharpley, A. N., Condron, L. M., Haygarth, P. M., & Brookes, P. C. (2001). Processes controlling soil phosphorus release to runoff and implications for agricultural management. Nutrient Cycling in Agroecosystems, 59(3), 269–284. doi: 10.1023/A:1014419206761

McLeod, M. (2023). Modelling Legacy Nitrogen Dynamics in the Transboundary Lake Erie Watershed [University of Waterloo]. Retrieved from https://uwspace.uwaterloo.ca/handle/10012/19122

Meals, D. W., Dressing, S. A., & Davenport, T. E. (2010). Lag time in water quality response to best management practices: A review. In Journal of Environmental Quality (Vol. 39, Issue 1, pp. 85–96). doi: 10.2134/jeq2009.0108

Mekonnen, M. M., & Hoekstra, A. Y. (2018). Global anthropogenic phosphorus loads to freshwater and associated grey water footprints and water pollution levels: A high-resolution global study. Water Resources Research, 54(1), 345–358. doi: 10.1002/2017wr020448

Meng, C., Liu, H., Li, Y., Wang, Y., Li, X., Shen, J., Gong, D., Zhang, M., & Wu, J. (2022). Landscape patterns of catchment and land-use regulate legacy phosphorus releases in subtropical mixed agricultural and woodland catchments. The Science of the Total Environment, 804, 150055. doi: 10.1016/j.scitotenv.2021.150055

Metson, G. S., Lin, J., Harrison, J. A., & Compton, J. E. (2017). Linking terrestrial phosphorus inputs to riverine export across the United States. Water Research, 124, 177–191. doi: 10.1016/j.watres.2017.07.037

Michalak, A. M., Anderson, E. J., Beletsky, D., Boland, S., Bosch, N. S., Bridgeman, T. B., Chaffin, J. D., Cho, K., Confesor, R., Daloglu, I., Depinto, J. V., Evans, M. A., Fahnenstiel, G. L., He, L., Ho, J. C., Jenkins, L., Johengen, T. H., Kuo, K. C., Laporte, E., … Zagorski, M. A. (2013). Record-setting algal bloom in Lake Erie caused by agricultural and meteorological trends consistent with expected future conditions. Proceedings of the National Academy of Sciences of the United States of America, 110(16), 6448–6452. doi: 10.1073/pnas.1216006110

Michigan department of environment, great lakes & energy (EGLE). (n.d.). Retrieved from https://www.michigan.gov/egle

Mishra, S. (2009). Uncertainty and sensitivity analysis techniques for hydrologic modeling. Journal of Hydroinformatics, 11(3-4), 282–296. doi: 10.2166/hydro.2009.048

Mississippi River/Gulf of Mexico Watershed Nutrient Task Force. Monitoring, Modeling, & Research Workgroup. (2004). A Science Strategy to Support Management Decisions Related to Hypoxia in the Northern Gulf of Mexico and Excess Nutrients in the Mississippi River Basin. U.S. Department of the Interior, U.S. Geological Survey. Retrieved from https://play.google.com/store/books/details?id=rs-uWPSieLMC

Motew, M., Chen, X., Booth, E. G., Carpenter, S. R., Pinkas, P., Zipper, S. C., Loheide, S. P., Donner, S. D., Tsuruta, K., Vadas, P. A., & Kucharik, C. J. (2017). The Influence of Legacy P on Lake Water Quality in a Midwestern Agricultural Watershed. Ecosystems , 20(8), 1468–1482. doi: 10.1007/s10021-017-0125-0

Muenich, R. L., Kalcic, M., & Scavia, D. (2016). Evaluating the Impact of Legacy P and Agricultural Conservation Practices on Nutrient Loads from the Maumee River Watershed. Environmental Science and Technology, 50(15), 8146–8154. doi: 10.1021/acs.est.6b01421

Muleta, M. K., & Nicklow, J. W. (2005). Sensitivity and uncertainty analysis coupled with automatic calibration for a distributed watershed model. Journal of Hydrology, 306(1), 127–145. doi: 10.1016/j.jhydrol.2004.09.005

National Land Cover Database (NLCD) 2019 products (ver. 2.0, June 2021). (2023, April 21). Retrieved from https://www.sciencebase.gov/catalog/item/5f21cef582cef313ed940043

Ncei., M. I. . July 1999 drought report. Retrieved from https://www.ncei.noaa.gov/access/monitoring/monthly-report/drought/199907

Newlands, N. K., Zamar, D. S., Kouadio, L. A., Zhang, Y., Chipanshi, A., Potgieter, A., Toure, S., & Hill, H. S. J. (2014). An integrated, probabilistic model for improved seasonal forecasting of agricultural crop yield under environmental uncertainty. Frontiers of Environmental Science & Engineering in China, 2. doi: 10.3389/fenvs.2014.00017

Nicholls, K. H., & Carney, E. C. (2011). The phytoplankton of the Bay of Quinte, 1972–2008: point-source phosphorus loading control, dreissenid mussel establishment, and a proposed

community reference. Aquatic Ecosystem Health & Management, 14(1), 33–43. doi: 10.1080/14634988.2011.550847

Nicholls, K. H., Hopkins, G. J., Standke, S. J., & Nakamoto, L. (2001). Trends in Total Phosphorus in Canadian Near–Shore Waters of the Laurentian Great Lakes: 1976–1999. Journal of Great Lakes Research, 27(4), 402–422. doi: 10.1016/S0380-1330(01)70656-9

Nwankwegu, A. S., Li, Y., Huang, Y., Wei, J., Norgbey, E., Sarpong, L., Lai, Q., & Wang, K. (2019). Harmful algal blooms under changing climate and constantly increasing anthropogenic actions: the review of management implications. 3 Biotech, 9(12), 449. doi: 10.1007/s13205-019-1976-1

NYSOGS. (2022, January 23). Cattaraugus creek integrated watershed action plan (IWAP). Esri. Retrieved from https://storymaps.arcgis.com/stories/369d69e8344a4856ac9729b178445eb0

Oenema, O., Oudendag, D., & Velthof, G. L. (2007). Nutrient losses from manure management in the European Union. Livestock Science, 112(3), 261–272. doi: 10.1016/j.livsci.2007.09.007

Ohio, E. P. A. (2006). Ohio Environmental Protection Agency. Post-Construction Storm Water Practices Available Online: Http://epa. Ohio. Gov/dsw/storm/technical_guidance. Aspx. Retrieved from https://epa.ohio.gov/

Orihel, D. M., Bird, D. F., Brylinsky, M., Chen, H., Donald, D. B., Huang, D. Y., Giani, A., Kinniburgh, D., Kling, H., Kotak, B. G., Leavitt, P. R., Nielsen, C. C., Reedyk, S., Rooney, R. C., Watson, S. B., Zurawell, R. W., & Vinebrooke, R. D. (2012). High microcystin concentrations occur only at low nitrogen-to-phosphorus ratios in nutrient-rich Canadian lakes. Canadian Journal of Fisheries and Aquatic Sciences. Journal Canadien Des Sciences Halieutiques et Aquatiques, 69(9), 1457–1462. doi: 10.1139/f2012-088

Paerl, H. W. (2009). Controlling Eutrophication along the Freshwater–Marine Continuum: Dual Nutrient (N and P) Reductions are Essential. Estuaries and Coasts, 32(4), 593–601. doi: 10.1007/s12237-009-9158-8

Paerl, H. W., Otten, T. G., & Kudela, R. (2018). Mitigating the Expansion of Harmful Algal Blooms Across the Freshwater-to-Marine Continuum. Environmental Science & Technology, 52(10), 5519–5529. doi: 10.1021/acs.est.7b05950

Parfitt, J., Barthel, M., & Macnaughton, S. (2010). Food waste within food supply chains: quantification and potential for change to 2050. Philosophical Transactions of the Royal Society of London. Series B, Biological Sciences, 365(1554), 3065–3081. doi: 10.1098/rstb.2010.0126

Peters, N. E., & Meybeck, M. (2000). Water Quality Degradation Effects on Freshwater Availability: Impacts of Human Activities. Water International, 25(2), 185–193. doi: 10.1080/02508060008686817

Phosphate rock - historical statistics (data series 140). Retrieved from https://www.usgs.gov/media/files/phosphate-rock-historical-statistics-data-series-140

Pick, F. R. (2016). Blooming algae: a Canadian perspective on the rise of toxic cyanobacteria. Canadian Journal of Fisheries and Aquatic Sciences. Journal Canadien Des Sciences Halieutiques et Aquatiques, 73(7), 1149–1158. doi: 10.1139/cjfas-2015-0470

Powers, S. M., Bruulsema, T. W., Burt, T. P., Chan, N. I., Elser, J. J., Haygarth, P. M., Howden, N. J. K., Jarvie, H. P., Lyu, Y., Peterson, H. M., Sharpley, A. N., Shen, J., Worrall, F., & Zhang, F. (2016). Long-term accumulation and transport of anthropogenic phosphorus in three river basins. Nature Geoscience, 9(5), 353–356. doi: 10.1038/ngeo2693

Pretty, J. N., Mason, C. F., Nedwell, D. B., Hine, R. E., Leaf, S., & Dils, R. (2003). Environmental costs of freshwater eutrophication in England and Wales. Environmental Science & Technology, 37(2), 201–208. doi: 10.1021/es020793k

Radcliffe, D. E., Reid, D. K., Blombäck, K., Bolster, C. H., Collick, A. S., Easton, Z. M., Francesconi, W., Fuka, D. R., Johnsson, H., King, K., Larsbo, M., Youssef, M. A., Mulkey, A. S., Nelson, N. O., Persson, K., Ramirez-Avila, J. J., Schmieder, F., & Smith, D. R. (2015). Applicability of Models to Predict Phosphorus Losses in Drained Fields: A Review. Journal of Environmental Quality, 44(2), 614–628. doi: 10.2134/jeq2014.05.0220

Ramankutty, N., Evan, A. T., Monfreda, C., & Foley, J. A. (2008). Farming the planet: 1. Geographic distribution of global agricultural lands in the year 2000. Global Biogeochemical Cycles, 22(1), 1–19. doi: 10.1029/2007GB002952

Ramankutty, N., & Foley, J. A. (1999). Estimating historical changes in global land cover: Croplands from 1700 to 1992. Global Biogeochemical Cycles, 13(4), 997–1027. doi: 10.1029/1999gb900046

Rao, Y. R., Howell, T., Watson, S. B., & Abernethy, S. (2014). On hypoxia and fish kills along the north shore of Lake Erie. Journal of Great Lakes Research, 40(1), 187–191. doi: 10.1016/j.jglr.2013.11.007

Reg. (2015). What is GLWQA. Retrieved from https://www.epa.gov/glwqa/what-glwqa

Reid, K., & Schneider, K. D. (2019). Phosphorus accumulation in canadian agricultural soils over 30 yr. Canadian Journal of Soil Science, 99(4), 520–532. doi: 10.1139/cjss-2019-0023

Reid, K., Schneider, K., & Joosse, P. (2019). Addressing Imbalances in Phosphorus Accumulation in Canadian Agricultural Soils. Journal of Environmental Quality, 48(5), 1156–1166. doi: 10.2134/jeq2019.05.0205

Report on GLWQ for 1972 [first annual report on great lakes water quality]. (2018, July 26). International Joint Commission. Retrieved from https://www.ijc.org/en/report-glwq-1972-first-annual-report-great-lakes-water-quality

Rosa, F., & Burns, N. M. (1987). Lake Erie Central Basin Oxygen Depletion Changes from 1929–1980. Journal of Great Lakes Research, 13(4), 684–696. doi: 10.1016/S0380-1330(87)71683-9

Russell, M. J., Weller, D. E., Jordan, T. E., Sigwart, K. J., & Sullivan, K. J. (2008). Net anthropogenic phosphorus inputs: spatial and temporal variability in the Chesapeake Bay region. Biogeochemistry, 88(3), 285–304. doi: 10.1007/s10533-008-9212-9

Sabo, R. D., Clark, C. M., Gibbs, D. A., Metson, G. S., Jason Todd, M., LeDuc, S. D., Greiner, D., Fry, M. M., Polinsky, R., Yang, Q., Tian, H., & Compton, J. E. (2021). Phosphorus Inventory for the Conterminous United States (2002–2012). In Journal of Geophysical Research: Biogeosciences (Vol. 126, Issue 4). doi: 10.1029/2020jg005684

Sabo, R. D., Clark, C. M., Gibbs, D. A., Metson, G. S., Todd, M. J., LeDuc, S. D., Greiner, D., Fry, M. M., Polinsky, R., Yang, Q., Tian, H., & Compton, J. E. (2021). Phosphorus Inventory for the Conterminous United States (2002–2012). Journal of Geophysical Research: Biogeosciences, 126(4), 1–21. doi: 10.1029/2020jg005684

Sarrazin, F. J., Kumar, R., Basu, N. B., Musolff, A., Weber, M., Van Meter, K. J., & Attinger, S. (2022). Characterizing catchment-scale nitrogen legacies and constraining their uncertainties. Water Resources Research, 58(4). doi: 10.1029/2021wr031587

Sattari, S. Z., Bouwman, A. F., Giller, K. E., & van Ittersum, M. K. (2012). Residual soil phosphorus as the missing piece in the global phosphorus crisis puzzle. Proceedings of the National Academy of Sciences of the United States of America, 109(16), 6348–6353. doi: 10.1073/pnas.1113675109

Scavia, D., Bocaniov, S. A., Dagnew, A., Long, C., & Wang, Y. C. (2019). St. Clair-Detroit River system: Phosphorus mass balance and implications for Lake Erie load reduction, monitoring, and climate change. Journal of Great Lakes Research. doi: 10.1016/j.jglr.2018.11.008

Schindler, D. W. (2001). The Cumulative Effects of Climate Warming and Other Human Stresses on Canadian Freshwaters in the New Millennium. In L. Bendell-Young & P. Gallaugher (Eds.), Waters in Peril (pp. 165–186). Boston, MA: Springer US. doi: 10.1007/978-1-4615-1493-0_11

Schindler, D. W., Carpenter, S. R., Chapra, S. C., Hecky, R. E., & Orihel, D. M. (2016). Reducing Phosphorus to Curb Lake Eutrophication is a Success. Environmental Science & Technology, 50(17), 8923–8929. doi: 10.1021/acs.est.6b02204

Schindler, D. W., Dillon, P. J., & Schreier, H. (2006). A review of anthropogenic sources of nitrogen and their effects on Canadian aquatic ecosystems. Biogeochemistry, 79(1), 25–44. doi: 10.1007/s10533-006-9001-2

Schindler, D. W., Hecky, R. E., & McCullough, G. K. (2012). The rapid eutrophication of Lake Winnipeg: Greening under global change. Journal of Great Lakes Research, 38, 6–13. doi: 10.1016/j.jglr.2012.04.003

Schippers, P., van de Weerd, H., de Klein, J., de Jong, B., & Scheffer, M. (2006). Impacts of agricultural phosphorus use in catchments on shallow lake water quality: About buffers, time delays and equilibria. The Science of the Total Environment, 369(1-3), 280–294. doi: 10.1016/j.scitotenv.2006.04.028

Schneider, K. D., McConkey, B. G., Thiagarajan, A., Elliott, J. A., & Reid, D. K. (2019). Nutrient Loss in Snowmelt Runoff: Results from a Long-term Study in a Dryland Cropping System. Journal of Environmental Quality, 48(4), 831–840. doi: 10.2134/jeq2018.12.0448

Scott, M. P., Edwards, J., Bell, C., Schussler, J., & Smith, J. S. (2006). Grain composition and amino acid content in maize cultivars representing 80 years of commercial maize varieties. Maydica, 51, 417–423. Retrieved from https://hygeia-analytics.com/wp-content/uploads/2018/02/Scott-et-al.-2006-corn-protein-amino-acids-historical-comparisons.pdf

Seitz, S., Goebes, P., Puerta, V. L., Pereira, E. I. P., Wittwer, R., Six, J., van der Heijden, M. G. A., & Scholten, T. (2018). Conservation tillage and organic farming reduce soil erosion. Agronomy for Sustainable Development, 39(1), 4. doi: 10.1007/s13593-018-0545-z

Sharpley, A., Foy, B., & Withers, P. (2000). Practical and innovative measures for the control of agricultural phosphorus losses to water: An overview. Journal of Environmental Quality, 29(1), 1–9. doi: 10.2134/jeq2000.00472425002900010001x

Sharpley, A., Jarvie, H. P., Buda, A., May, L., Spears, B., & Kleinman, P. (2013). Phosphorus legacy: Overcoming the effects of past management practices to mitigate future water quality impairment. Journal of Environmental Quality, 42(5), 1308–1326. doi: 10.2134/jeq2013.03.0098

Sharpley, A. N. (1995). Soil phosphorus dynamics: agronomic and environmental impacts. Ecological Engineering, 5(2), 261–279. doi: 10.1016/0925-8574(95)00027-5

Six, J., Conant, R. T., Paul, E. A., & Paustian, K. (2002). Stabilization mechanisms of soil organic matter: Implications for C-saturation of soils. Plant and Soil, 241(2), 155–176. doi: 10.1023/A:1016125726789

Smiley, G. (2002). Rethinking the Great Depression. Ivan R. Dee. Retrieved from https://play.google.com/store/books/details?id=LWAeAAAAQBAJ

Smith, D. R., King, K. W., Johnson, L., Francesconi, W., Richards, P., Baker, D., & Sharpley, A. N. (2015). Surface runoff and tile drainage transport of phosphorus in the midwestern United States. Journal of Environmental Quality, 44(2), 495–502. doi: 10.2134/jeq2014.04.0176

Smith, R. B., Bass, B., Sawyer, D., Depew, D., & Watson, S. B. (2019). Estimating the economic costs of algal blooms in the Canadian Lake Erie Basin. Harmful Algae, 87(June), 101624. doi: 10.1016/j.hal.2019.101624

Smith, V. H., & Schindler, D. W. (2009). Eutrophication science: where do we go from here? Trends in Ecology & Evolution, 24(4), 201–207. doi: 10.1016/j.tree.2008.11.009

Sohl, T., Reker, R., Bouchard, M., Sayler, K., Dornbierer, J., Wika, S., Quenzer, R., & Friesz, A. (2016). Modeled historical land use and land cover for the conterminous United States. Journal of Land Use Science, 11(4), 476–499. doi: 10.1080/1747423X.2016.1147619

Sprague, L. A., & Gronberg, J. A. M. (2012). Relating management practices and nutrient export in agricultural watersheds of the United States. Journal of Environmental Quality, 41(6), 1939–1950. doi: 10.2134/jeq2012.0073

Stackpoole, S. M., Stets, E. G., & Sprague, L. A. (2019). Variable impacts of contemporary versus legacy agricultural phosphorus on US river water quality. Proceedings of the National Academy of Sciences of the United States of America, 116(41), 20562–20567. doi: 10.1073/pnas.1903226116

Standard Geographical Classification (SGC) reference maps. (2016, November 10). Retrieved from https://www12.statcan.gc.ca/census-recensement/2011/geo/map-carte/ref/sgc-cgt/index-eng.cfm

Surhone, L. M., Tennoe, M. T., & Henssonow, S. F. (Eds.). (2011). National Chicken Council. Betascript Publishing. Retrieved from https://www.nationalchickencouncil.org/about-the-industry/statistics/per-capita-consumption-of-poultry-and-livestock-1965-to-estimated-2012-in-pounds/

Swaney, D. P., & Howarth, R. W. (2019a). County, subregional and regional phosphorus data derived from the net anthropogenic nitrogen/phosphorus inputs (NANI/NAPI) toolbox. Data in Brief, 25, 104265. doi: 10.1016/j.dib.2019.104265

Swaney, D. P., & Howarth, R. W. (2019b). Phosphorus use efficiency and crop production: Patterns of regional variation in the United States, 1987-2012. The Science of the Total Environment, 685, 174–188. doi: 10.1016/j.scitotenv.2019.05.228

Sweeney, R. A. (1974). Impact of detergent phosphate reductions on water quality.

Tam, B. Y., Szeto, K., Bonsal, B., Flato, G., Cannon, A. J., & Rong, R. (2019). CMIP5 drought projections in Canada based on the Standardized Precipitation Evapotranspiration Index. Canadian Water Resources Journal / Revue Canadienne Des Ressources Hydriques, 44(1), 90–107. doi: 10.1080/07011784.2018.1537812

Team, T. (2015). Recommended phosphorus loading targets for Lake Erie. Annex, 4, 2015–2006.

Thompson, S. E., Basu, N. B., Lascurain, J., Aubeneau, A., & Rao, P. S. C. (2011). Relative dominance of hydrologic versus biogeochemical factors on solute export across impact gradients. Water Resources Research, 47(7). doi: 10.1029/2010WR009605

Tilman, D. (1998, November). The greening of the green revolution. Nature Publishing Group UK. doi: 10.1038/24254

Tolson, B. A., & Shoemaker, C. A. (2007). Dynamically dimensioned search algorithm for computationally efficient watershed model calibration. Water Resources Research, 43(1). doi: 10.1029/2005WR004723

U.S. Action Plan for Lake Erie: Commitments and Strategy for Phosphorus Reduction. (2018). U.S. Environmental Protection Agency, Great Lakes National Program Office. Retrieved from https://play.google.com/store/books/details?id=JhTexQEACAAJ

US Census Bureau. (2023). Decennial Census of Population and Housing by Decades. Retrieved from https://www.census.gov/programs-surveys/decennial-census/decade.2020.html

USDA ERS. (2022). Livestock and Meat Domestic Data. Retrieved from https://www.ers.usda.gov/data-products/livestock-and-meat-domestic-data/

USDA - national agricultural statistics service - data and statistics. Retrieved from https://www.nass.usda.gov/Data_and_Statistics/index.php

USDA NRCS. (2008). Agricultural Waste Management Field Handbook - Chapter 4 Agricultural Waste Characteristics. Retrieved from https://directives.sc.egov.usda.gov/landingpage/86fc4bf7-b503-40bf-a112-91cc8ee87804

US Department of Commerce, & National Oceanic. (2018). NOAA’s national ocean service. Retrieved from https://oceanservice.noaa.gov/hazards

Us Epa, O. P. (2012). Clark Fork-pend oreille basin water quality study, conducted under section 525 of the clean water act of 1987, a summary of findings and a management plan. Bibliogov. Retrieved from https://www.epa.gov/laws-regulations/summary-clean-water-act

U.S. Geological Survey. (2005). Elevation derivatives for national applications (No. 2005-3049). U.S. Geological Survey. doi: 10.3133/fs20053049

Vallentyne, J. R. (1978). International Joint Commission (Canada/United States): Annual Review of Progress under the Great Lakes Water Quality Agreement of 1972—held in Windsor, Ontario, 17–20 July 1978. Environmental Conservation, 5(4), 308–308. doi: 10.1017/S0376892900006433

van Bochove, E., Thériault, G., Denault, J.-T., Dechmi, F., Allaire, S. E., & Rousseau, A. N. (2012). Risk of phosphorus desorption from Canadian agricultural land: 25-year temporal trend. Journal of Environmental Quality, 41(5), 1402–1412. doi: 10.2134/jeq2011.0307

Van Meter, K. J., & Basu, N. B. (2015). Catchment legacies and time lags: A parsimonious watershed model to predict the effects of legacy storage on nitrogen export. PloS One, 10(5). doi: 10.1371/journal.pone.0125971

Van Meter, K. J., Basu, N. B., & Van Cappellen, P. (2017). Two centuries of nitrogen dynamics: Legacy sources and sinks in the Mississippi and Susquehanna River Basins. Global Biogeochemical Cycles, 31(1), 2–23. doi: 10.1002/2016GB005498

Van Meter, K. J., Basu, N. B., Veenstra, J. J., & Burras, C. L. (2016). The nitrogen legacy: Emerging evidence of nitrogen accumulation in anthropogenic landscapes. Environmental Research Letters: ERL [Web Site], 11(3). doi: 10.1088/1748-9326/11/3/035014

Van Meter, K. J., McLeod, M. M., Liu, J., Tenkouano, G. T., Hall, R. I., Van Cappellen, P., & Basu, N. B. (2021a). Beyond the Mass Balance: Watershed Phosphorus Legacies and the Evolution of the Current Water Quality Policy Challenge. Water Resources Research, 57(10), 1–22. doi: 10.1029/2020WR029316

Van Meter, K. J., McLeod, M. M., Liu, J., Tenkouano, G. T., Hall, R. I., Van Cappellen, P., & Basu, N. B. (2021b). Beyond the mass balance: Watershed phosphorus legacies and the evolution of the current water quality policy challenge. Water Resources Research, 57(10). doi: 10.1029/2020wr029316

Van Staden, T. L., Van Meter, K. J., Basu, N. B., Parsons, C. T., Akbarzadeh, Z., & Van Cappellen, P. (2022). Agricultural phosphorus surplus trajectories for Ontario, Canada (1961–2016), and erosional export risk. The Science of the Total Environment, 818, 151717. doi: 10.1016/j.scitotenv.2021.151717

Van Staden, T., Van Meter, K., Saurette, D., Basu, N., Parsons, C., & Van Cappellen, P. (2019). Phosphorus Legacies and Water Quality Risks: A Vulnerability-Based Framework in Southern Ontario.

Vero, S. E., Basu, N. B., Van Meter, K., Richards, K. G., Mellander, P.-E., Healy, M. G., & Fenton, O. (2018). The environmental status and implications of the nitrate time lag in Europe and North America. Hydrogeology Journal, 26(1), 7–22. Retrieved from https://www.universityofgalway.ie/media/gene/Vero-et-al_2018_HJ.pdf

Villamil, M. B., Nafziger, E. D., & Behnke, G. D. (2019). New grain P and K concentration values for Illinois field crops. Crop, Forage & Turfgrass Management, 5(1), 180090. doi: 10.2134/cftm2018.11.0090

Vincent, R. K., Qin, X., McKay, R. M. L., Miner, J., Czajkowski, K., Savino, J., & Bridgeman, T. (2004). Phycocyanin detection from LANDSAT TM data for mapping cyanobacterial blooms in Lake Erie. In Remote Sensing of Environment (Vol. 89, Issue 3, pp. 381–392). doi: 10.1016/j.rse.2003.10.014

Vitousek, P. M., Aber, J. D., & Howarth, R. W. (1997). Human alteration of the global nitrogen cycle: sources and consequences. Ecological. doi: 10.1890/1051-0761(1997)007[0737:HAOTGN]2.0.CO;2

Vollmer-Sanders, C., Allman, A., Busdeker, D., Moody, L. B., & Stanley, W. G. (2016). Building partnerships to scale up conservation: 4R Nutrient Stewardship Certification Program in the Lake Erie watershed. Journal of Great Lakes Research, 42(6), 1395–1402. doi: 10.1016/j.jglr.2016.09.004

Wang, J., Qi, Z., & Bennett, E. M. (2022). Changes in Canada's phosphorus cycle 1961–2018: Surpluses and deficits. Global Biogeochemical Cycles, 36(8). doi: 10.1029/2022gb007407

Wang, J., Qi, Z., & Bennett, E. M. (2024). Managing mineral phosphorus application with soil residual phosphorus reuse in Canada. Global Change Biology, 30(1), e17001. doi: 10.1111/gcb.17001

Wang, R., Goll, D., Balkanski, Y., Hauglustaine, D., Boucher, O., Ciais, P., Janssens, I., Penuelas, J., Guenet, B., Sardans, J., Bopp, L., Vuichard, N., Zhou, F., Li, B., Piao, S., Peng, S., Huang, Y., & Tao, S. (2017). Global forest carbon uptake due to nitrogen and phosphorus deposition from 1850 to 2100. Global Change Biology, 23(11), 4854–4872. doi: 10.1111/gcb.13766

Water quality monitoring. Retrieved from https://www.usgs.gov/centers/california-water-science-center/science/science-topics/water-quality-monitoring

Water quality standards attainment and monitoring. Chesapeake Progress. Retrieved on 2022, Retrieved from https://www.chesapeakeprogress.com/clean-water/water-quality

Watson, S. B., Ridal, J., & Boyer, G. L. (2008). Taste and odour and cyanobacterial toxins: impairment, prediction, and management in the Great Lakes. Canadian Journal of Fisheries and Aquatic Sciences. Journal Canadien Des Sciences Halieutiques et Aquatiques, 65(8), 1779–1796. Retrieved from https://cdnsciencepub.com/doi/abs/10.1139/f08-084

Welch, H. L., Kingsbury, J. A., & Coupe, R. H. (2010). Occurrence of phosphorus in groundwater and surface water of northwestern Mississippi. W: Proceedings of the 2010 Mississippi Water Resources Conference [online]. Raymond.[Dostęp 10.02. 2015]. Dostępny W Internecie: Http://www. Wrri. Msstate. edu/pdf/welch10. Pdf Gy and Life Sciences in Falenty. It Was Found That, 1, 80–86. Retrieved from https://www.researchgate.net/profile/Heather-Welch/publication/252798261_Dissolved_Phosphorus_Concentrations_in_the_Mississippi_River_Valley_Alluvial_Aquifer_Northwestern_Mississippi/links/5922ffc0aca27295a8a7b5b3/Dissolved-Phosphorus-Concentrations-in-the-Mississippi-River-Valley-Alluvial-Aquifer-Northwestern-Mississippi.pdf

Williams, M. R., Welikhe, P., Bos, J., King, K., Akland, M., Augustine, D., Baffaut, C., Beck, E. G., Bierer, A., Bosch, D. D., Boughton, E., Brandani, C., Brooks, E., Buda, A., Cavigelli, M., Faulkner, J., Feyereisen, G., Fortuna, A., Gamble, J., … Yasarer, L. (2022). P-FLUX: A phosphorus budget dataset spanning diverse agricultural production systems in the United States and Canada. Journal of Environmental Quality, 51(3), 451–461. doi: 10.1002/jeq2.20351

Wilson, R. S., Beetstra, M. A., Reutter, J. M., Hesse, G., Fussell, K. M. D., Johnson, L. T., King, K. W., LaBarge, G. A., Martin, J. F., & Winslow, C. (2019). Commentary: Achieving phosphorus reduction targets for Lake Erie. Journal of Great Lakes Research, 45(1), 4–11. doi: 10.1016/j.jglr.2018.11.004

Winter, J. G., DeSellas, A. M., Fletcher, R., Heintsch, L., Morley, A., Nakamoto, L., & Utsumi, K. (2011). Algal blooms in Ontario, Canada: Increases in reports since 1994. Lake and Reservoir Management, 27(2), 107–114. doi: 10.1080/07438141.2011.557765

Wironen, M. B., Bennett, E. M., & Erickson, J. D. (2018). Phosphorus flows and legacy accumulation in an animal-dominated agricultural region from 1925 to 2012. In Global Environmental Change (Vol. 50, pp. 88–99). doi: 10.1016/j.gloenvcha.2018.02.017

Withana Herath, A. (2013). Chemical Fractions And Predictions For Long-term Releases of Phosphorus In Typical Canadian Agricultural Soils [University of Guelph]. Retrieved from https://atrium.lib.uoguelph.ca/items/039c0e76-1294-4e6c-98a9-30aa0feb5364

Withers, P. J. A., Neal, C., Jarvie, H. P., & Doody, D. G. (2014). Agriculture and Eutrophication: Where Do We Go from Here? Sustainability: Science Practice and Policy, 6(9), 5853–5875. doi: 10.3390/su6095853

Withers, P. J. A., Sylvester-Bradley, R., Jones, D. L., Healey, J. R., & Talboys, P. J. (2014). Feed the crop not the soil: Rethinking phosphorus management in the food chain. Environmental Science and Technology, 48(12), 6523–6530. doi: 10.1021/es501670j

Withers, P. J., Clay, S. D., & Breeze, V. G. (2001). Phosphorus transfer in runoff following application of fertilizer, manure, and sewage sludge. Journal of Environmental Quality, 30(1), 180–188. doi: 10.2134/jeq2001.301180x

Wolock, D. M., Winter, T. C., & McMahon, G. (2004). Delineation and evaluation of hydrologic-landscape regions in the United States using geographic information system tools and multivariate statistical analyses. Environmental Management, 34 Suppl 1, S71–S88. doi: 10.1007/s00267-003-5077-9

Worrall, F., Burt, T. P., Howden, N. J. K., & Whelan, M. J. (2012). The fluvial flux of nitrate from the UK terrestrial biosphere – An estimate of national-scale in-stream nitrate loss using an export coefficient model. Journal of Hydrology, 414-415, 31–39. doi: 10.1016/j.jhydrol.2011.09.020

Worrall, F., Howden, N. J. K., & Burt, T. P. (2015). Evidence for nitrogen accumulation: the total nitrogen budget of the terrestrial biosphere of a lowland agricultural catchment. Biogeochemistry, 123(3), 411–428. doi: 10.1007/s10533-015-0074-7

Yu, W., Li, G., Hartmann, T. E., Xu, M., Yang, X., Li, H., Zhang, J., & Shen, J. (2021). Development of a novel model of soil legacy P assessment for calcareous and acidic soils. Frontiers of Environmental Science & Engineering in China, 8. doi: 10.3389/fenvs.2020.621833

Zaimes, G. N., Tufekcioglu, M., & Schultz, R. C. (2019). Riparian Land-Use Impacts on Stream Bank and Gully Erosion in Agricultural Watersheds: What We Have Learned. WATER, 11(7), 1343. doi: 10.3390/w11071343

Zhang, T. Q., Tan, C. S., Zheng, Z. M., Welacky, T., & Wang, Y. T. (2017). Drainage water management combined with cover crop enhances reduction of soil phosphorus loss. The Science of the Total Environment, 586, 362–371. doi: 10.1016/j.scitotenv.2017.02.025

Zhang, T., Yang, Y., Ni, J., & Xie, D. (2020). Best management practices for agricultural non-point source pollution in a small watershed based on the AnnAGNPS model. Soil Use and Management, 36(1), 45–57. doi: 10.1111/sum.12535

Zhang, Y., Luo, P., Zhao, S., Kang, S., Wang, P., Zhou, M., & Lyu, J. (2020). Control and remediation methods for eutrophic lakes in the past 30 years. Water Science and Technology: A Journal of the International Association on Water Pollution Research, 81(6), 1099–1113. doi: 10.2166/wst.2020.218

1988 U.S. Drought/Heatwave. (2017). Homeland Security Digital Library. Retrieved from https://www.hsdl.org/c/tl/1988-u-s-droughtheatwave/

Appendix A- Supplemental Information for Chapter 2

S1. Methods

S1.1 Phosphorus in Fertilizer

Estimates of phosphorus fertilizer use on a county scale for the USA and Canada have been compiled for every year from 1930 to 2016. To maintain consistency across both countries, only farm fertilizer data was used in this study.

To calculate P fertilizer use in the USA between 1930-1944 county-specific scaling factors were employed. These factors were derived from the average ratio of fertilizer usage in each county to the total consumption of U.S. phosphate rock fertilizer during the years 1945-1949 (*USGS, Retrieved on 2019*). Subsequently, these scaling factors were applied to the mass of U.S. phosphate rock fertilizer consumed for each year between 1930 and 1944.

$$FERT_{30-44}(i,t) = FERT_{Prock}(t) * S_r(i) \quad \text{(Eq. S1.1)}$$

where $FERT_{30-44}(i,t)$ (kg-P y^{-1}) is the total P fertilizer used for county *i* in year *t*, $FERT_{Prock}(t)$ is the U.S. phosphate rock fertilizer consumed (*kg-P* y^{-1}) in year *t*, and $S_r(i)$ is the scaling factor.

Fertilizer use from 2013-2017 was obtained from scaling (*FAO, 2022*) national total mass to county-scale farm fertilizer using county-specific scaling factors. The scaling factors were the ratio between the yearly average of the county's agricultural fertilizer to FAO total mass.

$$FERT_{13-17}(i,t) = FERT_{nat}(t) * S_n(i) \quad \text{(Eq. S1.2)}$$

Where $FERT_{13-17}(i,t)$ P fertilizer use (*kg-P* y^{-1}) for county *i* in year *t*, respectively, $S_n(i)$ is the scaling factor and $FERT_{nat}$ is the FAO estimate of national P fertilizer use (kg-P y^{-1}).

For Canada, the total fertilizer applied to each county was approximated using the average provincial phosphorus fertilizer application rate. This rate was determined by multiplying provincial phosphate fertilizer sales and provincial crop area data from (Government of Canada et al., 2023b), under the assumption that all fertilizer sold was applied to farmland within the same year (Van Meter et al., 2021a).

$$FERT_C(i,t) = FERT_{sales}(t) * \frac{AREA_{crop}(i,t)}{AREA_{prov}(t)} \quad \text{(Eq. S1.3)}$$

$Where\ FERT_C\ (i,t)$ P fertilizer use (kg-P y^{-1}) for Canadian county i in year t, respectively, $AREA_{crop}\ (i,t)$ is crop area within i county in t year, $AREA_{prov}$ (i,t) is crop area in hectares for Ontario in t year and $FERT_{sales}$ (t) is the Ontario fertilizer sales data in kg-P y^{-1}.

S1.2 Phosphorus from Livestock Manure

P from livestock manure is calculated by multiplying livestock population, animal excretion rate and weight factor.

$$MAN(i,j,t) = INV(i,j,t) * p(j)_{lvstk,excr} * S_{wt}(j,t) \quad \text{(Eq. S1.4)}$$

Where, $MAN(i,j,t)$ is the P from livestock manure in kg-P yr^{-1}, $INV(i,j,t)$ is the livestock number of j category in i county on t year, $p(j)_{lvstk,excr}$ is the species-specific P excretion rate (kg -$head^{-1}yr^{-1}$), and is the $S_{wt}(j,t)$ weight factor based on 2008 for livestock type j in year t. Then they are linearly interpolated between the census year and normalized by county areas.

P excreted from livestock or P content in manure was calculated for census years using the reported heads of livestock, P content in manure generated from respective animals and weight factors of the animals. For calculating P content in manure, we used the *Agricultural Waste Management Field Handbook* (USDA NRCS, 2008). Conversion values are assumed to represent the manure P produced in 2008. Then we obtained a weight factor to accommodate the changes in livestock weight resulting from selective breeding and alterations in feed ((Byrnes et al., 2020)). Weight factor is the annual ratio of weights for a given year to 2008 which used surveyed yearly livestock weights (USDA ERS, 2022). Then we multiplied the yearly weight factor to the 2008 conversion value.

Table S1.1:P excretion rate from manure of different animal

Harmonized Livestock Category	***P excreted (kg/head/yr)***
Beef Cows	16.06
Broilers	0.12
Hogs and Pigs	2.35
Goats, Sheep and Lambs	1.16
Turkey	0.36
Horses and Ponies	8.44
Milk Cow	25.61
Other Chicken	0.18
Other Cattle (Heifers, Bulls, Steers, and Calves)	9.55

To ensure accurate comparisons between the livestock categories of the USA and Canada, we took special care to harmonize the data. While the USDA aggregates census categories, Agriculture Canada employs more detailed disaggregated categories. For instance, cattle are categorized by the USDA as beef cows, milk cows, and other cattle, while Agriculture Canada further breaks them down into beef cows, milk cows, heifers, steers, bulls, and calves. To maintain consistency, we used beef cows, milk cows, and other cattle, which include steers, heifers, bulls, and calves, for both countries.

Similarly, there were differences in how chicken data was reported. The USDA distinguishes between broiler and other chicken categories (layer, pullets for laying flock replacement), while Agriculture Canada uses categories like Broiler-roaster-cornish, Pullets under 19 weeks, and Laying hens, as of the census of 2012. To ensure comparability, we considered all types of chickens in the "other chicken" category for Canada, excluding broilers.

When facing missing data in both countries, we employed careful methodologies to estimate accurate values. For example, when broiler data was not reported for certain years in Canada, we averaged the broiler-to-total chicken ratio from surrounding years to estimate the missing values. Additionally, we assumed that the percentage change of broiler values remained consistent in both countries before 1969.

For data on broiler values between 1930 and 1961 in Canada, and 1930 to 1969 in the USA, we utilized the rate of change in broiler consumption (kg consumed) and broiler live weight (kg meat/chicken) to establish the percentage change of the national broiler inventory for each census year, as reported in the work by (Byrnes et al., 2020).

S1.3 Domestic Phosphorus Waste

Total flux for domestic P comprises P from laundry and dish detergent usage, human food consumption and food waste. Detergent P was estimated based on per capita detergent use and P content in detergents. Total waste generated by detergent (*DET (i,t)*) is determined as follows

$$DET\ (i,t) = (P_{laundry}(t) + P_{dish}(t)) * POP(i,t) \quad \text{(Eqn. S1.5)}$$

Where $P_{laundry}(t)$ is the annual per capita P from laundry detergent, $P_{dish}(t)$ is the annual per capita P from dishwashing detergent, and $POP(i,t)$ is the population of *i* county in *t* year.

Laundry and dish detergent used per person was estimated by assuming widespread usage of these detergents starting in 1935 (Han et al., 2012; Litke, 1999). The P content in detergent changed over time due to regulations, such as legislation to limit P in Great Lakes states in the mid-1970s (IJC, 2018)). This legislation restricted P content to 0.05 percent in the USA, while in Ontario, the limit was 2.2 percent (IJC, 2018). Detergent parameters for the USA were obtained from Han et al. (2012) and Ontario was obtained from (T. L. Van Staden et al., 2022).

Food P consumption was estimated based on annual population estimates, assuming human P consumption rates (P_{hum}) of 0.6 kg person^{-1} y^{-1} (Russell et al., 2008). Food P waste is quantified as a constant fraction (P_{food}) 0.11 times of food consumption (Parfitt et al., 2010). The total P waste generated by humans,

$$\text{HUM (i,t)} = POP(i,t) * (P_{hum} + P_{hum} * P_{food}) \quad \text{(Eqn. S1.6)}$$

Thus, total P waste

$$WASTE\ (i,t) = DET\ (i,t) + HUM\ (i,t) \quad \text{(Eqn. S1.7)}$$

Where, *HUM (i,t)* is total waste from human, and $POP(i,t)$ is the population for i county for t year.

S1.4 Phosphorus Uptake

Crop P uptake was calculated using county-scale crop production data from the Agricultural Census. First, we identified common field crops for each county across both countries. Next, we obtained crop area areas for census years and multiplied them with crop yield (kg/area) to convert the area into mass units. The mass of the crop harvested was converted into kg P by multiplying it with the P content of each crop (**Eqn. S1.8**). Finally, the P uptake for each crop was linearly interpolated between the census years and normalized with county area.

$$CROP\ (i,j,t) = AREA_{crop}\ (i,j,t) \times Y_{crop}\ (j,t) \times d\ (j) \times P_{crop}\ (j,t) \qquad \text{(Eqn. S1.8)}$$

Where *CROP (i,j,t)* P crop and pasture uptake in *i* county for *j* crop in t time $AREA_{crop}\ (i,j,t)$ is the harvested area of *j* crop or pasture in *i* county in *t* time (hectare), $Y_{crop}\ (j,t)$ is the provincial yield for *j* type in year *t*, *d(j)* is the crop-specific percent dry matter, and crop-specific P uptake values, p_{crop}(j). We added P uptake for each crop type to get the total crop P uptake for that county.

We collected data on crop mass in the USA from (Byrnes et al., 2020), which aggregated harvested crop area from the ICPSR data archive (1930–2012) (Haines et al., 2014) and NASS Quick Stats (2017) (USDA, 2017). For the USA side, we used all crops that have been used in TREND 2.0 by Byrnes et al., 2022. The harvested unit of each crop is available in either area (acres) or mass (lbs, cwt, tons) units for each census year between 1930 and 2016. Yearly survey data were available for 14 crops, and these were scaled using ratios of census data to survey data, following a methodology similar to that described by Byrnes et al. (2022). The yield data presented some challenges, as it was difficult to find time-varied yield, we used constant yield values throughout the years for our analysis of the USA (Byrnes et al., 2020).

For Canada, the same yield-based approach was used to calculate crop P mass. The crop area data, in hectares for each crop type, was collected from the Canadian Census of Agriculture ((Government of Canada et al., 2023a), which had data every 10 years from 1901 to 1951, and every 5 years thereafter. To account for temporal variations in crop yields, we utilized Ontario provincial data available from Statistics Canada which was available for every year (Government of Canada et al., 2023a). While attempting to maintain consistency across crop categories in both the USA and Canada, we excluded certain field crops and legumes from our analysis that were not significant (less than 0.1%) in the Lake Erie basin. For instance, in Canada, crops like rice,

sorghum, lentils, safflower, cotton, peanuts, and millet were omitted as they are less relevant to the region, although they are significant in the broader USA. Conversely, we included crops like buckwheat, mixed grain, and other field crops in Canada, which are not typically reported in the USA. These crops were included because they each contributed more than 1% to the total crop phosphorus mass. For example, mixed grains, primarily consisting of oats and barley used for feed, accounted for up to 16% of the total crop P mass. Additionally, the "other crops" category, which includes flax, camelina, hemp, miscanthus, quinoa, and switchgrass, was also significant, contributing up to 1.8% of the total crop P mass.

Table S1.2: Harmonized field crop categories and their P content

Harmonized Crop Category	**Fraction Dry Matter, d** **(kg-crop$_{dry}$/kg-crop)**	**Fraction P in Dry Matter, p$_{crop}$** **(kg-P /kg-crop$_{dry}$)**	**Fraction P in Dry Crop, d*p$_{crop}$ (kg-P/kg crop)**	**Citation**
Alfalfa hay	0.904	0.0026	0.00235	[1,2]
Barley	0.889	0.0042	0.003734	[2]
Beans	0.900	0.0054	0.00486	[3]
Canola	0.911	0.0062	0.005648	[3]
Corn, grain	0.867	0.00307	0.00266	[2]
Corn, silage	0.284	0.0019	0.00054	[2]
Flaxseed	0.941	0.0057	0.005364	[3]
Hay, (excl alfalfa)	0.867	0.0026	0.002254	[1]
Lentils	0.887	0.0043	0.003814	[3]
Oats	0.894	0.0037	0.003308	[2]
Potatoes	0.223	0.0025	0.000558	[2]
Rye	0.881	0.0037	0.00326	[2]
Soybeans	0.906	0.0057	0.00518	[2]
Sugar beets	0.191	0.0025	0.000478	[3]
Sunflower seeds	0.933	0.0063	0.005878	[3]
Tobacco	1.000	0.0021	0.0021	[2]
Triticale	0.891	0.0034	0.003029	[3]

Wheat	0.885	0.0031	0.0027	[2]
Hops*	0.7	0.005	0.0035	[3]
Millet*	0.9	0.0034	0.00306	[3]
Safflower*	0.924	0.006	0.00554	[3]
Sorghum, grain*	0.894	0.0035	0.00313	[2]
Sorghum, silage*	0.58	0.0021	0.00122	[2]
Sweet Potatoes*	0.318	0.0015	0.00048	[3]
Buckwheat**	-	-	0.0037	[4]
Mixed Grain**	-	-	0.0032	[4]
Other Field Crops**	-	-	0.0009	[5]

*Crop Categories used in only USA side
**Crop Categories used only in Canadian side

1. http://www.ipni.net/article/IPNI-3296; 2.(Swaney et al., 2019); 3. (Lander et al., 1998); 4. (T. Van Staden et al., 2019); 5. (Van Meter et al., 2021b)

We analyzed pasture data for both the USA and Canada. In the USA, pastureland is categorized into two types: cropland pasture and non-cropland pasture. According to (Byrnes et al., 2020), cropland pasture is defined as land that has been plowed within the last seven years and is currently used for grazing during the census period. Non-cropland pasture, on the other hand, includes all grazing areas that are not cultivated for crops, which encompasses woodland pastures and other low-quality pasture lands.

Table S1.3: P content in Pasture

Harmonized Crop Category	***P Content (kgP/kg/yr)***
Cropland/Improved Pasture	0.0055
Non-cropland /Unimproved Pasture	0.0044

For our Canada analysis, we equated cropland pasture with "Tamed or seeded pasture" and non-cropland pasture with "Natural land for pasture." The census defines "Tamed or seeded pasture" as grazable land that has been improved from its natural state through activities such as seeding, draining, irrigating, and fertilizing, aligning it closely with the USA's definition of cropland pasture. "Natural land for pasture" refers to grazable land that remains unimproved and includes areas such as native pastures, native hay, rangelands, and grazable bush, same as the USA's non-cropland pasture.

S1.5 Downscaling Phosphorus Mass Balance Component

The watershed-scale P surplus and its components were calculated from a downscaled version of the county-scale data. The resolution of the downscale version is 250m X 250m and it spans the entire Lake Erie Basin.

For the USA, we utilized the gridded dataset approach, which involved downscaling county-scale P fluxes to a 250-m grid based on land use/land cover and population densities. This process categorized P fluxes into agricultural, and urban, using historical and contemporary land-use datasets (Sohl LULC and NLCD) and decadal population maps to maintain temporal and spatial continuity from 1930-2016 (Sohl et al., 2016); (*National Land Cover Database (NLCD) 2019 products (ver. 2.0, June 2021)*, 2023). For Canada, we adopted a similar method by utilizing the annual crop inventory maps (ACI) from Agriculture and Agri-Food Canada (*Annual crop inventory, 2016*, *Annual crop inventory, 2021*). This downscaling involved converting county-scale P surplus components into a gridded format, focusing particularly on agricultural inputs such as fertilizers and manure, and outputs like crop uptake. Additionally, urban inputs like domestic P waste were downscaled based on developed land use data.

Agricultural P Components

Two distinct land use and land cover (LULC) datasets were used to define land-use patterns: the Sohl LULC dataset, which is modeled historically at 250 m resolution, and the National Land Cover Database (NLCD), available at 30 m resolution. These datasets were combined and synchronized to create detailed, continuous land-use trajectories from 1930 to 2017 across the Lake Erie USA side, all at a 250-m grid scale. The Sohl LULC data was employed annually from 1938 to 2005, and the NLCD data was used for the years 2006, 2008, 2011, 2013, and 2016. The NLCD data was adjusted from 30 m to 250 m resolution using the Nearest Neighbor Function.

Similarly, gridded maps of the Canada side of Lake Erie basin were produced using the same methodology as applied to the USA dataset. Due to the unavailability of high-resolution agricultural land cover data in Ontario, we used the ACI map from 2011 to 2016 to downscale the phosphorus components for those years and the 2011 map to downscale all years prior to 2011. The maps were originally at a 30 m resolution but were resampled to 250-m to ensure methodological consistency of the USA dataset. We used pixel codes 120 to 199 that include all field crops and pasture areas of the ACI land use map (Agri-food Canada, Agriculture, 2018, pp. 20–22).

To create a gridded map first we generated the annual binary map. The binary land-use maps were produced in 250-m grid size to classify as either agricultural or non-agricultural ($gLU_{ag}(k,t)$ = 0/1) , where k denotes the individual grid cell and t denotes the year. Here, agricultural land use includes both cropland and pasture. Any land that did not fall into the agricultural categories was classified as non-agricultural land ($gLU_{ag}(k,t)$ = 0). The total agricultural area for each county i in each year t, denoted as $AREA_{ag}(i,t)$ (ha), was determined by summing the areas of gridded agricultural land. For every component of the agricultural P mass balance, county-scale P flux values normalized by the agricultural area, $N_{ag,cnty}(i,j,t)$ (in kg ha-agland^{-1} y^{-1}), were computed by dividing the total P flux for each county by its agricultural area.

$$P_{ag,county}(i,j,t) = \frac{P_{cnty}(i,j,t)}{AREA_{ag}(i,t)} \quad \text{(Eqn. S1.9)}$$

To ensure that agricultural P fluxes were accurately assigned to grid cells designated as agricultural land, the county-scale flux values were multiplied by the binary values (0 or 1) from the land-use grid.

$$gP_{ag}(k,j,t) = P_{ag,county}(k,j,t) * gLU_{ag}(k,t) \quad \text{(Eqn. S1.10)}$$

Where k denoted each grid cell, j denoted each agricultural component of P mass balance and t represents year.

Domestic P Waste

For the USA side of the Lake Erie basin, domestic P waste was downscaled using gridded population-density data from (Fang et al., 2018). Among the five population models of varying complexities from their study, the M3 model was selected due to its optimal balance of complexity and proven accuracy, as verified by comparisons with county subdivision population data. Population estimates were interpolated linearly between modeled years and assumed a constant population from 2011 to 2017. Additionally, the annual 1-km human population maps were converted to a 250-m resolution using the nearest neighbor function.

For the Canadian side of the Lake Erie basin, domestic P waste was downscaled using the developed land area pixels from the ACI land use map (Agri-food Canada, Agriculture, 2018, pp. 20–22). For the domestic P components, we utilized the ACI map from 2011 to 2016 and applied constant values from 2011 for earlier years (1930-2010) due to the lack of high-resolution land cover data in Ontario. Similar to the agricultural map, a 30 m resolution was resampled to 250 m to ensure methodological consistency with the USA dataset. The downscaling methodology mirrored that of the agricultural land, except that it utilized developed land use to create a binary map ($gLU_{ur}(k,t)$ = 0/1) and domestic P fluxes to normalized to developed area ($P_{ur,county}(k,t)$) to calculate gridded domestic P maps. Where k denoted each grid cell and t represents the year. It is important to mention that these estimates do not account for the processing of waste by wastewater treatment facilities. The efficiency of these treatments has fluctuated across different regions and over the time span of the dataset. Including data on P removal via water treatment falls outside the scope of this study.

Table S1.4: Description of the Stations used in this study

Site Number	Site Name	Area (km2)	Lat	Long

04161820	Clinton River At Sterling Heights, MI	799.995	42.614	-83.027
04165500	Clinton River At Moravian Drive At Mt. Clemens, MI	1894.591	42.596	-82.909
04176500	River Rasin Near Monroe, MI	2689.766	41.961	-83.531
04186500	Auglaize River Near Fort Jennings OH	860.978	40.949	-84.266
04193500	Maumee River At Waterville OH	16943.426	41.500	-83.713
04197100	Honey Creek At Melmore	388.935	41.022	-83.110
04197170	Rock Creek At Tiffin	95.382	41.114	-83.168
04198000	Sandusky River Near Fremont	3250.011	41.308	-83.159
04199500	Vermilion River Near Vermillion, OH	687.618	41.382	-82.317
04208000	Cuyahoga River At Independence OH	1840.726	41.395	-81.630
04213500	Cattaraugus Creek At Gowanda, NY	1136.162	42.463	-78.934
04166500	River Rouge At Detroit, MI	476.512	42.281	-83.129
04199000	Huron River At Milan OH	949.087	41.301	-82.608
04200500	Black River At Elyria OH	1028.769	41.380	-82.105
04201500	Rocky River Near Berea	691.912	41.408	-81.883
04209000	Chagrin River At Willoughby	638.442	41.631	-81.403
04212100	Grand River Near Painesville, OH	1787.746	41.719	-81.228
04174500	Huron River At Ann Arbor, MI	1888.110	42.287	-83.734
04182000	Marys River Near Fort Wayne, IN	1973.57	40.988	-85.112
04183000	Maumee River At New Haven	5094.507	41.085	-85.022
04001304402	North Thames River Near Mitchell, ON	317.350	43.451	-81.207
04001305802	Thames River At Thamesville, ON	4540.905	42.514	-82.072
04001308002	Thames River At Innerkip, ON	150.419	42.732	-81.578
04002701202	Sydenham River Near Alvinston, ON	704.159	42.831	-81.851
16010900702	Big Otter Creek Above Otterville, ON	99.151	42.966	-80.543
16015900302	Lynn River At Simcoe, ON	140.686	42.823	-80.289

16016400102	Nanticoke Creek At Nanticoke, ON	179.242	42.810	80.076
16018400902	Nith River Near Canning, ON	1128.097	43.192	-80.383
16018401002	Grand River At Galt, ON	3487.452	43.279	-80.343
16018401602	Canagagigue Creek Near Elmi, ON	111.258	43.585	-80.535
16018402702	Grand River At Brantford, ON	5100.287	43.110	-80.245
16018403202	Nith River At New Hamburg, ON	549.355	43.375	-80.679
16018403402	Speed River Below Guelph, ON	526.131	43.534	-80.253
16018403602	Speed River Below Guelph, ON	547.554	43.484	-80.282
16018403702	Grand River Below Shand Dam, ON	788.521	43.725	-80.344
16018406702	Grand River Near Marsville, ON	665.071	43.862	-80.273
16018407702	Conestogo River At Glen Allan, ON	573.004	43.655	-80.702
16018409302	Fairchild Creek Near Brantford, ON	360.082	43.149	-80.172
16018409602	Mckenzie Creek Near Caledonia, ON	174.200	43.034	-79.950
16018409902	Speed River Near Armstrong Mills, ON	176.706	43.640	-80.270
16018410202	Eramosa River Above Guelph, ON	232.413	43.548	-80.182
16018410302	Grand River At West Montrose, ON	1157.295	43.588	-80.471
16018410602	Whitemans Creek Near Mount Vernon, ON	397.652	43.126	-80.384
16012401102	Big Creek At Walsingham, ON	565.759	42.686	-80.538
16010900802	Big Otter Creek At Calton, ON	655.778	42.711	-80.840
4002701602	Sydenham River At Florence, ON	1148.119	42.651	-82.009
16018409202	Grand, Yor, ON	6015.094	43.022	-79.892
4001305002	North Thames River Near Thorndale, ON	1337.125	43.096	-81.169
4001302702	North Thames River Below Fanshawe Dam, ON	1416.704	43.042	-81.195
10000200202	Canard River Near Lukerville, ON	159.000	42.159	-83.019
4001000302	Ruscom RiverNear Ruscom Station, ON	125.000	42.211	-82.629
4000100102	Little River At Windsor, ON	55.300	42.310	-82.928

4001302502	NA	11397.38	43.366	-81.019
4001302902	NA	13541.3	42.914	-81.314
4001304702	NA	323068.89	42.935	-81.422
4001306402	NA	14062.34	43.266	-81.084
16018405102	Canagagigue Creek At Woolwich	6478.17	43.616	-80.560

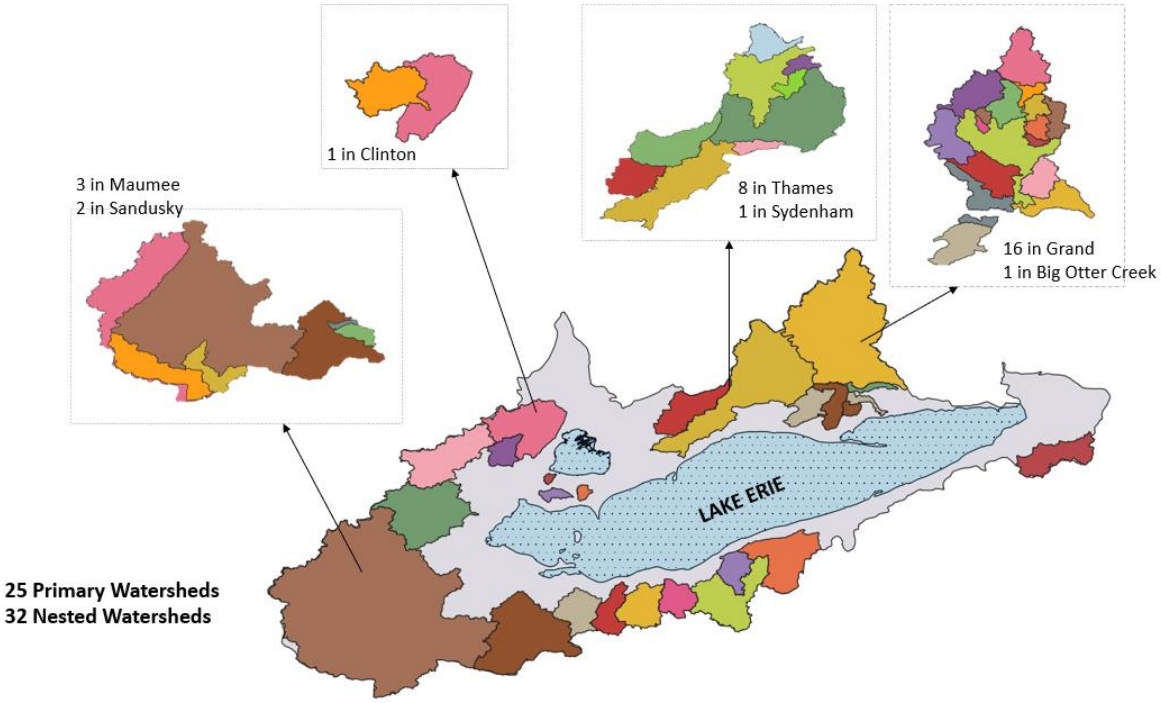


Figure S1.1:Studied 57 watersheds across the Lake Erie basin

Appendix B- Supplementary Materials for Chapter 3

Text S1 Source Zone Dynamics

S1.1 Organic P (Msop) in the Source Zone

The soil organic P *($M_{sop}(s,t)$)* pool is divided into two parts: a protected pool *($M_p(s,t)$)* with slower kinetics and an active pool *($M_a(s,t)$)*with faster kinetics. Furthermore, the organic protected P pools can move to the active pool, causing it to be subject to quicker mineralization kinetics. All three annual P surplus *($N_p(s,t)$)* **(Eq. 3.6-3.8)** cycles through these two pools and is divided between them based on a humification coefficient, *h* that varies based on land use and tillage practices (Janssen, 1984; Six et al., 2002; Van Meter et al., 2021). Both the active and protected pools lose mass over time due to mineralization and erosion, which are modelled as first-order processes with two different rate constants respectively (K_a, K_p) (Van Meter et al., 2021). The gross erosion rate constant (K_{eros}) is empirically quantified as a function of land use and annual discharge (de Vente et al., 2005; Van Meter et al., 2021). The P dynamics for the active and protected pools across different land-use trajectories can be described by differential equations.

$$\frac{dM_p(s,t)}{dt} = \begin{cases} hN_p(s,t) - k_p M_p(s,t) - k_{\text{eros}}(s,t) M_p(s,t), & \text{LU}(s,t-1) = 2 \\ hN_p(s,t) - \left(M_p(s,t) - 0.7M_{p,\text{pris}}\right) - k_{\text{eros}}(s,t) M_p(s,t), & \text{LU}(s,t) = 2 \text{ and } \text{LU}(s,t-1) \le 1 \end{cases}$$

$$\frac{dM_a(s,t)}{dt} = \begin{cases} (1-h)N_p(s,t) - k_a M_a(s,t) - k_{\text{eros}}(s,t) M_a(s,t), & \text{LU}(s,t) \le 1 \,\&\, \text{LU}(s,t-1) = 2 \\ (1-h)N_p(s,t) + \left(M_p(s,t) - 0.7M_{p,\text{pris}}\right) - k_{\text{eros}}(s,t) M_a(s,t), & \text{LU}(s,t) = 2 \text{ and } \text{LU}(s,t-1) \le 1 \end{cases}$$

(Eq. S1-S4)

S1.2 Mineral P (Mmin) in the Source Zone

Soil organic matter releases P that enters the mineral P pool, $M_{min}(s, t)$, which is in equilibrium between dissolved $M_{dis}(s, t)$ and sorbed pools $M_{sorb}(s, t)$. The mineralization framework was

based on the HYPE hydrological model ((Lindström et al., 2010; Van Meter et al., 2021) and the process follows the following equations

$$M_{min}(s,t) = M_{dis}\ (s,t) + M_{sorb,i}(s,t) + M_{sorb,r}(s,t) \quad \text{(Eq. S5)}$$

$$\frac{dM_{min}(s,t)}{dt} = k_a M_a(s,t) + k_p M_p(s,t) - J_s(s,t) - \left(k_{eros}(s,t) * \left(M_{sorb,i} + M_{sorb,r}\right)\right) \quad \text{(Eq. S6)}$$

where $M_a(s,\ t)$ and $M_p(s,\ t)$ are the active and protected soil P pools [$ML^{-2}T^{-1}$]; k_p and k_a are mineralization rate constants for the active and passive soil P pools respectively. $J_s(s,\ t)$, describes the leaching of dissolved P through the subsurface to the stream, K_{eros} is an erosional constant.

$$J_s(s,t) = M_{dis}(s,t)\frac{Q(t)}{V_w}, \quad when\ Q(t) * \delta t < V_w \quad \text{(Eq. S7)}$$

Or

$$J_s(s,t) = \frac{M_{dis}(s,t)}{\delta t}, \quad when \quad Q(t) * \delta t > V_w \quad \text{(Eq. S8)}$$

where V_w (=nsV) is the water volume in the source zone, with n being porosity, s is the mean soil saturation, and V is the volume of the soil column per unit area within the source zone (Van Meter et al., 2017).

The model also considered two sorbed P pools, $M_{sorb,r}$(s, t) which is reversibly adsorbed P and $M_{sorb,i}$(s, t) is irreversibly adsorbed or precipitated P. The partitioning of the mineral P between the dissolved and reversibly sorbed pool is described by the Freundlich Isotherm.

$$C_{eq}(s,t) = \left(\frac{M_{sort,r}(s,t)}{k_f}\right)^{nfr} \quad \text{(Eq. S9)}$$

$$M_{dis}(s,t) = C_{eq}(s,t) * V_w \quad \text{(Eq. S10)}$$

where C_{eq}(s, t) is the equilibrium concentration of source-zone dissolved P, k_f is the proportionality constant for the Freundlich model, nfr is an empirical constant related to the bonding energy of soil for phosphate, and V w is the volume of the source zone (mm) (Muindi et al., 2015).

S1.3 Dissolved P Fluxes: Travel Time-based Approach

ELEMeNT-P utilizes a travel time-based approach for modelling the movement of dissolved phosphorus in the subsurface. It considers the subsurface as a collection of stream tubes originating from various points on the landscape, each with its unique travel time to the outlet. The landscape is treated as a bundle of these stream tubes, characterized by a distribution of travel times (Liu et al., 2021; Van Meter et al., 2017, 2021). The model convolutes the mass leaving the source zone with the watershed travel time *f(t)* distribution to represent the time-varying contribution of subsurface P to P loading at the catchment outlet. The watershed-scale source function, $J_{s,wshd}(t)$ is determined by summing the P mass leaching from the source zone across different land-use trajectories, driven by factors such as annual precipitation dynamics, current-year surplus P inputs, and changes in legacy P stores.

$$J_{wshd}(t) = \sum_{I}^{n} J_s(s,t) \quad \text{(Eq. S11)}$$

where $J_s(s, t)$ is the leaching flux from each land use trajectory s at time t (S1.2). These P mass fluxes are influenced by factors such as annual precipitation patterns, phosphorus inputs for the current year to the source zone, and the varying levels of phosphorus stored from previous years in these source zones. It's important to note that phosphorus transport in the subsurface includes movement through both the shallow subsurface and deeper groundwater systems, as well as via tile drains. The model captures the travel times of these pathways through calibration. Additionally, mineral phosphorus in these subsurface flow paths is subject to retention, which is governed by a first-order sorption process using a rate constant, denoted as γ, in (**Eq.1**).

Text S2 Surface P Transport

Estimates of surface P erosion is derived using a modified version of the semi-quantitative Gavrilovic method, which considers both erosion and sediment retention at the watershed level (de Vente et al., 2005). This approach includes a sediment retention function that captures the retention of sediment within lakes and reservoirs in the watershed. Similar to the gross erosion rate constant, the sediment retention ratio, denoted as $K_{ret}(t)$ and unitless, changes with various factors within the watershed.

$$K_{ret}(t) = (1 - R(t)\left(\frac{\sqrt{O*Z}}{0.25*(L_n+10)}\right) \quad \text{(Eq. S12)}$$

Where R(t) (unitless) is a time-varying sediment delivery factor (0 to 3), O is the watershed perimeter, Z is the differential elevation for the watershed ($Z_{mzx} - Z_{min}$), and L_p is the length of the principal waterway. The R(t) values vary based on annual variations in discharge

$$R(t) = \begin{cases} 0.05 & Q(t) < Q_5 \\ 0.75 & Q(t) < Q_{25} \\ 1.50 & Q(t) < Q_{50} \\ 2.00 & Q(t) < Q_{75} \\ 2.75 & Q(t) < Q_{99} \\ 3.00 & Q(t) > Q_{99} \end{cases} \quad \text{(Eq. S13)}$$

Where Q_5-Q_{99} corresponds to a range of annual discharge values, from the 5th to 99th percentile.

The gross erosion rate constant, k_{eros} (s,t) quantified using an empirical equation

$$k_{eros}(s,t) = \theta * \pi * K_{e(s,t)^{\frac{3}{2}} * \frac{Q(t)}{C} * \frac{1}{Z_s}} \quad \text{(Eq. S14)}$$

Where θ is a temperature coefficient, Q (t) is the annual discharge (mm y^{-1}), C is the watershed runoff coefficient (Q_{mean}/ P_{mean}), K_e(s,t) is an erosion coefficient (m^2 $km^{-4/3}$ $mm^{-2/2}$), and Z_s is the depth of the source zone. The temperature coefficient,θ, is quantified as:

$$\theta = \sqrt{\frac{\vartheta}{10} = 0.1} \quad \text{(Eq. S15)}$$

Where θ is the mean annual temperature (^{o}C). The erosion coefficient, K_e (s,t) is a function of three descriptive variables and the average watershed slope, s(%), as follows

$$K_{sc}(s,t) = K_{sc}(s,t) * K_{sr} * \left(K_{ext} + \sqrt{s}\right) \quad \text{(Eq. S16)}$$

Where K_{sc} is the coefficient of soil cover (a soil protection factor ranging from 0 to 1, varying according to landuse), K_{sr} is the coefficient of soil resistance (an erosion factor ranging from 0 to 2), and K_{ext} is the coefficient of type and extent of erosion (ranging from 0 to 1) (de Vente et al., 2005).

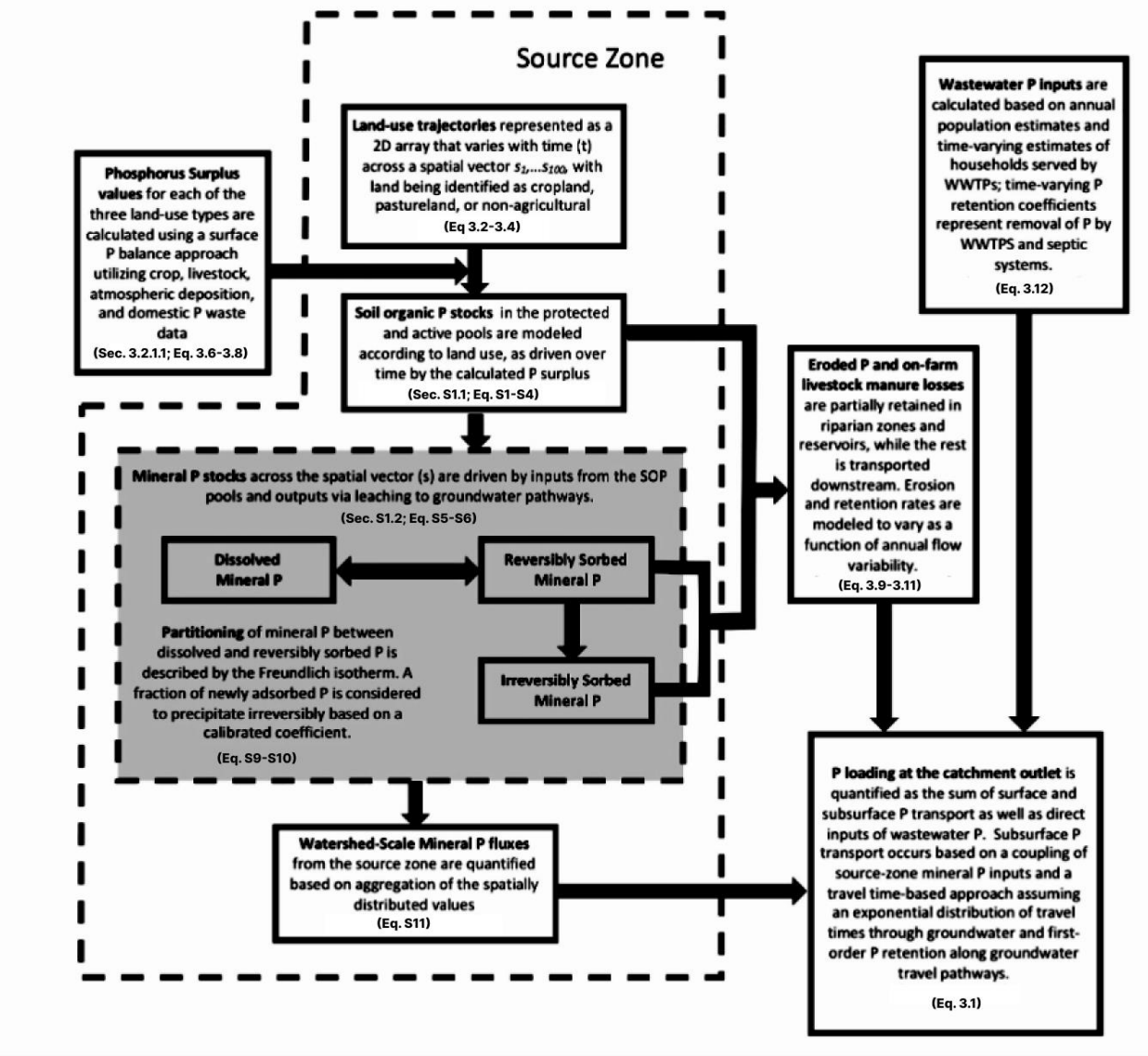


Figure S2.1 ELEMeNT-P modelling framework (Van Meter et al., 2021)

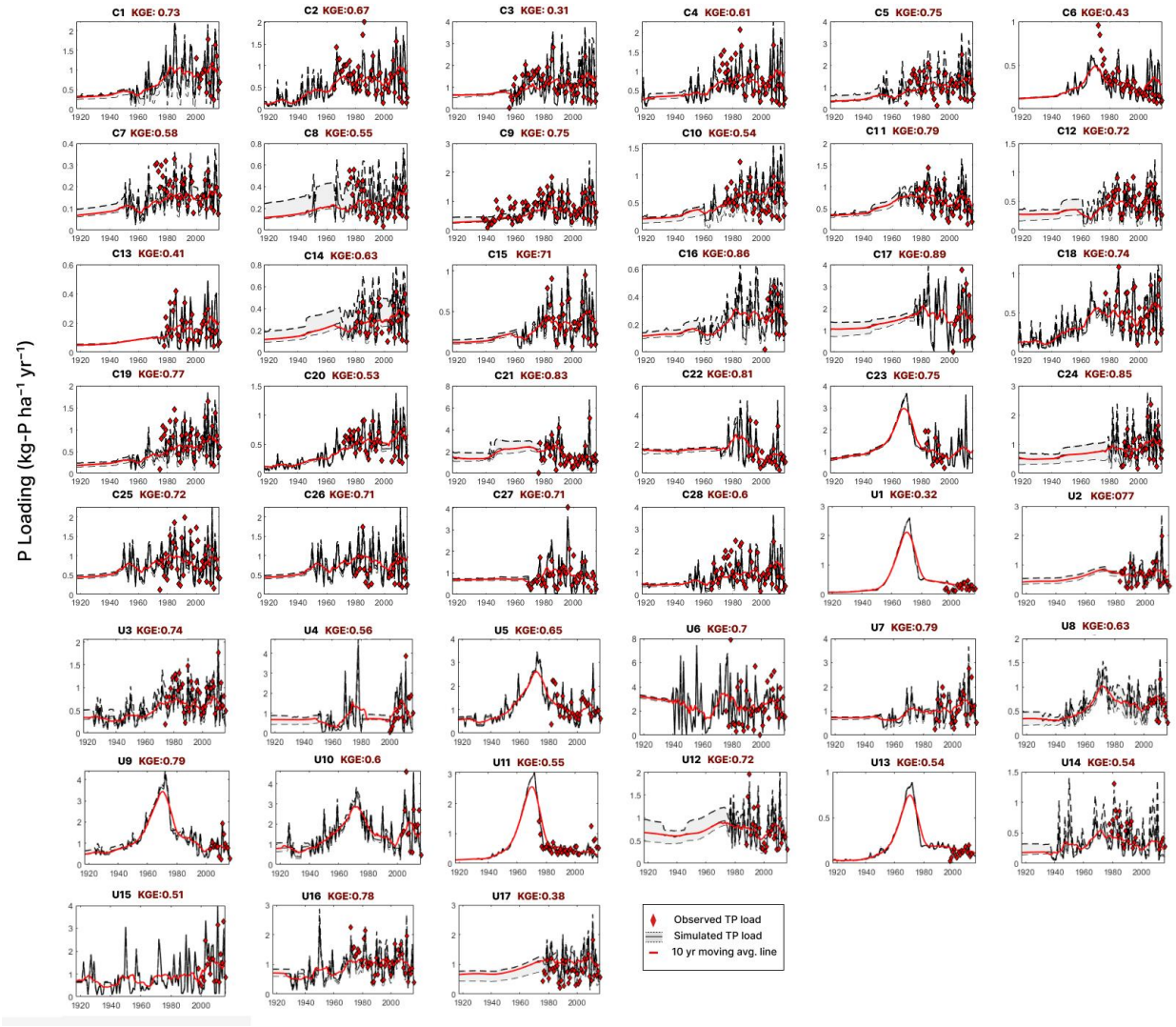


Figure S2.2: Modeled and measured loading at the outlet of 45 studied Lake Erie watersheds from 1920 to 2016. The KGE values represent the median KGE for each sub watershed's ensemble runs. The black line represents the median loading for ensemble runs of each watershed and grey bounds represent the upper and lower limit of loading. The red points represent the measured TP load.

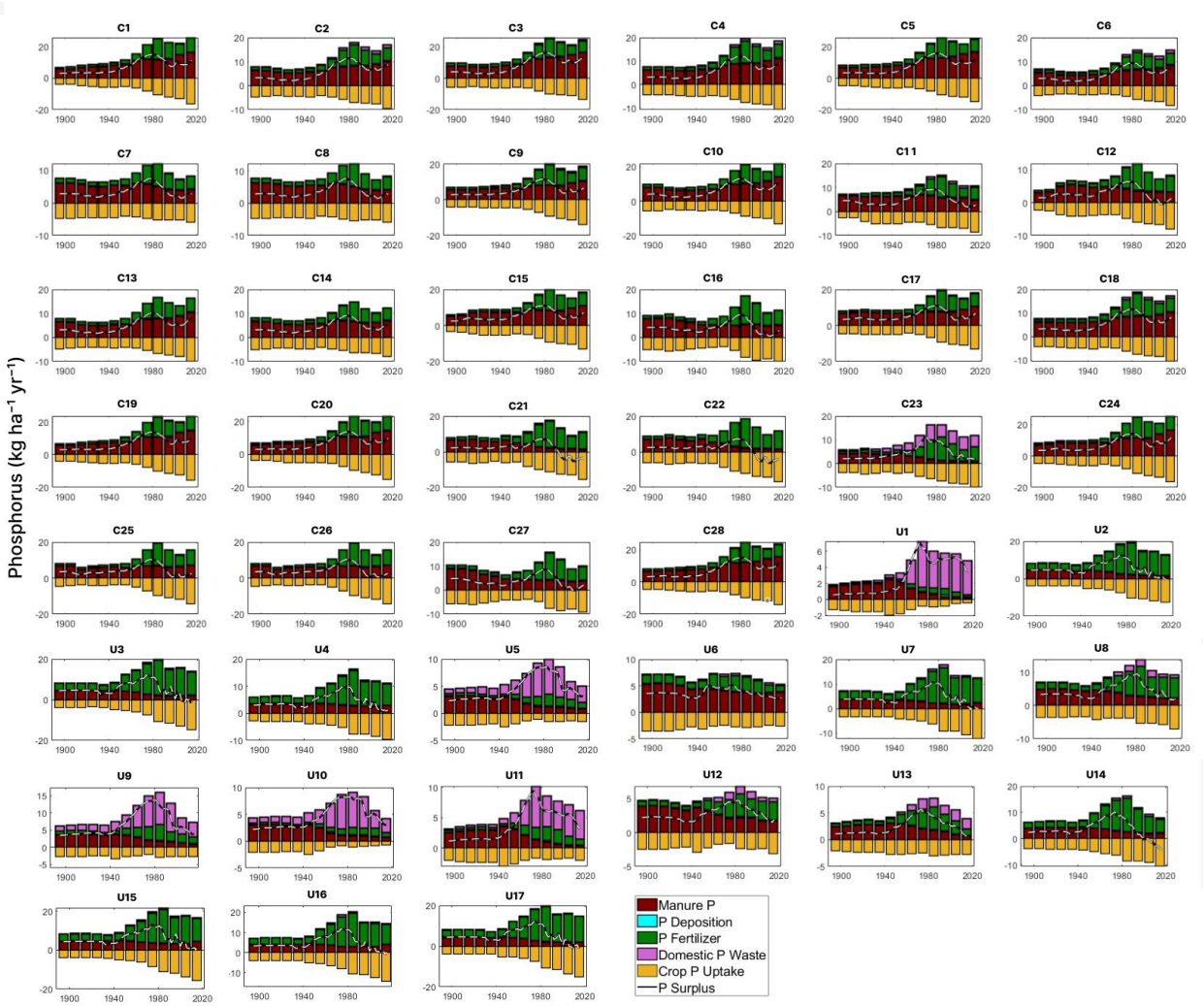


Figure S2.3: Trend of total P surplus and its component from 1901 to 2016 for 45 sub-watersheds in the Lake Erie basin.

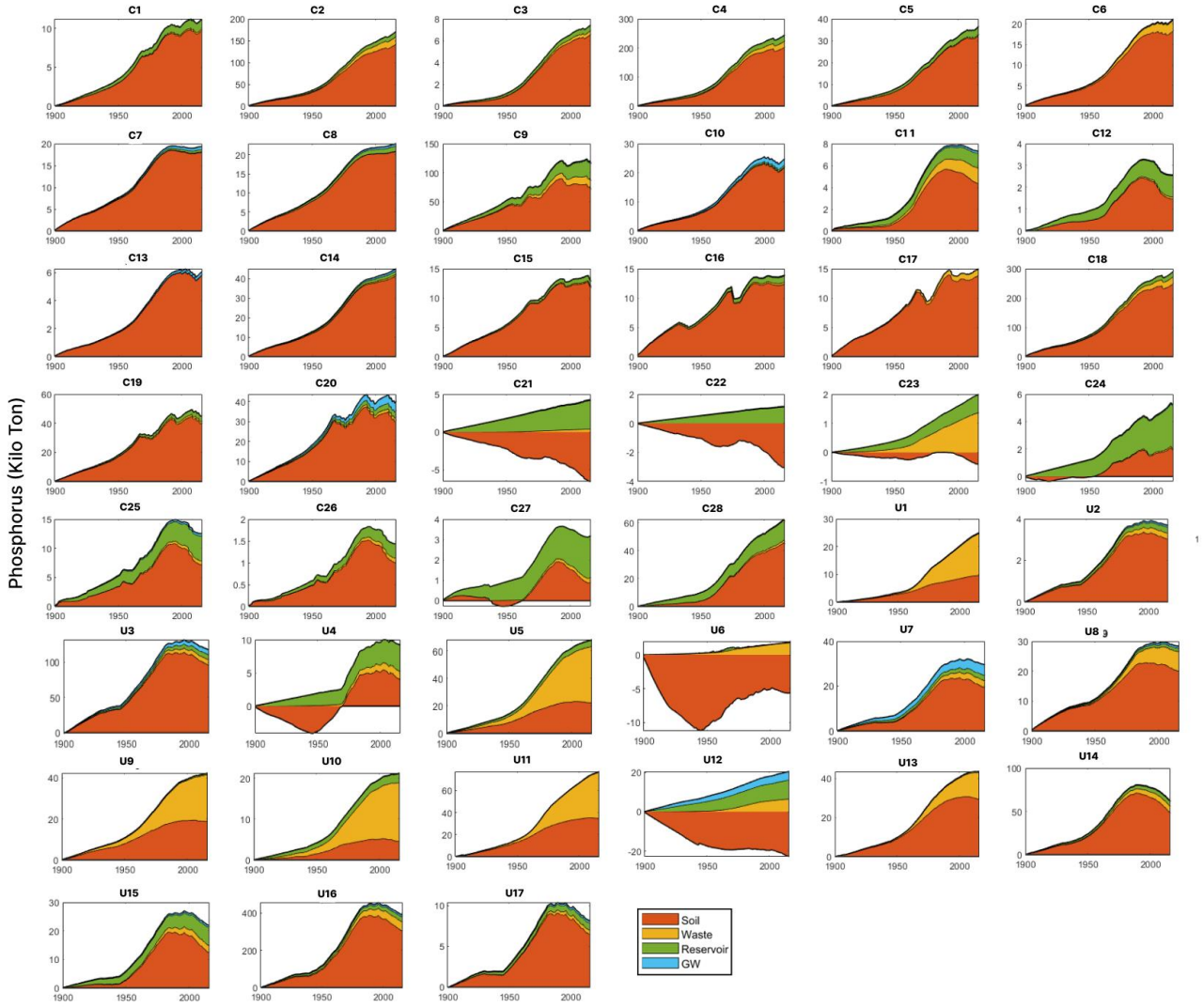


Figure S2.4: P accumulation trajectories in different land compartments for 45 watersheds in the Lake Erie basin.

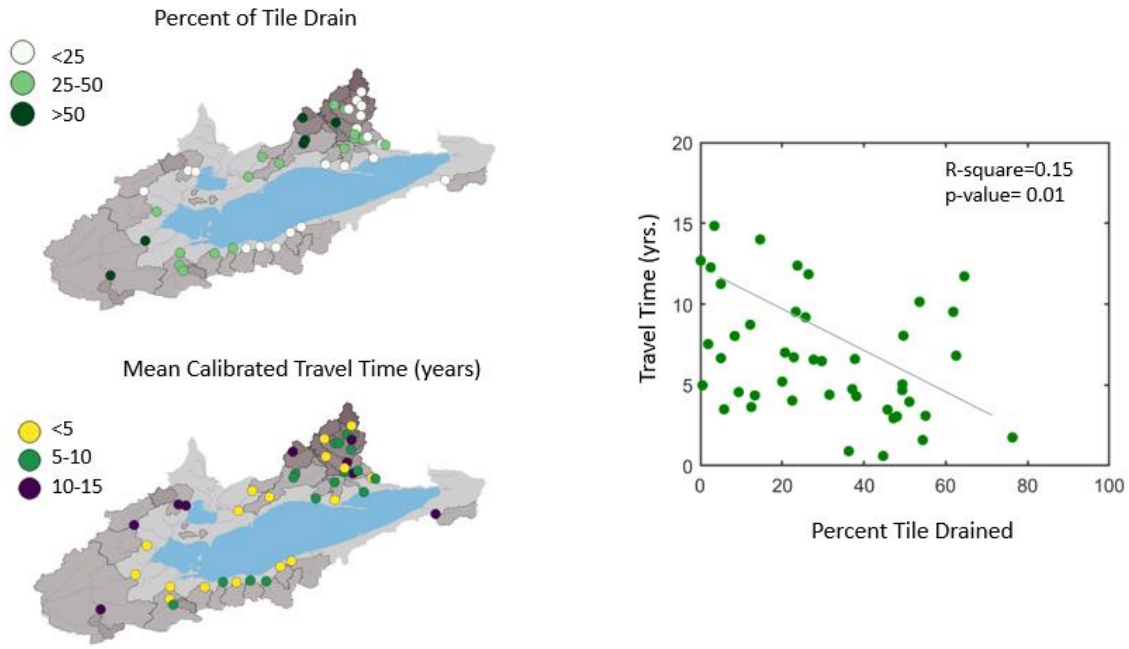


Figure S2.5: Relationship between percentage of tiled area and modeled travel time for studied sub-watersheds of Lake Erie basin.

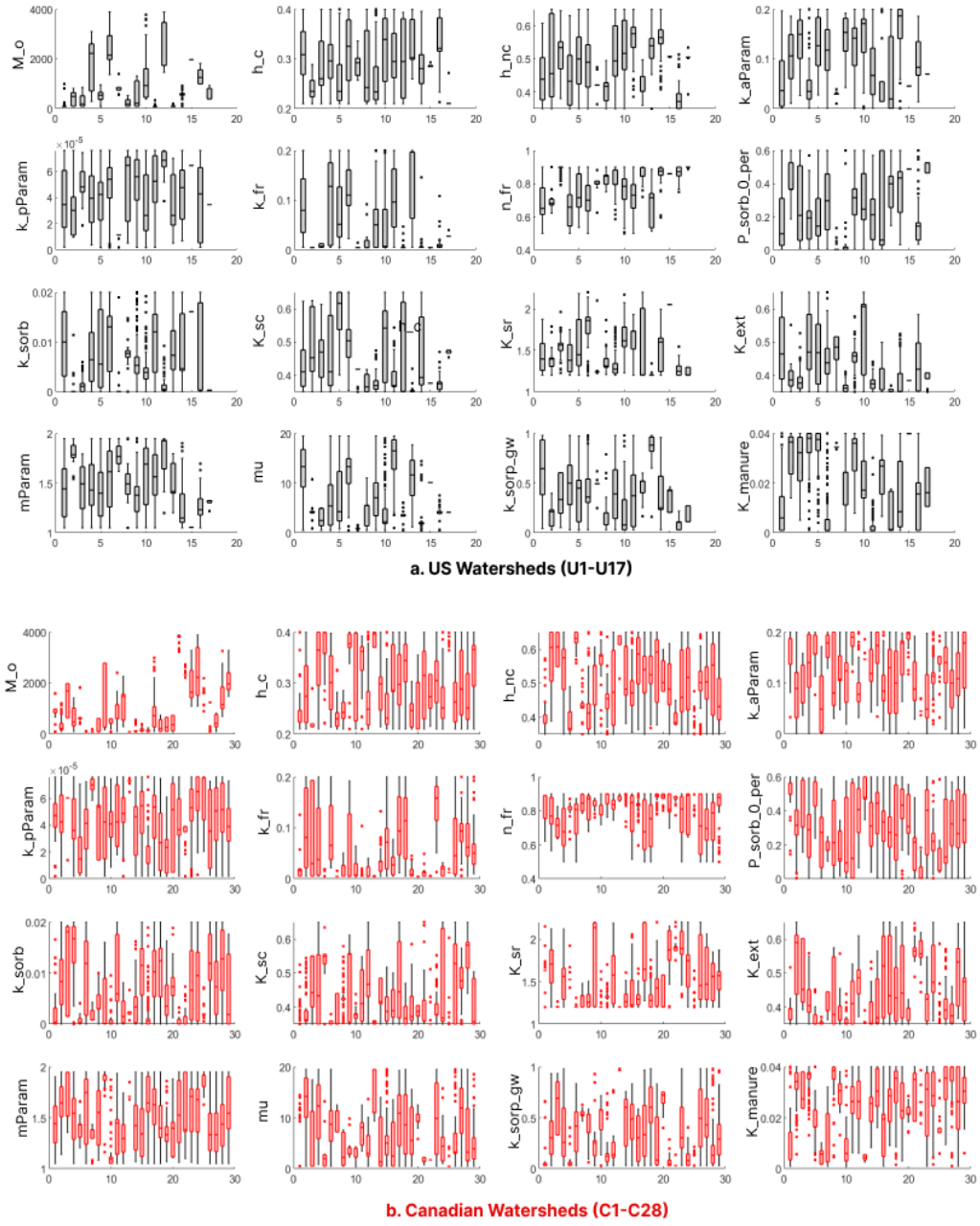


*Figure S2.6: Ranges of 16 calibrated parameters across 45 watersheds of the Lake Erie basin. a) parameter ranges for US watersheds, b) parameter ranges for Canadian watersheds. X-axis present the watershed ID of the USA and Canada (Table 3.1) and the Y axis represents the parameter ranges described in (**Table S3 in Appendix B**)*

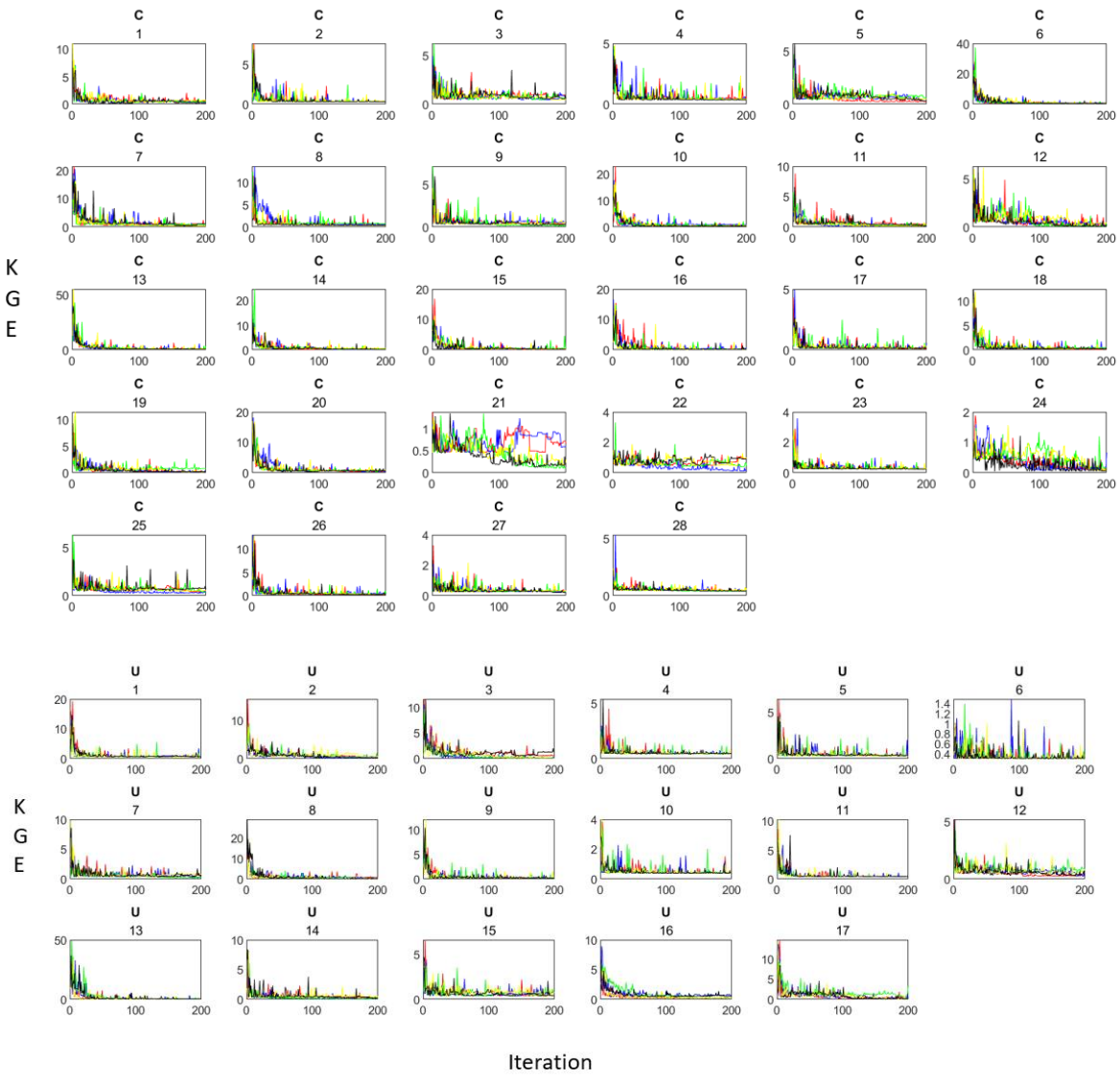


Figure S2.7: Model performance-KGE

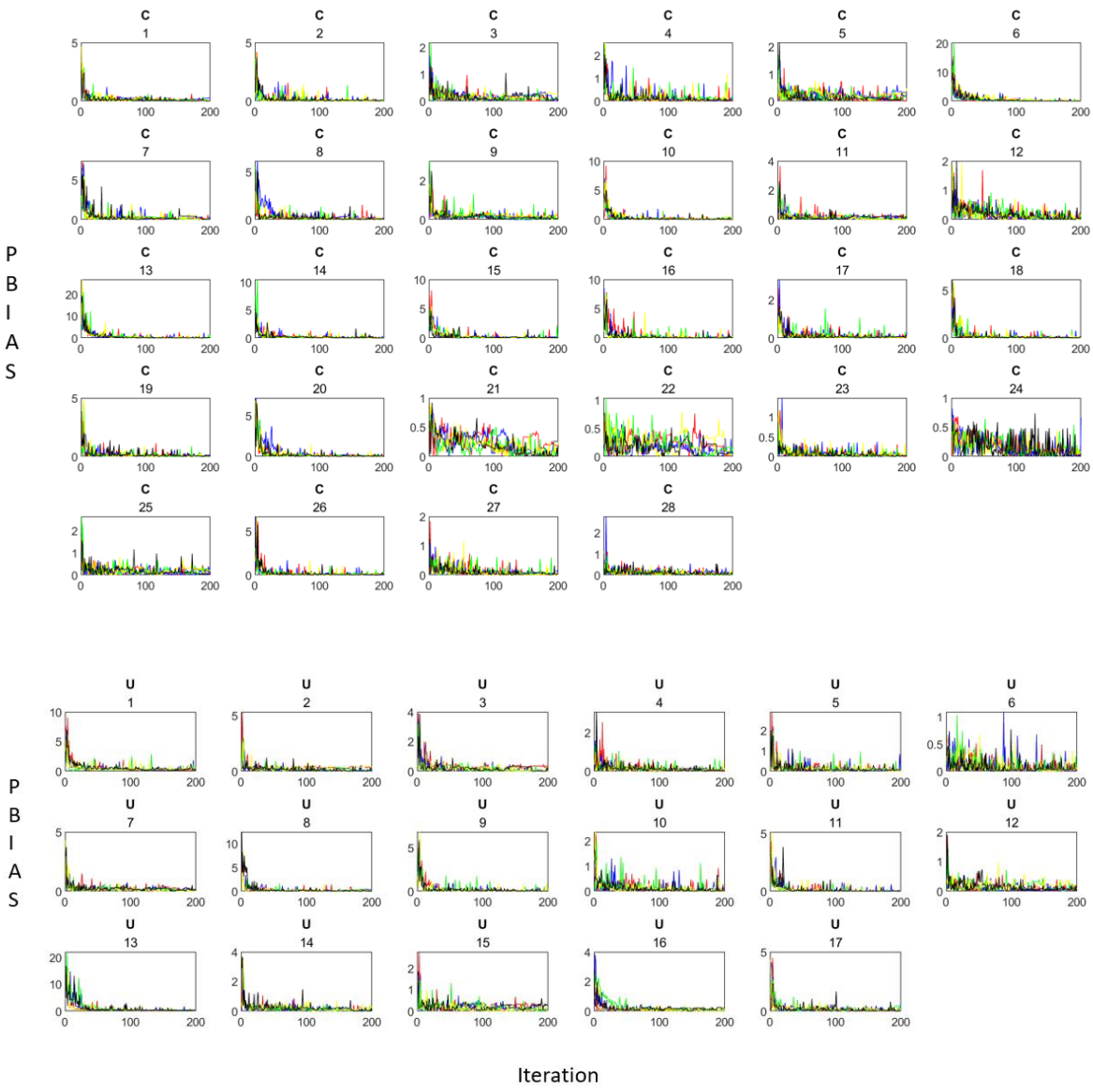


Figure S2.8: Model performance-p-Bias

Table S2.1: List of model performance parameters

ID	KGE	PBIAS		ID	KGE	PBIAS
U1	0.315	0.252		C7	0.582	0.197
U2	0.774	0.009		C8	0.554	0.019

U3	0.739	0.236		C9	0.748	0.201
U4	0.555	0.064		C10	0.539	0.290
U5	0.649	0.060		C11	0.758	0.101
U6	0.700	0.018		C12	0.722	0.153
U7	0.792	0.010		C13	0.405	0.002
U8	0.631	0.229		C14	0.632	0.048
U9	0.790	0.040		C15	0.714	0.017
U10	0.602	0.030		C16	0.858	0.022
U11	0.553	0.002		C17	0.878	0.035
U12	0.717	0.013		C18	0.744	0.042
U13	0.536	0.285		C19	0.769	0.172
U14	0.542	0.405		C20	0.534	0.062
U15	0.506	0.088		C21	0.825	0.005
U16	0.781	0.023		C22	0.812	0.052
U17	0.383	0.429		C23	0.751	0.049
C1	0.728	0.085		C24	0.850	0.010
C2	0.665	0.034		C25	0.727	0.007
C3	0.307	0.070		C26	0.714	0.038
C4	0.608	0.045		C27	0.716	0.040
C5	0.746	0.014		C28	0.596	0.048
C6	0.431	0.029				

Mean KGE 0.655

Mean Pbias 0.09

Median KGE 0.71

Median Pbias 0.04

Table S2.2: Change in P load from 2018 to 2045 under six different future scenarios.

ID	Future Scenarios					
	S1	S2	S3	S4	S5	S6
C1	0.16	-0.46	0.10	-0.54	-0.47	-0.54
C2	0.22	0.00	-0.06	-0.28	-0.06	-0.13
C3	0.12	0.03	-0.15	-0.25	0.01	-0.10
C4	0.17	-0.01	-0.11	-0.28	-0.04	-0.14
C5	0.23	-0.36	0.14	-0.45	-0.37	-0.43
C6	0.30	0.06	0.04	-0.18	-0.06	-0.08
C7	0.06	-0.30	-0.07	-0.40	-0.31	-0.37
C8	0.10	-0.15	-0.05	-0.31	-0.16	-0.24
C9	0.12	-0.28	-0.07	-0.48	-0.31	-0.36
C10	0.29	-0.48	0.21	-0.57	-0.48	-0.53
C11	-0.09	-0.39	-0.16	-0.47	-0.44	-0.45
C12	-0.04	-0.44	-0.09	-0.49	-0.45	-0.51
C13	0.28	-0.02	-0.03	-0.33	-0.03	-0.15
C14	0.17	-0.17	-0.07	-0.43	-0.19	-0.25
C15	0.11	-0.15	-0.36	-0.60	-0.16	-0.24
C16	0.12	-0.27	-0.01	-0.46	-0.28	-0.35
C17	0.11	-0.11	-0.22	-0.44	-0.11	-0.22
C18	0.15	-0.04	-0.20	-0.41	-0.10	-0.14
C19	0.16	-0.30	-0.17	-0.60	-0.31	-0.37
C20	0.22	-0.31	-0.01	-0.62	-0.32	-0.37
C21	-0.23	-0.41	-0.24	-0.41	-0.42	-0.48
C22	-0.27	-0.55	-0.27	-0.56	-0.55	-0.60
C23	-0.06	-0.18	-0.07	-0.18	-0.36	-0.29
C24	0.07	-0.41	0.04	-0.49	-0.41	-0.48
C25	-0.01	-0.50	-0.06	-0.55	-0.51	-0.57
C26	0.17	-0.14	-0.19	-0.51	-0.15	-0.22
C27	0.03	-0.16	-0.03	-0.22	-0.17	-0.32

C28	0.10	-0.14	-0.05	-0.30	-0.15	-0.26
U1	0.05	0.04	0.05	0.04	-0.50	-0.03
U2	-0.17	-0.33	-0.21	-0.37	-0.36	-0.43
U3	-0.19	-0.39	-0.31	-0.53	-0.41	-0.44
U4	-0.02	-0.12	-0.10	-0.21	-0.13	-0.27
U5	0.03	-0.02	0.01	-0.04	-0.17	-0.18
U6	0.01	-0.01	-0.01	-0.04	-0.02	-0.21
U7	-0.37	-0.52	-0.44	-0.58	-0.53	-0.56
U8	-0.20	-0.55	-0.24	-0.59	-0.59	-0.58
U9	0.01	-0.09	-0.01	-0.11	-0.35	-0.19
U10	0.02	-0.02	0.01	-0.03	-0.12	-0.17
U11	0.02	-0.02	0.01	-0.02	-0.52	-0.09
U12	-0.08	-0.24	-0.10	-0.27	-0.27	-0.33
U13	-0.03	-0.06	-0.06	-0.08	-0.60	-0.11
U14	-0.06	-0.09	-0.19	-0.22	-0.16	-0.21
U15	-0.07	-0.28	-0.21	-0.42	-0.30	-0.39
U16	-0.19	-0.33	-0.25	-0.41	-0.35	-0.40
U17	-0.43	-0.53	-0.45	-0.56	-0.53	-0.58

Table S2.3: Description of the calibration parameters with their mean value

Param	**Description**	**USA Mean**	**Canada Mean**
M_o	P mass in pristine soil(kg/ha)	1005.8	883.8
h_c	Protection coeff, cultivated land	0.296	0.297
h_nc	Protection coeff, non-cultivated land	0.493	0.512
k_aParam	mineralization rate constant y-1, active pool	0.107	0.116
k_pParam	mineralization rate constant y-1, protected pool	4.4e-5	4.2e-5
k_fr	Proportionality constant for Freundlich model	0.063	0.062

n_fr	emperical constant for Freundlich model	0.765	0.785
P_sorb_0_per	Fraction of sorbed soil P in pristine soil	0.255	0.298
k_sorb	Fraction of reversible sorbed source zone P	0.007	0.008
K_sc	coefficient of soil cover	0.452	0.433
K_sr	coefficient of soil resistance	1.520	1.540
K_ext	coefficient of type and extent of erosion (0 to 1)	0.438	0.444
mu	mean groundwater travel time	7.764	7.600
k_sorp_gw	GW P sorption coefficient	0.362	0.347
K_manure	Manure partitioning coefficient	0.019	0.028

Appendix C- Supplemental Information for Chapter 4

Table S3.1: Livestock phosphorus excretion parameters ($p_(_{lvstk,excr})$) for 2008. (USDA NRCS, 2008)

Livestock Type	**Livestock P Excretion, 2008 (kg-P head^{-1} y^{-1})**
Cattle, Beef	16.06
Cattle, Milk	25.61
Cattle, Other (heifers, bulls, steers, calves)	9.55
Goats	1.16
Sheep and Lambs	1.16
Horses	8.44
Pigs	2.35
Turkey	0.36
Broilers	0.12
Other Chickens	0.18

Table S3.2: Normalized livestock weights (1961-2021). Weights coefficient (Swt) of each livestock type are normalized to 2008 values, as reported by the (USDA NRCS, 2008)

Year	Beef cows	Cattle, milk	Other cattle (heifers, bulls, steers, and calves)	Pigs	Sheep & lambs	Broilers	Other chickens	Turkeys	Goats	Horses
2021	1.07	1.07	1.05	1.07	0.91	1.16	1.18	1.12	0.91	1.00
2020	1.07	1.07	1.05	1.08	0.93	1.15	1.19	1.11	0.93	1.00
2019	1.05	1.05	1.05	1.06	0.95	1.13	1.18	1.11	0.95	1.00
2018	1.05	1.05	1.05	1.06	1.01	1.12	1.12	1.07	1.01	1.00
2017	1.05	1.05	1.05	1.05	0.98	1.11	1.06	1.07	0.98	1.00
2016	1.06	1.06	1.06	1.05	0.99	1.10	1.04	1.06	0.99	1.00
2015	1.06	1.06	1.06	1.06	1.00	1.10	1.04	1.04	1.00	1.00

2014	1.04	1.04	1.04	1.06	0.99	1.08	0.99	1.05	0.99	1.00
2013	1.03	1.03	1.03	1.03	0.99	1.06	0.97	1.05	0.99	1.00
2012	1.02	1.02	1.02	1.02	1.06	1.05	0.96	1.03	1.06	1.00
2011	1.00	1.00	1.00	1.02	1.02	1.04	0.99	1.02	1.02	1.00
2010	1.00	1.00	1.00	1.02	0.99	1.02	0.99	1.01	0.99	1.00
2009	1.01	1.01	1.01	1.01	1.01	1.00	0.99	1.00	1.01	1.00
2008	1.00	1.00	1.00	1.00	1.00	1.00	1.00	1.00	1.00	1.00
2007	0.99	0.99	0.99	1.00	1.00	0.99	1.04	0.98	1.00	1.00
2006	0.99	0.99	0.99	1.00	1.00	0.98	1.06	0.97	1.00	1.00
2005	0.98	0.98	0.98	1.00	1.01	0.96	0.99	0.97	1.01	1.00
2004	0.97	0.97	0.97	0.99	1.00	0.94	0.98	0.94	1.00	1.00
2003	0.96	0.96	0.96	0.99	0.98	0.93	0.97	0.92	0.98	1.00
2002	0.98	0.98	0.98	0.99	0.98	0.92	0.93	0.92	0.98	1.00
2001	0.95	0.95	0.95	0.98	1.02	0.90	0.92	0.90	1.02	1.00
2000	0.95	0.95	0.95	0.98	0.99	0.90	0.92	0.88	0.99	1.00
1999	0.94	0.94	0.94	0.96	0.97	0.89	0.90	0.88	0.97	1.00
1998	0.94	0.94	0.94	0.96	0.96	0.87	0.89	0.85	0.96	1.00
1997	0.92	0.92	0.92	0.95	0.97	0.86	0.87	0.83	0.97	1.00
1996	0.91	0.91	0.91	0.95	0.93	0.86	0.90	0.82	0.93	1.00
1995	0.92	0.92	0.92	0.96	0.91	0.84	0.88	0.80	0.91	1.00
1994	0.93	0.93	0.93	0.95	0.91	0.83	0.86	0.78	0.91	1.00
1993	0.91	0.91	0.91	0.95	0.93	0.82	0.82	0.77	0.93	1.00
1992	0.91	0.91	0.91	0.94	0.91	0.81	0.82	0.75	0.91	1.00
1991	0.91	0.91	0.91	0.94	0.91	0.79	0.82	0.73	0.91	1.00
1990	0.89	0.89	0.89	0.93	0.91	0.78	0.81	0.73	0.91	1.00
1989	0.89	0.89	0.89	0.93	0.90	0.78	0.82	0.72	0.90	1.00
1988	0.88	0.88	0.88	0.93	0.90	0.77	0.79	0.72	0.90	1.00

1987	0.86	0.86	0.86	0.92	0.86	0.77	0.78	0.70	0.86	1.00
1986	0.86	0.86	0.86	0.92	0.85	0.76	0.78	0.69	0.85	1.00
1985	0.85	0.85	0.85	0.91	0.84	0.75	0.79	0.69	0.84	1.00
1984	0.85	0.85	0.85	0.91	0.84	0.75	0.77	0.68	0.84	1.00
1983	0.84	0.84	0.84	0.91	0.83	0.73	0.78	0.68	0.83	1.00
1982	0.84	0.84	0.84	0.91	0.83	0.72	0.77	0.67	0.83	1.00
1981	0.83	0.83	0.83	0.90	0.82	0.72	0.78	0.66	0.82	1.00
1980	0.83	0.83	0.83	0.90	0.81	0.71	0.76	0.64	0.81	1.00
1979	0.82	0.82	0.82	0.90	0.81	0.71	0.77	0.65	0.81	1.00
1978	0.81	0.81	0.81	0.89	0.80	0.70	0.75	0.65	0.80	1.00
1977	0.81	0.81	0.81	0.89	0.79	0.69	0.74	0.64	0.79	1.00
1976	0.80	0.80	0.80	0.89	0.79	0.68	0.76	0.63	0.79	1.00
1975	0.79	0.79	0.79	0.90	0.76	0.67	0.74	0.61	0.76	1.00
1974	0.82	0.82	0.82	0.91	0.76	0.68	0.76	0.63	0.76	1.00
1973	0.82	0.82	0.82	0.90	0.78	0.67	0.76	0.62	0.78	1.00
1972	0.82	0.82	0.82	0.89	0.76	0.67	0.77	0.63	0.76	1.00
1971	0.81	0.81	0.81	0.89	0.75	0.66	0.78	0.62	0.75	1.00
1970	0.82	0.82	0.82	0.90	0.76	0.65	0.80	0.62	0.76	1.00
1969	0.80	0.80	0.80	0.89	0.75	0.65	0.80	0.62	0.75	1.00
1968	0.80	0.80	0.80	0.90	0.74	0.64	0.80	0.61	0.74	1.00
1967	0.81	0.81	0.81	0.90	0.73	0.64	0.80	0.59	0.73	1.00
1966	0.80	0.80	0.80	0.91	0.74	0.63	0.81	0.57	0.74	1.00
1965	0.79	0.79	0.79	0.90	0.73	0.63	0.82	0.57	0.73	1.00
1964	0.81	0.81	0.81	0.91	0.71	0.62	0.83	0.56	0.71	1.00
1963	0.81	0.81	0.81	0.90	0.71	0.62	0.83	0.56	0.71	1.00
1962	0.80	0.80	0.80	0.90	0.71	0.61	0.84	0.55	0.71	1.00
1961	0.81	0.81	0.81	0.90	0.71	0.62	0.85	0.54	0.71	1.00

Table S3.3: Data for calculating P from laundry and dish detergent use for census years

Year	Laundry detergent per capita (kg- per capita/yr)[1]	Fraction of P in laundry detergent[2]	P in laundry detergent kg-P -per capita/yr)	P in dish detergent kg-P -per capita/yr)[2]
1961	4.839	0.15	0.726	0.067
1966	6.086	0.15	0.913	0.104
1971	6.451	0.087	0.561	0.144
1976	6.67	0.022	0.147	0.205
1981	6.67	0.022	0.147	0.241
1986	6.67	0.022	0.147	0.234
1991	6.67	0.022	0.147	0.233
1996	6.67	0.022	0.147	0.233
2001	6.67	0.022	0.147	0.233
2006	6.67	0.022	0.147	0.233
2011	6.67	0.005	0.033	0.013
2016	6.67	0.005	0.033	0.013
2021	6.67	0.005	0.033	0.013

1. Per capita laundry detergent use from (Han et al., 2012) was interpolated to fit Canadian census years.
2. Sourced from (Han et al., 2012), (Goyette et al., 2016) and fitted to Canadian census years.

Table S3.4: P content and fraction dry crop matter for all crop types.

Crop Type	**Fraction Dry Matter, d (kg-crop$_{dry}$/kg-crop)**	**Fraction P in Dry Matter, p$_{crop}$ (kg-P /kg- crop$_{dry}$)**	**Fraction P in Crop, d*p$_{crop}$ (kg-P/kg crop)**	**Citation**
Alfalfa hay	0.904	0.0026	0.00235	[1,2]
Barley	0.889	0.0042	0.003734	[2]
Beans	0.900	0.0054	0.00486	[3]
Canola	0.911	0.0062	0.005648	[3]
Corn, grain	0.867	0.00317	0.002748	[2]
Corn, silage	0.284	0.0019	0.00054	[2]
Flaxseed	0.941	0.0057	0.005364	[3]
Hay, (excl alfalfa)	0.867	0.0026	0.002254	[1]
Lentils	0.887	0.0043	0.003814	[3]
Oats	0.894	0.0037	0.003308	[2]
Potatoes	0.223	0.0025	0.000558	[2]
Rye	0.881	0.0037	0.00326	[2]
Soybeans	0.906	0.0066	0.00598	[2]
Sugar beets	0.191	0.0025	0.000478	[3]
Sunflower seeds	0.933	0.0063	0.005878	[3]
Tobacco	1.000	0.0021	0.0021	[2]
Triticale	0.891	0.0034	0.003029	[3]

Wheat	0.885	0.0040	0.00354	[2]
Buckwheat	-	-	0.0037	[4]
Mixed Grain	-	-	0.0032	[4]
Other Field Crops	-	-	0.0009	[5]

1. http://www.ipni.net/article/IPNI-3296; 2.(Swaney et al., 2019a); 3. (Lander et al., 1998); 4. (T. Van Staden et al., 2019) 5. (Van Meter et al., 2021)

Table S3.5: Livestock Phosphorus consumption parameters (P_{cons}) by livestock category for 2018 (USDA NRCS, 2008)

Livestock Type	**Livestock P Consumption, 2008 (kg-P head^{-1} y^{-1})**
Cattle, Beef	18.32
Cattle, Milk	33.02
Cattle, Other (heifers, bulls, steers, calves)	10.89
Goats	1.39
Sheep and Lambs	1.39
Horses	9.45

Table S3.6: Confinement factor (f_{conf}) considered for each province (USDA NRCS, 2008); The confinement factor refers to the fraction of each indicated livestock category that does not have access to pasture.

Canadian Province	**Beef Cow**	**Dairy Cow**	**Other Cow**
NL	0.1	0.8	0.368
PE	0.1	0.8	0.368
NS	0.1	0.8	0.368
NB	0.1	0.8	0.368
QC	0.133	0.833	0.412

ON	0.083	0.85	0.429
MB	0.075	0.85	0.401
SK	0.005	0.775	0.221
AB	0.01	0.75	0.223
BC	0.05	0.8	0.444

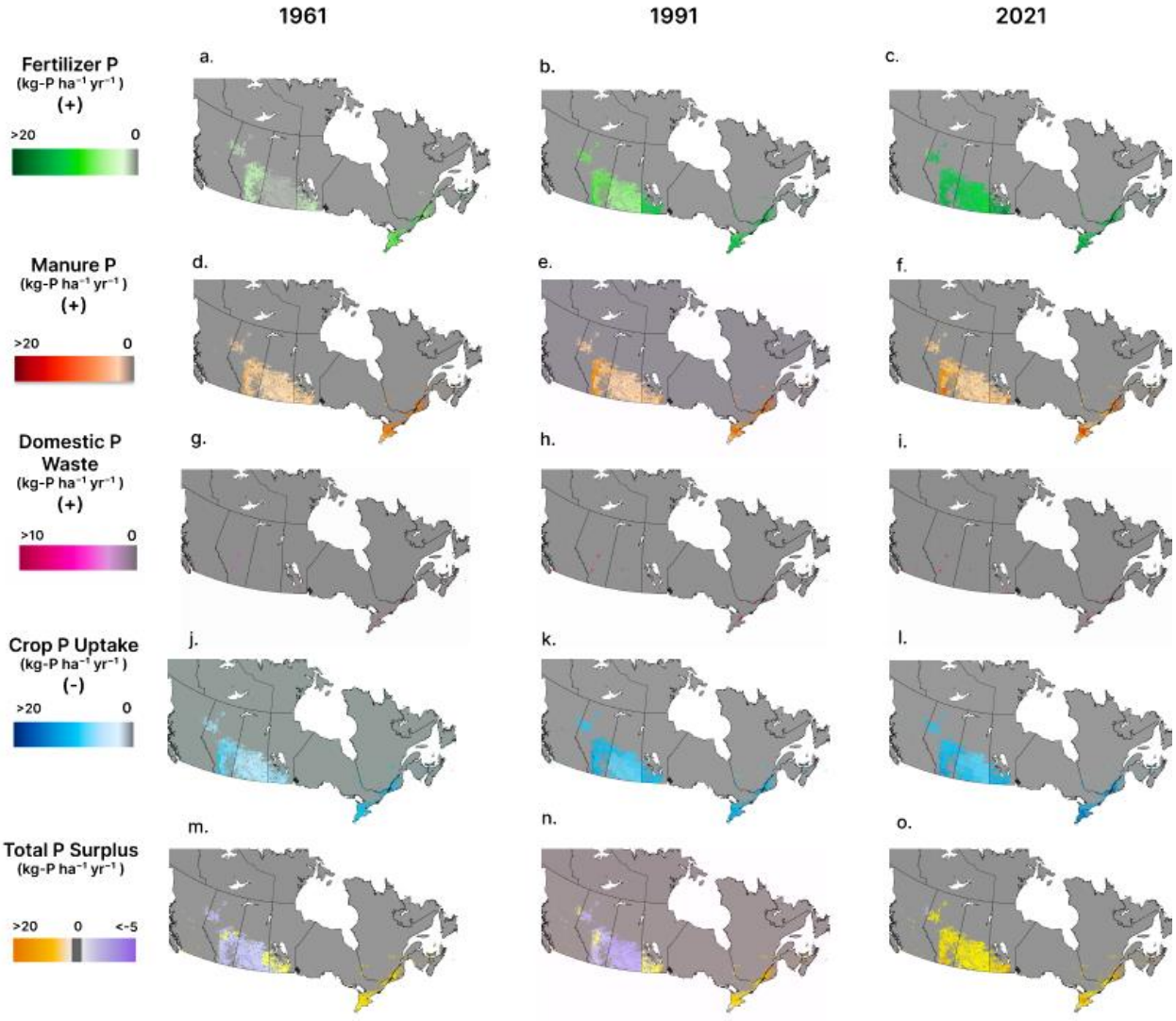


*Figure S3: Maps of the major components for the agricultural phosphorus mass balance***:** *(a-c) fertilizer P, (d-f) manure P, (g-i) domestic P waste, (j-l) crop uptake and (m-o) total P surplus all in kg-P* ha^{-1} yr^{-1}*. Each map is divided showing three time periods capturing the beginning, middle, and end of the time series.*

Table S3.7: Investigation report for mismatched county IDs.

Year	Province	County ID	Reason for not in map or table	Agriculture?
1961	NL	1010	Northern region	No
1962	NL	1010	Northern region	No
1971	NL	1009	This map was made & named after 1976 map, 1976 excel doesn't have 1009 county, so couldn't be sure that this county's ID is 1009. But, in 1981, this county has the same subdivision as 1971 which could mean that this county in 1971 can be ID'd as 1009.	No
1971	QC	2425	(In census not in map) - For some reason digitizing didn't save the edits to this polygon and is just a missing hole in the map in the county's shape.	No
1971	ON	3532	(In census not in map), This county doesn't exist in 1976 map which this was made from, & because the ID numbers don't line up it's unclear where this county is supposed to be.	(some) Near Toronto
1981	NL	1003	Maybe no agriculture due to being along the water?	No
1981	NL	1010	Northern region	No
1981	MB	4622	Northern region	No
1981	MB	4623	Northern region	No
1981	BC	5943	Maybe no agriculture due to being along the water?	No
1981	BC	5957	Northern & mountain region	No
1986	NL	1003	Maybe no agriculture due to being along the water?	No
1986	NL	1009	Northern region along the water?	No
1986	NL	1010	Northern region	No
1986	NB	1301	Narrow shape along the water	No
1986	QC	2498	Northern region	No
1986	ON	3520	Along the water	No
1986	MB	4622	Northern region	No
1986	MB	4623	Northern region	No
1986	SK	4718	Northern region	No

1986	AB	4815	Long county bordering AB & BC, unsure why it's not in excel, maybe just no agriculture	No
1986	BC	5923	Along the water	No
1986	BC	5929	Along the water	No
1986	BC	5943	Along the water	No
1986	BC	5945	Along the water	No
1986	BC	5947	Along the water	No
1986	BC	5957	Northern & mountain region	No
1991	NL	1003	Maybe no agriculture due to being along the water?	No
1991	NL	1009	Northern region along the water?	No
1991	NL	1010	Northern region	No
1991	NB	1301	Narrow shape along the water	No
1991	QC	2497	Northern region	No
1991	QC	2498	Northern region	No
1991	ON	3520	Along the water	No
1991	MB	4622	Northern region	No
1991	MB	4623	Northern region	No
1991	SK	4718	Northern region	No
1991	AB	4815	Long county bordering AB & BC, unsure why it's not in excel, maybe just no agriculture	No
1991	BC	5923	Along the water	No
1991	BC	5929	Along the water	No
1991	BC	5943	Along the water	No
1991	BC	5945	Along the water	No
1991	BC	5947	Along the water	No
1991	BC	5957	Northern & mountain region	No
1991	QC	2492	(In census not in map) - hole in map in the shape of a county that exists in previous years, maybe this is the missing space for the 2492 county?	No
1991	MB	4620	(In census not in map) - hole in map in the shape of a county that exists in previous years, maybe this is the missing space for the 4620 county?	No
1996	NL	1003	Maybe no agriculture due to being along the water?	No
1996	NL	1009	Northern region along the water?	No
1996	NL	1010	Northern region	No
1996	NB	1301	Narrow shape along the water	No

1996	QC	2497	Northern region	No
1996	QC	2498	Northern region	No
1996	QC	2499	Northern region	No
1996	ON	3520	Along the water	No
1996	MB	4622	Northern region	No
1996	MB	4623	Northern region	No
1996	SK	4718	Northern region	No
1996	AB	4816	Northern region	No
1996	BC	5943	Along the water	No
1996	BC	5957	Northern & mountain region	No
1996	BC	5959	Northern & mountain region	No

Text S7. This table addresses discrepancies involving mismatched county IDs identified during our analysis. There are two types of mismatches-1) IDs present in the census but absent on the census map; 2) IDs present in the shapefile but not reported in the census.

The counties not reported in the census are typically those without agricultural activity. Most of the counties mismatched are missing in original census table are tabulated here otherwise described as “In census not in map”. Upon identifying a mismatched county ID, we first examine the surrounding area to assess its land use condition. If it is in a non-agricultural region, we assume there is zero agricultural activity and disregard that area. However, if a county is located in an agricultural or populated region, we proceed to digitize the county boundary to ensure accurate representation in our dataset.